

**AN OCULAR MOTOR SYSTEM MODEL THAT SIMULATES  
CONGENITAL NYSTAGMUS, INCLUDING BRAKING AND  
FOVEATING SACCADES**

by

JONATHAN BRUCE JACOBS

Submitted in partial fulfillment of the requirements

For the degree of Doctor of Philosophy

Thesis Adviser: Louis F. Dell'Osso, Ph.D.

Department of Biomedical Engineering

CASE WESTERN RESERVE UNIVERSITY

May, 2001

Copyright © 2001 by Jonathan Bruce Jacobs

All rights reserved

CASE WESTERN RESERVE UNIVERSITY  
SCHOOL OF GRADUATE STUDIES

We hereby approve the thesis/dissertation of

Jonathan Bruce Jacobs

candidate for the Ph.D. degree \*.

(signed) David L. Wilson  
(chair of the committee)

L. A. Dell'Abate

Glover C. Almore

Mark Lutz

Neil P. Stani

(date) 3/27/2001

\*We also certify that written approval has been obtained for any proprietary material contained therein.

Do not write about nystagmus; it will lead you nowhere.

—Herman Wilbrand (1851-1935)

There are only two things we do not know about nystagmus:

The origin of the fast phase, and the origin of the slow phase.

—Unknown

You cannot depend on your eyes when your imagination is out of focus.

—Mark Twain (1835-1910)

The poet's eye, in a fine frenzy rolling,

Doth glance from heaven to earth, from earth to heaven;

And as imagination bodies forth

The forms of things unknown, the poet's pen

Turns them to shapes, and gives to airy nothing

A local habitation and a name.

—William Shakespeare, "A Midsummer Night's Dream"

## **DEDICATION**

To my parents, who taught me to love learning.

To Peggy, because, well, you know...

## TABLE OF CONTENTS

Table of Contents	vi
List of Tables	xiv
List of Figures	xv
Acknowledgements	xix
Abstract	xxi
Chapter	
1 Introduction and Background	1-74
1.1 Introduction	1
1.1.1. Why We Make Eye Movements	1
1.1.2 Congenital Nystagmus (CN)	4
1.1.3 Origin and Development of CN	8
1.1.4 Classification and Characteristics of CN	13
1.1.5 Treatments for CN	18
1.1.6 Misunderstandings about CN	23
1.1.7 Braking and Foveating Saccades	25
1.2 Techniques for Measuring Eye Movements	29
1.2.1 History of Eye Movement Recording	29
1.2.2 Electrooculography	30

1.2.3 Infrared Reflection	34
1.2.4 Videography	35
1.2.5 Magnetic Search Coil	36
1.3 Modeling	38
1.3.1 Fast Eye Movement (FEM) Subsystem	39
1.3.2 Smooth Pursuit (SP) Subsystem	45
1.3.3 Internal Monitor (IM)	46
1.3.4 Fixation Subsystem	48
1.3.5 Efference Copy vs Proprioception	49
1.3.6 Model Design Philosophy	52
1.3.7 Previous models of CN	56
1.3.8 Lineage of this CN model	58
1.4 Works Cited	60
2 Generation of Braking Saccades in Congenital Nystagmus	75-104
2.0 Abstract	75
2.1 Introductions	76
2.2 Methods	78
2.2.1 Recording	78
2.2.2 Protocol	79

	2.2.3 Analysis	80
	2.3 Results	87
	2.3.1 Phase Plane Timing	87
	2.3.2 Braking Effect	93
	2.3.3 Saccade Duration Effect	94
	2.3.4 Saccade Magnitude Effect	97
	2.3.5 Initial Position and Velocity Effects	97
	2.4 Discussion	97
	2.5 Works Cited	103
3	Characteristics of Braking Saccades in Congenital Nystagmus	105-158
	3.0 Abstract	105
	3.1 Introduction	106
	3.2 Methods	109
	3.2.1 Subjects	109
	3.2.2 Recording	111
	3.2.3 Protocol	111
	3.2.4 Analysis	112
	3.2.5 Models	119
	3.3 Results	122
	3.3.1 Peak Velocity vs. Amplitude	122

3.3.2	Duration vs. Amplitude	128
3.3.3	Skewness	133
3.3.4	Ramp-Step-Ramp	140
3.3.5	Models	143
3.4	Discussion	149
3.5	Acknowledgements	153
3.6	Works Cited	154
4	A Robust, Normal Ocular Motor System Model That Simulates Fixation, Saccades, and Pursuit Including Pendular Congenital Nystagmus Waveforms With Braking and Foveating Saccades and Extended Foveation	159-228
4.0	Abstract	159
4.1	Introduction	160
4.2	Methods	167
4.2.1	Recording	167
4.2.2	Protocol	168
4.2.3	Analysis	169
4.2.4	Computer Simulation	169
4.2.5	OMS Model Subsystems	175
4.2.6	Generation of CN	189

4.3	Results	189
4.3.1	Normal Behavior	189
4.3.2	'Evolution' of CN Waveforms	190
4.3.3	Responses to Step, Pulse-Step, Ramp, and Step-Ramp Stimuli: Normal and with CN	196
4.4	Discussion	214
4.4.1	Conceptual Basis for the Model	214
4.4.2	Fixation Subsystem Method	216
4.4.3	Foundations of the Model	216
4.4.4	Development of the Model	217
4.5	Works Cited	220
5	Conclusion	229-243
5.1	Summary	229
5.1.1	Generation of Braking Saccades	229
5.1.2	Characteristics of Braking Saccades	230
5.1.3	Model	231
5.2	Future Work	235
5.3	Conclusions	237
5.4	Works Cited	242

## Appendices

A	A Normal Ocular Motor System Model That Simulates the Dual-Mode Fast Phases of Latent/Manifest Latent Nystagmus	244-303
	A.0 Abstract	244
	A.1 Introduction	245
	A.2 Methods	251
	A.2.1 Recording and Protocol	251
	A.2.2 Analysis	252
	A.2.3 Computer Simulation	252
	A.2.4 Model Subsystems	257
	A.3 Results	266
	A.3.1 Normal Saccades	266
	A.3.2 Abnormal Saccades	266
	A.3.3 Manifest Latent Nystagmus (MLN)	270
	A.3.4 Latent Nystagmus (LN)	275
	A.3.5 Alternating Fixation	280
	A.3.6 Abducting-Eye Fixation	280
	A.4 Discussion	285
	A.4.1 Hypotheses of the Model	286
	A.4.2 Foundations of the Model	287

A.4.3 ‘Evolving’ the Model	287
A.4.4 The Dual-Mode Nature of the Model	289
A.4.5 Emergent Behavior of the Model	290
A.4.6 A Robust Ocular Motor System Model as a Research Tool	290
A.5 Acknowledgements	292
A.6 Works Cited	293
A.7 Model Details	298
A.7.1 Target Change Detection	298
A.7.2 Plant Model and Saccadic Logic	298
A.7.3 Target Velocity Reconstruction	299
A.7.4 Saccade Enable and Timing	299
A.7.5 Saccade Size	301
A.7.6 Saccade and Drift Blanking	302
A.7.7 Neural Integrator Control	302
A.7.8 Alexander’s Law	303
A.7.9 Braking Saccade Logic	303
B Summary of the Major Subsystems of the OMS Model	304-343
B.1 Overview of OMS Model and Internal Monitor	306
B.2 Saccadic Enable Subsystem and Sub-blocks	309

B.3 IM Subsystems I: Target Change Detect, Model Plant+, Saccadic Motor Command, and Associated Sub-blocks	313
B.4 Reconstruction of Position and Velocity of Eye and Target	316
B.5 Saccadic and Post-Drift Blanking	320
B.6 Braking/Foveating Saccade Logic and Sub-blocks	322
B.7 Fixation Subsystems	326
B.8 Neural Integrator Hold Controller	328
B.9 Saccadic Pulse Generator and Sub-blocks	330
B.10 Neural Integrator and Ocular Motor Neurons	334
B.11 Resettable Event Timer	336
Bibliography	344-357

## **LIST OF TABLES**

2-1 Summary of Braking Saccade Effect	93
3-1 Summary of Subjects in Studies	110

## LIST OF FIGURES

1-1 Orientation of pendular CN.	5
1-2 Ringing at onset of smooth pursuit.	11
1-3 Loss of attention during recording of CN subject.	15
1-4 Comparison of various nystagmus waveforms.	16
1-5 Effect of gaze angle on CN waveforms.	19
1-6 Comparison of various eye movement recording techniques.	32
1-7 Composition of signals that drive eye movement.	41
2-1 A braking saccade of “zero magnitude.”	82
2-2 Illustration of timing considerations in CN.	84-85
2-3 Phase-plane representation of CN data for S1.	89
2-4 Phase-plane representation of CN data for S2.	91
2-5 Cycle duration vs. braking saccade magnitude.	95
3-1 Saccadic onset and offset determination.	114
3-2 Open-loop model used to test the interaction between slow and fast phases.	120
3-3 Peak velocity vs. amplitude for S5’s $PP_{fs}$ waveform.	123
3-4 Peak velocity vs. amplitude for S7’s PC waveform.	126
3-5 Duration vs. amplitude for S5’s $PP_{fs}$ waveform.	129

3-6 Duration vs. amplitude for S7's PC waveform.	131
3-7 Skewness vs. duration for S5's $PP_{fs}$ waveform.	134
3-8 Skewness vs. duration for S7's PC waveform.	136
3-9 Histogram of the distribution of saccadic skewness for S9.	138
3-10 Ramp-step-ramp peak velocity vs. amplitude results for S9.	141
3-11 Model simulations of saccades made in the presence of smooth pursuit, I.	144
3-12 Model simulations of saccades made in the presence of smooth pursuit, II.	146
4-1 Block diagram of the ocular motor system model.	170
4-2 OMS details, and the smooth pursuit subsystem.	172-173
4-3 The internal monitor, and its saccade enable subsystem.	182-183
4-4 The fixation subsystem.	188
4-5 "Evolution" of pendular CN waveforms.	191-192
4-6 Voluntary saccades made during CN.	197
4-7 Pulse-step responses under normal and CN conditions.	200-202
4-8 Ramp and step-ramp responses under normal conditions.	205-206
4-9 Ramp and step-ramp responses with $P_{fs}$ .	208-209
4-10 Ramp and step-ramp responses with $PP_{fs}$ .	211-212

A-1 LMLN model—Functional block diagram.	253
A-2 LMLN model—Expanded block diagram.	255
A-3 LMLN model—Internal monitor.	261
A-4 LMLN model—Saccade enable & timing block.	263
A-5 LMLN model—Normal saccadic behavior.	267
A-6 LMLN model—Saccadic dysmetria.	269
A-7 LMLN model—Gaze-evoked nystagmus and myasthenia gravis.	271
A-8 LMLN model—Human subject with alternating fixation.	274
A-9 LMLN model—Simulation of MLN.	276
A-10 LMLN model—Simulation of LN.	278
A-11 LMLN model—Simulation of alternating fixation.	278
A-12 LMLN model—Simulation of adducting-eye fixation.	283
B-1 Overview of OMS model and internal monitor.	306-307
B-2 Saccadic enable subsystem and sub-blocks.	309-310
B-3 IM subsystems I: Target change detect, model plant+, saccadic motor command, and associated sub-blocks.	313-314
B-4 Reconstruction of position and velocity of eye and target.	316-317
B-5 Saccadic and post-drift blanking.	320
B-6 Braking/Foveating saccade logic and sub-blocks.	322-323
B-7 Fixation subsystems.	326

B-8 Neural integrator hold controller.	328
B-9 Saccadic pulse generator and sub-blocks.	330-332
B-10 Neural integrator and ocular motor neurons.	334
B-11 Resettable event timer.	336

## **ACKNOWLEDGEMENTS**

There is no way I could have done this without the help and support of a great many people. First, I owe a tremendous debt of gratitude to my research adviser, Dr. Louis F. Dell'Osso, who has taught me what it means to be a scientist and an engineer, by example. Over the past several years Lou has always been available to answer my questions and, as necessary, point me in the right direction. From the beginning he has treated me as a colleague and a friend. I hope I have lived up to this responsibility.

I am very grateful to Dr. R. John Leigh, for sharing his wealth of knowledge of ocular motor physiology. Without his exhortations to remember that behind the computer models there should be an actual brain, this work would be decidedly lacking.

I must also thank my committee members, Drs. Dave Wilson, Niels Otani and Cleve Gilmore for their many questions, comments and suggestions made during the course of my research, even the really tough ones during committee meetings. Even if it didn't really seem so at the time, I did appreciate their efforts.

Thanks also to many graduate students and ocular motility fellows I have worked with at the Ocular Motility Neurophysiology Laboratory at the Cleveland VA Medical Center, especially Ari Zivotofsky, Vallabh Das, Jeff Somers, John Stahl, and the late Lea Averbuch-Heller, whose untimely death stunned us all. I have learned much from all of

them, and, in that tradition, I thank the current students in the laboratory, Dun Shouchen, Helen Han and Arun Kumar for letting me learn how to teach as I have been taught.

Our secretary, Anne Rutledge, has been a life saver on more occasions than I can remember, and her willingness and uncanny ability to shield me from the VA bureaucracy has kept me sane.

I thank my parents for the encouragement and support they have given me all of my life. Mom and Dad, this is one of those rare occasions where I simply cannot summon the words to express how much you have meant to me.

Finally, I do not think I could have made it through these past years without your constant companionship, Peggy. You have seen me at my best and my worst, and to your everlasting credit, this did not scare you off. You have balanced my life and helped me grow more than I ever thought possible.

An Ocular Motor System Model That Simulates Congenital Nystagmus,  
Including Braking And Foveating Saccades

Abstract

by

JONATHAN BRUCE JACOBS

Congenital nystagmus (CN) is a disorder that causes the eyes to oscillate involuntarily towards and away from the attempted point of regard. Such uncontrolled movement is not conducive to good visual acuity, which decreases as either the distance from the fovea (the central portion of the retina) or the relative velocity between the fovea and the target increase. The ocular motor system (OMS) will attempt to counteract both of these potential degradations by interjecting fast eye movements into the slow-phase oscillation in the opposing direction. There are two types of these fast-phases, *foveating saccades* and *braking saccades*, each serving to improve vision by a different mechanism. The first part of this study investigated the conditions that lead to the generation of these saccades, examining the position and velocity of the eye over a range of times from 70 to 40 ms before the onset of the saccade. Next, several characteristic properties of these saccades were examined to determine how well they corresponded to normal, voluntary saccades, to demonstrate that braking and foveating saccades are also generated by the same neural

circuitry. Finally, these results were used in the design of a computer model, based on the normally-functioning OMS that could reproduce many common normal behaviors and non nystagmus-related dysfunctions, as well as simulate the pendular forms of CN, including braking and foveating saccades while maintaining these normal behaviors. The results of these simulations support the hypothesis that the OMS of a person with CN does not require any special abilities beyond those already inherent in the system and required to insure proper visual functioning during real-world conditions. Coping with the oscillations, and maintaining a normal percept of the world has simply exposed these capabilities, and offers a glimpse into the great power and complexity of the OMS.

# Chapter 1

## INTRODUCTION AND BACKGROUND

### 1.1 INTRODUCTION

#### *1.1.1 Why We Make Eye Movements*

Our eyes are constantly moving every waking minute, yet we are for the most part unaware of this motion. Most of our eye movements are purposive, enabling us to clearly see the world around us through a combination of *gaze-shifting* and *gaze-holding* maneuvers. We regularly redirect our attention from place to place with rapid eye movements called saccades, and track moving targets with slower movements (that can still be quite fast) known as smooth pursuit. Since our bodies and heads are also usually in constant motion throughout the day, signals sent from our vestibular apparatus, in the inner ear, act to oppose nearly exactly these movements (the *vestibulo-ocular reflex* or VOR), allowing us to maintain steady gaze—“fixation”—even under some of the most trying kinematic circumstances. The VOR usually acts in concert with the optokinetic reflex (OKR) which acts to move the eyes at about the same velocity as the visual environment during self-rotation. Even when held perfectly still (e.g., placed in head restraint) while fixing our gaze on a stationary target, we make very small movements,

called microtremors, that continue to move the eye about the target within an average of six minutes of arc. (It was once thought that their purpose was to prevent the image from fading, due to bleaching of photoreceptors but, given the normal motion of the head and eyes, that is unlikely).

It is interesting and important to note that not all eye movement is visually related. Even when we are asleep our eyes continue to move, especially during the dream portion of our sleep cycle. For many years, investigators believed that these movements *were* visual, suggesting that the dreamer was somehow “watching” the dream, and the rapid eye movements (REMs) that gave this level of sleep its name—REM sleep—were scans of the internally generated visual scene. It has since been shown (Winson, 1990) that this is not the case, and REMs are not visually motivated but are simply a response to the firing of neurons in the portions of the brainstem (the pons) that control, among other things, eye movement. These pontine neurons send impulses to the visual cortex and to the hippocampus (the structure considered to be the seat of memory formation), as well as to the muscles of the eyes. This neural activity aids in the processing of experience into memory and learning; the eyes move simply because, unlike the major muscles of the body, there is no reason to suppress them as eye movement does not hinder sleep.

Eye movement can also be made by blind subjects (Leigh & Zee, 1980; Leigh & Zee, 1999). These movements cannot aid vision (as in normals) and these properties reflect the loss of any sort of “calibration” due to the absence of meaningful visual input.

All this movement has implications for vision because the ability to see clearly depends on more than the refractive properties of the eye. For the highest possible visual acuity, the eye must be properly aimed at the object of interest so that the *fovea*, the central portion of the retina that contains the highest concentration of detail-sensitive photoreceptors, can be maximally stimulated. In humans, the best acuity falls within the central  $\pm 0.5^\circ$  of the eye, which is only about  $1/10,000^{\text{th}}$  the area of our full monocular visual field (Carpenter, 1988). The density of these receptors drops off quite quickly with increasing distance from the center of the fovea; as little as another half degree away from center, acuity drops by a factor of two or three (Carpenter, 1988). Clearly there is a pressing need to be able to redirect the fovea quickly and accurately, or detail-oriented vision would be very difficult, if not impossible.

As important as the *position* criterion's contribution to visual acuity is, the eye's *velocity* also plays a critical role. The eye must be properly stabilized so that there is a minimum of relative motion between the target image and the fovea, or acuity degrades. In psychophysics this is known as *dynamic visual acuity* (Sekuler & Blake, 1994) and can be measured by presenting a subject with a series of targets moving at ever-increasing speeds. The stimulus provided by an object moving past a fixed eye is equivalent to that seen when an eye moves at that same velocity past a fixed object. The disparity in either case is called *retinal slip*. Although exact values for image degradation with retinal slip may vary between studies and subjects, it is generally agreed that it becomes noticeable almost immediately, and even the low value of  $1^\circ/\text{sec}$  can be shown to have the

equivalent effect as two diopters of myopia (Burr & Ross, 1982). Clearly we need an accurate and rapidly responding ability to keep retinal slip within manageable limits.

### *1.1.2 Congenital Nystagmus (CN)*

There are some people who cannot maintain this degree of stability during fixation because their eyes are continuously moving due to a disorder of the ocular motor system called congenital nystagmus (CN). The term nystagmus comes from the Greek *νυσταγμος*, or “nodding.” In CN the eyes oscillate involuntarily, towards and away from the point of interest. (It was once believed that the eyes oscillated around the target, but with the systematic use of accurate, objective recording techniques (Dell'Osso, 1976), this misconception has been laid to rest, see Figure 1-1.) Like many forms of nystagmus, this oscillation is composed (in its simplest form) of a slow-phase movement that takes the eye off target, followed by a fast-phase movement (a *foveating saccade*) that attempts to bring it back. The temporal frequency of CN oscillations ranges from <2 to about 10 Hz, with 3-5 Hz being most typical. CN amplitude ranges from quite small, on the order of <1 degree peak-to-peak, to large movements that can exceed 30-40°, a significant fraction of the orbital range of the eye; the usual amplitudes are 2-6° peak-to-peak.

Recalling the earlier statement about equivalence of stimuli whether it is the eye or the target that is moving, one might expect that the constant uncontrollable eye movements of CN would make vision nearly impossible and that someone with CN should see the world as being in constant motion, swinging wildly to and fro.

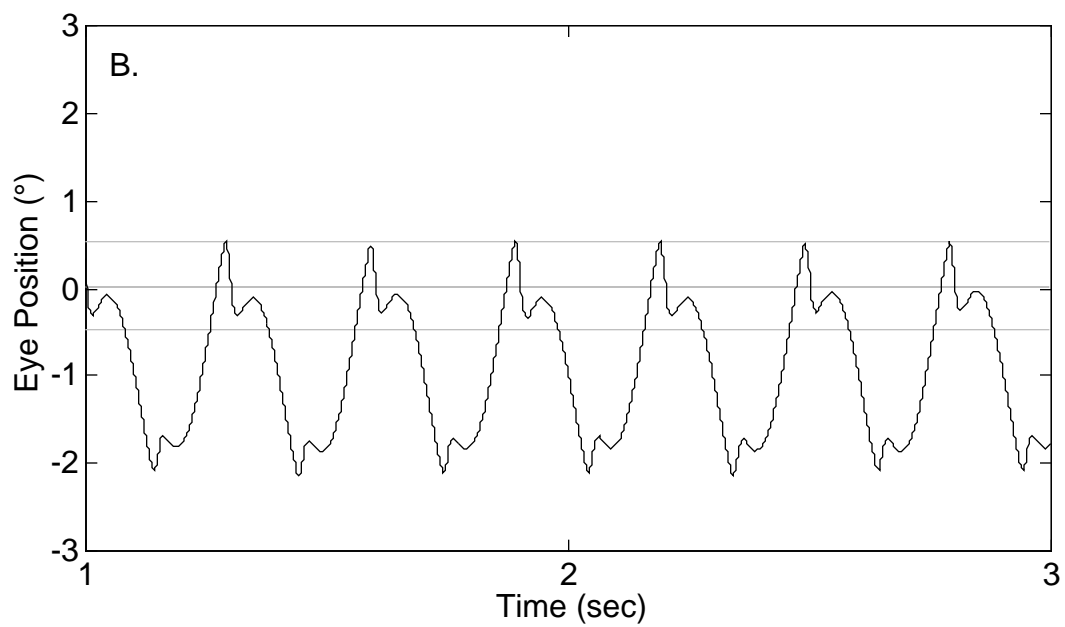
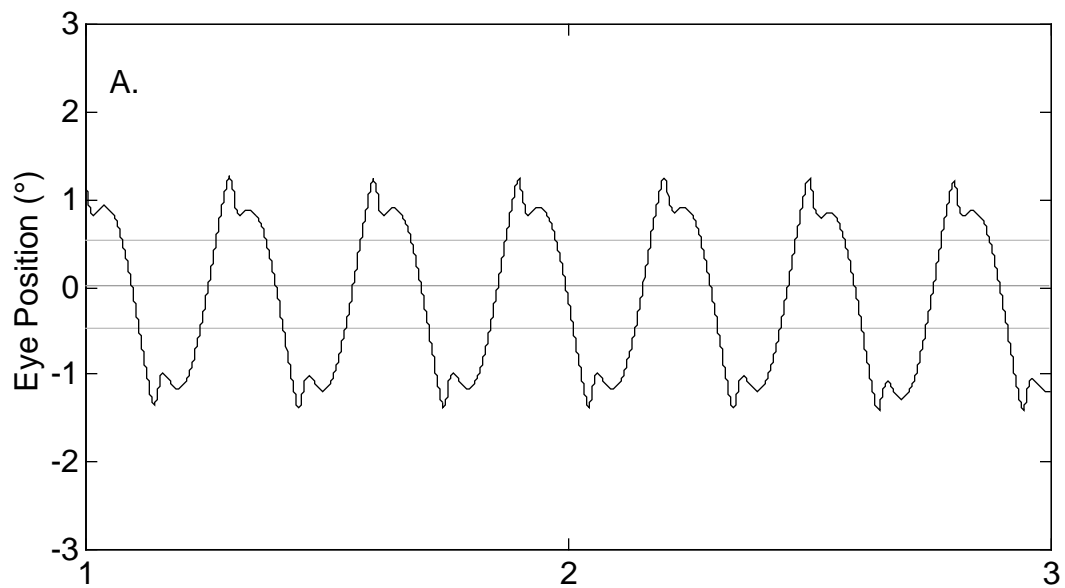


Figure 1-1

Orientation of pendular CN. The lines at  $\pm 0.5^\circ$  represent the extent of the fovea, the line at  $0^\circ$  represents the attempted point of fixation. A.) Incorrect. Before accurate recording and calibration techniques, it was assumed that CN oscillated *around* the target. In this case the fovea spends almost no time on the target, making little contribution to good visual acuity. B.) Proper representation. The bottom saccades now serve to bring the fovea onto the target, and it stays there much longer, leading to better vision.

Indeed, it is very easy to convince oneself of this by gently moving one's eye with a finger at the lateral border and noting the rather disturbing effect as the visual scene jumps back and forth with each manipulation. Fortunately this disturbance, known as *oscillopsia*, occurs only rarely in individuals with CN because, during development, the brain learns to account for the motor signals sent to the eyes, a phenomenon called *efference copy* (ECPY) (see section 1.3.5). It can, in essence, subtract the resulting extraneous visual movement from the retinal input, resulting in a correctly interpreted percept (Bedell & Currie, 1993; Dell'Osso & Leigh, 1995). In fact, this ability to compensate for internally generated oscillations is an easy and generally reliable way to differentiate congenital nystagmus from nystagmus that is acquired later in life.

CN is just one of over forty-five forms of nystagmus (Dell'Osso & Daroff, 1999) and can be distinguished from the others by several important characteristics, especially its distinctive waveforms (eye position plotted against time). The name "congenital" nystagmus is actually somewhat of a misnomer, for even though it typically appears at or shortly after birth (i.e., in the first few months of life) and very rarely manifests later in life—although in these cases it is quite likely that the oscillations have been present since infancy, albeit sub-clinically (Gresty, Bronstein, Page, & Rudge, 1991), it is only one of many forms of nystagmus that are seen in infants. It is most often confused with latent nystagmus, which arises from a failure to develop binocular vision, from which it can be distinguished by the different slow-phase characteristics, and with spasmus nutans (SN), which is far less common, and is characterized by a triad of signs: pendular oscillations

that are not phase-locked, but vary with time from in-phase to anti-phase motion; head nodding; and torticollis (Weissman, Dell'Osso, Abel, & Leigh, 1987; Dell'Osso & Daroff, 1999). By contrast, CN is typically conjugate, that is, both eyes move together, in phase, with approximately equal amplitude. Besides the phase characteristics, CN and SN can be differentiated by the fact that SN amplitude can be quite unequal in each eye (and can even be monocular), and that SN is truly a disorder of infancy, usually disappearing within the first few years of life. Such dissociated pendular nystagmus may, however, indicate a brain tumor and imaging may be necessary to rule that out. One other interesting contrast between SN and CN is found in the nodding head movements that sometimes appear. In SN, these movements can be vertical or horizontal, and can actually be *compensatory*, using the VOR to cancel the nystagmus (Gresty, Leech, Sanders, & Eggars, 1976). In CN, however, the head movements are predominantly horizontal and do not act to oppose the eye movements, but are simply the offshoot of the same central oscillatory signals that drive the eyes applied to the muscles of the neck (Gresty, Halmagyi, & Leech, 1978; Dell'Osso & Daroff, 1986).

### *1.1.3 Origin and Development of CN*

CN frequently accompanies a wide variety of afferent defects of the visual system (e.g. congenital cataracts). However there are many instances when this is not true, and the CN arises in isolation; in these cases the nystagmus is said to be of idiopathic origin. It is most probably due to a fundamental instability of the ocular motor system; cases

associated with afferent defects probably also have this instability at their core, although here it may not be as pronounced, therefore requiring the afferent deficit to exacerbate the instability.

Some families have a genetic predisposition to CN (Forssman, 1971; Dell'Osso, Flynn, & Daroff, 1974; Hayasaka, 1986); the mode of transmission may be X-linked and passed down from unaffected mother to affected son. There are also instances of autosomal dominant forms (Kerrison, Koenekoop, Arnould, D., & Maumenee, 1998; Oetting, Armstrong, Holleschau, DeWan, & Summers, 2000).

When CN first appears in infants, it has been reported to start as a large, triangular waveform of up to  $\pm 20^\circ$  and 1 to 2 Hz (Reinecke, 1995). Even at this early stage, the infant's developing visual and ocular motor systems are beginning to work in concert as evidenced by the appearance of foveation periods at either the left or right extreme of the waveform. These foveation periods can aid in the diagnosis of the infant's visual status (Hertle, Dell'Osso, & Movaghar, 1995). As the infant ages, the waveform begins to resemble those seen in adult CN, becoming pendular or jerk, with all the hallmarks associated with CN, including good fixation and pursuit abilities and a null point.

More recent studies, however, using more reliable techniques (infrared reflection (IR) and magnetic search coil instead of electrooculography (EOG)—see “Recording Techniques” section below) have failed to corroborate the presence of triangular waves (Hertle & Dell'Osso, 1999), and have instead found infant CN waveforms to be essentially of the type seen in adults. While the authors of the more recent study suggest

the possibility that the lessened linear range of their recording technique could mask the triangular waveform, it is also possible that the older EOG method may be *losing* detail that “rides” on the slowly varying baseline, yielding only the triangular waveform. There is evidence that the underlying triangular wave may be a *extended slow phase* (ESP) as recorded in infants (Goldstein, 1995). Goldstein found that this oscillation falls in the same range of frequency (under 2 Hz) and magnitude (5–25°) as the triangular waveform. This ESP is evoked when the subject’s attention is directed away from visual tasks.

CN oscillations are most often in the horizontal plane, although they occasionally appear vertically; recent evidence suggests that there is also usually a torsional component (Dell’Osso & Daroff, 1999). A possible reason for the rarity of vertical CN is the inherent difference in stability between the horizontal and vertical pursuit subsystems. Because we live in a predominantly “flat” world, i.e., one where the vast majority of our required daily eye movements are horizontal, it has been hypothesized that evolution has preferentially enhanced our ability to accurately track horizontal movements (Collewijn & Tamminga, 1984). From the study of control systems engineering, it has been shown that, in the tradeoff between speed and accuracy, optimization of the former usually results in a system that “rings,” or oscillates slightly when stimulated; the gain is just on the border of instability. In normal human horizontal pursuit, this is in fact the case, and the onset of pursuit is accompanied by a rapidly decaying series of velocity oscillations, shown in Figure 1-2, between 3 and 4 Hz (Robinson, Gordon, & Gordon, 1986), which happens to be the most typical frequency range of CN.

From Robinson et al., 1986

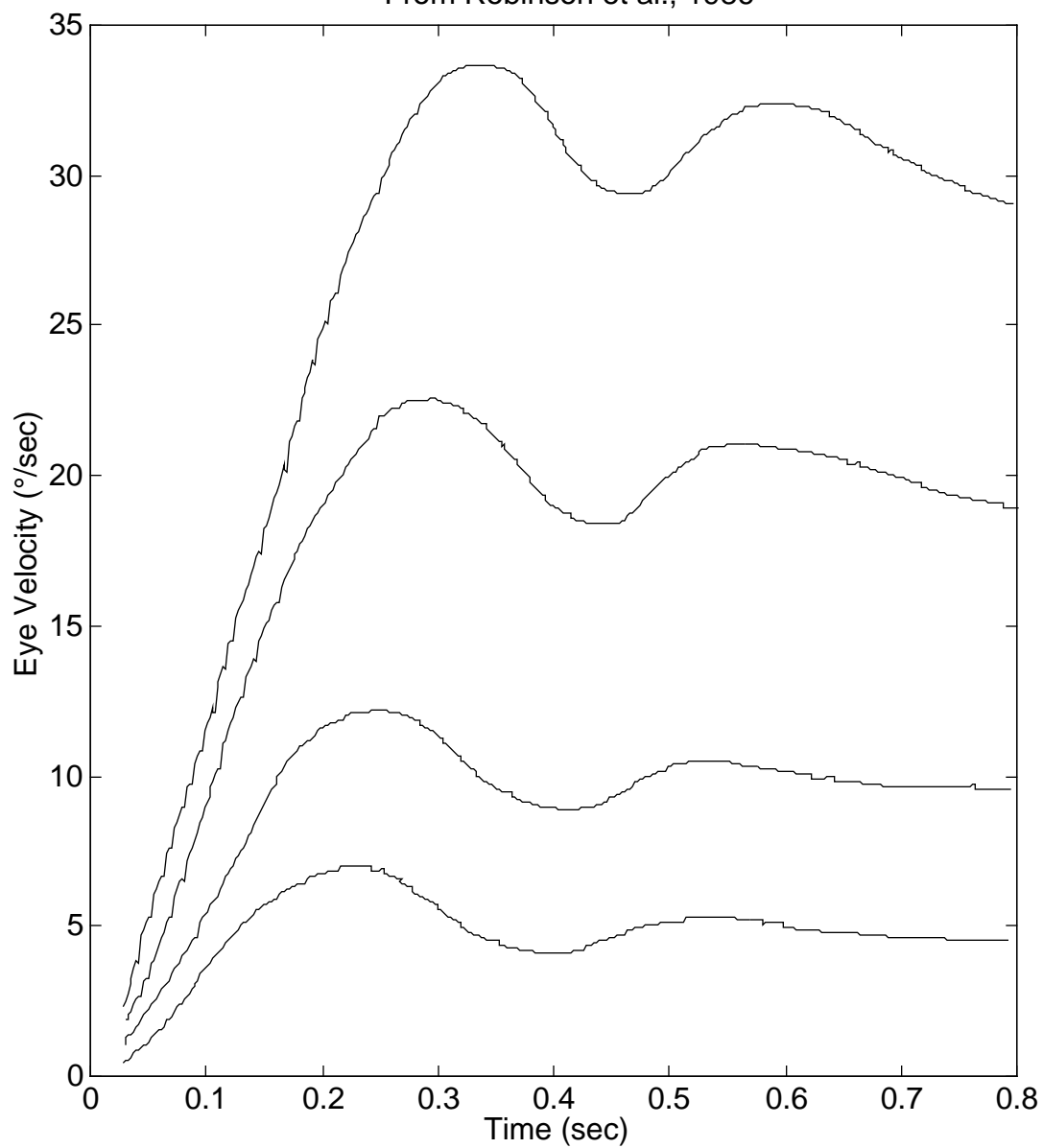


Figure 1-2

Ringing in velocity accompanying the onset of smooth pursuit in a normal subject. The ringing decays exponentially within a few cycles as the subject matches the target velocity. As pursuit velocity increases, so does the magnitude of the oscillation, although the frequency remains constant. (Adapted from Robinson et al., 1986.)

It is also important to note that since no oscillopsia is perceived by normals even during these oscillations, and since nature tends to be conservative, the same basic mechanism is probably responsible for the stable-world percept among people with CN—they need no newly developed function. However it should also be noted some subjects can have a more immediate initiation (i.e. a greater initial acceleration) for their vertical pursuit onset than for their horizontal pursuit (Rottach, Zivotofsky, Das, Averbuch-Heller, DiScenna, Poonyathalang, & Leigh, 1996). This supports separate subsystems for horizontal and vertical pursuit, and therefore there may be additional factors that act to stabilize vertical pursuit.

#### *1.1.4 Classification and Characteristics of CN*

In general, CN waveforms are classified as either *jerk* or *pendular*, based on the shape of the slow-phase oscillation. Because people with CN often (but not invariably) have visual system problems, for many years there was the mistaken belief that jerk and pendular CN had different causes, with pendular being associated with visual deficits and therefore often referred to as “sensory” congenital nystagmus, and jerk being due to motor system defects and subsequently called “motor” congenital nystagmus. This is not a realistic set of classifications, for many individuals with CN, with and without afferent defects, have both jerk and pendular waveforms. In fact, the motor system instability mentioned above can be considered as a necessary precondition for CN, and reduced vision can act as a trigger, either because it reduces the available information necessary

for the calibration of the developing ocular motor system, or because of the well-known relationship between visual effort and CN, where greater attempts to see increase the magnitude of the CN (Dell'Osso & Daroff, 1999; Leigh & Zee, 1999).

Conversely, CN diminishes when the subject is not actively engaged in a visual task, such as when daydreaming or sleeping. An example is shown in Figure 1-3. This must be separated however, from simply placing him in the dark; visual effort is not the same as actually *seeing*; it is quite possible for CN to persist under this condition—all that is necessary is for the subject to concentrate on a target, even if it is only imaginary (Dell'Osso & Daroff, 1999). Although the old pendular = sensory and jerk = motor hypothesis is incorrect, there is growing evidence that the pendular and jerk forms of CN may, in fact, be due to instabilities in different portions of the ocular motor system.

Examples of jerk and pendular waveforms are shown in Figures 1-4A and B. Jerk waveforms consist of accelerating (exponentially *increasing*) slow phases (although in cases of low magnitude this component can appear to be linear) followed by foveating saccades. Pendular waveforms, as the name suggests, have underlying sinusoidal slow phases. It is these slow phase characteristics that serve as an important and powerful way to distinguish CN from many of the other forms of nystagmus. For example, a form of vestibular nystagmus, caused by a tonic imbalance in the tonic activity levels in the vestibular nuclei (Leigh & Zee, 1999) has a linear slow phase, while in latent/manifest latent nystagmus (LMLN—which is often mistaken for CN) the slow phases are either linear or of *decreasing* exponential form, as shown in Figure 1-4C.

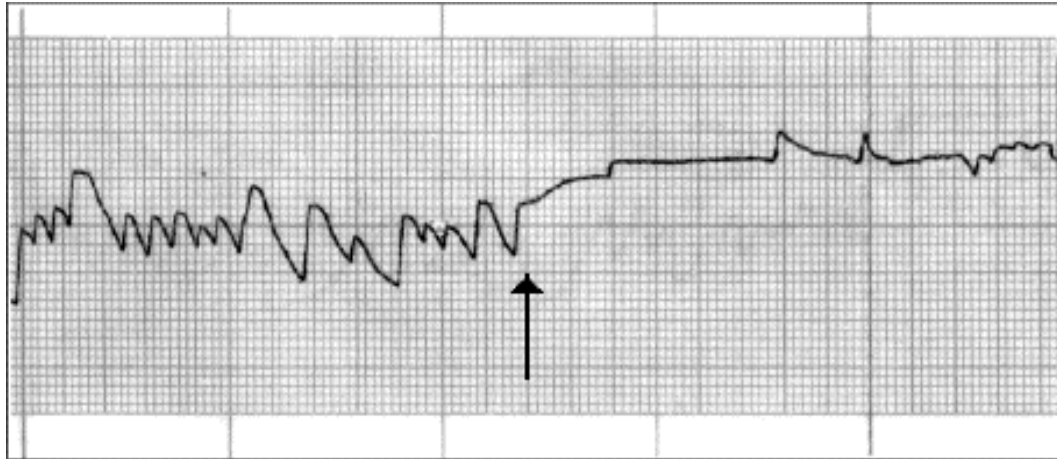
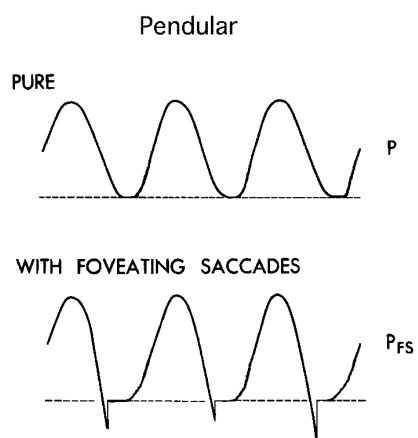


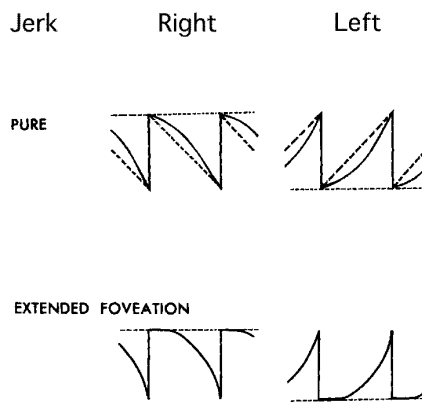
Figure 1-3

Loss of attention during recording from a subject with CN. The amplitude diminishes to almost zero as the subject loses interest in the visual task. Another sign that the subject has stopped attending to the target is that the eye has drifted away from the fixation point. The waveform is jerk right with extended foveation.

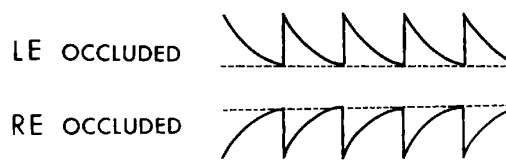
A.



B.



C.



D.

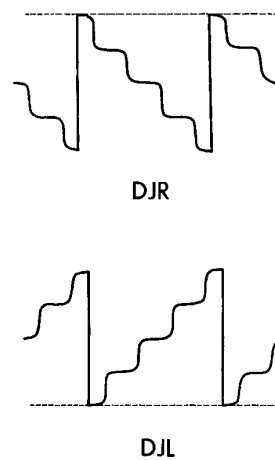


Figure 1-4

Schematized examples of different nystagmus waveforms. A.) Pure pendular is quite rare, while pendular with foveating saccades is much more common because the extended foveation leads to better vision. B.) Unidirectional jerk. Note that the slow phase starts off slowly and then accelerates away from the fixation point. Once again, extended foveation leads to better vision. C.) Latent/manifest latent nystagmus. While looking very similar to jerk CN, this is a very different condition. Note that here the saccades take the eye *away* from the target, whereas in CN, they take the eye *to* the target. D.) Dual jerk waveforms. Careful inspection reveals that the waveform is composed of a sinusoidal oscillation that rides atop a jerk waveform. This suggests that there is probably more than one source of instability for the different forms of CN. (Adapted from Dell'Osso, 1999.)

There are also CN waveforms containing two oscillatory components. The second oscillation is typically pendular, of much smaller magnitude and usually of a higher frequency (typically around 10 Hz) than the primary, suggesting a distinct origin than the primary instability. In the resultant waveform, the fast oscillation appears to ride upon the slower one, giving rise to a waveform called “dual jerk,” the “dual” referring to the two underlying oscillations, *not* two jerk elements. Figure 1-4D shows dual-jerk nystagmus.

#### *1.1.5 Treatments for CN*

Most subjects' CN waveforms are *not* uniform across all gaze angles. Instead, the amplitude, frequency (to a lesser extent), and type of oscillation can vary greatly as the subject fixes at targets of varying eccentricity; this is important information that should be carefully recorded when attempting to classify their nystagmus. In many cases, there is a *gaze-angle null* where the amplitude of the nystagmus is significantly reduced (the frequency is usually fairly constant), as shown in Figure 1-5. This null can occur at any point in the orbit, and can often be appreciated clinically by observing the patient and noting a preferred head turn to the opposite direction that places the eye in the favored position when attempting to direct gaze straight ahead. A common surgical treatment for CN, the Anderson-Kestenbaum (A-K) operation, exploits the gaze-angle null by detaching the lateral and medial recti muscles from the globe, recessing and resecting them so that the eyes, when at rest will be in a position equal and opposite to the null.

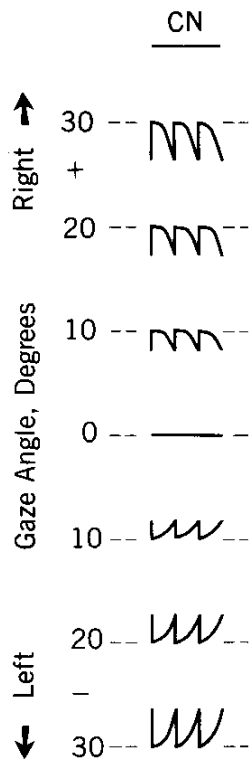
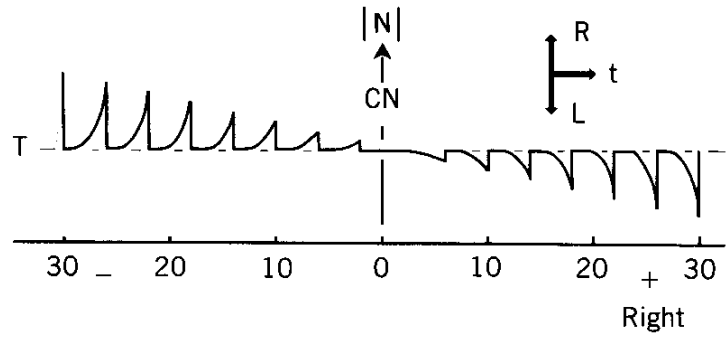


Figure 1-5

Drawing of how CN amplitude and direction can vary with gaze angle. The amplitude of the oscillation is minimal when the eye is directed straight ahead. As gaze is directed further to either side, the amplitude increases. Note that as gaze is directed left of the null, the nystagmus is left beating, and right of the null, it is right beating. (This is a hypothetical example—not everyone with CN has a null, and in those who do, the null can occur at any gaze angle.) (Adapted from Dell’Osso, 1979.)

The patient will then need to provide the same amount of innervation to place the eyes straight ahead into primary position as they had used previously to put them into the null position.

In addition, some patients may have a *convergence null*; that is, their CN damps when they force their eyes to converge, as when viewing a target that moves from far to near (to within a few inches of the eyes). This works only when the patient has good alignment of their eyes, and is capable of using them in concert to properly perceive *stereoscopic*, or three-dimensional, images. It should be noted that a significant fraction (~30%) (Dell'Osso, 1994) of people with CN also have *strabismus*, a congenital misalignment of the eyes that, if not treated surgically within the first years of life, will prevent the development of the structures in the visual cortex necessary to correctly interpret the slight visual disparities coming from each retina that form the basis of stereoscopic vision. (It is also important to mention that strabismus is a necessary (but not sufficient) condition for the development of LMLN, and that the number of people with CN and strabismus is probably greater than the number of people with LMLN, often leading to the improper diagnosis of the latter condition instead of CN.) In cases of CN without strabismus, there are also therapeutic alternatives that can exploit the null. First, there is a non-invasive approach, using base-out prisms (in conjunction with a  $-1.00$  diopter spherical correction added to the patient's normal correction to counter the convergence-associated lens accommodation that occurs as part of the near triad) to move images medially, forcing the eyes to converge to avoid double vision, or *diplopia*. This

therapy can be an end in itself, or can be a test for the suitability of another surgery, the “artificial divergence” or *bimedial recession* (BMR) where the medial recti muscles are detached from their original insertions and reattached in a more posterior location on the globe. The result of this is that the patient must now make a convergence effort to hold the eyes in primary position, or they will point laterally. Both of these techniques will only work, however, with someone who has sufficient stereoscopic capabilities; otherwise only the fixating eye will be affected and the unused eye will simply “go along for the ride.”

When both a gaze-angle null and a convergence null are present, it is the convergence null that usually has the greater damping effect on the nystagmus. If there is no convergence null, and the gaze-angle null is in primary position, or is very close to it, traditionally it was believed that there was no surgical procedure that could help, as the effect of the A-K procedure was believed to come solely from the rotation of the globe to move the null to primary position. Therefore, it was reasoned, if there was no complementary angle to which the eye could be rotated, there was no benefit to be gained. However, a study of the outcomes of A-K surgeries (Dell'Osso & Flynn, 1979; Flynn & Dell'Osso, 1979) showed a decrease in nystagmus intensity (Amplitude \* Frequency) at all angles, an effect beyond the simple predicted shifting of the intensity vs. gaze angle curve. Specifically, the intensity at primary position was now lower than that of the original null. Furthermore, the range of gaze angles with damped CN was *broadened* by the surgery. For almost twenty years this information sat unexplored by

surgeons, even though it clearly suggested that there was an effect more important than the actual rotation of the globe. Further investigation led to the development of a surgery (Dell'Osso, 1997; Hertle, Dell'Osso, Williams, & Jacobs, 1998; Dell'Osso, Hertle, Williams, & Jacobs, 1999) that demonstrated the efficacy of a simplified approach where the muscles were tenotomized, i.e., separated from their original insertion, and then reattached with neither resection nor recession. It was hypothesized the major effect (the global reduction of intensity) was due to the interruption of a dynamic feedback system involving the muscle plant and their proprioceptive organs (Dell'Osso et al., 1999) that may act as a local “tensioning loop,” that adjusts the stiffness of the muscle response. (This study raises many interesting questions, especially about the magnitude range of eye movements affected by tenotomy—for example whether the characteristics of saccades changed by the hypothesized de-tensioning of the plant. This suggests pre- and post-surgical analysis of saccades. If this hypothesis is true, then the effect should be seen in any patient that has received any four-muscle surgery, and quite possibly may apply to two-muscle surgeries as well.)

#### *1.1.6 Misunderstandings about CN*

Several important misconceptions about CN can be traced to a lack of appreciation of the properties of the gaze angle null and of basic control theory. The *gain* of a system is defined as its output divided by its input. Although true, that is not the complete definition; there is a *critical qualification* that must be observed to properly

calculate gain. The more comprehensive definition is: gain is the output of the system divided by its input *and can be measured only at those times when the output is a direct consequence of the input*. When calculating smooth pursuit subsystem gain in the absence of CN, other type of slow-phase oscillation, or induced motion (VOR or OKR), this distinction can usually be ignored with impunity, because the velocity of the eye will be affected only by the velocity of the target being tracked. However when CN or any type of nystagmus is present, it adds another slow-phase signal that moves the eye without regard to the target stimulus. Therefore it is possible, when comparing output to input, to mistakenly use the simple ratio of eye-velocity to target-velocity as a measure of gain at all times. Since the eye is only actually pursuing during periods of foveation in CN, and is moving independently at all other times, such an oversimplified approach is fated to yield abnormal pursuit gains, and can lead to the mistaken belief that patients with CN have insufficient smooth pursuit ability (Optican, Zee, Chu, & Cogan, 1983). When faced with the seeming need to make such dramatic pronouncements about possible severe deficits a patient may face, it is of vital importance to first insure that they agree with real-world observation. Unless a CN patient has other, more serious visual system problems, such as afferent defects or very limited stereopsis, they are usually quite capable of performing well at tasks that require tracking ability, such as sports. In fact, many have normal pursuit gain, as measured during their foveation periods (Dell'Osso, Gauthier, Liberman, & Stark, 1972; Dell'Osso, 1986; Kurzan & Büttner, 1989; Dell'Osso, Van der Steen, Steinman, & Collewijn, 1992b).

A pair of related phenomena, “reversed pursuit” (Optican & Zee, 1984) and “reversed optokinetic nystagmus” (OKN) (Yamazaki, 1979; Yee, Baloh, & Honrubia, 1981) also fall by the wayside when subjected to such analysis. However, the story in these cases is a bit more complex, for to understand them required the discovery that the gaze angle null is not *static*, but is *dynamic*, and during pursuit it moves in the opposite direction, proportional to the pursuit effort (Dell’Osso et al., 1972; Halmagyi, Gresty, & Leech, 1980; Dell’Osso, Van der Steen, Steinman, & Collewijn, 1992a; Dell’Osso et al., 1992b; Dell’Osso, Van der Steen, Steinman, & Collewijn, 1992c). When combined with the knowledge that jerk CN waveforms beat away from the null point, i.e., in the direction of the pursuit, this means that the slow-phase component will be directed opposite to pursuit. This yields an analogous result as the above discussion of gain: only the foveation periods reflect true smooth pursuit effort and can be used to calculate true gains; the rest of the waveform—the oscillation of the SP subsystem—was not a response to the target’s motion.

### *1.1.7 Braking and Foveating Saccades*

The complex waveforms of CN are a result of the insertion of braking and foveating saccades into the underlying slow-phase oscillation. Depending on the waveform, either or both of these fast phases can occur. The simplest waveforms, jerk (J) and jerk with extended foveation ( $J_{ef}$ ) have only foveating saccades, while the most complex-appearing waveform, pseudopendular with foveating saccades ( $PP_{fs}$ ) has both. It

is possible to have only braking saccades such as seen in pseudocycloid (PC), pseudopendular (PP), and triangular (T) although the latter two are only transitional waveforms and not seen for more than a few cycles at a time.

Foveating saccades, as mentioned above, appear in CN waveforms and serve to bring the target image onto the fovea, using positional error information and a knowledge of the eye's velocity to calculate, program and execute an appropriately sized saccade. While at first this may seem like an improbable ability for a person with CN to have, it is actually just one more example of the complex interplay between the fast and slow eye movement subsystems that we have learned to take for granted in normals. It is a foundation of the foveate ocular motor system, and allows us to make accurate saccades to moving targets, and to make corrective saccades while engaged in pursuit. This is such a fundamental ability that we would be lost without it, but it also serves to confound study of the smooth pursuit subsystem alone. It requires the design of carefully calculated "Rashbass" stimuli (composed of a step to one direction followed by a ramp in the other) to isolate it from the saccadic subsystem by removing the need to make a saccade. The ocular motor system, when presented with this stimulus, calculates that *no* saccade will be needed for the eye to land on target during the beginning of pursuit. Since people with CN generally have good pursuit abilities, the presence of the CN has not interfered with this ability, but seems instead to have adopted it for making accurate saccades in the presence of an incessant pursuit-like signal.

Braking saccades were first described twenty-five years ago (Dell'Osso & Daroff, 1976). Their main function is to oppose the runaway slow-phase portion of the CN waveform. They tend to be stereotyped and their magnitude is generally quite small, usually less than a degree or so. Unlike foveating saccades, braking saccades at first appear to serve no obvious visual function, for they do not typically lead to foveation (although it is possible in some small-amplitude CN waveforms to get a secondary foveation period following the braking saccade; however it tends to be shorter than the primary, and is not as stable, showing a greater variance in position, so that its contribution to visual acuity is not as great). Because of this, it was initially difficult to see what, if any, benefit they offered.

The benefit of braking saccades is indirect and lies in their effect on the waveform. By acting in opposition to the runaway, the braking saccade reduces the distance the eye travels from the target and therefore reduces the amount of time until the ocular motor system can refoveate the target, allowing more foveation time each second. Paradoxically, this can have the effect of slightly increasing the frequency of the nystagmus, which at first might sound inconsistent with improved vision, but the point to remember about acuity in nystagmus is that *foveation time* is by far the most important criterion—not amplitude, not frequency.

The first study that will be presented in this dissertation examines the criteria and mechanisms responsible for the *generation* of braking saccades: what are the conditions that must be met to cause the ocular motor system to program and execute a braking

saccade. At first glance, this might seem like a trivial question; after all, since the saccadic subsystem is driven by positional error, shouldn't that be the impetus to make a braking saccade? Remember also, however, that braking saccades are *non-visual*, and therefore we need to examine the role of velocity error as well. This is crucial, for they occur in the dark (much like the fast phases of vestibular nystagmus), where obviously there can be no visual feedback information, and therefore no positional error signal acting as to drive the saccadic subsystem.

In the second study, the *characteristics* of braking (and foveating) saccades will be examined. In particular we will look at the *peak velocity* and *duration* of these saccades, as they relate to the saccades' *magnitudes*. These properties have been referred to as the *main sequence* for saccades for reasons that are historical (and not exactly appropriate). In general these relationships are quite good, although there are a few caveats that must be kept in mind when relying upon them. First and foremost, these relationships are an attempt to quantify the behavior of a biological system, and therefore should not be expected to yield invariant results, but rather should reflect the inherent variability that is the hallmark of such systems (Boghen, Troost, Daroff, Dell'Osso, & Birkett, 1974). In particular, these results can vary from subject to subject, or even within a single subject depending on any of a host of conditions including level of attention, time of day, age, medications (prescribed or otherwise) and health.

Not all saccades that fail to satisfy these relationships are necessarily pathological, however. As will be shown in this study, braking saccades and foveating saccades *can*

fall outside of the normal saccadic velocity- and duration-amplitude relationships, yet as will be shown, they are *not* abnormal. This is analogous to the effects seen during the summation of slow- and fast-phase eye movements in VOR (Jürgens, Becker, Reiger, & Widderich, 1981; Winters, Nam, & Stark, 1984).

Finally, in the third study, we will consider a model of the ocular motor system that simulates not only normal and common pathological behaviors, but also the most complex-appearing CN waveforms, the pendular family with combinations of braking and foveating saccades. The model generates and executes these saccades according to the criteria and relationships determined in the previous two studies.

## **1.2 TECHNIQUES FOR MEASURING EYE MOVEMENT**

### *1.2.1 History of Eye Movement Recording*

As has already been stressed several times over the preceding pages, it is impossible to study nystagmus properly without the use of accurate recording techniques. Even though nystagmus has been described clinically since at least the mid-nineteenth century (Duke-Elder & Wybar, 1949) (and has probably been noted since the beginnings of human civilization), any systematic and quantifiable study of the subject had to wait until the twentieth century and the advent of precision sensors and electronics. This does not dismiss many ingenious approaches to the problem attempted earlier, based on mechanical, optical and cinematographic techniques. Indeed, the roots of modern practice

can often be traced directly back to these attempts. One of the more notable of these early efforts was by Ohm (1928) who used a rod resting on the upper eyelid to measure corneal displacement; also of interest were Orchansky's use of a small mirror attached to a contact lens to reflect light for photographic recording (1898), and de la Barre who recorded eye movements transduced by a plaster contact lens to a smoked drum (1898). (A true use of smoke and mirrors?) Perhaps the strangest of all was Hering's use (1879) of a miniature stethoscope to actually distinguish the difference between background noise due to drifts and tremors and the clicks of microsaccades! While each of these techniques had mixed levels of success, they were all limited in both spatial and temporal resolution, seldom providing accuracy of much better than  $1^\circ$ , or 10 ms.

The most common modern recording techniques commonly used are electrooculography, infrared reflection, magnetic search coil, and video oculography.

### *1.2.2 Electrooculography*

Electrooculography (EOG), which measures the dipole potential of the eye, requires some strong precautions to be useful for accurate recording of eye movements. EOG uses silver-silver chloride (Ag-AgCl) electrodes placed on the skin to either side of the eye to measure the potential difference between the electrically neutral cornea and the electronegative retina. There are potential problems with this approach. Chief among them is noise, both internal biological noise, as well as external noise. Because the electrodes are of the same type that are used to measure other biological signals such as

electrocardiogram, electroencephalogram, or especially, electromyogram, they are also able to pick up the potentials generated by the muscles surrounding the orbit of the eye and the large facial muscles. Therefore, if the subject moves more than minimally, the resulting muscle noise can easily swamp the eye-movement signal being measured. The leads connecting the electrodes are also a source of noise, acting like antennas to pick up the 60 Hz signals that permeate the space in and around any modern building. The chemical interface between the electrodes and skin is also a source of difficulty, for the properties of this interface can change drastically with temperature and with changes in the skin as the subject sweats. These can cause changes in voltage, leading to large drifts in apparent eye position. The main benefits of EOG are its ability to measure horizontal and vertical movement simultaneously (although lid movement confounds the latter), and its extreme ease of use, although that is becoming less of a consideration as other non-invasive techniques, such as IR and video, have become more user-friendly. Figure 1-6A shows a subject prepared for simultaneous horizontal and vertical EOG recording. Note that 9 electrodes are needed: 2 per eye per direction for a total of 8, plus a reference voltage electrode.

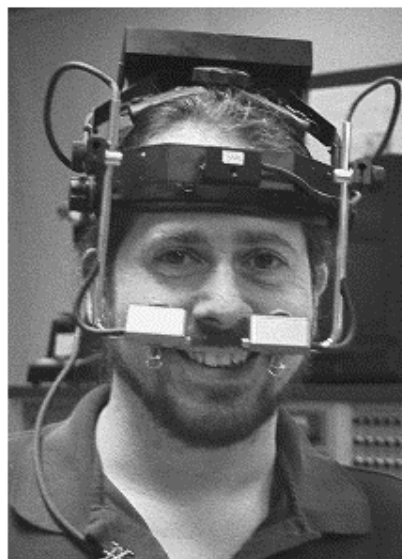
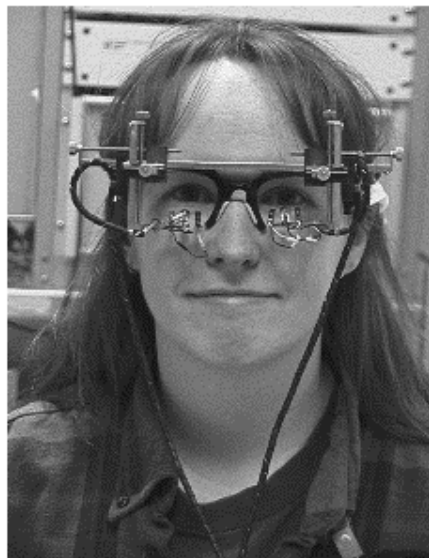


Figure 1-6

The most common eye movement measurement techniques. A.) EOG, requiring 9 electrodes to measure horizontal and vertical, binocularly. B.) A head-mounted IR reflection system. The diodes are positioned just below, and facing up at the eyes. C.) A head-mounted high-speed video system. One camera is aimed at each eye, and there is a lower-speed camera mounted on the headband to measure head movement. D.) Scleral search coil. Note the wire embedded in the silicone just around the iris, and exiting at the inner corner of the eye.

### 1.2.3 Infrared Reflection

Infrared reflection (IR) is one of the earliest of the modern methods to record in the horizontal or vertical planes. In general IR systems record only one plane at a time, but some IR systems can record movement in both planes simultaneously (Carpenter, 1988), but care must be taken to insure that the level of crosstalk between planes (i.e., movement in one plane that appears as movement in the other) is minimized. IR's chief advantage is its simplicity, requiring only rudimentary equipment to get started. IR also has the advantage of being relatively inexpensive, reliable and accurate to within a tenth of a degree, and linear over approximately  $\pm 20^\circ$ . Also, IR is a *noninvasive* technique, so there is no need for direct contact between the patient and the equipment, providing an extra level of safety and comfort. Instead, the subject's eye is illuminated with low-level infrared light, imperceptible to them, and the resulting reflection is measured by photo diodes aimed at the left and right borders between the iris and sclera (the white portion of the globe). These signals are filtered and passed to a differential amplifier that compares the signal return seen in each sensor. If they are equal, the eye is pointing straight ahead; if there is more return to one sensor it is because there is more infrared being reflected from the sclera and therefore the eye is pointing in the other direction.

For the best results, the sensors should be head-mounted, typically on a pair of eyeglass frames, to reduce the possibility of artifactual noise due to relative motion between the head and the sensors. The patient's head should be restrained, so that targets straight ahead are viewed with the eyes in primary position, unless the experimenter also

uses a head-based sensor that can accurately measure head position. It is also necessary to explicitly adjust the eye position sensors for each eye, by having the subject look at targets at known angles, to calibrate the system for the subject. This can be quite difficult for subjects who have gaze palsies or poorly controlled nystagmus, and is a potential shortcoming for all methods that calibrate the subject rather than the equipment itself. A major disadvantage of IR is its susceptibility to “light pollution,” requiring measurements to be made under conditions of dim illumination or DC-powered lighting. Some IR systems can only measure one direction (i.e., horizontal or vertical) at a time, rather than simultaneously. If the subject requires visual correction, only contact lenses will not interfere with the recording apparatus. Furthermore, the eyelids will interfere with recording whenever the subject blinks. A subject wearing head-mounted IR sensors is shown in Figure 1-6B.

#### *1.2.4 Videography*

Only recently, with the explosion of cheap computing power and inexpensive high-speed video cameras, have video recording techniques become suitable for scientific study of eye movements. Previously these systems were limited by poor temporal sampling rates of 60 to 120 Hz, fast enough for psychophysical and VOR studies, and for investigations of slow-phase characteristics, but were of limited usefulness for any sort of fast-phase studies, such as saccadic dynamics. Current high-end systems can now sample at rates up to 250 Hz, and some can measure eye movements in all three planes

simultaneously, as well as head movements, making them much more attractive and placing them in the middle ground between IR and SC. In these systems, a compact high-speed video camera is aimed at each eye, centering the entire eye in its field. At each sample time, the size and centroid of the pupil is calculated and geometric transforms performed to calculate the precise angle of the eye. Also, some systems use corneal reflection (the first Purkinje image) as a supplemental visual technique. The use of this additional information greatly reduces the sensitivity to artifacts due to movement of the camera with respect to the head, for the distance between the two reflections is affected only by eye rotation. A subject wearing head-mounted cameras from a 250 Hz video system is shown in Figure 1-6C.

#### *1.2.5 Magnetic Search Coil*

Magnetic search coil (Robinson, 1963) is often considered the Cadillac of eye movement recording techniques because of its ability to simultaneously record horizontal, vertical and torsional movements, as well as vertical and horizontal head position. This is accomplished by the use of time-varying magnetic fields of harmonically unrelated frequencies placed at right angles to each other (horizontal and vertical). A circular coil of wire embedded in a silicone annulus that surrounds the cornea is placed in the subject's eye. Unlike the previous three methods where the equipment must be calibrated for each subject, the search coil is itself calibrated with the magnetic field before being placed in the subject's eye, making this method invaluable for recording

more difficult cases. However, the exact zero position must be based on the subject's fixation data. As the eye moves, carrying the coil, an electrical signal representing horizontal and vertical movement is generated in the wire courtesy of the principles of electrostatics. To measure torsional movements, an additional wire must be added to the annulus, wound in a figure-of-eight pattern. To measure head movements, another coil is simply attached to the forehead. This signal can then be subtracted from the eye signals to calculate the eye-in-head position.

Although the search-coil method is highly regarded for its precision, resolution, linearity and completeness, it is very expensive and complex to set up, requiring very precise electronic instrumentation to sense and amplify the small electrical signals generated in the coils. Furthermore, this method is invasive, requiring great care placing the coil in the eye, which must be anesthetized. As a consequence, many investigators limit coil recording sessions to not much longer than thirty minutes (although others frequently will exceed an hour). Among the reasons for this are discomfort for the subject and the possibility of increased intraocular pressure. As with any foreign object in the eye, there is a risk (albeit small) of scratching the cornea. These reasons make this technique generally unsuitable for measuring the eye movements of infants and small children. An eye with coil is shown in Figure 1-6D.

### 1.3 MODELING

When we attempt to model a physical system, we must make a series of tradeoffs to balance the complexity of the resulting model against the level of behavior we wish to simulate. Any system interesting enough to study is almost invariably so complex that we must decide ahead of time what aspects of it we can afford to ignore, as well as the behaviors we must be able to replicate. There is danger inherent in this approach however, for the temptation exists to simplify our model beyond what is realistic and necessary. As Albert Einstein said, “Everything should be made as simple as possible, but not simpler.” This has proven especially true with some models of CN that serve only to replicate some particular waveform by removing the model’s ability to generate anything but CN. While occasionally useful as a didactic device, this approach misses the basic presumption that the ocular motor system in CN is not fundamentally different from that of a normal person, which is one of the fundamental hypotheses of the model presented later in this dissertation.

So what should a good model of CN do? Obviously we will need to model several of the most important clinical aspects of CN, listed earlier in this section, but more importantly, we must first be able to demonstrate the ability to simulate the most important aspects of a *normal* ocular motor system, in keeping with the principal hypothesis mentioned just above. It should also be biologically plausible, based on what is known about actual organization and function whenever possible. Therefore, the

organization of the ocular motor system determines the design of the model. Figure 4-1 in Chapter 4 presents an overview of the OMS and the model. The model should also make predictions that can be tested experimentally.

### 1.3.1 Fast Eye Movement (FEM) Subsystem

The FEM portion of model must be able to reproduce basic saccadic behavior, such as the ability to make realistic saccades over the range of the ocular motor system. “Realism” does not necessarily mean “accuracy,” for in reality most people do not make perfectly orthometric saccades at all magnitudes, but actually make slightly hypermetric saccades below  $5^\circ$  and hypometric saccades around  $17^\circ$  and up. These over- or undersized saccades are then followed, with short latency (approximately 125 ms), by a small *corrective saccade* that brings the fovea onto the target. Note that this is a shorter latency than a saccade made using visual feedback, which requires around 200 ms for the information to make its way from the retina, passing through cortical processing and finally through the saccadic subsystem and to the extra ocular muscles. Obviously there is some other pathway in effect here, allowing for much more rapid reaction to improperly directed saccades. This will be discussed in greater detail shortly.

The signal that drives the eye, modeled as a two-pole plant, is composed of a large, brief *pulse* needed to overcome the viscosity of the orbital tissue that acts to quickly move the eye towards its desired position. This is followed by a *step* to oppose

the elastic restoring forces trying to return the globe to central orbital position, that maintains the position, as illustrated in Figure 1-7A.

For horizontal saccades, the pulse is created by excitatory burst neurons in the paramedian pontine reticular formation (PPRF) that are normally inhibited by the omnipause neurons of the nucleus raphe interpositus that must relax their inhibition for a saccade to be generated. Stimulating the omnipause neurons can arrest saccades in mid-flight (Keller & Edelman, 1994). (The pulse for vertical and torsional saccades comes from cells in the rostral interstitial nucleus of the medial longitudinal fasciculus (riMLF).) The step is created from the pulse by integration in the neural integrator (NI), a structure that is a collection of interconnected cell groups in the brainstem—the nucleus prepositus hypoglossi and the medial vestibular nucleus—responsible for gaze holding. (Vertical movements are served by a different cell group, the interstitial nucleus of Cajal.) These two components are combined into a pulse-step in the ocular motor neurons, as illustrated in Figure 1-7B. (Strictly speaking, the use of a two-pole plant and pulse-step is a simplification, for the actual driving signal looks more like a pulse-slide-step, and the globe and extraocular muscles behave more like a two-pole, one-zero plant. Some have proposed sixth-order models for the plant. However for the purposes of the material to be presented here, the simpler plant will suffice.)

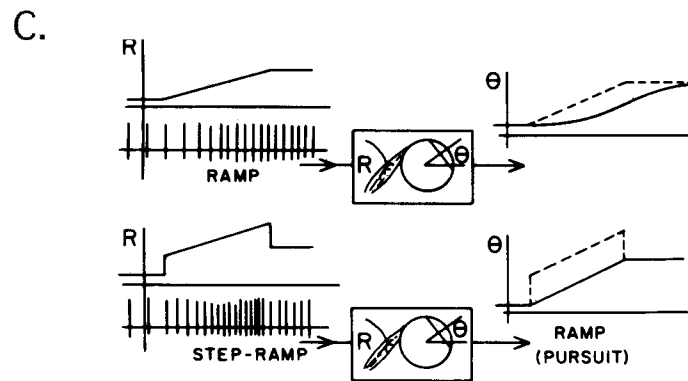
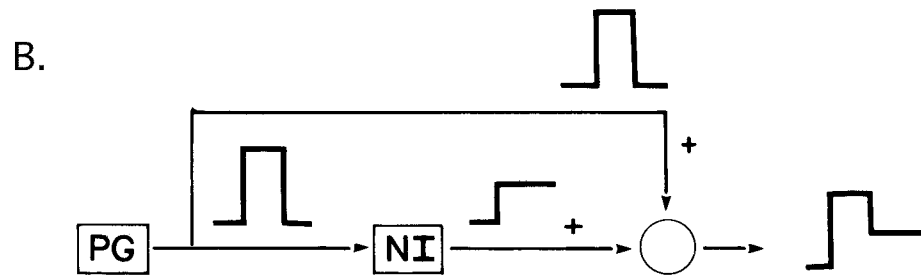
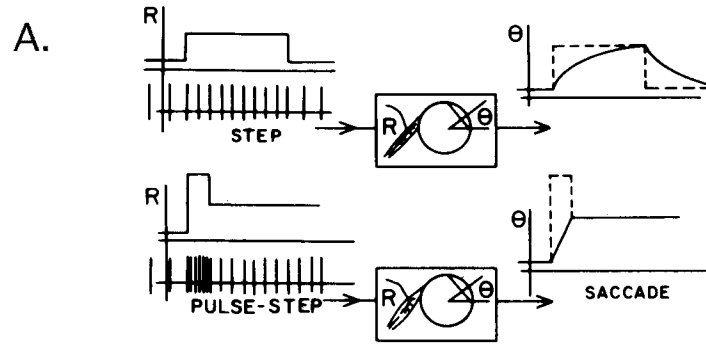


Figure 1-7

A.) With only a step of innervation (top), a saccade takes much longer to get the eye to the target,  $\Theta$ , than when driven by a pulse-step signal (bottom). B.) Creation of a pulse-step by summing the pulse with a step created by integration of the pulse. C.) Use of a step ramp (bottom) to increase pursuit performance, in a manner analogous to the pulse-step for saccades. (Adapted from Robinson, DA: Oculomotor control signals. In Lennerstrand G, Bach-y-Rita P (eds.): Basic Mechanisms of Ocular Motility and their Clinical Applications. New York, Pergamon Press, 1975.)

Other FEM properties that a good model should be able to reproduce range from the trivially simple, such as saccadic latency, to the more subtle and complex, such as the pulse-step response. Latency, which is due mostly to the long delay in feedback of visual information, is easily dealt with by the judicious distribution of simple delay elements throughout the model so that there is a 200 ms lag between a target jump and the ensuing saccade. The pulse-step behavior is a consequence of the ocular motor system acting like a sampled-data system, i.e., one where visual input can be used only at discrete times to program eye movement. If a target jump is briefly presented (the “pulse”) to the subject, and then it jumps to a new location (the “step”), the response of the saccadic subsystem depends on the duration of the initial pulse. If it is less than about 50 ms, it will be ignored in favor of the position of the step presentation. This implies that there is a finite duration required to program a saccade—this is the sample time of a discrete system, and as a result determines how the saccadic must be implemented in a model.

We must also be able to simulate the saccadic subsystem’s refractory period, i.e., the minimum time after which one saccade is executed before another can be made. (Actually, the story is a bit more complicated than this, for there are instances when saccades can be made back-to-back, with no intervening rest. This can be seen in the double saccadic pulse (Doslak, Dell’Osso, & Daroff, 1983; Leigh & Zee, 1999), which is a saccadic intrusion during fixation, where a pair of small saccades take the fovea off target and then immediately return it. A more extreme case of this is flutter, which is a

saccadic oscillation that is due to a failure in the pause neurons that normally inhibit saccadic burst cells (Zee & Robinson, 1979). This model will not deal with that particular pathology, however.) This has great implications for normal behavior, as well as for how braking and foveating saccades will be generated in the full model when CN is present, and how these saccades will affect the attempt to make voluntary refixation saccades. Because subjects with CN are capable of making accurate voluntary saccades despite the continuous demand being placed on their saccadic subsystems, a proper model of CN, based on the normal ocular motor system should be able to do the same. In fact, it will be shown in Chapter 4 that this is the case, and that the resulting behavior mimics quite well that seen in CN subjects. This result comes about simply from the basic rules used to design the normal saccadic subsystem, without the need to explicitly postulate any particular neural circuitry to achieve it. (In this model, the refractory period is modelled using a timing circuit, which is obviously not particularly realistic physiologically. It is possible to construct circuitry based on exponential time decay of membrane voltages, but at the cost of greater computational complexity, that would not have added anything towards the understanding of the phenomena for which the model was constructed.)

Also, taking the normal saccadic subsystem model and challenging it by interfering with its ability to make orthometric saccades of *any* magnitude (by changing the gain at the output) should lead to a model that will make a *series* of corrective saccades that will eventually reach the target. If the gain is *too low*, i.e., under 1.0, these saccades will stair-step their way to the target. For a gain of 0.5 (50%), each successive

saccade covering half the error left by the previous saccade. (This brings to mind Zeno's paradox where Achilles can never catch the tortoise once it has been given a head start, because to do so would require him to keep covering an infinite series of half-distances as the tortoise patiently plods to the next point. Fortunately, the saccadic subsystem isn't quite so literal minded, and has the ability to ignore errors that fall within a certain small range—here, set to about a quarter of a degree, saving us from making an infinite series of ever-decreasing corrective saccades.)

If the gain is *too high* (i.e., greater than 1.0 but less than 2.0), then the result is a series of corrective saccades that oscillate around the point of fixation, eventually reaching the dead zone and achieving the target. If however, the gain reaches 2.0, then the saccades will never be able to correct, for the error will never decrease, but will instead simply flip its sign *ad infinitum*, leading to a condition known as *macro saccadic oscillation*, a dramatic hallmark of cerebellar disease.

### 1.3.2 Smooth Pursuit (SP) Subsystem

Just as we had to consider FEM properties, so we must also consider which SP properties are crucial for inclusion in the model. Once again, we have to distribute delays throughout the visual path so that there is an approximately 130 ms delay between the appearance of a pursuit target and subsequent eye movement, although shorter durations have been reported (Carl & Gellman, 1987). This delay includes the processing times due higher cortical areas of the brain that are involved in perceiving motion, such as the

primary visual cortex (V1); the medial temporal (MT) and medial superior temporal (MST) areas; and the frontal and supplementary eye fields (FEF and SEF, respectively).

The pursuit subsystem must also be able to perform accurately even in the presence of a potentially confounding signal such as the internally generated “noise” of nystagmus. Somehow the pursuit subsystem needs to be able to separate the apparent movement of the target caused by oscillation of the eye from the actual movement of the target. Also, we need to be able to somehow segregate the smooth pursuit subsystem from the saccadic subsystem so that it doesn’t react falsely to velocity errors caused by the rapid gaze shifting caused by the execution of saccades.

Just as the eye needs a pulse-step to generate a saccade, it requires a *step-ramp* drive signal to pursue. The step overcomes the viscous properties of the orbit, and the ramp keeps the eye moving. This is shown in Figure 1-7C.

This SP subsystem in this model will be based upon a well-known SP model (Robinson et al., 1986) that reproduces the velocity ringing that accompanies the onset of pursuit, and is hypothesized to be the origin of the instability at the heart of pendular CN.

### *1.3.3 Internal Monitor (IM)*

These types of required calculations suggest an additional level of processing that interconnects and coordinates the smooth pursuit and saccadic subsystems. In our model, the IM keeps track of (among other signals) eye position and velocity commands, eye position and velocity errors, and saccadic commands; it uses them to reconstruct target

position and velocity and then sends appropriate commands to the SP and saccadic subsystems, dependent on the states of those subsystems. Expanding upon the example in the last paragraph, the SP subsystem is prohibited from sampling velocity error while a saccade is executing, and for a period of 70 ms afterwards (to allow the eye to fully respond to the saccadic command), by turning off an enabling signal that is necessary to allow the SP subsystem's normal functioning. After the necessary time has elapsed, the SP subsystem is once again allowed to sample and respond to its inputs. This disabling and re-enabling of subsystems can be viewed as the inhibition and re-enabling of the cell groups.

In our model, the IM determines whether ECPY-based or visual feedback-based saccades are eligible to be made by enforcing a set of rules based on measured saccadic latencies for both cases and knowledge of which can take precedence over the other, according to observations of actual behavior.

One last very important function performed by our IM is the logic necessary for the detection of conditions that should trigger braking and foveating saccades, and the calculations to make accurate foveating saccades. This is done by monitoring the velocity of the eye due to the nystagmus, knowing where the eye is at the time of the decision to make the saccade, and where it is predicted to be when the saccade is executed.

Philosophically, any model that keeps track of a portion of its internal state and uses that information to determine future actions can be said to have an internal monitor. The history of this model's IM will be presented in detail in the towards the end of this

chapter, and more detail about the design and implementation of the IM will appear in Chapter 4, and Appendix B.

#### *1.3.4 Fixation Subsystem*

On occasion, fixation has been referred to as “smooth pursuit at zero velocity.” However there is a great deal of evidence that supports the modeling of fixation as a separate subsystem. Perhaps most important, is a study that found neurons active during fixation but not during pursuit (Lynch, Mountcastle, Talbot, & Yin, 1977). Similarly, in monkeys, stimulation of neurons associated with pursuit only act to change eye velocity *during* pursuit, and will not *initiate* pursuit while the test subject is fixing on a non-moving target (May, Keller, & Crandall, 1988; Komatsu & Wurtz, 1989). Also, there are behavioral observations that the ringing that normally accompanies the onset of pursuit is absent at its termination (Robinson et al., 1986). Finally, there is a report of patients whose eyes are stable during fixation, but break into CN-like oscillations when attempting to pursue a moving target (Kelly, Rosenberg, Zee, & Optican, 1989). Based on the strength of these arguments, the model to be presented has been designed with distinct pursuit and fixation subsystems.

Two implementations of the fixation subsystem were considered: first, the possibility that the fixation subsystem acts as a gain modulator of the smooth pursuit signal, normally operating at full gain until fixation is desired, at which time the gain drops towards zero, slowing the eye briefly. Second, and as implemented in the final

model, fixation could be achieved by use of a “counter-signal,” i.e., when fixation is desired, the subsystem attempts to cancel out the slow-phase oscillation with a velocity signal that is of the same magnitude, but oppositely directed.

### *1.3.5 Efference Copy vs Proprioception*

Recalling the discussion of corrective saccades earlier in this section, it was stated that there had to be some internalized, non-visual way to monitor eye position. There are two possible mechanisms for this extraretinal signal: one is *proprioception*, which is the information fed back from sensory organs in the peripheral musculature. Proprioception is a very powerful sensory modality (sometimes referred to as our sixth sense) that provides us with our “body sense,” i.e., our non-tactile, non-visual awareness of body position. The strength of proprioception is so great that it can frequently persist in amputated limbs (or even in limbs that never developed) giving rise to the so-called “phantom limb.” In extreme cases, complete paraplegics (high-cervical injury) report still having a sense of their bodies. (Melzack, 1992). Even more strange are the case studies of people who have, through chemical or traumatic means, lost their proprioceptive ability (Sacks, 1987); they report a continual feeling of disorientation and disconnection from their bodies, and are often incapable of any but the simplest physical activities without extensive retraining. Even then they must frequently monitor their movements visually to be able to function. From these examples, it is easy to see why proprioception was considered such a strong candidate for the internal monitoring of eye position.

The other possible mechanism is called *efference copy*, which is, as its name suggests, a secondary record of the motor commands sent out to the eye muscles. Sometimes this is referred to as *corollary discharge*. (These are actually not exactly the same, but are closely related; the difference is really semantic: corollary discharge is the process of sending the information and efference copy is the image of the information. For simplicity, the term efference copy will be used throughout this dissertation.) Efference copy can be thought of as information that is *fed forward* to some other portion of the brain in anticipation of a motor action, in effect setting the stage for the anticipated new state. The first experiments that demonstrated its existence were performed independently by Sperry (1950)—who called it corollary discharge—and von Holst and Mittelstaedt (1950)—who called it *reafferenzprinzip*. In each case it was shown that there was a signal coming from the structures of/around the eye that when reversed (by physically inverting the eye) caused the experimental preparations (fish and insects, respectively) to go into oscillatory behavior, rather than settle down, due to the accentuation rather than cancellation of illusory outside movement.

So, is it proprioception or efference copy that is responsible for our ocular motor system's ability to "know" the position of our eyes? This question is almost as old as the study of eye movement itself. Helmholtz first postulated that knowledge of eye position was due to "the effort of will" put forth to move the eyes (1866), discounting proprioceptive information by presenting the case of a patient with a partially paralyzed eye; here the proprioceptive information was intact, yet there was still diplopia present.

He concluded that this could only be because the brain expected a different retinal image in that eye based on “knowledge” of where it expected the eye to actually point. A further experiment involved passive eye movements (i.e., the eye was moved by pulling on it with forceps) and afterimages confirmed this result for they *did not move* with the fovea as they would have during *voluntary* refixations. Sherrington (1918), on the other hand, believed that the stretch receptors in the extra ocular muscles provided this information to the ocular motor system, based on work done over the span of more than twenty years examining the anatomy and physiology of the sensory nerves of the eye muscles. He performed experiments that purported to demonstrate that these structures provided clear position sense of eye position. Unfortunately, however, there were questions about the validity of these experiments (Merton, 1964), and subsequent studies failed to reproduce his results (Ludveigh, 1952a; Ludveigh, 1952b).

Bridley and Merton (1960) anesthetized the surface of the eye and inner eyelids of a human subject and covered the cornea with an opaque cap to remove all visual cues. They then moved the eye by pulling on the horizontal recti muscles with forceps, creating movements on the order of 20°, repeatedly. The subjects was unable to tell when his eye was moved.

Guthrie, Porter and Sparks (1983) found that elimination of proprioceptive information by transection of the ophthalmic nerve at the junction with the trigeminal ganglion did not remove the ability of rhesus monkeys to perform saccadic tracking tasks

that relied on the presence of some form of extraretinal signal, leading to the conclusion that efference copy (called corollary discharge) was the responsible mechanism.

It should be noted that there is no evidence that says proprioception cannot play *some* role in providing eye position information to the ocular motor system, just that it is not primary. Skavenski (1972) points out that the results of Brindley and Merton (1960) are not conclusive because of the insensitivity of the psychophysical techniques they employed, and because any physical discomfort resulting from their rather invasive experimental technique could act as a distracter. When a more sensitive forced-choice psychophysical approach was used, and less distracting methods were used to move the eye, Skavenski found that inflow information could be used to *contribute* to the detection and control of eye movement; no claim was made that this was the sole source of the extraretinal information. Finally, more complete mapping of the central terminations of afferent nerve fibers from extraocular muscles (Porter, 1986) and the recent discovery of motor cells in tendons of extraocular muscles (Blumer, Lukas, Aigner, Bittner, Baumgartner, & Mayr, 1999) suggests that proprioception may play a greater role than previously thought.

### *1.3.6 Model Design Philosophy*

The model to be presented is based on a control systems approach that is block-oriented, with the functional blocks connected by distinct signal lines. It attempts to retain physiological accuracy by modeling known neurophysiological functions as

discrete blocks whenever possible (e.g., the common neural integrator), but also takes some liberties with the creation of large, complex blocks that may not have actual analogous functions, but represent the grouping of many (sometimes hypothetical) functions. The best example of this approach is the IM, a functional block that subsumes all the computation required for the reconstruction of eye and target position and velocity, and for the programming of saccades and pursuit. Such a grouping is not made on an anatomical basis, but purely on a functional basis. It is interesting to note, however, that recent work suggests that structures in the paramedian tract (PMT) may contain many of the signals required by the IM (Buttner-Ennever, Horn, & Schmidtke, 1989; Nakamagoe, Iwamoto, & Yoshida, 2000).

This approach does not negate the importance of more physiologically or anatomically “realistic” modeling methods, especially those using neural networks. It is simply a more direct approach acceptable when the goal is to partition a problem as a set of “black-box”-type functions. In fact, either approach should yield the same results, because from a purely theoretical point of view, any mathematical function where the output varies smoothly with the input can be implemented as a neural net if there is no interest in understanding the details of the function’s internal organization and operation (Robinson, 1994; Russell & Norvig, 1995). In a neural network it is not even possible to divine such details from its organization. Also, except for signals at the input and the output of the network, no clearly-defined, physically-interpretable intermediate signals exist in the net; what is available inside of the network are weighted combinations of the

input and output signals. In a neural net implementation all we have are these input and the output signals with no indication of how we got from point A to point B, so to speak—the neural net is the ultimate “black box.”

One very powerful aspect of neural network modeling is that, as in nature, complex behavior can arise from many simple elements operating together following simple rules. For example, neurons can be viewed as either “on” or “off,” and combining just a dozen or so of them in the appropriate topology with the appropriate synaptic values gives rise to an enormous variety of possible operations beyond those simple “on” or “off” values. This should not be a surprising result for anyone familiar with control systems analysis, where one of the first lessons learned is that the *organization* of the system (which is analogous to the structure and interconnectedness of a neural network) rather than the transfer functions of the boxes that is the primary determinant of its ultimate behavior.

The chief advantage of the selected approach is that partitioning the modeling process allows for the independent development of each subsystem, reducing the hazard that minor—and in some cases, even major—changes in implementation of one set of functions will completely confound the proper operation of the other blocks or of the model as a whole. This allows for the substitution of new subsystems as better alternatives become available (e.g., it would be relatively simple to incorporate a different smooth pursuit subsystem if future work were to indicate it as offering more suitable behavior).

Overall, it is reasonable to look at the developmental process for this model as analogous to the evolution of a biological system in that we have started with a simplicity of form and function and slowly built complexity and optimality (whenever feasible) as the behavioral requirements were increased. As is the case in nature, much is possible, but far less actually turns out to be workable, let alone optimal. Each design choice is, in essence, a hypothesis that can be tested and, if successful, incorporated into the model. Of course, this process is not a natural evolution so much as a guided one, but the pathway is the same.

Another crucial property that must be incorporated into a good model is *robustness*. There are two separate (but related) definitions of this term, depending on whether you have been reading eye movement literature or control theory literature. Mathematically, a control system is robust if it has a large *stability margin*. In practical terms, this means that it is relatively insensitive to disturbances at its inputs and to internal noise and modeling errors or malfunctions.

An ocular motor model is robust if it is capable of simulating both normal and abnormal responses to given inputs, and if the presence of a motor disorder does not interfere with normal responses seen in patients with that disorder. Primarily, this means that both the saccadic and smooth pursuit subsystems must function normally, able to make voluntary refixations and track moving targets, with corrective saccades when required even in the presence of a potentially confounding signal such as the internally generated oscillations of nystagmus. Secondly, the response of the model should

remain “reasonable,” i.e., within the range of realistic ocular motor behaviors when presented with “difficult” or “bad” inputs; for example, it would be unacceptable if a small input signal were to drive the model into sustained extreme lateral gaze. Finally, the model should be able to continue operating even when challenged with the digital equivalent of lesions of cell groups or signal pathways, and degrade performance gracefully, letting other mechanisms take over for the missing components wherever possible, preserving as much functionality as possible.

If all these goals are met, then ideally the model should be capable of making predictions that can be tested experimentally.

### *1.3.7 Previous models of CN*

Prior to the model to be presented in Chapter 4, there have been several attempts to model CN, with varying degrees of success. The chief problem with most of these has been their limited design; they were intended to reproduce only some CN waveforms, not a normal ocular motor system that has CN. As repeatedly stated above, this approach is too narrow to capture the breadth of CN behavior, and is unable to provide much insight into either the actual mechanisms responsible for CN or the function of the normal ocular motor system. As a result, it is easy to lose sight of the real world when building such models, and often they lead to unrealistic assumptions about the possible underlying mechanisms of CN; this can lead to models that *appear* to be reasonable, but have one or more serious flaws. (Of course these models are usually unable to do anything but

simulate some particular aspect of CN; normal behavior truly remains beyond their abilities.)

In Chapter 4, four other models in particular will be discussed. Three are especially noteworthy for they all use the same mechanism to generate CN, an overly large positive feedback loop around the neural integrator. This excessive feedback causes these models to produce the exponentially increasing runaway slow phases characteristic of jerk CN. While the output of these models looks like the eye movement data recorded from subjects with CN, there are problems that limit their suitability. Optican and Zee's (1984) model is incapable of making pendular oscillations except around a null region, and even then they are of very low amplitude. Second, and far more damaging, there can be *two* nulls, something that has never been verified in CN. Tusa, Zee, Hain & Simonz' (1992) model is based on a patient that does not have CN, based on the clinical findings they report. From this false start they end up proposing reversed neural wiring to provide an inverted signal in the fixation subsystem. To date, no CN patient has ever been shown to have such a midline defect. Harris (1995) makes some very important contributions, but once again proposes a model that ignores much real-life data: namely that there are many people whose CN does *not* arise from afferent deficits of the visual system, but is instead of an idiopathic origin. On the positive side, all three of these models do produce jerk CN, a waveform that the model to be presented in this dissertation does not yet simulate. Although this simple waveform is easy to simulate (Dell'Oso & Daroff, 1981),

the most probable source for this instability has not yet become clear; the sources proposed in the above models are not good candidates.

#### *1.3.8 Lineage of this CN model*

The most striking feature of the model is the IM, mentioned earlier. During the design of this current model, it became apparent that the functions incorporated into the IM, such as the challenge of separating eye motion from target motion, are necessary for the functioning of the *normal* ocular motor system; its ability to continue to function properly even when confronted by conditions that push it beyond the limits of normal operation is simply the extension of its fundamental design.

Dell'Osso (1968) presented a model of CN based on contemporary models of saccadic and smooth pursuit systems and incorporated what can be viewed as the genesis of the IM: a feedback loop that used a copy of a stylized CN motor signal (an externally-generated sawtooth) combined with the retinal signal to cancel out the eye's oscillation. This cancellation allowed the model to continue to properly track the step and ramp targets that it had tracked before the addition of the CN-like signal. This model marked a departure from previous attempts to simulate the ocular motor system without the use of efference copy.

The gaze-evoked nystagmus and myasthenia gravis models by Abel and co-investigators (Abel, Dell'Osso, & Daroff, 1978; Abel, Dell'Osso, Schmidt, & Daroff, 1980) further extended the IM by increasing the number of signals it had to keep track of

when determining where the eye needed to be directed. (These models also introduced the resettable neural integrator as the basis of the saccadic subsystem and the introduction of controls on the common neural integrator—that is, not all pulses from the pulse generator were automatically and fully integrated.)

The IM matured significantly in the LMLN model (Jacobs & Dell'Osso, 1999; Dell'Osso & Jacobs, 2000) that is the immediate predecessor of the model to be presented here. This greatly enhanced IM was significantly more complex because it now had to detect target changes, reconstruct eye position and velocity, target position and velocity, generate both foveating and defoveating saccades, and corrective and voluntary saccades, all with proper latency and precedence. In addition, it had to control whether or not the NI fully integrated a saccade (foveating saccades) or not (defoveating saccades). These requirements insured that the IM became more complex than many entire models.

The adoption of a “whole system” approach as the basis for this model should not be taken as a dismissal of the use of smaller, simpler models, for they can offer great insights into function, and are usually much simpler to test. A model of the complexity as the one presented in this dissertation is much harder to test, and can perhaps obscure some details that smaller models can address directly. However, a model of this complexity is a starting place for understanding the rules that govern the interaction of the many interconnected subsystems of the OMS.

## 1.4 WORKS CITED

Abel, L. A., Dell'Osso, L. F., & Daroff, R. B. (1978). Analog model for gaze-evoked nystagmus. *IEEE Trans Biomed Engng*, **BME(25)**, 71-75.

Abel, L. A., Dell'Osso, L. F., Schmidt, D., & Daroff, R. B. (1980). Myasthenia gravis: Analogue computer model. *Exp Neurol*, **68**, 378-389.

Bedell, H. E., & Currie, D. C. (1993). Extraretinal signals for congenital nystagmus. *Invest Ophthalmol Vis Sci*, **34**, 2325-2332.

Blumer, R., Lukas, J.-R., Aigner, M., Bittner, R., Baumgartner, I., & Mayr, R. (1999). Fine structural analysis of extraocular muscle spindles of a two-year-old human infant. *Invest Ophthalmol Vis Sci*, **40**, 55-64.

Boghen, D., Troost, B. T., Daroff, R. B., Dell'Osso, L. F., & Birkett, J. E. (1974). Velocity characteristics of normal human saccades. *Invest Ophthalmol*, **13**, 619-623.

Brindley, G. S., & Merton, P. A. (1960). The absence of position sense in the human eye. *J. Physiol.*, **153**, 127-130.

Burr, D. C., & Ross, J. (1982). Contrast sensitivity at high velocities. *Vision Res*, **22**, 479-484.

Buttner-Ennever, J. A., Horn, A. K., & Schmidtke, K. (1989). Cell groups of the medial longitudinal fasciculus and paramedian tracts. *Revue Neurologique*, **145**(8-9), 533-539.

Carl, J. R., & Gellman, R. S. (1987). Human smooth pursuit: stimulus-dependent responses. *Journal of Neurophysiology*, **57**(5), 1446-1463.

Carpenter, R. H. S. (1988) *Movements of the Eyes, 2nd Edition.*, Pion: London.

Collewijn, H., & Tamminga, E. P. (1984). Human smooth and saccadic eye movements during voluntary pursuit of different target motions on different backgrounds. *J Physiol*, **351**, 217-250.

de la Barre, E. B. (1898). A method of recording eye-movements. *American Journal of Psychology*, **9**, 572-574.

Dell'Osso, L. F. (1968) *A Dual-Mode Model for the Normal Eye Tracking System and the System with Nystagmus. (Ph.D. Dissertation)*. In: Electrical Engineering (Biomedical)., University of Wyoming: Laramie. p. 1-131

Dell'Osso, L. F. (1976) Prism exploitation of gaze and fusional null angles in congenital nystagmus. In: S. Moore, *Orthoptics : Past, Present, Future* (pp. 135-142). New York: Symposia Specialists.

Dell'Osso, L. F. (1986). Evaluation of smooth pursuit in the presence of congenital nystagmus. *Neuro ophthalmol*, **6**, 383-406.

Dell'Osso, L. F. (1994). Congenital and latent/manifest latent nystagmus: Diagnosis, treatment, foveation, oscillopsia, and acuity. *Jpn J Ophthalmol*, **38**, 329-336.

Dell'Osso, L. F. (1997). Extraocular muscle tenotomy, dissection, and suture: A hypothetical therapy for congenital nystagmus. *J Pediatr Ophthalmol Strab*, **35**, 232-233.

Dell'Osso, L. F., & Daroff, R. B. (1976). Braking saccade--A new fast eye movement. *Aviat Space Environ Med*, **47**, 435-437.

Dell'Osso, L. F., & Flynn, J. T. (1979). Congenital nystagmus surgery: a quantitative evaluation of the effects. *Arch Ophthalmol*, **97**, 462-469.

Dell'Osso, L. F., & Daroff, R. B. (1981) Clinical disorders of ocular movement. In: B. L. Zuber, *Models of Oculomotor Behavior and Control* (pp. 233-256). West Palm Beach, CRC Press Inc.

Dell'Osso, L. F., & Daroff, R. B. (1986) Abnormal head position and head motion associated with nystagmus. In: E. L. Keller, & D. S. Zee, *Adaptive Processes In Visual and Oculomotor Systems* (pp. 473-478). Oxford: Pergamon Press.

Dell'Osso, L. F., & Leigh, R. J. (1995). Oscillopsia suppression: Efference copy or foveation periods? *Invest Ophthalmol Vis Sci*, **36**, S174.

Dell'Osso, L. F., & Daroff, R. B. (1999) Nystagmus and saccadic intrusions and oscillations. In: J. S. Glaser, *Neuro-Ophthalmology* (pp. 369-401). Baltimore: Lippincott Williams & Wilkins.

Dell'Osso, L. F., & Jacobs, J. B. (2000) A robust, normal ocular motor system model with latent/manifest latent nystagmus (LMLN) and dual-mode fast phases. In: J. A.

Sharpe, *Neuro-ophthalmology at the Beginning of the New Millennium* (pp. 113-118). Englewood: Medimond Medical Publications.

Dell'Osso, L. F., Flynn, J. T., & Daroff, R. B. (1974). Hereditary congenital nystagmus: An intrafamilial study. *Arch Ophthalmol*, **92**, 366-374.

Dell'Osso, L. F., Gauthier, G., Liberman, G., & Stark, L. (1972). Eye movement recordings as a diagnostic tool in a case of congenital nystagmus. *Am J Optom Arch Am Acad Optom*, **49**, 3-13.

Dell'Osso, L. F., Van der Steen, J., Steinman, R. M., & Collewijn, H. (1992a). Foveation dynamics in congenital nystagmus I: Fixation. *Doc Ophthalmol*, **79**, 1-23.

Dell'Osso, L. F., Van der Steen, J., Steinman, R. M., & Collewijn, H. (1992b). Foveation dynamics in congenital nystagmus II: Smooth pursuit. *Doc Ophthalmol*, **79**, 25-49.

Dell'Osso, L. F., Van der Steen, J., Steinman, R. M., & Collewijn, H. (1992c). Foveation dynamics in congenital nystagmus III: Vestibulo-ocular reflex. *Doc Ophthalmol*, **79**, 51-70.

- Dell'Osso, L. F., Hertle, R. W., Williams, R. W., & Jacobs, J. B. (1999). A new surgery for congenital nystagmus: effects of tenotomy on an achiasmatic canine and the role of extraocular proprioception. *J Am Assoc Pediatr Ophthalmol Strab*, **3**, 166-182.
- Doslak, M. J., Dell'Osso, L. F., & Daroff, R. B. (1983). Multiple double saccadic pulses occurring with other saccadic intrusions and oscillations. *Neuro ophthalmol*, **3**, 109-116.
- Duke-Elder, S., & Wybar, K. (1949) *Ocular motility and strabismus (Vol IV)*. System of Ophthalmology., Mosby: St. Louis.
- Flynn, J. T., & Dell'Osso, L. F. (1979). The effects of congenital nystagmus surgery. *Ophthalmol AAO*, **86**, 1414-1425.
- Forssman, B. (1971). Hereditary studies of congenital nystagmus in a Swedish population. *Ann Hum Genet (London)*, **35**, 119-138.
- Goldstein, H. P. (1995). Extended slow phase analysis of foveation, waveform and null zone in infantile nystagmus. *Invest Ophthalmol Vis Sci*, **36**, S174.

Gresty, M. A., Halmagyi, G. M., & Leech, J. (1978). The relationship between head and eye movement in congenital nystagmus with head shaking: objective recordings of a single case. *Br J Ophthalmol*, **62**, 533-535.

Gresty, M. A., Leech, J., Sanders, M. D., & Eggars, H. (1976). A study of head and eye movement in spasmus nutans. *Br J Ophthalmol*, **160**, 652-654.

Gresty, M. A., Bronstein, A. M., Page, N. G., & Rudge, P. (1991). Congenital-type nystagmus emerging in later life. *Neurology*, **41**, 653-656.

Guthrie, B. L., Porter, J. D., & Sparks, D. L. (1983). Corollary discharge provides accurate eye position information to the oculomotor system. *Science*, **221**, 1193-1195.

Halmagyi, G. M., Gresty, M. A., & Leech, J. (1980). Reversed optokinetic nystagmus (OKN): mechanism and clinical significance. *Ann Neurol*, **7**, 429-435.

Harris, C. M. (1995) Problems in modeling congenital nystagmus: Towards a new model. In: J. M. Findlay, R. Walker, & R. W. Kentridge, *Eye Movement Research: Mechanisms, Processes and Applications* (pp. 239-253). Amsterdam: Elsevier.

Hayasaka, S. (1986). Hereditary congenital nystagmus. A Japanese pedigree. *Ophthalmic Pediatr Genet*, **7**, 73-76.

Helmholtz, H. v. (1866) *Handbuch der Physiologen Optik.*, Voss: Leipzig.

Hering, E. (1879). Über Muskelgeräusche des Auges. *Sitzungsberichte der Akademie der Wissenschaften un Wein: Mathematisch-Naturwissenschaftliche Klasse, Abeiling* **3**, **79**, 137-159.

Hertle, R. W., & Dell'Osso, L. F. (1999). Clinical and ocular motor analysis of congenital nystagmus in infancy. *J Am Assoc Pediatr Ophthalmol Strab*, **3**, 70-79.

Hertle, R. W., Dell'Osso, L. F., & Movaghar, M. (1995). Clinical and oculographic analysis of congenital nystagmus (CN) in infancy. *Invest Ophthalmol Vis Sci*, **36**, S174.

Hertle, R. W., Dell'Osso, L. F., Williams, R. W., & Jacobs, J. B. (1998). Extraocular muscle tenotomy (the Dell'Osso procedure): Damping of congenital (CN) and see-saw (SSN) nystagmus in the achiasmatic Belgian sheepdog (ABS). [ARVO Abstract]. *Invest Ophthalmol Vis Sci*, **39**, S149.

Jacobs, J. B., & Dell'Osso, L. F. (1999). A dual-mode model of latent nystagmus [ARVO Abstract]. *Invest Ophthalmol Vis Sci*, **40**, S962.

Jürgens, R., Becker, W., Reiger, P., & Widderich, A. (1981) Interaction between goal-directed saccades and the vestibulo-ocular reflex (VOR) is different from interaction between quick phases and VOR. In: A. F. Fuchs, & W. Becker, *Progress in Oculomotor Research* (pp. 11-18). Amsterdam: Elsevier.

Keller, E. L., & Edelman, J. A. (1994). Use of interrupted saccade paradigm to study spatial and temporal dynamics of saccadic burst cells in superior colliculus in monkey. *Journal of Neurophysiology*, **72**(6), 2754-2770.

Kelly, B. J., Rosenberg, M. L., Zee, D. S., & Optican, L. M. (1989). Unilateral pursuit-induced congenital nystagmus. *Neurology*, **39**, 414-416.

Kerrison, J. B., Koenekoop, R. K., Arnould, V. J., D., Z., & Maumenee, I. H. (1998). Clinical features of autosomal dominant congenital nystagmus linked to chromosome 6p12. *Am J Ophthalmol*, **125**, 64-70.

Komatsu, H., & Wurtz, R. H. (1989). Modulation of pursuit eye movements by stimulation of cortical areas MT and MST. *J Neurophysiol*, **62**, 31-47.

Kurzan, R., & Büttner, U. (1989). Smooth pursuit mechanisms in congenital nystagmus.

*Neuro ophthalmol*, **9**, 313-325.

Leigh, R. J., & Zee, D. S. (1980). Eye movements of the blind. *Invest Ophthalmol Vis*

*Sci*, **19**, 328-330.

Leigh, R. J., & Zee, D. S. (1999) *The Neurology of Eye Movements, Edition 3*

(*Contemporary Neurology Series*)., Oxford University Press: New York.

Ludveigh, E. (1952a). Possible role of proprioception in the extraocular muscles. *A. M. A.*

*Arch. Opth.*, **48**(436-441).

Ludveigh, E. (1952b). Control of ocular movements and visual interpretation of

environment. *A. M. A. Arch. Opth.*, **48**(442-448).

Lynch, J. C., Mountcastle, V. B., Talbot, W. H., & Yin, T. C. T. (1977). Parietal lobe

mechanisms for directed visual attention. *J Neurophysiol*, **40**, 362-389.

- May, J. G., Keller, E. L., & Crandall, J. (1988). Changes in eye velocity during smooth pursuit tracking induced by microstimulation in the dorsolateral pontine nucleus of the macaque. *Soc Neurosci Abstr*, **11**, 79.
- Melzack, R. (1992). Phantom limbs. *Scientific American*, (April), 120-126.
- Merton, P. A. (1964) Absence of conscious position sense in the human eyes. In: M. B. Bender, *The Oculomotor System* (pp. 314-320). New York: Harper and Row.
- Nakamagoe, K., Iwamoto, Y., & Yoshida, K. (2000). Evidence for brainstem structures participating in oculomotor integration. *Science*, **288**, 857-859.
- Oetting, W. S., Armstrong, C. M., Holleschau, A. M., DeWan, A. T., & Summers, G. C. (2000). Evidence for genetic heterogeneity in families with congenital motor nystagmus (CN). *Ophthalmic Genetics*, **21**(4), 227-233.
- Ohm, J. (1928). Die Hebelnystagmographie. *Albrecht von Graefes Archiv für Ophthalmologie*, **120**, 235-252.
- Optican, L. M., & Zee, D. S. (1984). A hypothetical explanation of congenital nystagmus. *Biol Cyber*, **50**, 119-134.

- Optican, L. M., Zee, D. S., Chu, F. C., & Cogan, D. G. (1983). Open loop pursuit in congenital nystagmus. [ARVO Abstract]. *Invest Ophthalmol Vis Sci*, **24(Suppl)**, 271.
- Orschansky, J. (1898). Eine Methode die Augenbewegungen direkt zu untersuchen (Ophthalmographie). *Zentralblatt für Physiologie*, **12**, 785-790.
- Porter, J. D. (1986). Brainstem terminations of extraocular muscle primary afferent neurons in the monkey. *J Comp Neurol*, **247**, 133-143.
- Reinecke, R. D. (1995) Development of congenital and infantile nystagmus. In: R. J. Tusa, & S. A. Newman, *Neuro-Ophthalmological Disorders - Diagnostic Workup and Management* (pp. 175-186). New York, Basel, Hong Kong: Marcel Dekker, Inc.
- Robinson, D. A. (1963). A method of measuring eye movement using a scleral search coil in a magnetic field. *IEEE Trans Bio Med Electron*, **BME(10)**, 137-145.

- Robinson, D. A. (1994) Implications of neural networks for how we think about brain function. In: P. Cordo, & S. Harnad, *Movement Control* (pp. 42-53). Cambridge: Cambridge University Press.
- Robinson, D. A., Gordon, J. L., & Gordon, S. E. (1986). A model of smooth pursuit eye movements. *Biol Cyber*, **55**, 43-57.
- Rottach, K. G., Zivotofsky, A. Z., Das, V. E., Averbuch-Heller, L., DiScenna, A. O., Poonyathalang, A., & Leigh, R. J. (1996). Comparison of horizontal, vertical and diagonal smooth pursuit eye movements in normal human subjects. *Vision Res*, **36**, 2189-2195.
- Russell, S. J., & Norvig, P. (1995) Learning in Neural and Belief Networks. In: *Artificial Intelligence, A Modern Approach* (pp. 563-598). Englewood Cliffs, NJ: Prentice Hall.
- Sacks, O. W. (1987) The disembodied lady. In: *The man who mistook his wife for a hat and other clinical tales* (pp. 43-54). New York: Harper and Row—Perennial Library.
- Sekuler, R., & Blake, R. (1994) *Perception.*, McGraw-Hill, Inc.: New York.

Sherrington, C. S. (1918). Observation on the sensual role of the proprioceptive nerve supply of the extrinsic ocular muscles. *Brain*, **41**, 332-343.

Skavenski, A. A. (1972). Inflow as a source of extraretinal eye position information. *Vision Res*, **12**, 221-229.

Sperry, R. W. (1950). Neural basis of the spontaneous optokinetic response produced by visual inversion. *J Comp Physiol Psychol*, **43**, 482-489.

Tusa, R. J., Zee, D. S., Hain, T. C., & Simonsz, H. J. (1992). Voluntary control of congenital nystagmus. *Clin Vis Sci*, **7**, 195-210.

Von Holst, E., & Mittelstaedt, H. (1950). Das Reafferenzprinzip (Wechselwirkungen zwischen Zentralnervensystem und Peripherie). *Naturwiss*, **37**, 464-476.

Weissman, B. M., Dell'Osso, L. F., Abel, L. A., & Leigh, R. J. (1987). Spasmus nutans: A quantitative prospective study. *Arch Ophthalmol*, **105**, 525-528.

Winson, J. (1990). The meaning of dreams. *Scientific American*, (Nov 1990), 86-96.

Winters, J. M., Nam, M. H., & Stark, L. W. (1984). Modeling dynamical interactions between fast and slow movements: Fast saccadic eye movement behavior in the presence of the slower VOR. *Math Biosci*, **68**, 159-185.

Yamazaki, A. (1979) Abnormalities of smooth pursuit and vestibular eye movements in congenital jerk nystagmus. In: K. Shimaya, *Ophthalmology* (pp. 1162-1165). Amsterdam: Excerpta Medica.

Yee, R. D., Baloh, R. W., & Honrubia, V. (1981). Eye movement abnormalities in rod monochromacy. *Ophthalmology*, **88**, 1010-1018.

Zee, D. S., & Robinson, D. A. (1979). A hypothetical explanation of saccadic oscillations. *Annals of Neurology*, **5**(5), 405-414.

## Chapter 2

# GENERATION OF BRAKING SACCADES IN CONGENITAL NYSTAGMUS

### **2.0 ABSTRACT**

We examined eye movement records of two congenital nystagmus (CN) subjects, whose waveforms contained braking saccades, to test the hypothesis that eye velocity, rather than eye position, is the more important criterion for braking saccade generation. Specifically, we wished to determine the criteria and timing used by their ocular motor systems in triggering these unique saccades. For the records analyzed, eye movements were measured by either scleral search coil or IR limbic reflection and data were sampled at rates from 200—488 Hz with a resolution of 12 bits for analysis by custom software. Both position and velocity were used to determine critical timing points in CN cycles, including saccadic onset, duration, offset and magnitude. Phase planes at various times (between 40 and 70 ms) prior to saccade onset helped determine (using foveation window criteria for best acuity) the conditions to generate a braking saccade. Braking saccades do brake CN slow phases, with average slowing (unrelated to braking-saccade size) of 62 and 119% for the two waveforms studied. At 70 ms prior to braking saccades both eye position and velocity usually still satisfied the criteria for good acuity established in the previous foveation period; by 40 ms, velocity no longer did. Thus, high eye velocity was

the only criterion that could be used for saccade generation. Braking saccades result in longer foveation times per second for CN waveforms. Eye velocity is the main criterion used to trigger braking saccades and the determination to trigger them occurs closer to 40 than 70 ms prior to their execution. Braking saccades can increase the nystagmus acuity function and allow better acuity.

## 2.1 INTRODUCTION

The ability to see clearly depends on more than just the refractive properties of the lens and cornea. The object of interest must also lie within the fovea, a central region of approximately one-half degree radius, and must be relatively stable, with less than  $4^\circ/\text{sec}$  motion relative to the retina for a reliable, repeatable period of time. In congenital nystagmus (CN), an instability of the ocular motor system (most probably in the smooth pursuit subsystem (Dell'Osso, Gauthier, Liberman, & Stark, 1972; Dell'Osso, Averbuch-Heller, & Leigh, 1997)) may prevent the eye from maintaining either of these goals. Because some patients with CN have visual acuity equal to that of normals, there must be a mechanism responsible for controlling the eyes' movements and forcing them to behave for this crucial portion of the CN cycle, known as the "foveation period."

*Braking saccades* were first described twenty years ago (Dell'Osso & Daroff, 1976) yet, to this day, their presumed purpose and the ocular motor conditions responsible for their generation remain unstudied. Braking saccades are fast eye movements that appear in certain CN waveforms: pseudopendular (PP), pseudopendular

with foveating saccades ( $PP_{fs}$ ), triangular (T), pseudojerk (PJ), bidirectional jerk (BDJ) and pseudocycloid (PC) (Dell'Osso & Daroff, 1975). They appear to slow, halt, or even reverse the CN slow phases and are similar to the more well-known fast-phase component seen in CN, the *foveating saccade*. Because foveating saccades also act to interrupt a runaway slow phase, they are a special case of braking saccade. The major difference, however, is that foveating saccades are visually guided, bringing the fovea to the target while slowing the eye enough to allow for best acuity. Braking saccades do not appear to be goal-directed and do not cause a significant change in the position of the eye. The occurrence of braking and foveating saccades (and the resulting CN waveforms) is idiosyncratic.

We examined two criteria for best possible visual acuity (position and velocity) to determine their importance in deciding when to generate a braking saccade. We also investigated the conditions prompting the decision to trigger a braking saccade. Specifically, do either (or both) eye position or eye velocity exceed values that are required for good visual acuity prior to the generation of a braking saccade? Sometime after the previous cycle's foveation period and before the generation of a braking saccade, either the eye position, velocity, or both must achieve values that reduce acuity before a braking saccade is triggered. As the results of this study show, it is likely that the most important criterion is eye velocity and the decision is made less than 70 ms (closer to 40 ms) before the beginning of the braking saccade.

## 2.2 METHODS

Data for this study came from two subjects previously recorded in this laboratory. Both subjects had idiopathic CN without any acquired nystagmus. They were healthy, with no neurological deficits. Both subjects' waveforms included  $PP_{fs}$  and PC cycles and they were chosen for this study because their waveforms were typical of those recorded in hundreds of other CN subjects. In primary gaze, S1's waveform was almost exclusively  $PP_{fs}$ , with PC occurring only at extreme gaze angles ( $40^\circ$  left gaze). S2's CN was mainly PC in primary gaze, with occasional runs of  $PP_{fs}$ . S2 was not recorded extensively at other gaze angles, and consequently only the data for straight-ahead viewing was used. Records were chosen for study only if they contained repeated runs of braking saccades, to avoid using transitional cycles. When selecting PC cycles, care was taken to properly differentiate them from jerk with extended foveation ( $J_{ef}$ ), a similar appearing waveform; if the distance from the apparent end of the saccade and the point of foveation was under  $0.5^\circ$ , the saccade was considered foveating, rather than braking, and the cycle was discarded. By using both  $PP_{fs}$  and PC waveforms from the two subjects, we were able to perform an internal crosscheck, comparing our results both across subjects as well as across the waveforms for each subject.

### 2.2.1 Recording

Some horizontal eye movement recordings were made using infrared reflection (Applied Scientific Laboratories, Waltham, MA). In the horizontal plane the system was

linear to  $\pm 20^\circ$  and monotonic to  $\pm 25\text{-}30^\circ$  with a sensitivity of  $0.25^\circ$ . The IR signal from each eye was calibrated with the other eye behind cover to obtain accurate position information and to document small tropias and phorias hidden by the nystagmus. Eye positions and velocities (obtained by analog differentiation of the position channels) were displayed on a strip chart recording system (Beckman Type R612 Dynograph). The total system bandwidth (position and velocity) was 0-100 Hz. The data were digitized at 400 Hz with 12-bit resolution. The remaining data from S1 were taken from recordings made in the laboratory of Dr. R.M. Steinman using a phase-detecting revolving magnetic field technique. The sensor coils consisted of 9 turns of fine copper wire imbedded in an annulus of silicone rubber molded to adhere to the eye by suction. The signals were digitized at 488 Hz with a resolution of 16 bits. The system's sensitivity was less than one minute of arc, with linearity of one part in 14,014 and drift of 0.2-0.3 minarc/hour. Noise was less than two minarc and eye position was stored to the nearest minarc. Further details of this system can be found elsewhere (Steinman & Collewijn, 1980).

### *2.2.2 Protocol*

Subjects were seated in a chair with headrest and either a bite board or a chin stabilizer, far enough from an arc of red LEDs to prevent convergence effects ( $>5$  feet). At this distance the LED subtended less than  $0.1^\circ$  of visual angle. The room was dimly illuminated to minimize extraneous visual stimuli. Written consent was obtained from subjects before the testing. All test procedures were carefully explained to the subject before the experiment began, and were reinforced with verbal commands during the

trials. An experiment consisted of from one to ten trials, each lasting under a minute with time allowed between trials for the subject to rest. Trials were kept this short to guard against boredom because CN intensity is known to decrease with inattention. All trials were fixation trials with the subject kept stationary; no pursuit or vestibuloocular reflex (VOR) was involved. This research, involving human subjects, followed the Declaration of Helsinki and informed consent was obtained after the nature and possible consequences of the study were explained. The research was approved by an institutional human experimentation committee.

### *2.2.3 Analysis*

Data were sampled at 200 or 488 Hz and were digitized with a resolutions of 12 or 16 bits, respectively. Only eye position was measured directly, with velocity derived from the position data by means of a variable degree central-point differentiator. For a sampling frequency of 488 Hz, the -3 dB cutoff frequency of 55 Hz is slightly lower than the recommendation of 70 Hz by Juhola and Pyykkö (1987). However, careful comparisons of the differentiated signals to unfiltered signals, in both the time and frequency domains, confirmed that the filtering did not change the timing of the saccades, though it could lead to a slight decrease (~10%) in saccadic amplitudes. All analysis was carried out in the MATLAB environment using software written for this study.

Peak velocity: When measuring the peak velocity of the saccade, the velocity of the slow phase must be accounted for. Simply using the peak of the velocity record is not sufficient; the slow-phase velocity at the beginning of the saccade must be added.

Measuring only the velocity from zero to the peak ignores a major portion of the saccade (the segments that occur before the first zero crossing, and after the second zero crossing), leading to a false, low value for the velocity. Winters et al. recognized this when they studied normal saccades in the presence of large velocity VOR (Winters, Nam, & Stark, 1984).

Magnitude: There are several ways to calculate the magnitude of the saccade. The first, and easiest, is simply to use position-derived onset and offset points, and calculate the difference in position at these times. The problem with this approach is that it leads to artificially small saccades, for it doesn't take into account that the eye was moving with great velocity in the other direction and, therefore, took some amount of time to slow and reverse. This is clearly illustrated in Figure 2-1; the position record shows no change in eye position, yet the velocity record clearly indicates that a braking saccade has occurred. This saccade has *zero magnitude*, which would not be possible if the slow-phase velocity had not reduced the saccade's magnitude.

An approximation that may be used to determine "true" saccadic size is: simply calculate the distance the eye traveled between the time the velocity-derived saccade onset occurred and the time the position-derived onset occurred and add this distance to the magnitude obtained by using only the position-derived onset and offset. It must be stressed that this is a first approximation, and that we plan to examine others.

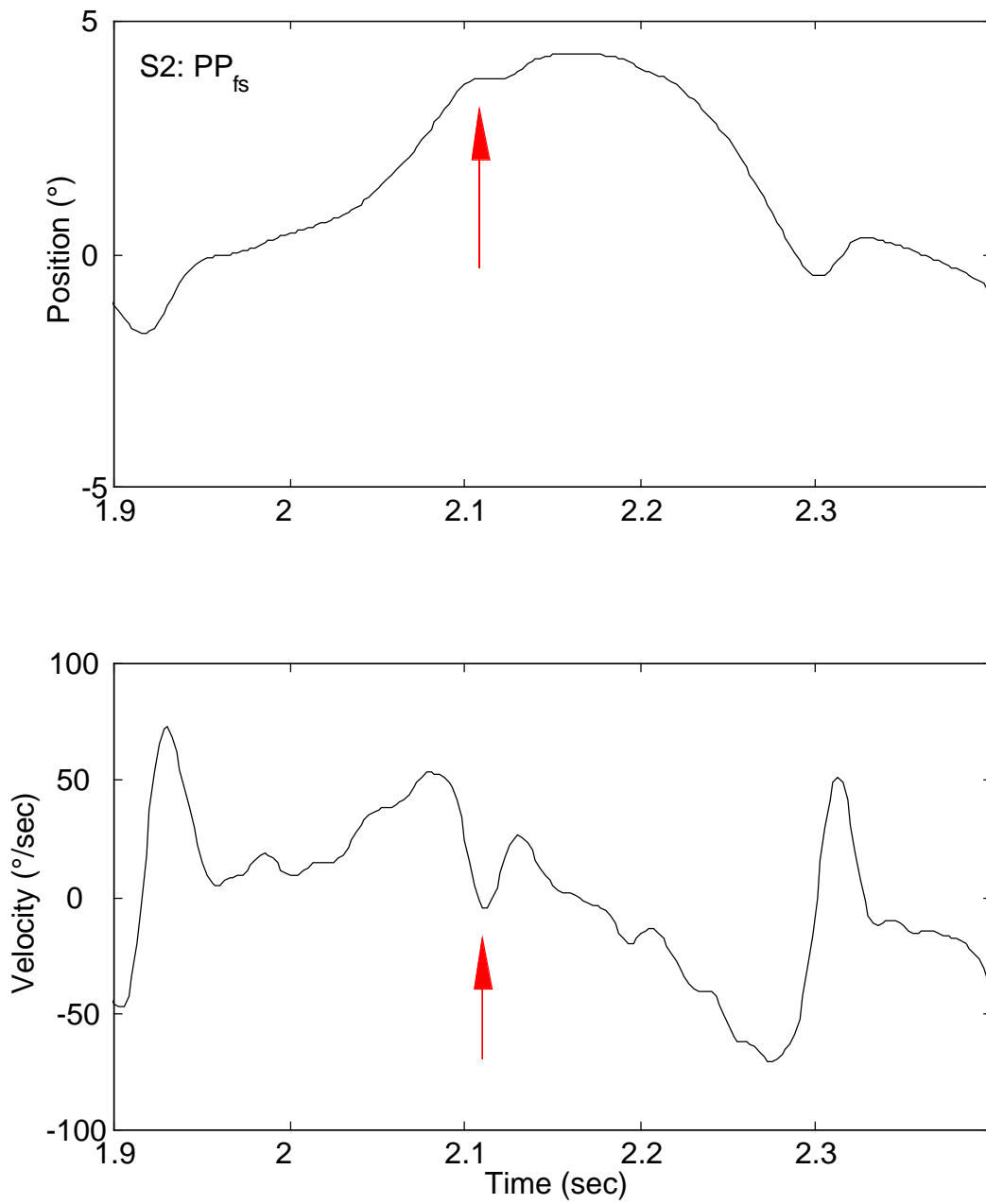


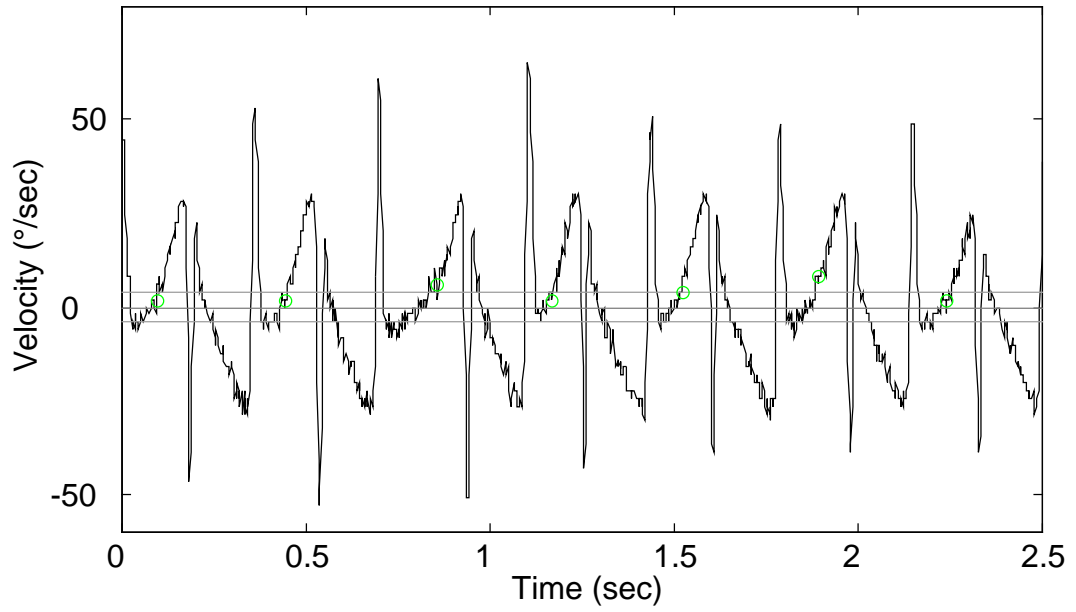
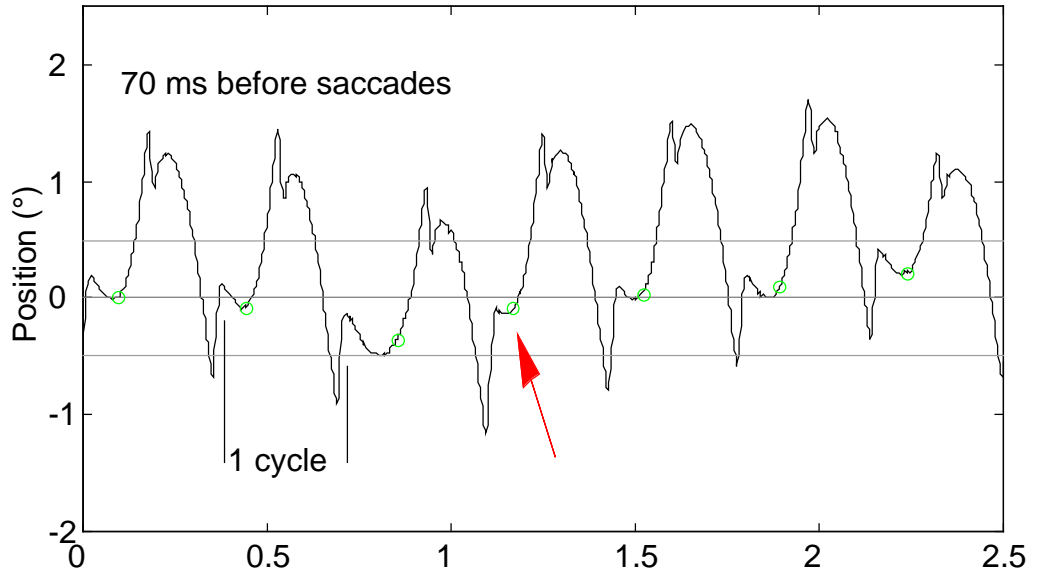
Figure 2-1

A braking saccade of “zero magnitude.” The position trace shows no change in eye position (arrow), yet the velocity trace shows that there is clearly a saccade (arrow).

Period of CN and critical times in the CN cycle: To study CN, a cyclic phenomenon, we must first define when a cycle of CN starts, and when it ends. Dell'Osso et al. chose the center of the foveation period as the beginning of each cycle (and therefore the end of the preceding cycle) (Dell'Osso, Van der Steen, Steinman, & Collewijn, 1992). It is often a difficult task to know where the center of the foveation period is, and no accuracy is lost by choosing the end of the foveating saccade, just prior to the start of the foveation period, as the beginning of a cycle (Figure 2-2A).

Time of Generation: We examined the eye's behavior, looking backwards in time from the beginning of each saccade, starting at -40 ms and working back to -70 ms. We chose -40 ms as the closest time, for this is about the shortest interval Bruce and Goldberg found between when a command could be issued to move the eye and the eye's subsequent movement (Bruce & Goldberg, 1985). The bulk of this delay is distributed in the brainstem, the neuromuscular junction and the contraction time of the extraocular muscle. We stopped at -70 ms because, as can be seen by the arrow in Figure 2-2A, to go much beyond this point would involve moving out of the cycle being examined, and into the previous one. Such results would be meaningless, for the braking saccade is affected only by the events of the cycle in which it occurs. At each time under consideration we first measured the eye's position. If the target was seen to be within the fovea, then the need to make a saccade should not exist. Likewise, if at that time, the velocity was within slip limits, there would be no impetus to generate a saccade to slow the eye. The position and velocity behavior can be summarized in a single plot, known as a phase plane.

A.



B.

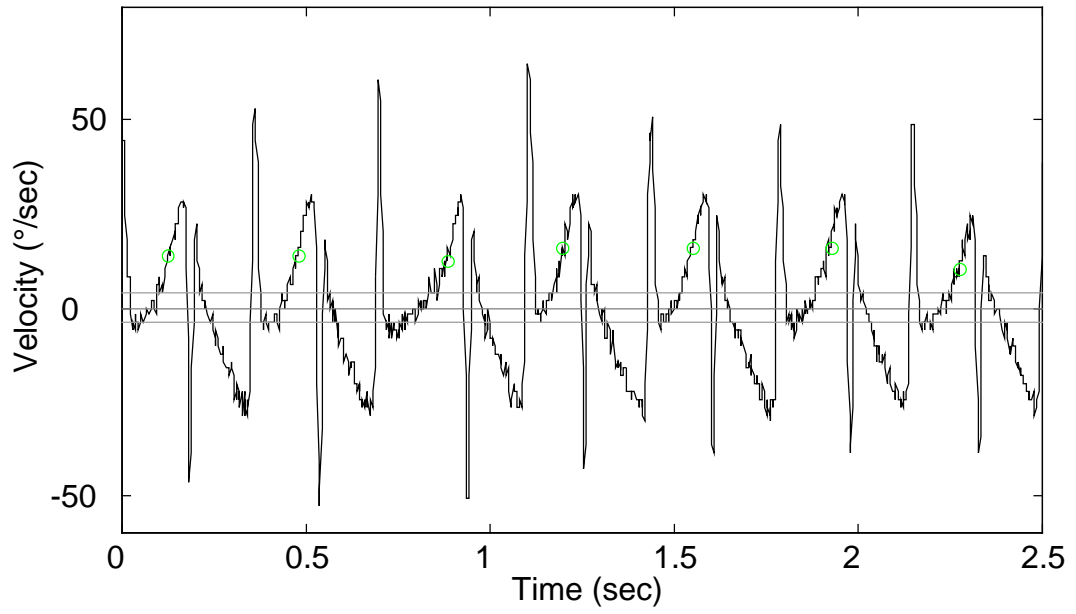
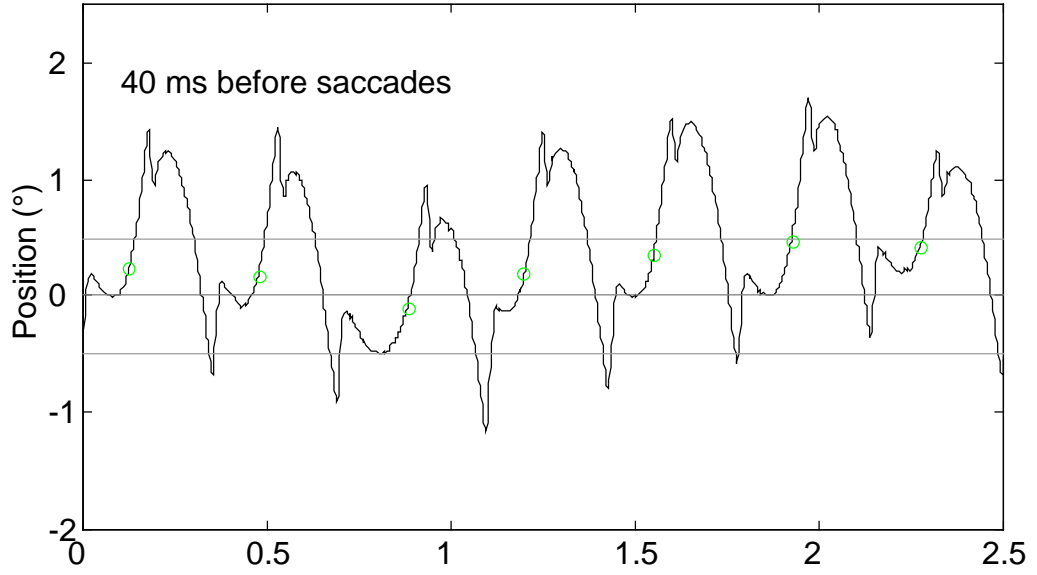


Figure 2-2

Five-second excerpt from S1's  $PP_{fs}$  waveform. The beginning of the cycle has been defined to occur at the end of the foveating saccade which precedes it. A.) One cycle is indicated by the vertical lines in the position trace. Note the reliability and repeatability of the foveation periods. Circles indicate the sample that occurred closest to 70 ms before saccade onset. The majority of these samples fall within the foveal extent. The velocity yields analogous results. The majority of samples at -70 ms fall within the slip velocity limits. B.) As above, but for 40 ms before saccades. Note that position samples are still within the foveal extent, but that velocity samples are well outside slip limits. The point indicated by the arrow is discussed in the text.

Phase plane analysis: Control systems engineers have used phase planes to analyze complex periodic and pseudo-periodic behavior for decades. In a phase plane, one variable is plotted against its derivative, resulting in a trajectory of the system's behavior. Dell'Osso et al. introduced this approach to the study of CN cycles (1992). It is also possible to use the phase plane to look only at a particular aspect of eye movement, as we have done in this study, examining the eye's behavior at discrete times prior to the onset of a saccade. In the center of the phase plane is a box whose limits are the foveal extent ( $\pm 0.5^\circ$ ) and the slip velocity ( $\pm 4.0^\circ$ ), referred to as the "foveation window." Points which appear in this region represent times when the target appears with best acuity, for the target is relatively stable with respect to the fovea, and is imaged on its most sensitive region.

## **2.3 RESULTS**

### *2.3.1 Phase Plane Timing*

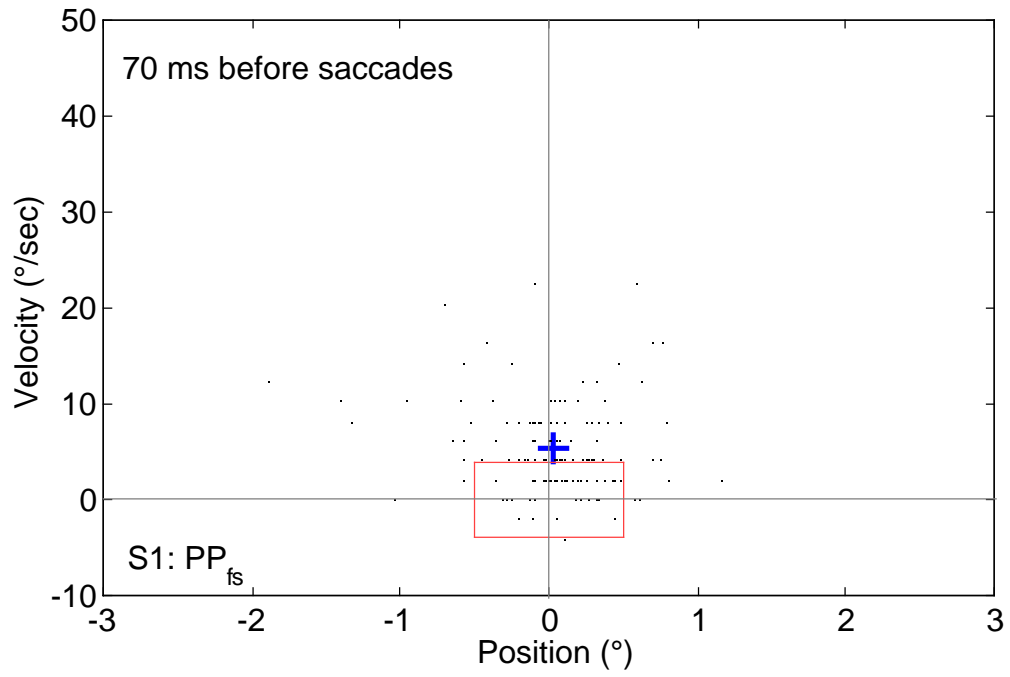
To estimate time of braking saccade generation required examination of both the eye's position and velocity at selected instants in time prior to the actual onset of the saccade. By plotting these points in a phase plane, it was possible to determine when either, both, or neither of the crucial position and velocity criteria were being met. Figure 2-2A shows a five-second excerpt from the position and velocity records of S1, for times when his waveform was  $PP_{fs}$ . This is a very well-behaved, stable CN where the subject

was consistently able to keep his eyes within  $\pm 1^\circ$  of the target throughout the oscillation, and had repeatable foveation periods with durations ranging from 50 to 70 ms. The circles indicate the sample that occurred closest to 70 ms before the onset of the braking saccade, as determined from the velocity-derived criterion. It should be noted that at -70 ms, the vast majority of circles occurred well within the foveal extent of  $\pm 0.5^\circ$ . Similar results can be seen for the velocity record (Figure 2-2B); with few exceptions the velocity fell within the slip-velocity limits. Figure 2-3B shows the phase plane for all saccades recorded from this subject. We calculated the average position and velocity of all the points and plotted it along with the individual points. The average position fell well within the foveal limits, and the average velocity fell at  $5^\circ/\text{sec}$ , just outside the strict  $\pm 4^\circ/\text{sec}$  limit we imposed for minimal decrease in acuity, but still low enough to insure very little blurring.

Figure 2-3B shows the phase plane analysis for points 40 ms before the saccades. As was the case for -70 ms, the average position of the target was still within the fovea, but now the average velocity was well beyond even the most liberal limits for velocity, at about  $15^\circ/\text{sec}$ .

Figure 2-4, analogous to the previous two figures, is for S2 during the intervals that he exhibited PC waveforms. As above, in part A, at 70 ms the average position and velocity were more likely to fall within their respective limits, with the image position just beyond the fovea. In Figure 2-4B, 40 ms prior to saccade onset, both the average position and average velocity were well outside the foveation window, making it less likely to satisfy its slip criterion.

A.



B.

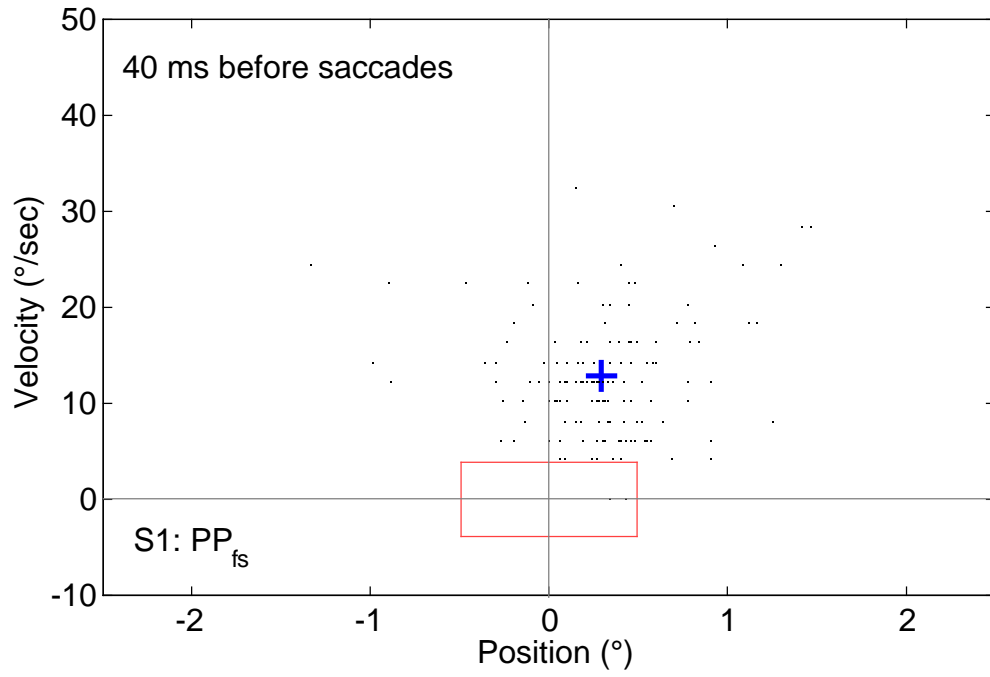


Figure 2-3

Phase-plane representation of S1's PPfs waveform. In this and subsequent Figures, the rectangular box centered around the origin is the foveation window ( $\pm 0.5^\circ$  by  $\pm 4^\circ/\text{sec}$ ) and the crosses represent the position and velocity averages. A.) At 70 ms before saccades, the average position lies within the fovea, and the average velocity is just on the slip velocity border. B.) At 40 ms before saccades, the average position remains on the fovea, but now average velocity is well beyond the slip velocity border.

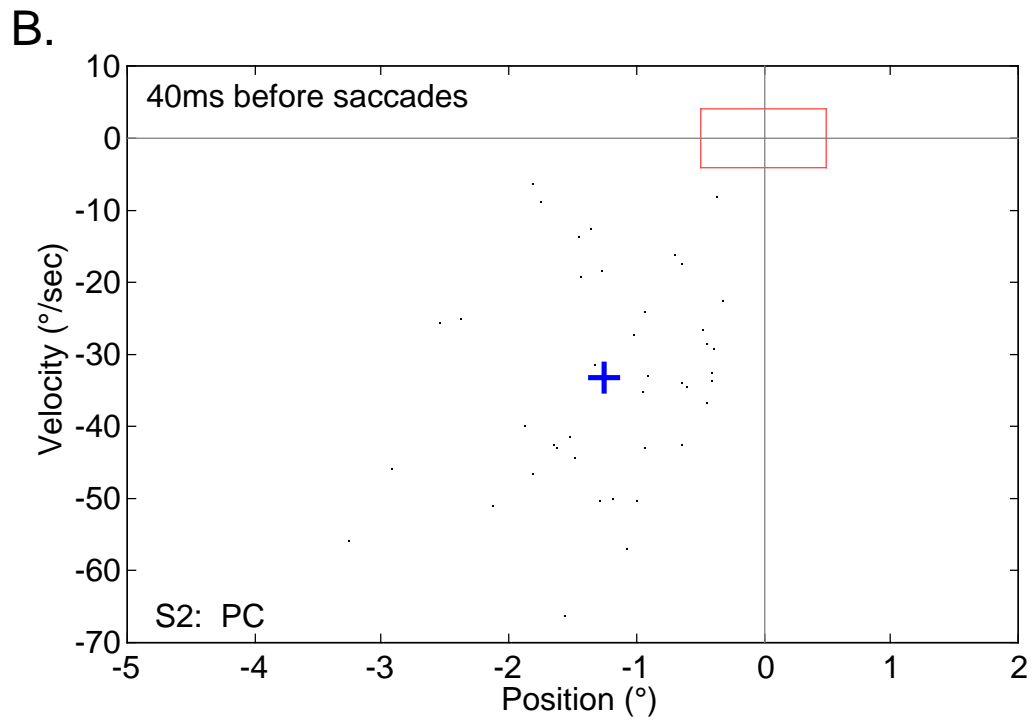
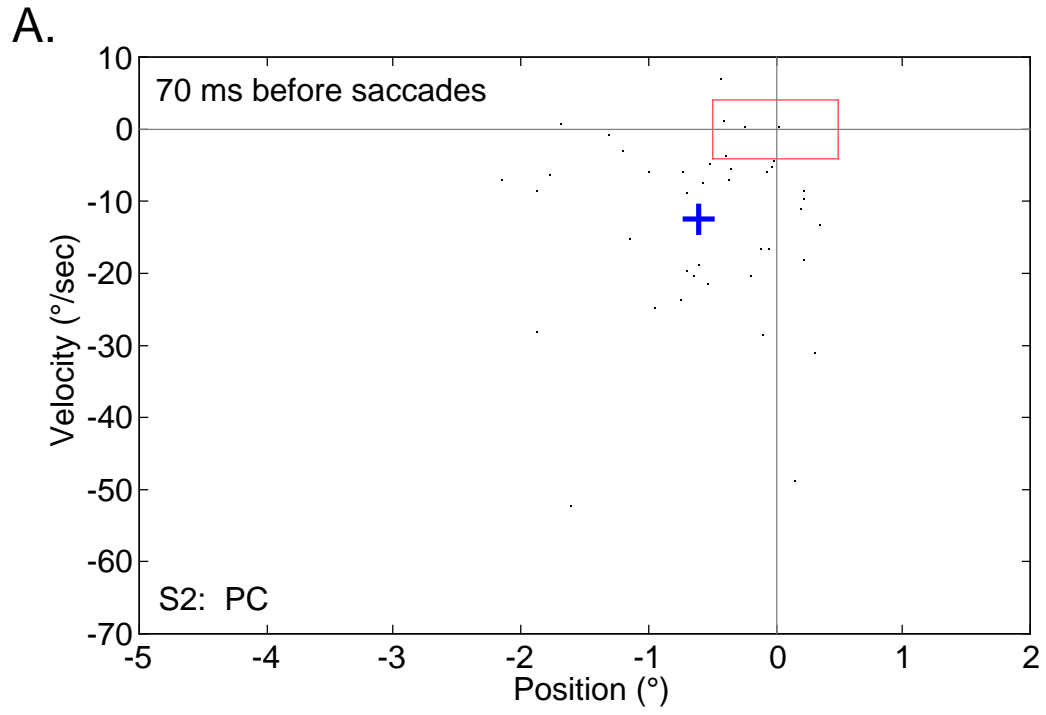


Figure 2-4

Phase-plane representation of S2's pseudocycloid (PC in this and subsequent Figures) waveforms. A.) At 70 ms before saccades, the average position is just on the edge of the fovea, while average velocity is  $12^\circ/\text{sec}$ . B.) At 40 ms before saccades, both the average position and average velocity have moved far beyond the limits for good visual acuity.

### 2.3.2 Braking Effect

Because braking saccades are purported to slow the eye, we calculated how effective they were by taking the absolute difference (the velocity of the slow phase just prior to beginning of the saccade minus the velocity of the slow phase just after completion of the saccade) and also expressing braking as a percentage reduction (difference/presaccadic velocity). S1's PC, and S2's PP<sub>fs</sub> results were similar. In both subjects, for *both* their waveforms, the saccades acted to slow the eye. However, the range of the effect differed for each waveform. For S1's PP<sub>fs</sub>, the braking ranged from about a 20% reduction for the less effective saccades, to 100% for saccades that completely stopped the eye, to >100% for saccades that caused eye to reverse its direction. The average amount of braking was 61.99%. For the PC waveform, the saccade *always* acted to change the direction of the eye, regardless of subject, so the amount of braking seen was always greater than 100%. For S2 this range was as high as 146.9%, with an average slowdown of 119.4%. Table 2.1 details the average and maximum braking effect for both waveforms in each subject.

Table 2.1. Braking Effect

Subject	Waveform			
	PP <sub>fs</sub>		PC	
	Mean %	Max %	Mean %	Max %
S1	61.99*	128.6	125.5	151.6
S2	74.4	100	119.4	146.9

\* Subject's preferred waveform

### *2.3.3 Saccade Duration Effect*

We next determined if the magnitude of the braking saccade influenced the duration of the CN cycle. Figure 2-5A shows a plot of intercycle interval vs. the magnitude of the braking saccade. As the magnitude of the braking saccade increased, there was a general decrease in the time between successive cycles. For a more qualitative illustration of this phenomenon, Figure 2-5B shows a several-second record of a switch between pendular with foveating saccades ( $P_{fs}$ ) and  $PP_{fs}$  waveforms for S1. As can easily be seen, when there was no braking saccade ( $P_{fs}$ ), the eye traveled further from the target before reversing and returning to primary position. This extra distance led to an increase in the time between successive cycles. Compare this to the case when a braking saccade was present ( $PP_{fs}$ ): the maximum excursion was reduced, leading to a shorter time between cycles. We calculated the nystagmus acuity function (NAF) (Sheth, Dell'Osso, Leigh, Van Doren, & Peckham, 1995) for each waveform in both subjects. For S1, the NAF was 0.603 during  $PP_{fs}$  and decreased by approximately 50-66% (0.301 - 0.218) during PC. For S2, the NAF was 0.271 for the PC waveform and the  $PP_{fs}$  waveform was too transient to calculate an NAF (i.e., no runs greater than 1.5 sec were found).

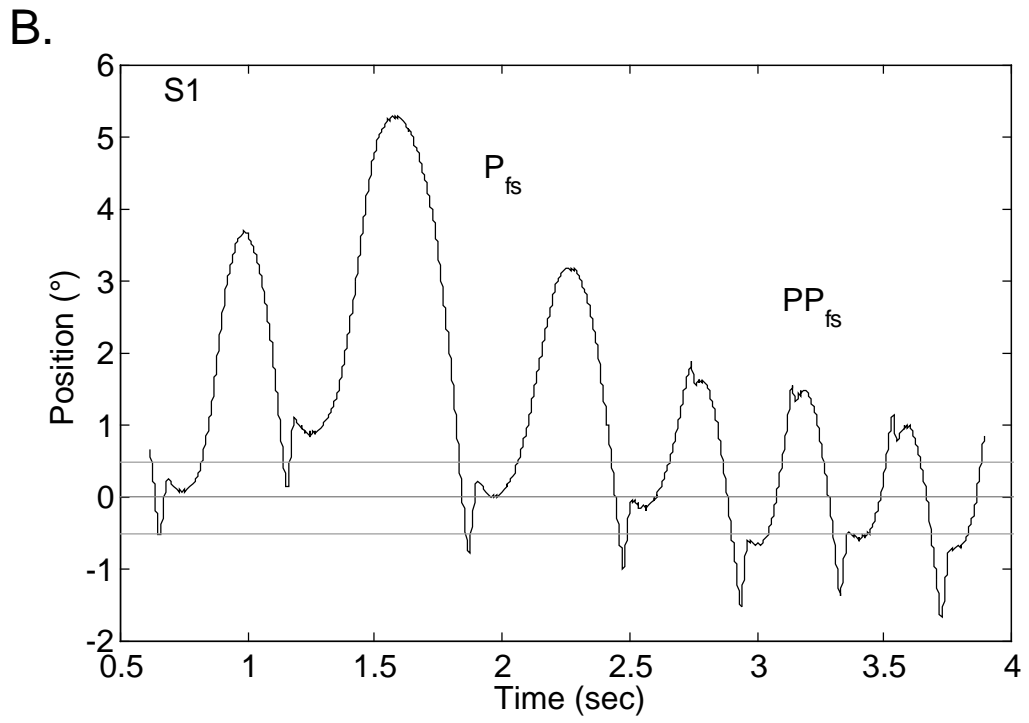
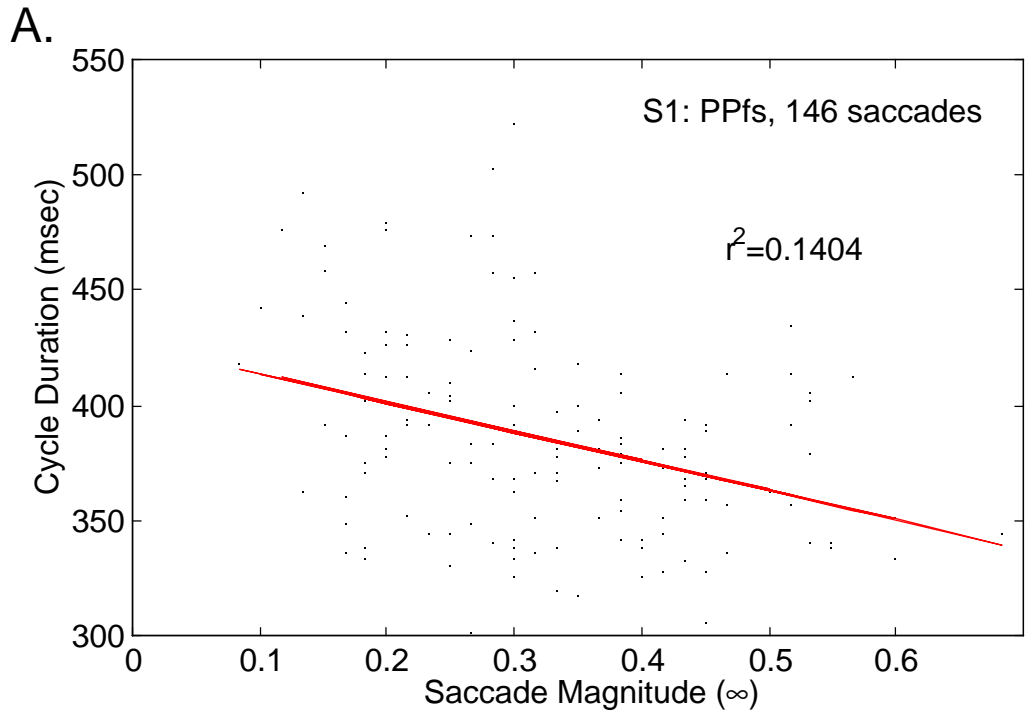


Figure 2-5

A.) Cycle duration vs. braking saccade magnitude for S1. B.) Transition between pendular with foveating saccades ( $P_{fs}$ ) and  $PP_{fs}$ . Note the increased magnitude and duration of the slow phase when there is no braking saccade to oppose the runaway.

### *2.3.4 Saccade Magnitude Effect*

We next investigated whether the amount of braking effect was dependent on the magnitude of the braking saccade. For S1's PP<sub>fs</sub> waveform, there did not appear to be a discernibly strong relationship between the size of the saccade and the amount of braking that it provided. For S2's PC waveform, again, no strong relationship between saccade magnitude and braking slowdown was observed.

### *2.3.5 Initial Position and Velocity Effects*

To answer the question of whether the magnitude of the braking saccade depends on the behavior of the eye at the time of generation, we considered the position, velocity and acceleration of the eye at various times from 40 ms to 70 ms before saccade onset. For neither S1's PP<sub>fs</sub> nor S2's PC waveforms, was there any dependence of the size of braking saccades on either eye position, velocity, or acceleration at any time between 40 and 70 ms prior to the saccade. Thus, any size braking saccade may occur no matter what the initial conditions of the eye's motion.

## **2.4 DISCUSSION**

The goals of this study were to investigate the conditions for the generation of braking saccades and their effect on CN waveforms and to test the hypothesis that braking saccades are primarily determined by eye velocity. This included determining

which criteria (the position and velocity signals that the ocular motor system may monitor) are used to decide when there is a need to slow the eye, as well as the time at which the braking saccade is programmed. We chose position and velocity because they are the most important variables in determining visual acuity; the target image must be within the central one degree of vision (on the fovea), and must not be moving too rapidly across the retina (slip-velocity limit).

Our results suggest the velocity criterion is the stronger of the two, based on the results of Figures 2-4 and 2-5. The eye's behavior 70 ms before the onset of the braking saccade indicates that its mean velocity still remains within the slip-velocity limit established during the previous foveation period. Therefore, given the velocity requirements necessary for good visual acuity, there is no compelling need to slow the eye further and there should be no impetus to generate a braking saccade. When, on the other hand, we consider the eye at 40 ms before onset, the mean eye *velocity* increases to a value well beyond even the most generous upper value for the slip-velocity limits, prompting a need to slow the eye's runaway and leading to the generation of a braking saccade. These data suggest that the time at which the saccade is programmed is more likely to be nearer -40 ms than -70 ms.

Using this same reasoning, it appears that the position criterion is not important for the triggering of a braking saccade because, at all times between 40 and 70 ms before saccade onset, the mean eye position remains within the foveal extent, and thus, there is no reason to change the eye's *position*.

These results are also intuitively pleasing, for the braking saccade does not appear to be affected by visual input. We state this based on several observations: First, the braking saccade leads to no significant change in the position of the eye, as would be expected if the ocular motor system were reacting to a target (such as the change caused by a foveating saccade). Second, the duration of the low-velocity period following the completion of a braking saccade (which can be seen as analogous to the foveation period which follows a foveating saccade), is considerably shorter, ranging from 10 ms to 40 ms (mean =  $20.3 \pm 6.02$  ms), than that of the foveation period. Foveation periods ranged from 50 ms to well over 100 ms in both these subjects; in other subjects they have been measured to be up to 450 ms. Additionally, the magnitudes of braking saccades were fairly constant, not appearing to have any strong dependence on where the eye was pointing at the suspected time of generation. Finally, this conclusion is strengthened by noting that waveforms with braking saccades still appear when the subject is in the dark with no target.

We found that the size of the saccade that is programmed does not depend on the position, velocity or acceleration of the eye at the time the decision to generate a braking saccade was made. This suggests that the braking saccade is an automatic response to the monitored velocity signal rising above threshold, requiring a minimum of processing time. This is consistent with our selection of 40 ms before saccade onset as the time at which the saccade is most likely generated. The qualitatively similar, though quantitatively different, results seen for the different waveforms in each subject may be due to the fact that each subject appears to have a “favored” waveform, and tends to use

that waveform to achieve his best visual acuity. When S1's CN shifted to the secondary waveform, the NAF, and hence acuity, tended to decrease. For S2, the secondary waveform was merely a transient occurrence of several cycles at a time and could not be used to calculate visual acuity over a 2-5 sec interval. As a consequence of the shift from primary to secondary waveform, the position and velocity criteria for generating a braking saccade may have been relaxed to reflect this lessened demand on the visual and ocular motor systems. This is mostly in agreement with the conclusion reached by Abadi & Dickinson (1986), although we stress that their "waveform shape" should not be read to simply mean "waveform." For example, in their prior work (Dickinson & Abadi, 1985) they suggested that PC waveforms yielded better sensitivity than did pendular (P) or  $P_{fs}$  waveforms, owing to longer foveation periods in the PC case. However, we have shown that it is possible for at least one subject (S1) to consistently display  $PP_{fs}$  cycles with longer low-velocity intervals than seen in his PC cycles; the crucial factor is foveation time in the waveform, not the waveform itself.

The main benefit of the braking saccade appears to be an increase in NAF and visual acuity. As shown above in Figure 2-5B, when the braking saccades are made, the time between corresponding points of successive CN cycles has been decreased, which means that the frequency of the nystagmus has been *increased*. At first, this might appear to be a paradox: an increase in nystagmus frequency leading to an increase in visual acuity. In reality, there is no contradiction, for when considering visual acuity, frequency is *not* the important feature of the waveform. Instead, one must consider the *foveation periods*, which are the times when the target is within the fovea and moving slower than

the slip velocity limit with respect to it. Visual acuity in CN is highest when these foveation periods are repeated reliably from cycle to cycle. (Dell'Osso et al., 1992) Note that when the CN is of low amplitude, the braking saccade can actually bring the eye near the target, giving a “double shot” of foveation for that particular cycle. In these cases we expect, and have demonstrated, (Dell'Osso et al., 1992) that acuity would increase even more, for there are now two separate foveation periods in one CN cycle, although (as mentioned above) the one following the braking saccade is of shorter duration.

The braking saccade appears to serve just as its name suggests, applying the brakes to a runaway ocular motor system. In all CN cycles we examined, the braking saccade slowed the eye, and in some cases stopped it, or even caused it to reverse direction. As shown above, the PC waveform *always* experienced a reversal in velocity while the PP<sub>fs</sub> only rarely was completely halted or reversed. Braking saccades appear to function in the same way as vestibular or optokinetic fast phases.

Note that the braking saccade seen in the PC waveform looks, at first glance, to be a foveating saccade. This is not the case, however, for the saccade does *not* serve to bring the fovea to the target, but instead stops short, requiring that the slow eye movement system must complete the motion. It is also worth mentioning that the duration of slow-velocity periods following PC braking saccades was longer than those that follow PP<sub>fs</sub> braking saccades in our subjects. This re-emphasizes that the periods following braking saccades can either serve a visual purpose (foveation), as for PC waveforms, or not, as for PP<sub>fs</sub> waveforms.

The velocity criterion that we have found appears to be necessary but not always sufficient to generate a braking saccade. As noted above, there are very similar CN waveforms which appear to differ only by whether a braking saccade is present (e.g.,  $P_{fs}$  and  $PP_{fs}$ ). The decision to include a braking saccade may also depend on the specific and varied demands the subject makes of their visual system at the time, i.e., if their visual acuity is not sufficient for the task at hand then the interjection of braking saccades may act to increase acuity as needed.

## 2.5 WORKS CITED

- Abadi, R. V., & Dickinson, C. M. (1986). Waveform characteristics in congenital nystagmus. *Doc Ophthalmol*, **64**, 153-167.
- Bruce, C. J., & Goldberg, M. E. (1985). Primate frontal eye fields. I. Single neurons discharging before saccades. *J Neurophysiol*, **53**, 603-635.
- Dell'Osso, L. F., & Daroff, R. B. (1975). Congenital nystagmus waveforms and foveation strategy. *Doc Ophthalmol*, **39**, 155-182.
- Dell'Osso, L. F., & Daroff, R. B. (1976). Braking saccade--A new fast eye movement. *Aviat Space Environ Med*, **47**, 435-437.
- Dell'Osso, L. F., Averbuch-Heller, L., & Leigh, R. J. (1997). Oscillopsia suppression and foveation-period variation in congenital, latent, and acquired nystagmus. *Neuro Ophthalmol*, **18**, 163-183.
- Dell'Osso, L. F., Gauthier, G., Liberman, G., & Stark, L. (1972). Eye movement recordings as a diagnostic tool in a case of congenital nystagmus. *Am J Optom Arch Am Acad Optom*, **49**, 3-13.

- Dell'Osso, L. F., Van der Steen, J., Steinman, R. M., & Collewijn, H. (1992). Foveation dynamics in congenital nystagmus I: Fixation. *Doc Ophthalmol*, **79**, 1-23.
- Dickinson, C. M., & Abadi, R. V. (1985). The influence of nystagmoid oscillation on contrast sensitivity in normal observers. *Vision Res*, **25**, 1089-1096.
- Juhola, M., & Pyykkö, I. (1987). Effects of sampling frequencies on the velocity of slow and fast phases of nystagmus. *Int J Bio Med Comp*, **20**, 253-263.
- Sheth, N. V., Dell'Osso, L. F., Leigh, R. J., Van Doren, C. L., & Peckham, H. P. (1995). The effects of afferent stimulation on congenital nystagmus foveation periods. *Vision Res*, **35**, 2371-2382.
- Steinman, R. M., & Collewijn, H. (1980). Binocular retinal image motion during active head rotation. *Vision Res*, **20**, 415-429.
- Winters, J. M., Nam, M. H., & Stark, L. W. (1984). Modeling dynamical interactions between fast and slow movements: Fast saccadic eye movement behavior in the presence of the slower VOR. *Math Biosci*, **68**, 159-185.

## Chapter 3

# CHARACTERISTICS OF BRAKING SACCADES IN CONGENITAL NYSTAGMUS

### 3.0 ABSTRACT

Several of the characteristic waveforms of congenital nystagmus (CN) contain braking saccades. We test the hypothesis that braking (including foveating) saccades, while not always satisfying the standard relationships for saccades, are normal; any differences are due to the presence of large-velocity, slow-phase eye movements. Better measurements of saccadic properties, including position- and velocity-based measures and skewness, can eliminate some of this apparent distortion. We also evoked an analogous effect in normal subjects by use of a ramp-step-ramp stimulus. Finally we used a model to further demonstrate this distortion in the saccades of normals, deviating from their intended magnitude as a function of the magnitude of the opposing velocity. The saccadic analysis methods developed herein are applicable to all saccades made during ongoing eye movements, either normal or pathological. The above findings support the hypothesis that the braking saccades integral to many CN waveforms are normal and the result of a normal saccadic system's responses to the oscillation.

### 3.1. INTRODUCTION

For over twenty-five years, a standard set of relationships has been used to relate the magnitude of a saccade to its duration and peak velocity (Zuber & Stark, 1965; Yarbus, 1967; Boghen, Troost, Daroff, Dell'Osso, & Birkett, 1974; Bahill, Clark, & Stark, 1975). Although the relationship is generally good, there is a scarcity of data for small saccades ( $<1^\circ$ ), and the different studies do not fully agree with one another. Furthermore, these relationships are frequently represented as lines, suggesting that saccades must lie on, or very near, them lest they be considered “abnormal.” While this is a useful didactic device, it is somewhat of an oversimplification, as it ignores the inherent variability of biological systems. Indeed, these saccadic relationships vary from person to person, and can even vary within the same subject (Boghen et al., 1974). Boghen et al. was also one of the few studies to include variability in the curves, calculating 95% confidence intervals for high and low peak saccadic velocities. Properly put, even in the hypothetical “normal” or “average” subject, the so-called saccadic “main sequence” is not nearly as exact—or limited—as its astronomical name suggests. (In astronomy, the main sequence is a very narrow band in a diagram of a star’s luminosity versus its apparent temperature; a star’s position in this band depends on its mass (Shu, 1982). This is not a permanent property of the star, however, for it lies along the main sequence only during the first epoch—its hydrogen-burning phase—of its existence; as it evolves, it will move out of this band and will follow one of many possible paths. Indeed, only a small fraction of the observable universe occupies the main sequence.) Despite the use of this

term by some, what is really being described is a much more relaxed fit—sometimes approaching a cloud—to these lines (Van Opstal & Van Gisbergen, 1989).

Saccades can also fail to follow these standard relationships for a variety of reasons, not limited to ingestion of alcohol or other drugs (Abel & Hertle, 1988), neurological diseases such as Huntington's chorea or spinocerebellar degeneration (Zee, Optican, Cook, Robinson, & Engel, 1976), or even the normal aging process (Sharpe & Zackon, 1987; Abel & Dell'Osso, 1988; Hainline, 1988). These saccades generally have a smaller peak velocity and greater duration, although it is possible, for example, to encounter faster, shorter saccades in myasthenia gravis (Schmidt, Dell'Osso, Abel, & Daroff, 1980a; Schmidt, Dell'Osso, Abel, & Daroff, 1980b; Wirtschafter & Weingarden, 1988). It has also been shown that saccades elicited under different conditions (e.g., visual vs. non-visual) conditions can have greatly different properties, with visually evoked saccades being faster and shorter in duration than saccades made to remembered targets (Sharpe, Troost, Dell'Osso, & Daroff, 1975; Smit, Van Gisbergen, & Cools, 1987a; Whittaker & Cummings, 1990) or those made during antisaccade paradigms (Smit, Van Gisbergen, & Cools, 1987b). These differences may be attributed, in part at least, to the effects of higher cortical processing.

In previous work (Jacobs, Erchul, & Dell'Osso, 1996; Jacobs, Dell'Osso, & Erchul, 1999) we examined *braking saccades* (Dell'Osso & Daroff, 1976)—small, somewhat stereotyped, apparently non-visually driven, fast eye movements that act to oppose (i.e., brake) the large slow-phase velocities (often in the range of 40-50°/sec or even faster) seen in congenital nystagmus (CN), an oscillation probably originating in the

smooth pursuit system (Dell'Osso, Gauthier, Liberman, & Stark, 1972; Dell'Osso, Averbuch-Heller, & Leigh, 1997). Many CN waveforms also contain *foveating* saccades, which are braking saccades that also foveate the target. Braking saccades appear in several waveforms, including pseudopendular (PP), pseudopendular with foveating saccades (PP<sub>fs</sub>), pseudocycloid (PC), bidirectional jerk (BDJ), triangular (T) and pseudojerk (PJ) (Dell'Osso & Daroff, 1975). During our initial analysis of these saccades, we discovered that they did not always fit the standard relationships (Jacobs et al., 1996; Jacobs & Dell'Osso, 1997), and for some subjects could appear slower than “normal.” This caused us some concern, for nonstandard saccades can suggest the possibility of pathology, yet all the data came from subjects with idiopathic CN and no known neurological deficits.

We hypothesize that braking saccades (including foveating saccades) are, in fact, normal saccades and that they do not fit the standard relationships simply because they occur in the presence of, and act to oppose, CN's large slow-phase velocities that tend to confound the accurate measurement of braking-saccade properties. We examined the techniques and assumptions usually made for the measurement of saccades, paying particular attention to the question of when saccades can be said to begin and to end, based on both position and velocity information.

## **3.2. METHODS**

### *3.2.1 Subjects*

Data for this study came from seven CN subjects, five recorded explicitly for this study and two previously recorded in this laboratory, as well as four normal subjects who participated in the complementary ramp-step-ramp paradigm (discussed at the end of this section). Subjects are summarized in Table 1. All CN subjects had idiopathic CN without any acquired nystagmus and all subjects were healthy, with no neurological deficits. The CN subjects' waveforms included either  $PP_{fs}$  or PC cycles, and two subjects (S5 and S7) contained both. In primary gaze, S5's waveform was usually  $PP_{fs}$ , with PC occurring only at extreme gaze angles ( $40^\circ$  left gaze). S7's CN was mainly PC in primary gaze, with occasional intervals of  $PP_{fs}$ . S7 had not been recorded extensively at other gaze angles, and consequently only the data for straight-ahead viewing was used. S2 and S6's waveforms contained predominantly  $PP_{fs}$  cycles, whereas S1, S3 and S4 displayed predominantly PC cycles. Records were chosen for study only if they contained repeated runs of braking saccades, to avoid using transitional cycles. When selecting PC cycles, care was taken to properly differentiate them from jerk with extended foveation, a similar-appearing waveform; if the distance from the apparent end of the saccade and the point of foveation was under  $0.5^\circ$ , the saccade was considered "foveating," rather than braking, and the cycle was discarded. By using both  $PP_{fs}$  and PC waveforms from two subjects, we were able to perform an internal crosscheck, comparing our results both

across subjects as well as across the waveforms for each subject. For S5 and S6's PP<sub>fs</sub> waveforms, we also analyzed foveating saccades for comparison with braking saccades.

TABLE 1. Summary of subjects used for this study

	Subject	Sex	Age	Waveform	Number of Saccades	Method
CN	1	M	33	PC*	116	IR
	2	F	49	PP <sub>fs</sub> —BS	66	IR
	3	F	14	PC	139	IR
	4	F	25	PC	214	Coil
	5	M	43	PP <sub>fs</sub> —BS	146	IR
				PP <sub>fs</sub> —FS	118	IR
			58	PC	31	Coil
	6	M	28	PP <sub>fs</sub> —BS	126	IR
				PP <sub>fs</sub> —FS	126	IR
	7	M	13	PP <sub>fs</sub> —BS	44	IR
PC				42	IR	
					Total: 1168	
Normal	8	F	47	RSR	178	IR
	9	M	40	RSR	187	IR
	10	F	33	RSR	168	IR
	11	M	28	RSR	180	IR
					Total: 713	

- \* PC waveforms have only braking saccades
- PP<sub>fs</sub> — pseudopendular with foveating saccades
- PC — pseudocycloid
- BS — braking saccades
- FS — foveating saccades
- RSR — ramp-step-ramp paradigm

### *3.2.2 Recording*

Some horizontal eye movement recordings were made using infrared reflection (Applied Scientific Laboratories, Waltham, MA). In the horizontal plane, the system was linear to  $\pm 20^\circ$  and monotonic to  $\pm 25\text{-}30^\circ$  with a sensitivity of  $0.25^\circ$ . The IR signal from each eye was calibrated with the other eye behind cover to obtain accurate position information and to document small tropias and phorias hidden by the nystagmus. Eye positions and velocities (obtained by analog differentiation of the position channels) were displayed on a strip chart recording system (Beckman Type R612 Dynograph). The total system bandwidth (position and velocity) was 0-100 Hz. The data were digitized at 400 or 500 Hz with 12- or 16-bit resolution. The remaining data were recorded by means of a phase-detecting revolving magnetic field technique. The sensor coils consisted of 9 turns of fine copper wire imbedded in an annulus of silicone rubber molded to adhere to the eye by suction. The signals were digitized at 488 or 500 Hz with a resolution of 16 bits. The system's sensitivity was less than one minute of arc, with linearity of one part in 14,014 and drift of 0.2-0.3 minarc/hour. Noise was less than two minarc and eye position was stored to the nearest minarc. Further details of this system can be found elsewhere (Steinman & Collewijn, 1980).

### *3.2.3 Protocol*

Written consent was obtained from subjects before the testing. All test procedures were carefully explained to the subject before the experiment began, and were reinforced with verbal commands during the trials. Subjects were seated in a chair with headrest and

either a bite board or a chin stabilizer, far enough from an arc of red LEDs to prevent convergence effects (>5 feet). At this distance the LED subtended less than  $0.1^\circ$  of visual angle. The room light could be adjusted from dim down to blackout to minimize extraneous visual stimuli. A CN experiment consisted of from one to twelve trials, including required *monocular* and *binocular* calibrations, each lasting up to one minute with time allowed between trials for the subject to rest. Trials were kept short to guard against boredom because CN intensity is known to decrease with inattention. All trials were fixation trials with the subject kept stationary; no pursuit or vestibuloocular responses (VOR) were involved.

Ramp-step-ramp (RSR) experiments were performed monocularly and consisted of eight trials of up to 75 seconds of a random series of constant-velocity ramps of 10, 20, and  $30^\circ/\text{sec}$  interrupted in the center by a step (of 1, 5, or  $10^\circ$ ) that was either in the same direction as the ramp or in opposition (“with” and “against” cases). The step was then followed by the resumption of pursuit at the same velocity. Each subject was presented with 3 of every possible combination of ramp and step. Prior to the pursuit trials, the subjects were presented with two series of target jumps of the same magnitude as the steps, but without the pursuit ramp, to provide a baseline for saccadic parameters.

#### 3.2.4 Analysis

Only eye position was sampled directly, with velocity derived from the position data by means of a variable degree central-point differentiator. All analysis was carried

out in the MATLAB environment (The MathWorks, Natick, MA) using software written for this study.

*Saccade Duration:* To calculate the properties of a braking saccade, we are interested in its beginning, its end, and the point at which the maximum saccadic velocity is reached. However, these measures are not as straightforward as one might hope, because braking saccades are made in the presence of a high-velocity, accelerating slow phase that has a confounding effect on them. When examining the position record, the first inclination might be to state that the beginning of the saccade occurs when the eye position reaches a local maximum (or minimum) and then reverses itself (Figure 3-1). Similarly, we might consider the end of the saccade to be the time when the eye resumes its movement in the opposite direction. If not for the presence of the CN oscillation and its associated velocity, this would be a reasonable approach. This can be seen by examining the velocity record. The beginning of a saccade made in the presence of a non-negligible slow-phase velocity can be determined in the same manner as that of a saccade when the slow-phase velocity is zero, or nearly so. The saccade appears as a large “V”-shaped event, with its beginning and end marked by the outer points of the “V”, i.e., the points at which the velocity reverses (Figure 3-1). This differs from the usual method (used later for saccadic outputs from the model), where the first point that exceeds a threshold baseline velocity ( $5^\circ/\text{sec}$ ) is considered the point of onset. This is because in CN there is no reliable velocity baseline, as the slow-phase velocity is accelerating. The difference between these two methods is quite minor, fortunately, generally just a sample point, leading to potential errors of  $\pm 2$  msec (at 500 Hz) at either end.

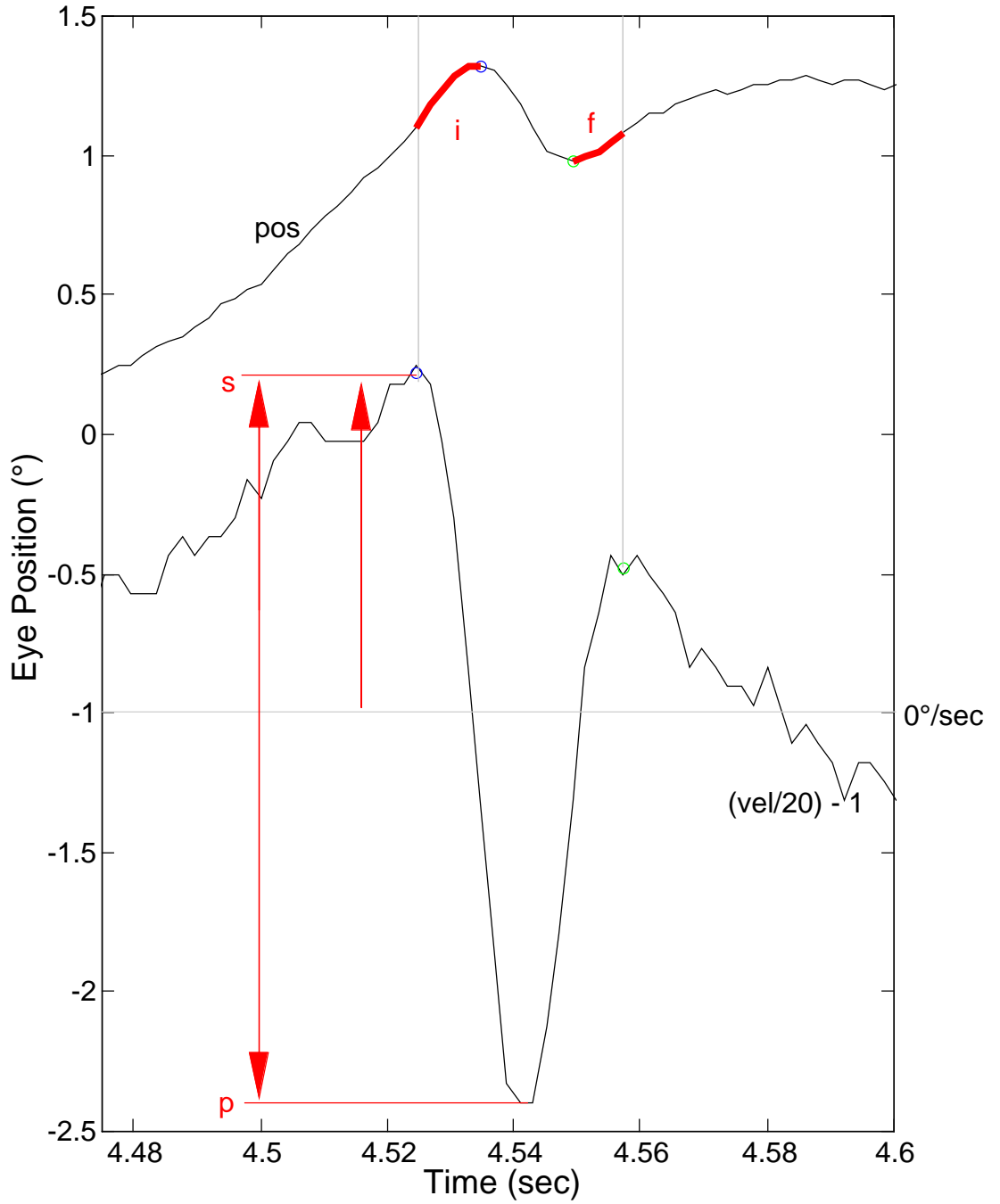


Figure 3-1

A schematic representation of the determination and differences between points of saccadic onset and offset. Top trace shows position, bottom shows velocity (divided by 20 and shifted for clarity). The two dotted vertical lines represent the beginning- and end-points of the saccade as determined by the velocity data. Note that these points occur earlier and later than their position-derived points, respectively. The single-headed arrow shows the value of slow-phase velocity ('s') preceding the saccade, whose apparent peak velocity is 'p'; the double-headed arrow shows the proper peak-velocity measurement, including the velocity of the preceding slow phase (p + s). The heavy segment, 'i,' on the position trace is the distance the eye traveled between the time the velocity- and position-derived saccade onsets. Similarly, the segment 'f' is the distance traveled between position- and velocity-derived saccade offsets.

However, comparison of these onset/offset pairs will show that the saccadic onset derived from the position record does not correspond with the onset derived from the velocity record; nor do the offsets. The velocity-derived onset occurs several milliseconds before the position-derived onset, and the velocity-derived offset occurs after the position-derived offset. Specifically, the position-derived points occur between the velocity-derived points (Figure 3-1) at the zero-crossings of the saccadic velocity record, as would be expected since the position-derived offsets mark the points where the eye has changed direction and, therefore, briefly has no velocity. If there were no slow-phase velocity, the position- and velocity-derived points would correspond.

We considered the use of acceleration-derived onset/offset points, in the hope that they would help us further segregate the effects of the slow-phase velocity from the saccade dynamics. However, even after filtering, the acceleration signal was too noisy to allow reliable identification of onset/offset points in any consistent fashion. This added an extra level of uncertainty on the order of  $\pm 2-3$  samples for each point, which in some cases could coincide with the timing of the velocity-derived points, or could even be less reliable.

*Peak velocity:* When measuring the peak velocity of a braking saccade, once again the velocity of the slow phase must be accounted for. Simply measuring the peak of the velocity record is not sufficient, the slow-phase velocity at the beginning of the saccade must be added. This is also illustrated in Figure 3-1. To count only the velocity from zero to the peak ('p') ignores a major portion of the saccade (the segments that

occur before the first zero crossing, and after the second zero crossing) and therefore leads to a false, low value for the velocity. Winters, Nam, & Stark recognized this when they studied normal saccades in the presence of large-velocity VOR (1984). Therefore, we must add the magnitude of the initial slow-phase velocity ('s') to obtain a more accurate measurement of peak velocity (indicated by the double-headed arrow).

*Magnitude:* We considered several methods of calculating the magnitude of a braking saccade. The first, and easiest, is simply to use the position-derived onset and offset points, and calculate the difference in position at these times. The problem with this standard approach (used for normal saccades between stationary targets) is that it leads to artificially small measures of amplitude, for it doesn't take into account that the eye was moving with great velocity in the other direction due to the CN and therefore took some amount of time to slow and reverse. As an analogy, consider a car with manual transmission, waiting at a stop light, facing uphill. Suppose the driver takes his foot off the brake when the light turns green, but it takes him a second or so to let out the clutch. The car will begin rolling downhill, accelerating with gravity, its backwards velocity growing rapidly. When the driver finally does engage the clutch, the car will begin to slow but will continue its descent. Eventually, the forward energy from the engine will cancel the pull of gravity, and shortly thereafter the car will climb the hill. This is the time analogous to the positional-derived saccadic onset. It should be obvious that, had the car not been moving backwards, the forward energy applied would have led to greater forward motion, or to complete the analogy, a larger saccade.

These considerations lead to two simple approximations that may be used in an attempt to determine “true” saccadic size. For the first modification to saccade size, we simply add the distance the eye traveled between the time the velocity-derived saccade onset occurred and the time the position-derived onset occurred (labeled ‘i’ in Figure 3-1) to the magnitude obtained by using only the position-derived onset and offset. For the second modification to saccade size, we also add the distance traveled in the time between the position-derived and the velocity-derived offsets (labeled ‘f’).

*Skewness:* Skewness is a measure of the symmetry of a saccade’s velocity profile, i.e., acceleration and deceleration. It provides more information about saccade dynamics than is available in the three standard parameters. Smaller saccades appear more symmetrical (i.e., their accelerating and decelerating phases are roughly equal), whereas larger saccades tend to accelerate to their peak velocity quickly and then “coast” the rest of the way, yielding a skewness below 0.5.

There are several methods to calculate skewness; some of them are quite mathematically intense, requiring the use of gamma functions (Smit et al., 1987a), or the computation of higher order central moments. Fortunately, all give similar results so we used the simplest one, the ratio between the time to peak velocity of the saccade and its duration (Van Opstal & Van Gisbergen, 1987). A symmetrical saccade therefore has a skewness of 0.5, one that is slow to accelerate to peak velocity,  $>0.5$ , and one with a long decelerating “tail”  $<0.5$ . Because skewness depends on saccade duration, we compared skewness results calculated by use of position- and velocity-derived saccadic onsets and offsets.

*Foveating Saccades:* The above analyses were also performed for foveating saccades from S5 and S6's  $PP_{fs}$  waveform (PC waveforms do not have a foveating saccade; the braking saccade starts the eye towards the target and the slow phase brings it to the target).

*Ramp-Step-Ramp:* Saccades made by the normal subjects were subjected to the same analyses of peak velocity, duration, and skewness as those made by the CN subjects. Results of the saccades made either with or against pursuit ramps of different velocities were compared to those made when no initial velocity was present.

### 3.2.5 Models

We constructed two simplified, open-loop control system models of the saccadic system in the MATLAB/Simulink environment, consisting of a pulse generator, neural integrator, ocular motor neurons and plant (Figures 3-2A and B). The first model used components from our previous models of both latent and congenital nystagmus (Jacobs & Dell'Osso, 1999; Jacobs & Dell'Osso, 2000), creating a pulse-step to drive a 2-pole plant with time constants of 7 ms and 180 ms. The second model, which used a pulse-slide-step to drive a 2-pole, 1-zero plant (zero at 80 ms, real poles at 300 ms and 13 ms, and a pair of complex poles), came from Zee, Fitzgibbon & Optican (1992), with modifications to allow symmetric operation without being connected in push-pull. Both models had two independent inputs: a saccadic command, and a pursuit (velocity step) command. We verified that these models could make accurate saccades in the absence of an initial velocity. We then generated saccades of specific intended magnitudes in the presence of a

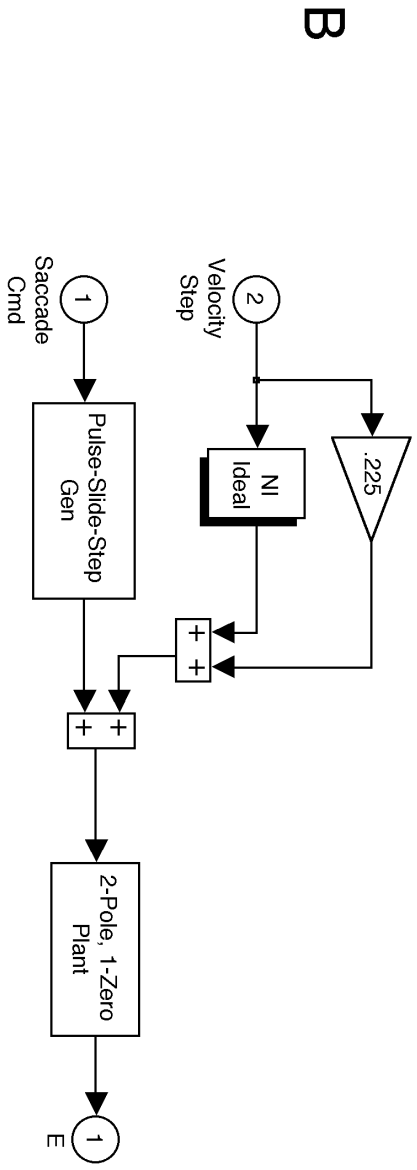
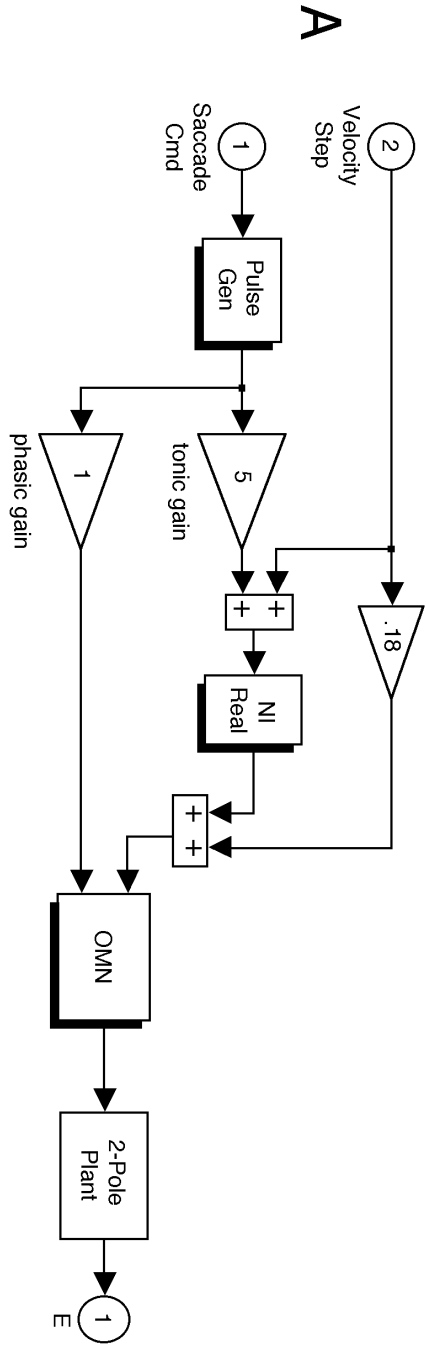


Figure 3-2

Open-loop model used to test the interaction between slow and fast phases. The pulse generator, neural integrator (NI), ocular motor neurons (OMN) and 2-pole plant are taken from previous models. The 2-pole, 1-zero model comes from Zee et al. (1992).

variety of constant velocities, as great as 50°/sec, comparable to the slow-phase velocities typical of CN. Ramps and saccades were combined in both the “with” (ramp facilitating saccade) and “against” (ramp opposing saccade) directions. We measured the resulting saccades, comparing them to their intended magnitudes and durations.

### **3.3. RESULTS**

#### *3.3.1 Peak Velocity vs. Amplitude*

Figure 3-3A-F shows the results for peak velocity plotted vs. magnitude for S5's  $PP_{fs}$  waveform for both braking ('x') and foveating ('+') saccades. The braking saccades are quite small, frequently under 1°, and the foveating saccades range from approximately 1° to just under 4°. There is a small amount of overlap between the upper range of braking saccades and the lower range of the foveating saccades. There are six subplots displayed, representing the possible combinations resulting from two methods of measuring peak velocity and three methods of measuring amplitude. Panels A, B, and C show peak-velocity calculations that do not account for the initial slow-phase velocity; D, E and F are recalculated to include this velocity. In panels A and D the saccadic magnitudes are recorded using only the position-derived onset and offset points. Panels B and E incorporate the addition of the distance the eye traveled between the velocity- and position-derived onsets. Finally, Panels C and F include the onset correction in addition to the distance traveled between the position- and velocity derived offset times. The same criteria were used to calculate the data in each panel in Figures 3-4 through 3-6. The solid

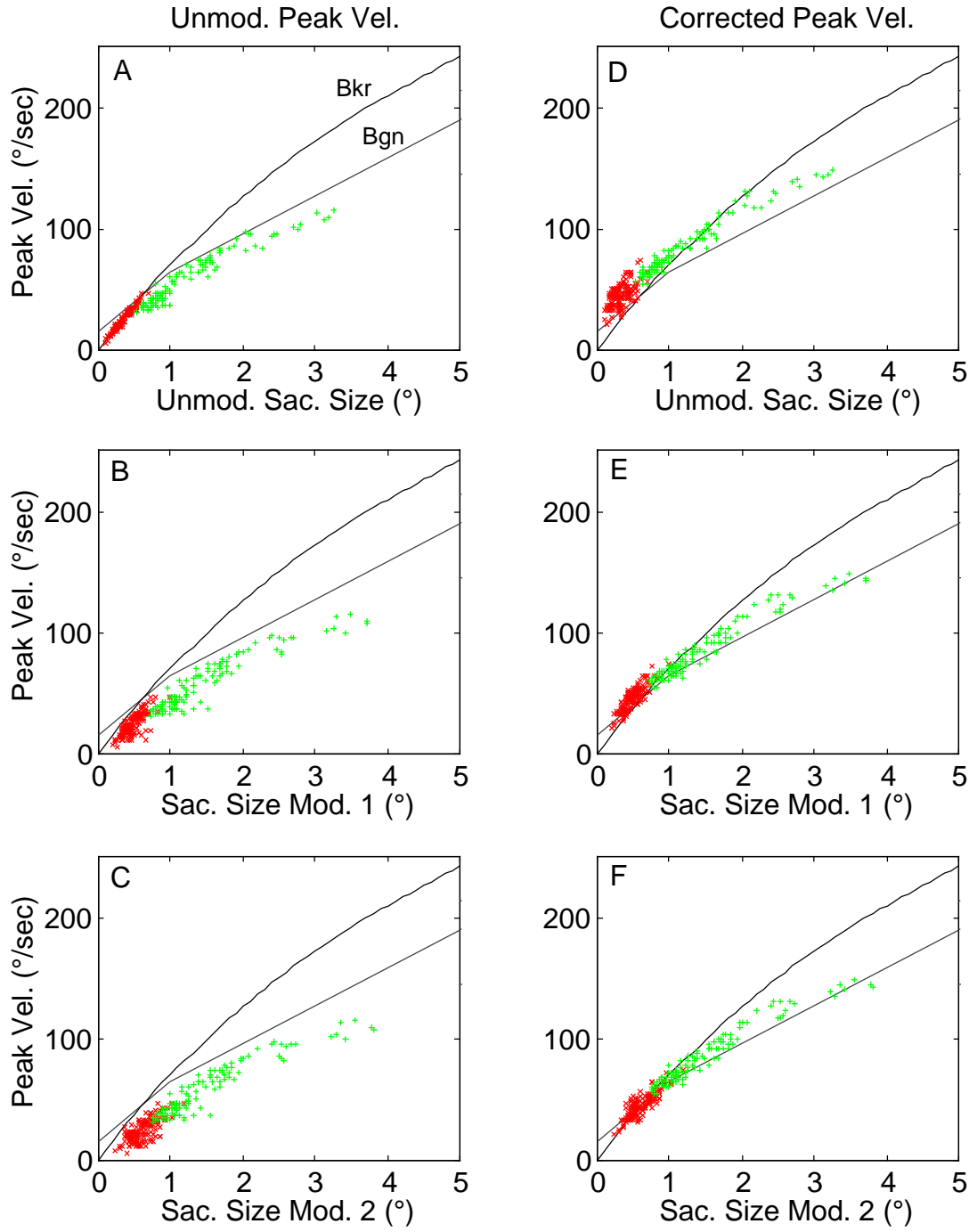


Figure 3-3

Peak velocity vs. amplitude for S5's  $PP_{fs}$  waveform. Panels A-F show the six calculated possible corrections based on three ways of adjusting the magnitude and two ways to measure peak velocity. In this and Figures 3-4 through 3-6, left column (A-C) is uncorrected peak velocity, and right column (D-F) is corrected peak velocity. First row (A, D) is unmodified saccade magnitude; second row (B, E) adds the initial saccadic segment; third row (C,F) adds initial and terminal saccadic segments as discussed in the text. In this and Figures 3-4 and 3-9, the solid line comes from Becker ('Bkr') and the dashed line comes from Boghen et al. ('Bgn'), representing mean peak velocity (high and low limits for 95% of measured saccades start at  $5^\circ$ —beyond the range of these data—and therefore are not shown). In this and Figures 3-5 and 3-7, braking saccades are represented by 'x'; foveating saccades are represented by '+.' Note that the lower range of foveating saccades and the upper range of braking saccades overlap.

line ('Bkr') is the peak velocity vs. amplitude relationship from Becker (1989), and the dashed line ('Bgn') is from Boghen et al. (1974). The 95% intervals for the fastest and slowest peak velocities are not displayed here, as they begin at 5°, which is beyond the upper end of these saccades.

In the left three panels (A-C), when we do *not* include the slow-phase velocity in the calculation of peak velocity, all the saccades appear to be somewhat slow, albeit within the "acceptable" range. As we apply the magnitude corrections, to include more of the saccade that had been masked by the runaway, the fit worsens as the points shift towards higher magnitudes.

The right three panels (D-F), show the opposite result; now that the entire change in velocity is included in the measurement of peak velocity, the saccades are shifted so that they appear to be slightly faster than average. As more of the saccade is included in the magnitude calculation, the points move closer to the average line. Note that in all six panels, the larger a saccade is, the greater its peak velocity. No matter how we measure the velocity and the magnitude, this general relationship holds.

It is also important to mention that the region between the Becker and Boghen et al. lines, that the saccades occupied after application of position and velocity corrections, is the same area where all four of our normal subjects' saccades (n=713) lay. That is, the saccadic peak velocity vs. amplitude data from normals measured in our lab coincide with the published data from Becker and the region between the average peak velocity and upper 95% boundary of Boghen et al.

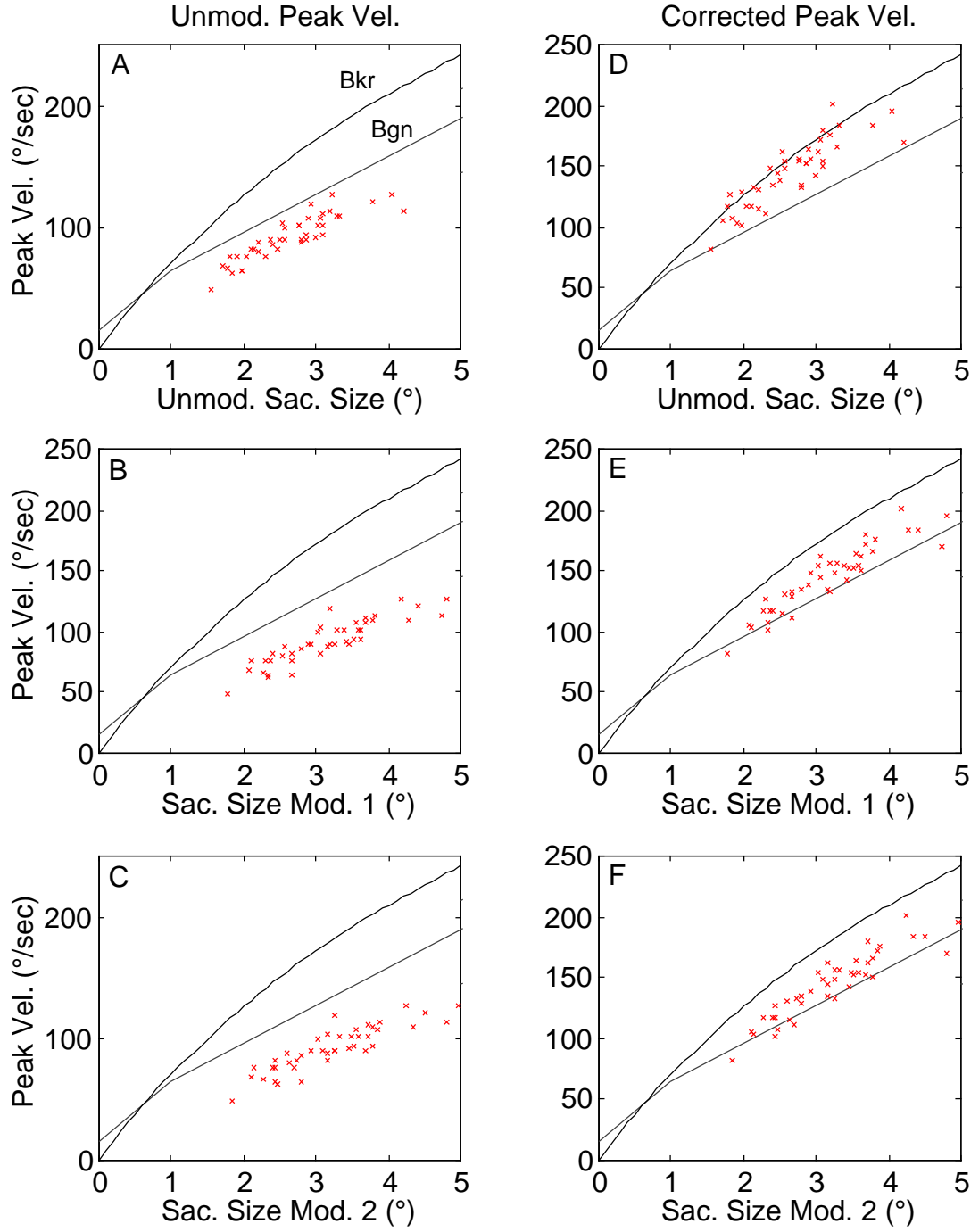


Figure 3-4

Peak velocity vs. amplitude for S7's PC waveform. Panels A-F show the six calculated possible corrections based on three ways of adjusting the magnitude and two ways to measure peak velocity.

The results for peak velocity vs. magnitude for S7's PC waveform are plotted in Figure 3-4. These saccades are much larger than those seen in S5's PP<sub>fs</sub> waveform. As with S5, the saccades follow the general principle that peak velocity increases with magnitude, regardless of measurement methodology. Once again, prior to the peak-velocity correction, saccades appear slow, and after the velocity correction they conform more closely to normal values, regardless of whether the magnitude correction is applied. For approximately 50% of the subjects however, the velocity correction alone results in peak velocities that exceed the average peak velocities of normals. In those cases, it is necessary to apply both the velocity and magnitude corrections (see Discussion).

### 3.3.2 *Duration vs. Amplitude*

Figure 3-5A-F shows the results for duration vs. magnitude for S5's PP<sub>fs</sub> waveform. As in Figure 3-3, both braking and foveating saccades are shown and there are six subplots in this Figure, representing the combinations of the two ways to measure duration and the three to measure magnitude. The solid line represents the duration vs. magnitude data from Yarbus (1967). The fit for the position-derived duration comes closer to the standard lines than does that for the velocity-derived duration.

Duration vs. magnitude results are plotted in Figure 3-6A-F for S3's PC waveform. In contrast to the case above, before the corrections are applied, these saccades appear to be of shorter duration than average; after correction, they are closer to average. As expected, no matter what correction was attempted, the larger a saccade, the

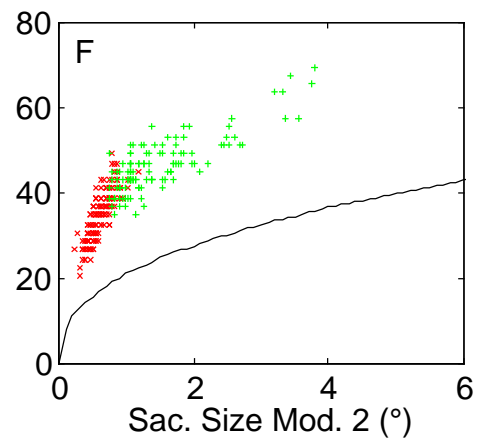
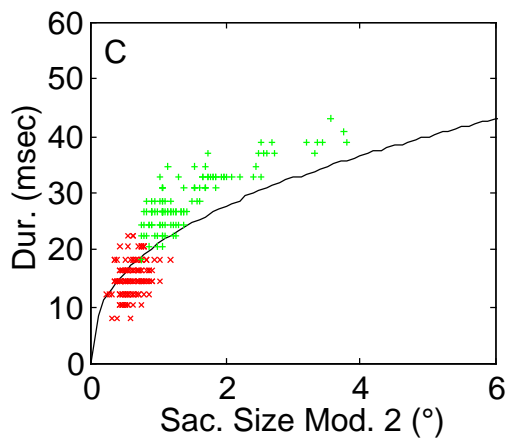
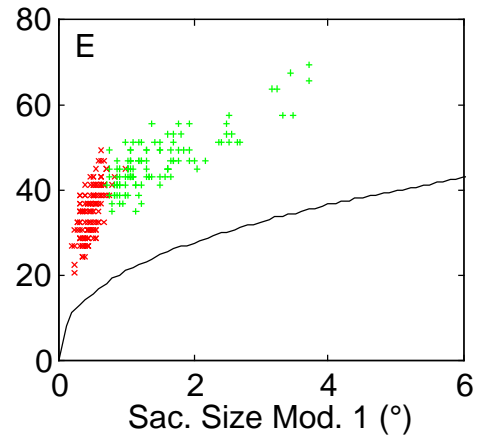
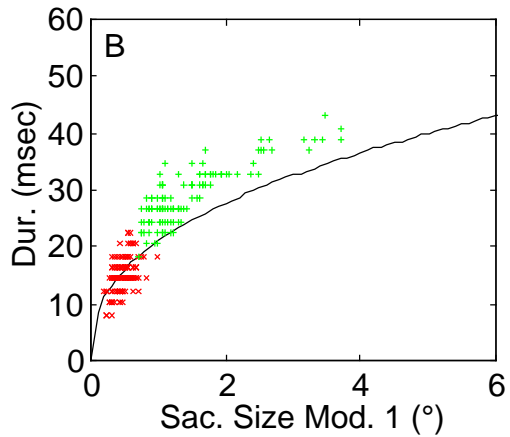
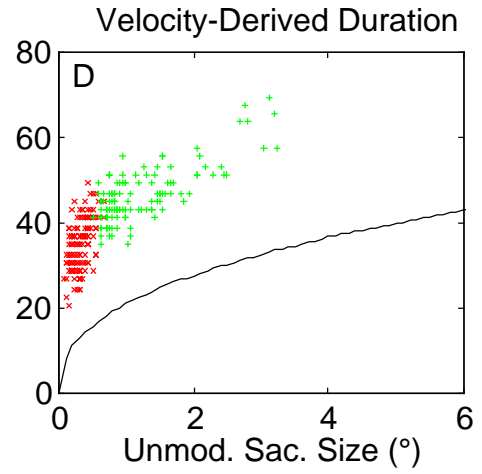
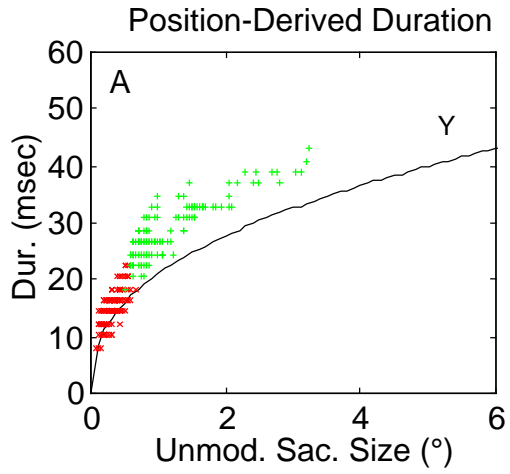


Figure 3-5

Duration vs. amplitude for S5's  $PP_{fs}$  waveform. Panels A-F show the six calculated possible corrections based on three ways of adjusting the magnitude and two ways to measure duration. In this and Figure 3-6, line 'Y' comes from Yarbus. Note that the lower range of foveating saccades and the upper range of braking saccades overlap.

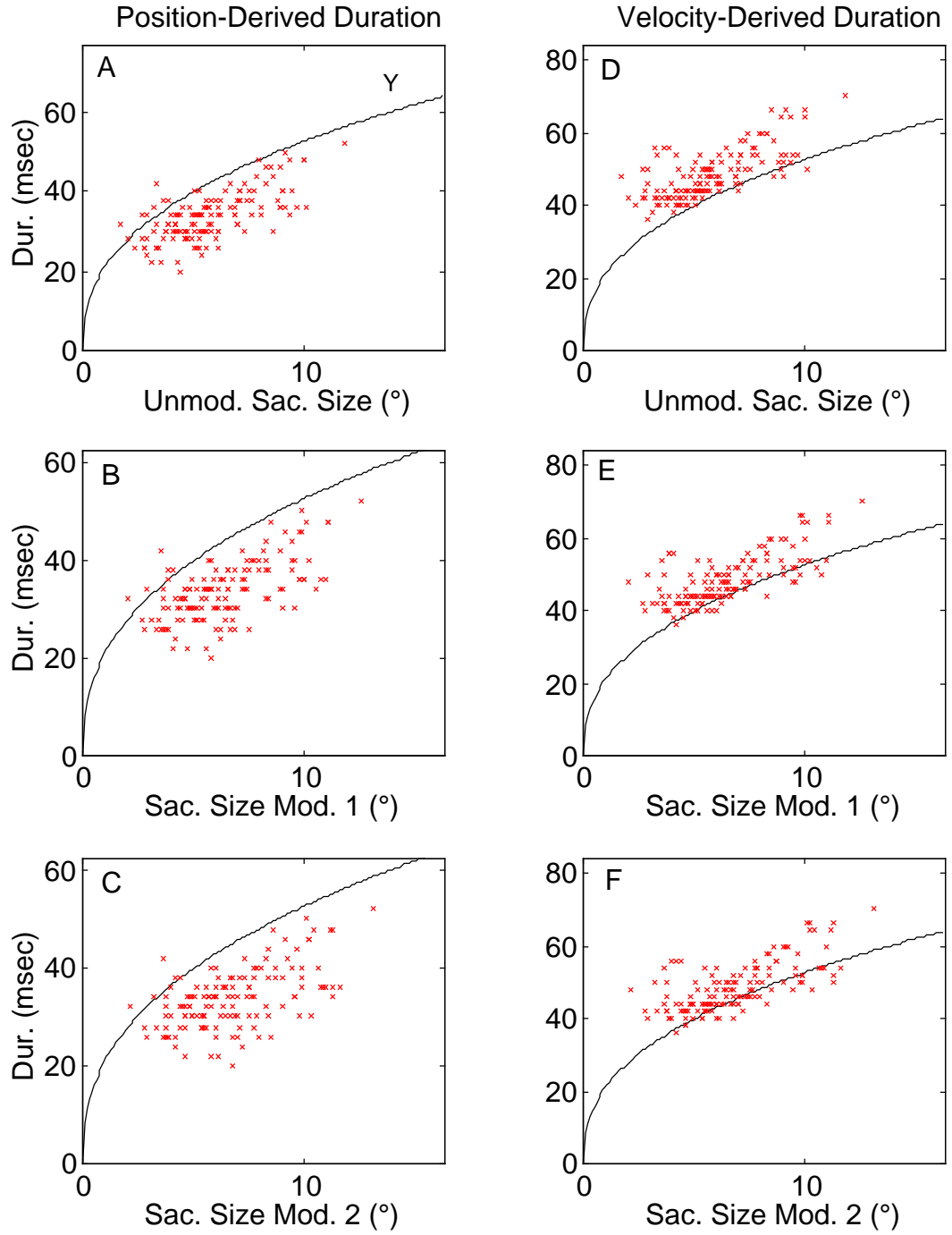


Figure 3-6

Duration vs. amplitude for S7's PC waveform. Panels A-F show the results after applying the possible corrections.

longer its duration. Thus, the duration, peak velocity, and magnitude general relationships hold regardless of methodology.

### 3.3.3 Skewness

Figure 3-7 shows a plot of skewness vs. duration for S5's  $PP_{fs}$  waveform, for both braking ('x') and foveating ('+') saccades. The dashed lines are adapted from van Opstal and van Gisbergen (1987) and show the approximate bounds of their results. Note that the upper range of the braking saccades overlaps well with the lower end of the foveating saccades. For the foveating saccades ("+"), the velocity-derived duration in plot 7B yields a better fit to reported results than do the position-derived durations seen in plot 7A, while the braking saccades do not show quite as much improvement. Analysis of S7's PC waveform yielded similar results.

In Figure 3-8 the skewness of S7's PC braking saccades using velocity-derived durations again offer much better correspondence than do the position-derived ones. The histogram in Figure 3-9-Bottom using the velocity-derived durations are distributed around 0.5, as would be expected for saccades that fall in this range (smaller than  $5^\circ$ ), whereas the distribution for the position-derived durations result in a higher average skewness (i.e., longer time to peak velocity), as is usually seen in smaller saccades. Compare this to the skewness distribution for normal subject S9 (Figure 3-9-Top), showing a peak more strongly centered on 0.5 than the skewness of braking and foveating saccades made by the CN subjects, who as a group, tended to have a looser distribution around 0.5.

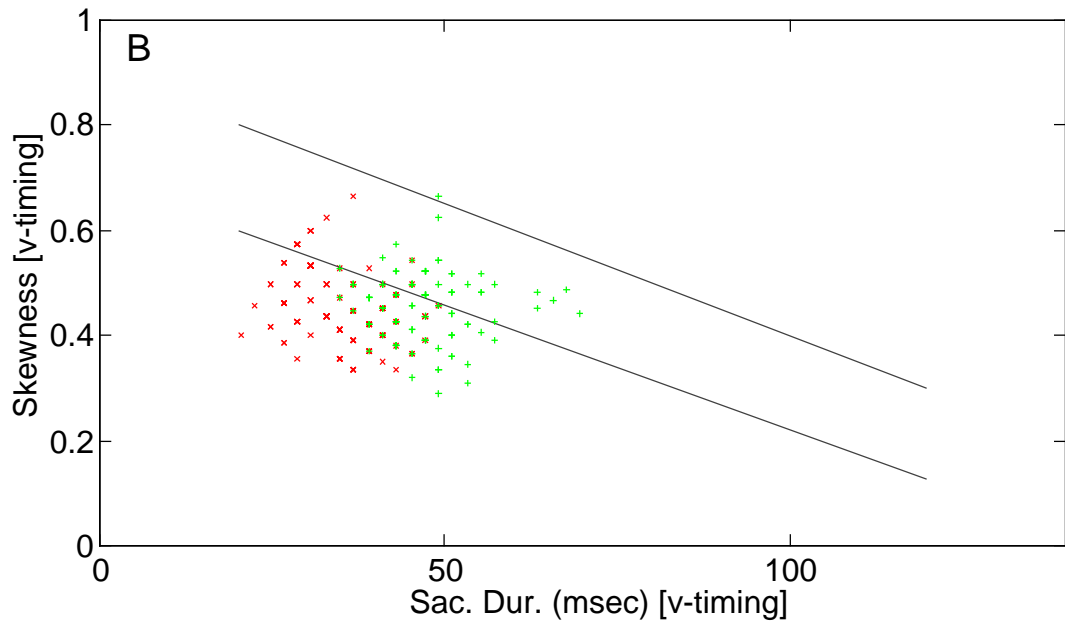
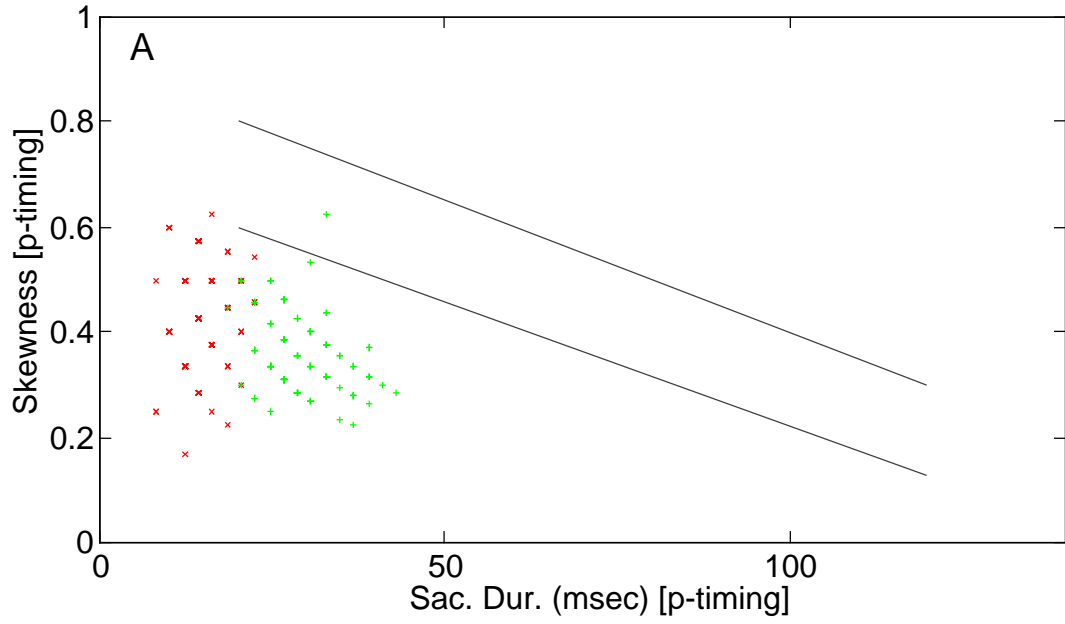


Figure 3-7

Skewness vs. duration for S5's  $PP_{fs}$  waveform. A) using velocity-derived onset/offset points. B) using position-derived onset/offset points. Dashed lines represent upper and lower bounds of skewness from van Opstal and van Gisbergen.

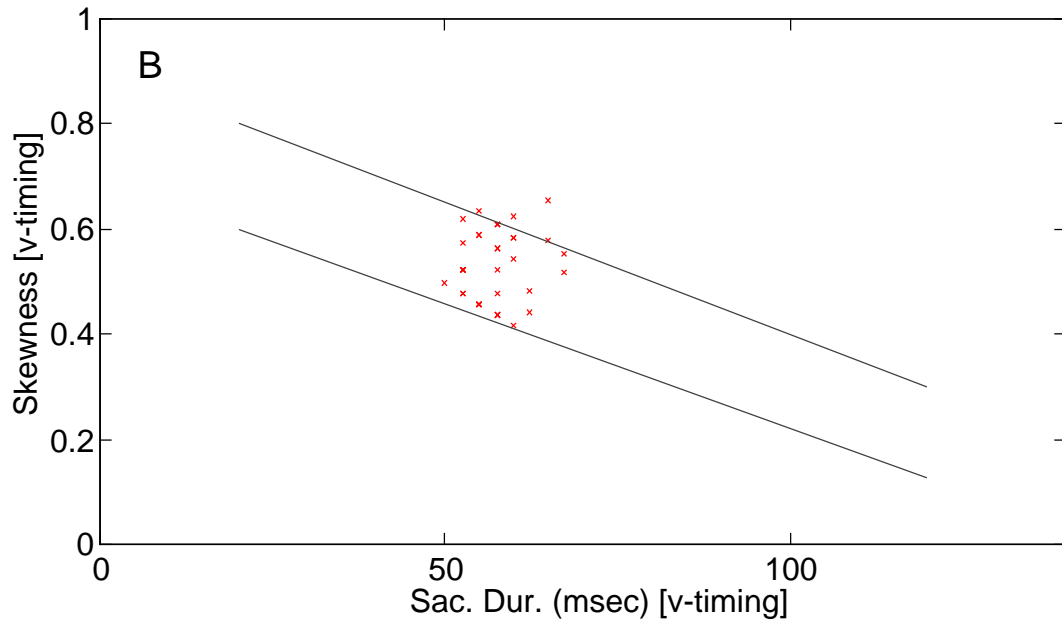
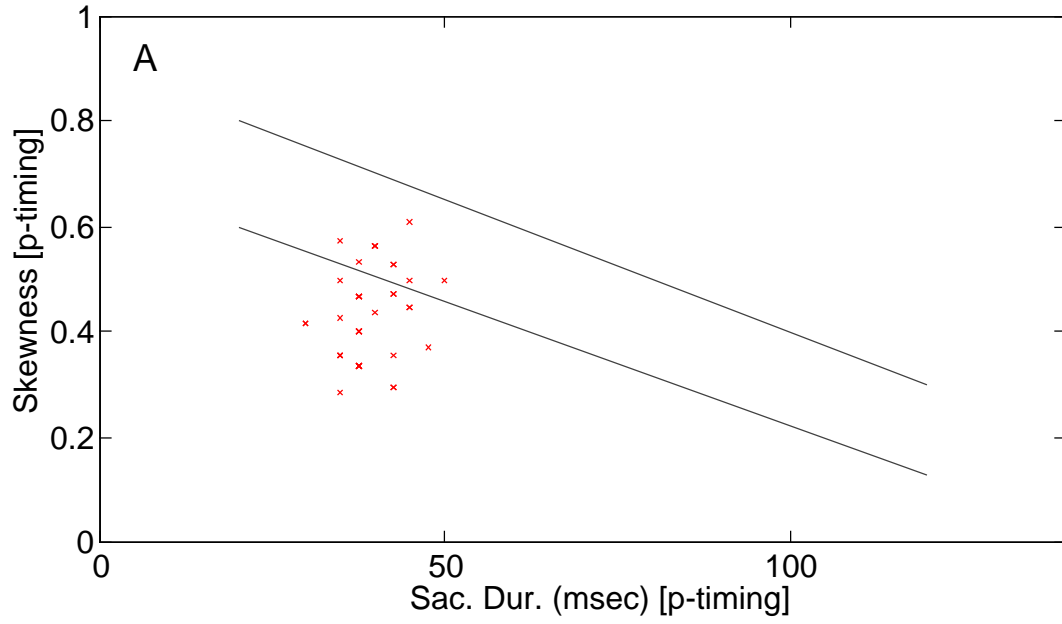


Figure 3-8

Skewness vs. duration for S7's PC waveform. A) using velocity-derived onset/offset points. B) using position-derived onset/offset points.

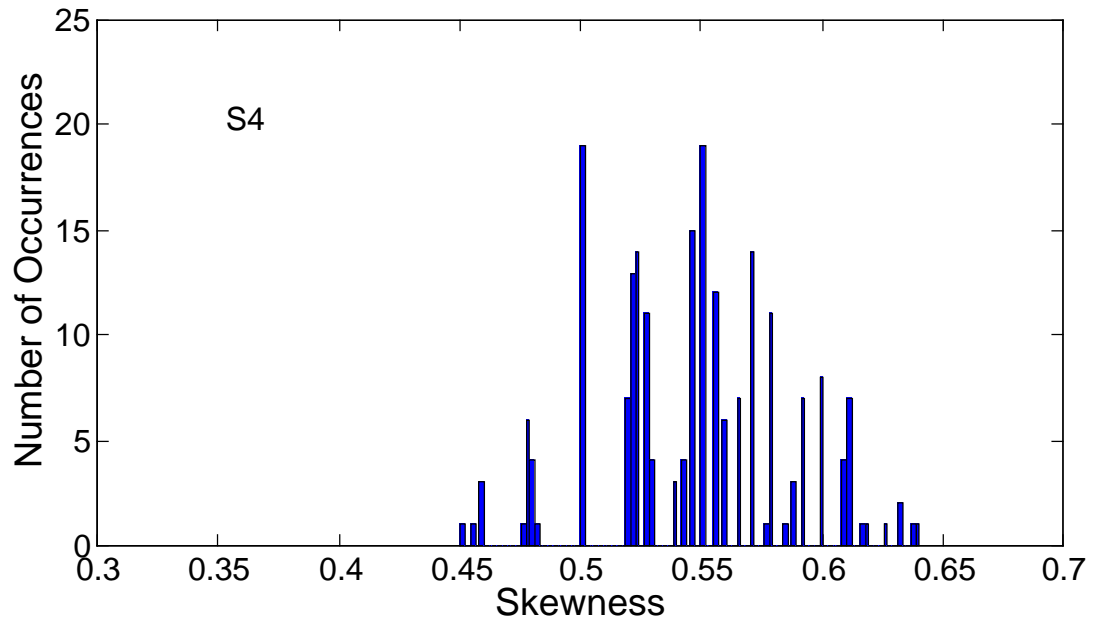
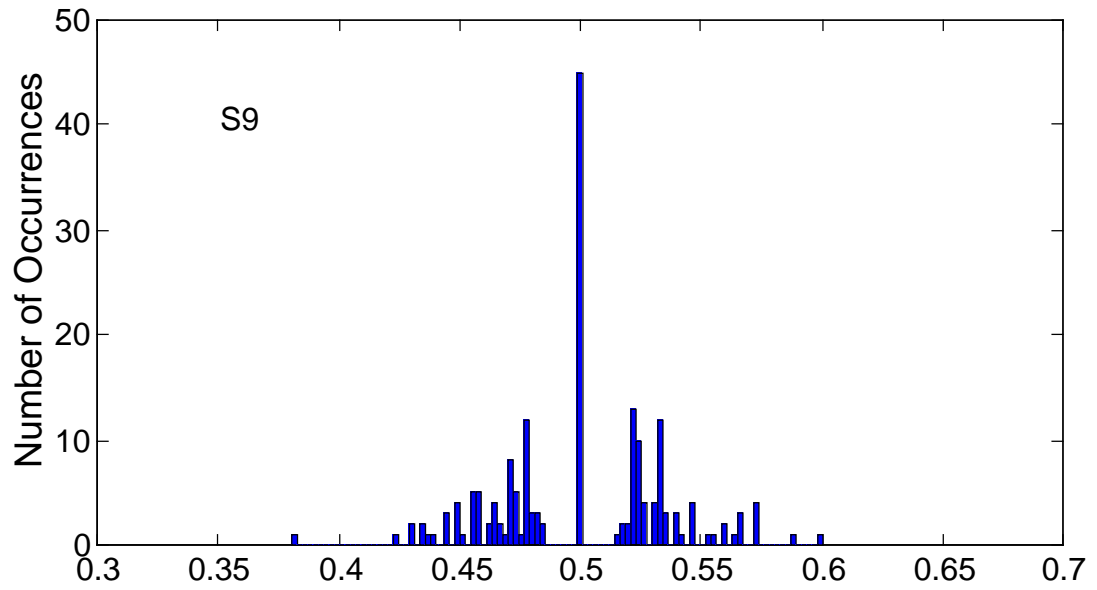


Figure 3-9

Histogram of the distribution of saccadic skewness for S9, a normal subject (Top panel), and S4, a CN subject with a PC waveform (Bottom panel). The normal subject is more symmetrically and sharply distributed around 0.5, denoting saccades of equal skewness.

### 3.3.4 Ramp-Step-Ramp

Normal subject S9's performance in the RSR paradigm is summarized in Figure 3-10 as a plot of peak velocity vs. magnitude for saccades made with no pursuit ('o'), saccades made against pursuit ramps ('x'), and saccades made in the same direction as pursuit ('+'). Note the distinct separation for these three cases, with saccades that must overcome the opposing pursuit having a larger peak velocity than static saccades, which in turn have a higher peak velocity than those saccades that "ride along" in the same direction as pursuit.

Examination of saccadic durations, however, reveals little if any change for saccades made during no pursuit; when pursuit was  $\pm 10^\circ/\text{sec}$ , the velocity-derived timing tended to yield slightly longer saccades, frequently adding a sample point or more at each end. For pursuits of  $\pm 20^\circ/\text{sec}$  and  $\pm 30^\circ/\text{sec}$  the difference could be more noticeable, up to three sample points at either end. This was not an invariant result, however; it was possible for pursuit cases to show no change in duration between position- and velocity-derived points, and for slow pursuit to be several samples longer at either end. Also, these differences were seen regardless of whether the pursuit was in the same direction as the saccade or in opposition.

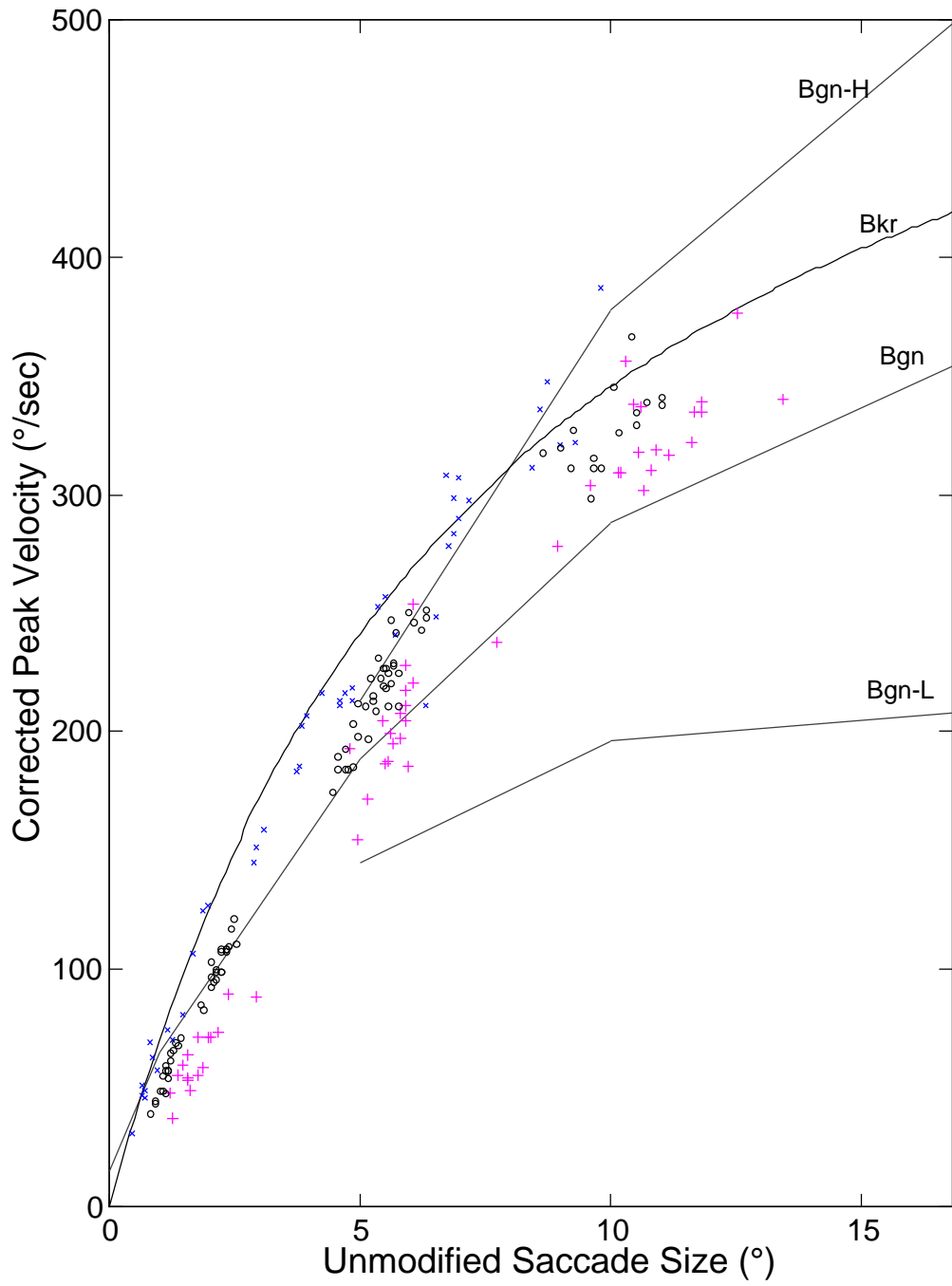


Figure 3-10

Ramp-step-ramp peak velocity vs. amplitude results for normal subject S9. Saccades made in the absence of smooth pursuit are represented by 'o'; against smooth pursuit by 'x,' with smooth pursuit by '+.'

### 3.3.5 Models

The interaction between initial smooth-pursuit velocities and resulting saccadic sizes is demonstrated by outputs from the 2-pole model shown in Figure 3-11, for a 1°-programmed leftward saccade, combined with ramps ranging from 0°/sec to 50°/sec in the opposite direction. For lower velocities, the magnitude of the resulting saccade is only slightly affected, but at the highest velocity (50°/sec), the cancellation is so severe that the saccade appears nearly flat, in effect a saccade of “zero magnitude,” a phenomenon we reported in previous work (Jacobs et al., 1999). Equivalent results were obtained with the 2-pole, 1-zero model.

Figure 3-12 quantifies the relationships between intended and actual saccades produced by both models for three cases: 1) saccades with no additional slow-phase velocity; 2) saccades with a slow-phase in same direction as the saccades; and 3) saccades with an oppositely directed slow-phase velocity. The dashed line in all four panels is the line of saccadic equality; i.e., points along this line are those whose intended and actual magnitudes are identical. Note that the 2-pole model's output for no slow-phase velocity falls just below this line at the higher magnitudes ( $\geq 15^\circ$ ) while the 2-pole, 1-zero model's output lies along the line. This is due to the design of the 2-pole model's saccade generator, that attempts to realistically simulate the common human tendency to be slightly hypometric for larger saccades.

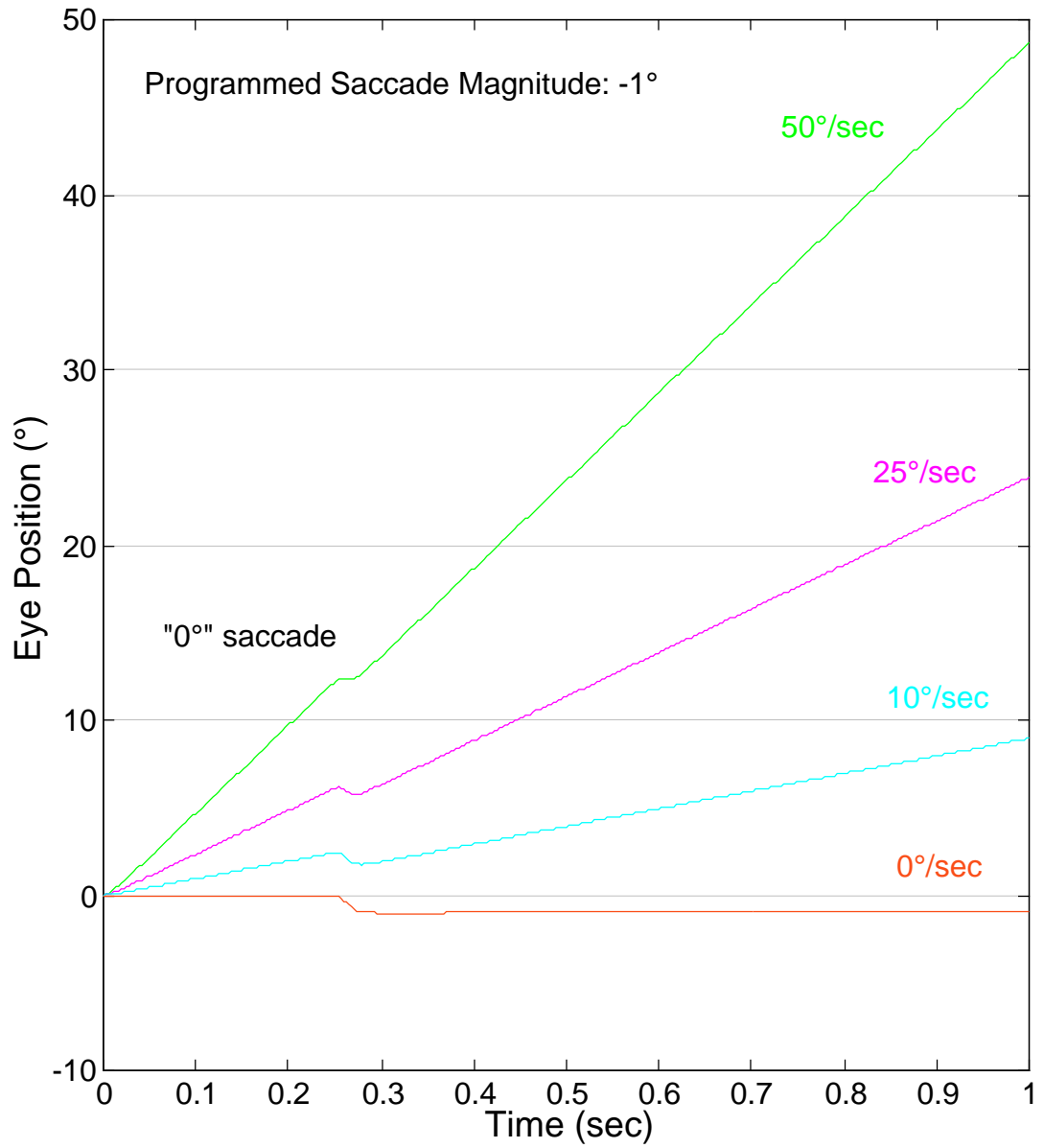


Figure 3-11

Examples of  $-1^\circ$  (intended magnitude) saccades made in the presence of smooth pursuit in the opposite direction for the 2-pole model. Labeled outputs are shown for velocities ranging from  $0^\circ/\text{sec}$  to  $50^\circ/\text{sec}$ . Note the greatly diminished saccade in the  $50^\circ/\text{sec}$  case; it is nearly a “saccade of zero magnitude.”

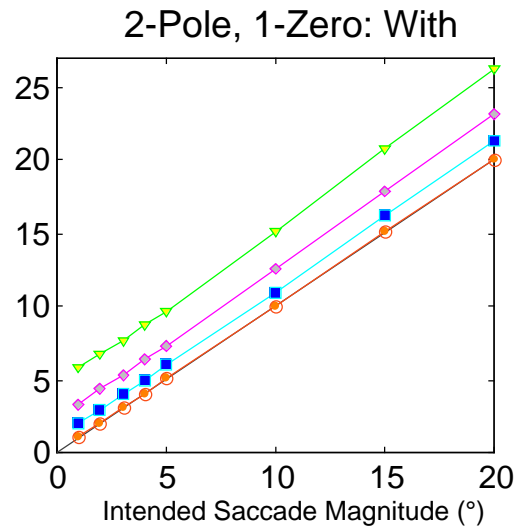
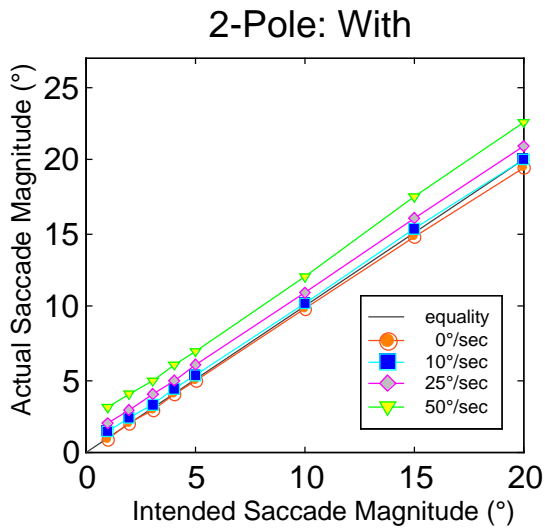
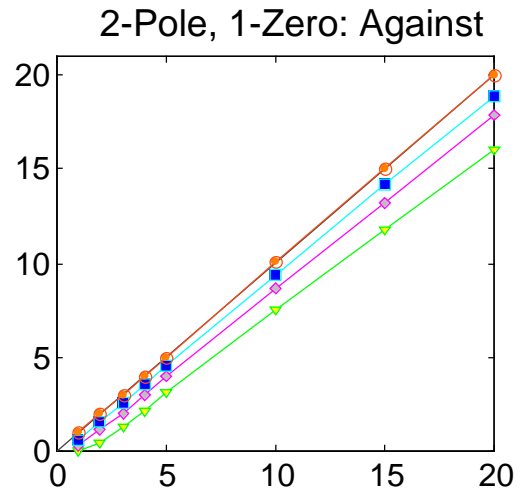
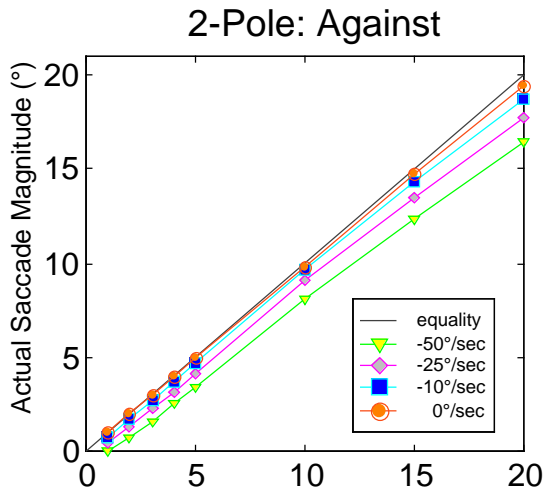


Figure 3-12

Relationships between inputs and outputs of the model, testing summation of slow phases with opposing fast phases. Left column shows response data of the 2-pole model and right column, of the 2-pole, 1-zero model. Top row represents saccades made against the slow-phase velocity and bottom row, saccades made with the slow-phase velocity. Note that the 2-pole model's larger saccades for  $0^\circ/\text{sec}$  slow phase are just below the dashed line of equality, due to real-life characteristics of the model's saccadic system.

As predicted, when the initial velocity and the saccade are oppositely directed, the resulting saccade is smaller than its programmed value (the lines for  $-10^\circ/\text{sec}$ ,  $-25^\circ/\text{sec}$ , and  $-50^\circ/\text{sec}$ ). Conversely, when the initial velocity and the saccade are in the same direction, the resulting saccade is appreciably larger than it would have been in the absence of a pre-existing velocity, with the effect growing more pronounced as that velocity rises to  $50^\circ/\text{sec}$ . The data in this figure are for rightward saccades; the results for leftward saccades are identical.

The amount of diminution or enhancement depends on the programmed magnitude of the saccade, the initial velocity, and the characteristics of the plant. The 2-pole, 1-zero plant shows an obviously greater effect when saccades and initial velocity are in the same direction, and a slightly greater effect when they are in opposition. When viewed as a percentage change, the effect is most pronounced for smaller saccades, and decreases as programmed saccade magnitude increases. The effect is also greater when the pursuit velocity increases, as expected.

Finally, we measured the duration of the saccade, as determined by velocity criteria, for all combinations of saccade and initial-velocity magnitude and direction using both models. In all cases the duration of a saccade of a given pre-programmed magnitude remained the same (within  $\pm 1$  sample onset and offset) regardless of the magnitude and direction of the slow-phase velocity, confirming that this method (perhaps in combination with acceleration and/or jerk) is a more accurate way to determine duration.

### **3.4. DISCUSSION**

The goal of this study was to examine the characteristics of braking saccades and attempt to reconcile them with the standard relationships used to characterize other types of fast-phase movements. It had been hypothesized that the complex waveforms of CN were created by the responses of a normal saccadic system to an ongoing oscillation (Dell'Osso & Daroff, 1975; Jacobs & Dell'Osso, 2000). Because braking saccades act to oppose the runaway slow-phase velocities of CN, there is some degree of interaction between the two motions. We have studied and modeled the simplest possible interaction, namely the simple linear increase and decrease of saccadic magnitudes, peak velocities, and durations due to the summation and cancellation of fast and slow phases at the plant.

We examined two reasonable approaches to correct saccadic magnitude, adding an approximation of the distance the eye traveled during the times between when position-derived and velocity-derived timing indicated the saccade occurred. It appears that the most appropriate metric is the saccadic duration; from this value it is then possible to work 'backwards' to approximate the range of the programmed braking saccade. The methodology developed to study braking saccades is directly applicable to all saccades made during eye movements induced either in normals or by ocular motor dysfunction.

Upon initial inspection, it might appear that by adding the "missing" pieces to the saccades' duration (e.g., Figure 3-5), we have made them far too long; the position-

derived saccade duration looks like a better fit in some subjects. However, examination of skewness properties supports the conclusion that the velocity-derived timing is correct. (In the RSR responses, saccadic durations also were increased for saccades both with and against the pursuit, a strong argument for the exclusive use of velocity points to determine timing.) When the peak-velocity correction is also included, some CN subjects who did not previously appear to have normal characteristics now fit the standard relationships. Bahill, Brockenbrough, & Troost (1981) concluded that duration was not as reliable a metric as previously stated. By comparison, normals seemed more stereotyped from subject to subject in duration than CN subjects. This is a good illustration of the variability inherent in biological systems, especially when the system is perturbed from its nominal operating range.

Using the velocity-derived duration in the calculation of skewness yielded better results for both the PC and  $PP_{fs}$  waveforms. However, the improvement for S5's  $PP_{fs}$  braking saccades were not as noticeable, merely shifting the points towards the expected range rather than into it (between the dashed lines), while the foveating saccade improvements were more obvious, shifting most of the saccades into the expected range. As noted earlier, the smaller a saccade, the more likely it is to be affected by the interaction with the slow-phase velocity. In this case, the slow phase just before the onset of either the braking or foveating saccades is essentially the same, but since foveating saccades are larger, they suffer less from the admixture, and therefore show more "normal" characteristics when examined. This is supported by S7, for these braking saccades are larger still, and show excellent fit to the expected range.

The histograms of skewness distribution (Fig. 3-9-Bottom) for S4's PC waveform, using velocity-derived timing, also showed a distribution centered just above 0.5, as we would expect for the range of saccades that we examined. Using the position-derived timing yields a left-skewed ( $<0.5$ ) result (not shown), less appropriate for saccades of this range.

The broader skewness distributions for CN-related saccades vs. normal saccades may reflect an artifact of the method used to determine saccadic endpoints. More probably, it might reflect the higher degree of difficulty in programming the former than the latter. That is, the CN slow phases were accelerating whereas the smooth pursuit velocities were constant. A similar effect was seen to a lesser degree in the RSR responses of the normal subjects (i.e., saccades with and without pursuit).

As the models demonstrated, the simple mechanical interaction between the saccade and the initial velocity is enough to significantly truncate the magnitude of the braking saccade, an effect that is well explained by the earlier analogy of the car on a hill. The presence of this mechanical interaction does not rule out the possible existence of further interaction at a more central neural level (e.g., cancellation of motor commands) but such a mechanism does not appear to be necessary to explain braking-saccade characteristics.

The 2-pole, 1-zero model's increased response to the slow-phase/saccade interaction was due to its plant's greater sensitivity to stimuli, a consequence of the inertia-reducing zero. We have included the results of both models to demonstrate that the cancellation/potential effect is not limited to the more "realistic" 2-pole, 1-zero

plant, but is also present in the simpler 2-pole plant. The latter is perfectly adequate for use in modeling that does not require exact simulation of initial trajectory dynamics, but is more concerned with later dynamics and the steady-state response.

Note that the greatest effect occurred for the smaller saccades (under  $5^\circ$ ) which is also the range for most braking saccades. For larger saccades the effect is still noticeable, although apparent only at higher velocities. This suggests that larger foveating and refixation saccades are probably also affected to a lesser degree, perhaps not enough to be obviously noticeable except in the most intense CN waveforms.

There have been other studies that included small saccades (i.e., saccades under  $1^\circ$ ) (Zuber & Stark, 1965; Steinman, Haddad, Skavenski, & Wyman, 1973; Kapoula, Robinson, & Hain, 1986; Abadi, Scallan, & Clement, 2000). In general, our data compare favorably with those of Kapoula et al. and Abadi et al., who both published peak-velocity values that fit standard relationships well (although neither examined duration). The data of Smit et al. (1987b) overlap the Boghen and Becker curves. Abadi and Worfolk (1989) found a statistically significant reduction in peak velocities for CN subjects versus normal subjects. However, their methods do not mention how peak velocities were calculated, so it is possible that the small differences between the two groups could be due to a failure to account for the slow-phase velocity just before the saccade. Furthermore, their data fall on or near Becker and the high Boghen curves, well within normal variation. Finally, their statistical method may not have been sufficient for the analyses required; i.e., they applied the Student's t-test to each amplitude-cluster of data. The multiple t-tests may capitalize on the chance event of finding a significant effect. An analysis of the

regression lines or an Analysis of Variance followed by a *post-hoc* test, such as Bonferroni, would have been better choices to support the contention of differences.

Too strong a dependence on the strict interpretation of saccadic velocity- and duration-amplitude relationships can lead to the discovery of problems where none actually exist. Although, at first glance, braking saccades do not always fit these standard relationships, a deeper examination of their properties suggests that they are not pathological, but are normal, non-visually-triggered, fast-phase eye movements whose magnitudes have been diminished by their opposition to the runaway slow phases that characterize CN.

While it may be possible to find a complex non-linear method to “correct” braking saccade magnitudes, i.e., attempt to elicit their original preprogrammed values, the effort to do so seems unnecessary, given the strong evidence supporting the hypothesis that braking saccades are generated by the same mechanisms responsible for other types of rapid eye movements.

### **3.5 ACKNOWLEDGEMENTS**

We gratefully acknowledge the assistance of Cleve Gilmore for his incisive comments on statistical methods.

### 3.6 WORKS CITED

- Abadi, R. V., & Worfolk, R. (1989). Retinal slip velocities in congenital nystagmus. *Vision Research*, **29**, 195-205.
- Abadi, R. V., Scallan, C. J., & Clement, R. A. (2000). The characteristics of dynamic overshoots in square-wave jerks, and in congenital and manifest latent nystagmus. *Vision Research*, **40**, 2813-2829.
- Abel, L. A., & Hertle, R. W. (1988) Effects of psychoactive drugs on ocular motor behavior. In: C. W. Johnston, & F. J. Pirozzolo, *Neuropsychology of Eye Movements* (pp. 83-114). Hillsdale, Lawrence Erlbaum Associates.
- Abel, L. A., & Dell'Osso, L. F. (1988). Correlations between saccadic latency and velocity in neurologic patients and elderly, but not young, normal subjects. *Investigative Ophthalmology and Visual Science*, **29**, 347.
- Bahill, A. T., Clark, M. R., & Stark, L. (1975). The main sequence: A tool for studying human eye movements. *Mathematical Bioscience*, **24**, 191-204.
- Bahill, A. T., Brockenbrough, A., & Troost, B. T. (1981). Variability and development of a normative database for saccadic eye movements. *Investigative Ophthalmology and Visual Science*, **21**, 116-125.
- Becker, W. (1989) Metrics. In: R. M. Wurtz, & M. E. Goldberg, *The neurobiology of saccadic eye movements* (pp. 13-67). Amsterdam: Elsevier Science Publishers BV.
- Boghen, D., Troost, B. T., Daroff, R. B., Dell'Osso, L. F., & Birkett, J. E. (1974). Velocity characteristics of normal human saccades. *Investigative Ophthalmology*, **13**, 619-623.

- Dell'Osso, L. F., & Daroff, R. B. (1975). Congenital nystagmus waveforms and foveation strategy. *Documenta Ophthalmologica*, **39**, 155-182.
- Dell'Osso, L. F., & Daroff, R. B. (1976). Braking saccade—A new fast eye movement. *Aviation Space and Environmental Medicine*, **47**, 435-437.
- Dell'Osso, L. F., Averbuch-Heller, L., & Leigh, R. J. (1997). Oscillopsia suppression and foveation-period variation in congenital, latent, and acquired nystagmus. *Neuro-Ophthalmology*, **18**, 163-183.
- Dell'Osso, L. F., Gauthier, G., Liberman, G., & Stark, L. (1972). Eye movement recordings as a diagnostic tool in a case of congenital nystagmus. *American Journal of Optometry and Archives of the American Academy of Optometry*, **49**, 3-13.
- Hainline, L. (1988) Normal lifespan developmental changes in saccadic and pursuit eye movements. In: C. W. Johnston, & F. J. Pirozzolo, *Neuropsychology of Eye Movements* (pp. 31-64). Hillsdale: Lawrence Erlbaum Associates.
- Jacobs, J. B., & Dell'Osso, L. F. (1997). Congenital nystagmus braking saccade characteristics. ARVO abstracts. *Investigative Ophthalmology and Visual Science*, **38**, S650.
- Jacobs, J. B., & Dell'Osso, L. F. (1999). A dual-mode model of latent nystagmus. ARVO abstracts. *Investigative Ophthalmology and Visual Science*, **40**, S962.
- Jacobs, J. B., & Dell'Osso, L. F. (2000). A model of congenital nystagmus (CN) incorporating braking and foveating saccades. ARVO abstracts. *Investigative Ophthalmology and Visual Science*, **41**, S701.

- Jacobs, J. B., Erchul, D. M., & Dell'Osso, L. F. (1996). Braking saccade generation in congenital nystagmus. ARVO abstracts. *Investigative Ophthalmology and Visual Science*, **37**, S277.
- Jacobs, J. B., Dell'Osso, L. F., & Erchul, D. M. (1999). Generation of braking saccades in congenital nystagmus. *Neuro-Ophthalmology*, **21**, 83-95.
- Kapoula, Z. A., Robinson, D. A., & Hain, T. C. (1986). Motion of the eye immediately after a saccade. *Experimental Brain Research*, **61**, 386-394.
- Schmidt, D., Dell'Osso, L. F., Abel, L. A., & Daroff, R. B. (1980a). Myasthenia gravis: Saccadic eye movement waveforms. *Experimental Neurology*, **68**, 346-364.
- Schmidt, D., Dell'Osso, L. F., Abel, L. A., & Daroff, R. B. (1980b). Myasthenia gravis: Dynamic changes in saccadic waveform, gain and velocity. *Experimental Neurology*, **68**, 365-377.
- Sharpe, J. A., & Zackon, D. H. (1987). Senescent saccades. *Acta Oto-Laryngologica (Stockholm)*, **104**, 422-428.
- Sharpe, J. A., Troost, B. T., Dell'Osso, L. F., & Daroff, R. B. (1975). Comparative velocities of different types of fast eye movements in man. *Investigative Ophthalmology*, **14**, 689-692.
- Shu, F. H. (1982) Evolution of the Stars. In:., *The Physical Universe. An Introduction to Astronomy* (pp. 144-158). Mill Valley, California: University Science Books.
- Smit, A. C., Van Gisbergen, J. A. M., & Cools, A. R. (1987a) Dynamics of saccadic tracking responses: Effects of task complexity. In: J. K. O'Regan, & A. Levy-Schoen, *Eye movements: from physiology to cognition* (pp. 7-16). North Holland: Elsevier Science Publishers BV.

- Smit, A. C., Van Gisbergen, J. A. M., & Cools, A. R. (1987b). A parametric analysis of human saccades in different experimental paradigms. *Vision Research*, **27**, 1745-1762.
- Steinman, R. M., & Collewijn, H. (1980). Binocular retinal image motion during active head rotation. *Vision Research*, **20**, 415-429.
- Steinman, R. M., Haddad, G. M., Skavenski, A. A., & Wyman, D. (1973). Miniature eye movement. *Science*, **181**, 810-819.
- Van Opstal, A. J., & Van Gisbergen, J. A. M. (1987). Skewness of saccadic velocity profiles: A unifying parameter for normal and slow saccades. *Vision Research*, **27**, 731-745.
- Van Opstal, A. J., & Van Gisbergen, J. A. M. (1989). Scatter in the metrics of saccades and properties of the collicular motor map. *Vision Research*, **29**, 1183-1196.
- Whittaker, S. G., & Cummings, R. W. (1990). Foveating saccades. *Vision Research*, **30**, 1363-1366.
- Winters, J. M., Nam, M. H., & Stark, L. W. (1984). Modeling dynamical interactions between fast and slow movements: Fast saccadic eye movement behavior in the presence of the slower VOR. *Mathematical Bioscience*, **68**, 159-185.
- Wirschafter, J. D., & Weingarden, A. S. (1988) Neurophysiology and central pathways in oculomotor control: Physiology and anatomy of saccadic and pursuit movements. In: C. W. Johnston, & F. J. Pirozzolo, *Neuropsychology of Eye Movements* (pp. 5-30). Hillsdale: Lawrence Erlbaum Associates.
- Yarbus, A. L. (1967) *Eye movements and vision.*, Plenum Press: New York.

Zee, D. S., Fitzgibbon, E. J., & Optican, L. M. (1992). Saccade-vergence interactions in humans. *Journal of Neurophysiology*, **68**, 1624-1641.

Zee, D. S., Optican, L. M., Cook, J. D., Robinson, D. A., & Engel, W. K. (1976). Slow saccades in spinocerebellar degeneration. *Archives of Neurology*, **33**, 243-251.

Zuber, B. L., & Stark, L. (1965). Microsaccades and the velocity-amplitude relationship for saccadic eye movements. *Science*, **150**, 1459-1460.

## Chapter 4

# A ROBUST, NORMAL OCULAR MOTOR SYSTEM MODEL THAT SIMULATES FIXATION, SACCADES, AND PURSUIT INCLUDING PENDULAR CONGENITAL NYSTAGMUS WAVEFORMS WITH BRAKING AND FOVEATING SACCADES AND EXTENDED FOVEATION

### **4.0 ABSTRACT**

The pendular waveforms of congenital nystagmus (CN) appear to be quite complex, composed of a sustained sinusoidal oscillation punctuated by foveating and/or braking saccades and periods of extended foveation. Previously, we verified that these quick phases are generated by the same mechanism as voluntary saccades. We propose a computer model of the ocular motor system that simulates the responses of individuals with pendular CN (including its variable waveforms) based upon the instability common in the pursuit subsystem and its interaction with other components of the normal ocular motor control system. Fixation data were recorded from subjects with CN using both infrared and magnetic search coil oculography and used as templates for our simulations.

Our ocular-motor model accurately simulates ocular motility data during fixation and in response to complex stimuli made by individuals with CN. The responses to target steps, pulse-steps, ramps and step-ramps provide a hypothetical explanation for the conditions that result in sustained pendular oscillation and the rules for the corrective saccadic responses that shape this underlying oscillation into the well-known family of pendular CN waveforms: pendular (P), pseudopendular (PP), pendular with foveating saccades ( $P_{fs}$ ), and pseudopendular with foveating saccades ( $PP_{fs}$ ). As is the case for normal physiological saccades, position error determined the saccadic amplitudes of foveating saccades, whereas braking saccades were stereotypical, their amplitudes not dependent on visual information. Finally we propose a possible structure and method of operation for the fixation subsystem, and use it to prolong the slow phases that immediately follow foveating saccades. This model supports the hypothesis that the pendular nystagmus seen in CN is due to an exacerbation of the normally damped, pursuit-system velocity oscillation (functionally, it is *pursuit-system* nystagmus—PSN).

#### **4.1 INTRODUCTION**

Congenital nystagmus (CN) consists of involuntary oscillations of the eyes towards and away from an attempted point of fixation. CN waveforms can be variations of either pendular or jerk waveforms, and the slow-phase portion tends to take the form of an increasing-velocity (or “runaway”) exponential, though approximately linear slow phases can be found in some less common waveforms, such as triangular (T) or

bidirectional jerk (BDJ), as well as pure jerk (Dell'Osso & Daroff, 1997). This slow-phase characteristic differentiates most CN waveforms from other types of nystagmus, such as latent/manifest latent nystagmus (LMLN) that has a linear or *decreasing* slow phase, or vestibular nystagmus, with its linear slow phase.

There are several further characteristics of CN that help to distinguish it from the many other types of nystagmus. These characteristics are important to note, for they must serve as the underlying fundamentals of any attempt to develop a control systems model of CN. Such a model must be capable of reproducing these basic behaviors to be considered biologically relevant. CN is conjugate, affecting both eyes similarly, even when strabismus is present. While the amplitude of the oscillations may not be equal, the frequency is, and the eyes are phase locked, in contrast to spasmus nutans, where the eyes move in and out of phase.

Over the years, many of the ocular motor subsystems have been suggested as the origin of CN, or at least to be severely deficient, including the optokinetic subsystem (Yee, Baloh, & Honrubia, 1980; Kommerell & Mehdorn, 1982), the saccadic subsystem (Dell'Osso, Gauthier, Liberman, & Stark, 1972; Abadi & Worfolk, 1989), and the smooth pursuit (SP) or vestibular subsystems (Yamazaki, 1979; Kommerell & Mehdorn, 1982; St. John, Fisk, Timney, & Goodale, 1984). However careful observation and study of most of these candidate systems have ruled them out.

The smooth pursuit gain is normal in CN (Dell'Osso, 1986; Kurzan & Büttner, 1989; Dell'Osso, Van der Steen, Steinman, & Collewijn, 1992b). For many years it had been believed, incorrectly, that CN was due to a deficit of smooth pursuit, and that

pursuit could even be “reversed,” i.e. the eyes would move in the direction *opposite* to that of the target (Lueck, Tanyeri, Mossman, Crawford, & Kennard, 1989). This mistaken belief arose from a misunderstanding of the true definition of “gain,” namely a failure to recognize that it can be calculated only during those intervals when the output is a direct result of the input. Also, the vestibulo-ocular gain is normal (Dell'Osso, Van der Steen, Steinman, & Collewijn, 1992a). There is also evidence (Abadi, Dickinson, & Lomas, 1982; Abadi & Dickinson, 1985; Shallo-Hoffmann, Wolsley, Acheson, & Bronstein, 1998) that the optokinetic subsystem does in fact behave properly.

Similarly, the fast eye movement system operates normally, and subjects make accurate saccades that compare favorably with those made by normals. During their foveation periods, subjects with CN can maintain fixation almost as accurately as can normals (SD within 13 minutes of arc for CN vs. 6 minutes of arc for normals (Dell'Osso, Van der Steen, Steinman, & Collewijn, 1992c)). CN can exist despite failures (found in one family with CN) of the common neural integrator (NI) responsible for maintaining eye position (Dell'Osso, Weissman, Leigh, Abel, & Sheth, 1993). This is especially important to note for, as we will discuss shortly, certain assumptions made by existing models of CN fail to recognize this fact.

Another important point to note about CN is that oscillopsia is *only rarely* present. This has critical implications for modeling because it constrains the origin of the oscillations to be within the efference copy loop where they are properly accounted for when calculating the reconstructed target velocity. This is in marked contrast to other

forms of nystagmus, whose origin appear outside of this compensating mechanism resulting in a sometimes debilitating global sense of movement.

What is the origin of CN? CN is known to be driven by attempts at fixation or pursuit, regardless of whether the target is real or imaginary (Dell'Osso, 1973a); CN can exist in total darkness, absent of any physical target. Conversely, it has been shown to damp (or even disappear) when the subject is inattentive. These facts suggested that there is a variable gain at the heart of CN (Dell'Osso, 1973b). We propose that, for the pendular waveforms of CN, this gain resides in the smooth pursuit (SP) subsystem, but it is a gain *internal* to the subsystem, *not* the overall pursuit gain.

Several models of some CN waveforms have been proposed over the years. Four in particular deserve special attention. Optican and Zee (1984), Tusa, Zee, Hain, & Simonsz (1992), and Harris (1995) are all based on a similar mechanism, namely a large, inappropriate positive feedback around the neural integrator (NI), that leads to the runaway slow phases. The fourth (Broomhead, Clement, Muldoon, Whittle, Scallan, & Abadi, 2000) starts from a different premise, namely that the responsible mechanism can be traced to insufficiencies in the saccadic subsystem, based on a conclusion from an earlier study (Abadi & Worfolk, 1989) that found the peak velocities of saccades made by CN subjects appear to be slower than those made by controls.

The first three models all share some basic flaws owing to their common heritage. First, and perhaps most serious, is the hypothesis that the gain around the common neural integrator is excessive; CN has been studied in a family with gaze-evoked nystagmus (GEN) due to a leaky (i.e., low-gain) neural integrator (Dell'Osso et al., 1993). The gain

cannot simultaneously be too high (causing CN) and too low (causing GEN). Also, many individuals with CN exhibit long periods of extended foveation (several hundred milliseconds) before the eye accelerates off target, suggesting a stable neural integrator. Another flaw is the model's difficulty in reproducing the most basic pendular waveforms. Optican and Zee's model (1984) has a very narrow range of positions where pendular oscillations are possible. Even then, these are very small and limited to exist only around a null region. This is not in agreement with the many individuals with CN who display pendular waveforms over a wide range of positions, and those who do not have any significant null region yet still have pendular waveforms. In addition, this model exhibited *two* null regions, something that has never been seen in CN that was documented with eye-movement recordings. While this model is incapable of simulating pendular CN, it does have the ability to generate some CN waveforms by the simple alteration of key model parameters.

Tusa et al. (1992) purport to model an unusual form of CN. However the symptoms of the patients they describe are frequently the exact opposite of those typically seen in CN. For example, their subjects could make their nystagmus *disappear* by fixation attempt. Also, one of these subjects complained of oscillopsia, which is not present in CN but is usually an indication of some form of acquired or vestibular nystagmus where the source of the oscillation is outside of the efference copy loop. Although the condition may have been "congenital" in their patients, it did not fit the clinical or waveform criteria for CN. They proposed a mechanism of reversed signals in the fixation subsystem in the form of an "abnormal loop" that acted as an extra positive

feedback, and suggested that there might be a physical midline defect causing CN, namely the inappropriate decussation of axonal fibers carrying velocity information, something that has not, as of yet, been found in anyone with CN and has been ruled out in others (Shallo-Hoffmann et al., 1998). This model also uses pulse-step mismatches as an “ignition source” for initial generation of CN. While this is required for their model, this sort of mismatch is not seen in those with CN, whose nystagmus is a function of gaze angle, *regardless* of how that position was achieved (e.g., large and small saccades, slow pursuit, or slow VOR).

Harris’ model (1995) rejects the misrouting hypothesis and instead proposes that CN is due to a maladaptation to early visual deprivation; this does not address the etiology of those whose CN was present *at birth*. While still a possible explanation for some, this ignores a great wealth of CN patient data that clearly show no major afferent visual deficits, i.e., patients with idiopathic or hereditary CN. On the positive side, he agrees that CN is highly dependent on attention-based gain, although he defines this gain as the overall smooth pursuit gain, and refers to it as excessive. As stated above, this contradicts known CN behavior, where the SP gain has been shown to be normal (Dell’Osso et al., 1972; Dell’Osso, 1986; Kurzan & Büttner, 1989; Dell’Osso et al., 1992b).

The model by Broomhead et al. (2000), while also able to reproduce some waveforms, does so by arguing for a deficit in the saccadic subsystem, i.e., that CN saccades are slower than normal. This foundation is suspect, however, for it has been shown elsewhere (Jacobs & Dell’Osso, 1997; Jacobs, Dell’Osso, & Leigh, 2001) that the

differences in peak velocities are due to artifacts of measuring techniques and simple mechanical summation-cancellation of the commands for saccadic and smooth pursuit signals sent to the plant via the ocular motor neurons. The model is also appears to be incompatible with the saccadic accuracy demonstrated by individuals with CN when refixing on new targets. Ocular motor data from hundreds of CN patients supports the concept that the causes of the oscillation are slow eye movements (i.e., the slow phases) and the saccades are corrective in nature and the result of a normal saccadic subsystem attempting to either brake the runaway eye movements or to also refoveate the target.

Braking saccades are small, automatic (i.e., non-visually triggered), stereotyped fast phases that appear in some CN waveforms—pseudopendular (PP), pseudopendular with foveating saccades ( $PP_{fs}$ ), triangular (T), pseudojerk (PJ), bidirectional jerk (BDJ) and pseudocycloid (PC) (Dell'Osso & Daroff, 1975). Braking saccades act to oppose the runaway slow phase, slowing the eye, and in some cases reversing its direction (Dell'Osso & Daroff, 1976; Jacobs, Dell'Osso, & Erchul, 1999). These saccades are triggered by extraretinal velocity efference signals; when the eye's velocity motor command exceeds some critical velocity, say  $4^\circ/\text{sec}$ —the retinal slip velocity—leading to decreased visual acuity, there is cause to attempt to arrest the eye's runaway.

It is our hypothesis that pendular CN waveforms, although appearing complex, are actually quite simple, created by an oscillation already present in the smooth pursuit subsystem and shaped by the interposition of braking and foveating saccades. There is evidence that, in some infants, CN may start as almost purely slow-phase pendular or triangular movements (Reinecke, Suqin, & Goldstein, 1988) and as the ocular motor

system develops during the first years of life, saccades begin to appear leading to the establishment of familiar CN waveforms. However, our records over the past 35 years document many infants whose waveforms mimic those of adults, already containing braking and foveating saccades (Hertle & Dell'Osso, 1999), and further development of the ocular motor system serves to increase the accuracy and duration of foveation periods.

## **4.2 METHODS**

### *4.2.1 Recording*

The ocular motility recordings of ~750 subjects and patients with CN made in our laboratory over the past 35 years, as either part of a clinical evaluation or specific research protocol, are the foundations for the model presented in this paper. Over that time period we used two methods. Some of the horizontal eye movement recordings were made using infrared reflection (Applied Scientific Laboratories, Waltham, MA). In the horizontal plane the system was linear to  $\pm 20^\circ$  and monotonic to  $\pm 25\text{-}30^\circ$  with a sensitivity of  $0.25^\circ$ . The IR signal from each eye was calibrated with the other eye behind cover to obtain accurate position information and to document small tropias and phorias hidden by the nystagmus. Eye positions and velocities (obtained by analog differentiation of the position channels) were displayed on a strip chart recording system (Beckman Type R612 Dynograph). The total system bandwidth (position and velocity) was 0-100 Hz. The data were digitized at 400 Hz with 12-bit resolution. The remaining data were

recorded by means of a phase-detecting revolving magnetic field. The sensor coils consisted of 9 turns of fine copper wire imbedded in an annulus of silicone rubber molded to adhere to the eye by suction. The signals were digitized at 200 Hz with a resolution of 16 bits. The system's sensitivity was less than  $0.1^\circ$ , with linearity of greater than  $\pm 20^\circ$ .

#### *4.2.2 Protocol*

Written consent was obtained from subjects before the testing. All test procedures were carefully explained to the subject before the recording began, and were reinforced with verbal commands during the trials. During IR recording, the subject was seated at the center of a 5-ft radius arc containing LED targets. At this distance the LED subtended less than  $0.1^\circ$  of visual angle. During search-coil recording, a laser target was back-projected onto a translucent screen 1-2 meters from the subject. The head was stabilized in primary position and the subject was instructed to move only the eyes to view each target as it was illuminated. The room light could be adjusted from dim down to blackout to minimize extraneous visual stimuli. A recording session consisted of from one to ten trials, each lasting under a minute with time allowed between trials for the subject to rest. Trials were kept this short to guard against boredom because CN intensity is known to decrease with inattention.

#### *4.2.3 Analysis*

Data analysis, filtering, statistical computation of means and standard deviations, and graphical presentation were performed using custom software written in MATLAB (The MathWorks, Natick MA), a development environment for scientific computing. Data was first filtered in the forward direction, and the result was reversed and filtered to insure zero phase shift.

#### *4.2.4 Computer Simulation*

The ocular motor system (OMS) model was designed and implemented using the Simulink component of MATLAB, a control systems simulation package capable of performing simulations in both continuous and discrete time. As the block diagram of Figure 4-1 shows, the model is of modular, hierarchical design, consisting of the functional building blocks thought to be required for accurate ocular motor control. This modular design allows for easy substitution of any block by an equivalent block, based on new data, personal preference, or to demonstrate other possibilities. It also facilitates expansion of the model to include additional subsystems (e.g., the vestibuloocular and optokinetic subsystems) and preserves the separation of functions required to produce the wide variety of ocular motor responses exhibited by humans, both normal subjects and those with specific dysfunction. In addition to modularity, the model contains distributed delays that duplicate those shown to exist by neurophysiological studies (Figure 4-2A). The components of the smooth pursuit and saccadic subsystems are shown along with the fixation subsystem and neural integrator hold circuitry (see below).

# OMS Block Diagram

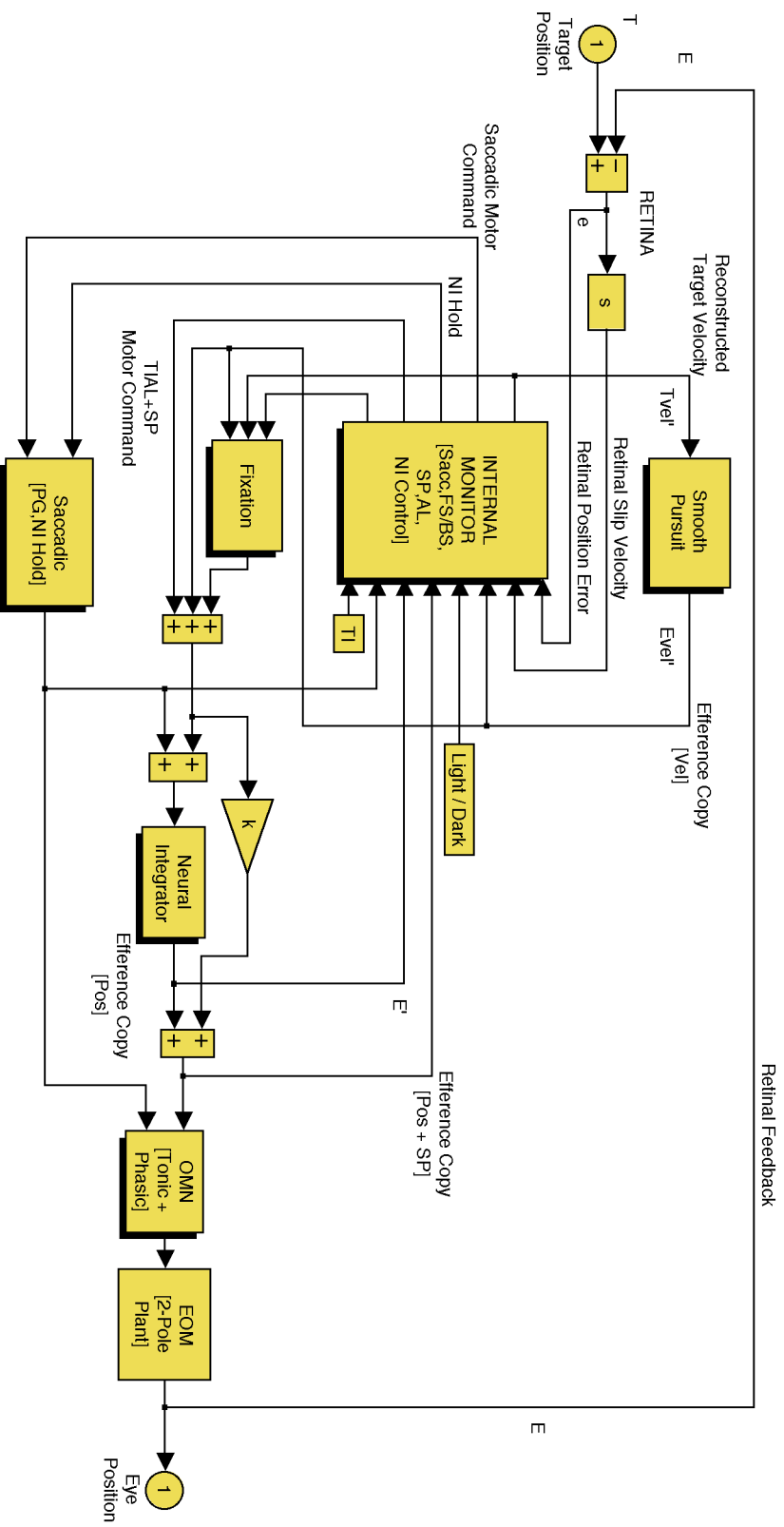


Figure 4-1

A functional block diagram of the ocular motor system (OMS) model showing the basic organization of subsystems and major components: saccadic, smooth pursuit, fixation, internal monitor, final common neural integrator (NI), ocular motor neurons (OMN), and extraocular muscles and globe (plant) (EOM). In this and the following Figures, T—target, E—eye, e—retinal error, Tvel'—reconstructed (perceived) target velocity, Evel'—eye-velocity motor command, E'—eye-position motor command, PG—pulse generator, [Sacc, SP, AL, NI Control]—saccadic, smooth pursuit, Alexander's law and neural integrator control functional blocks (respectively) in the internal monitor, and other symbols within square brackets are signals used by other blocks. Transfer functions of various blocks are shown in their Laplace notation within the block. Drop shadows on a functional block indicate that other functional blocks are contained within.





Figure 4-2

A.) Ocular motor system (OMS) model showing distributed delays, pursuit subsystem components, pulse generator and neural integrator hold. B.) The smooth pursuit subsystem, modified as described in the text with provision for oscillations in the PMC+ circuitry.

At the simplest level, our OMS model is in essence smooth pursuit and saccadic subsystems whose behaviors are coordinated by an “Internal Monitor” (IM), that receives inputs from the retina and both subsystems (position and velocity efference copy) and sends motor control signals back to the motor subsystems, including the fixation subsystem. The model is of unilateral, bidirectional architecture (Dell’Osso, 1994), that is, both sides of the brainstem are combined into one model capable of both positive and negative signals that drive one—the fixating—eye. Provision also exists to drive a second, non-fixating eye for studies of conditions where the eyes are unyoked due to strabismus or paresis. This type of model suffices for the simulation and study of most disorders that result in conjugate oscillations of the eyes, such as CN.

Based on the recorded saccadic and pursuit responses of the CN subjects described above, we have hypothesized that their ocular motor systems are *not* dramatically different from normals. Thus, our model’s subsystems (smooth pursuit (SP) and saccadic) should be capable of normal behavior, as well as being able to also simulate many common clinical dysfunctions and their effects on fixation, saccadic refixation, and smooth pursuit.

#### *4.2.5 OMS Model Subsystems*

**SMOOTH PURSUIT SUBSYSTEM:** We constructed several published models of the SP subsystem (Robinson, Gordon, & Gordon, 1986; Krauzlis & Lisberger, 1989; Krauzlis & Miles, 1996) and evaluated their suitability for inclusion in our model. We selected the Robinson model because of its simplicity of design that nonetheless yields

realistic results. However with a few minor modifications we could substitute any other SP model in its place.

A defining feature of Robinson's model is the damped oscillation ("ringing") that occurs with the onset of pursuit. This ringing affects only *initial* pursuit, not steady-state performance, for the oscillation dies away within a few cycles. The source of this ringing is in the pre-motor circuitry (PMC) sub-block. The frequency of the oscillation depends on the length of delay,  $\tau_3$ , in the feedback branch of this block. As the delay is increased from its default value of 30 ms, the frequency of the oscillation decreases and the amplitude increases. Conversely, if  $\tau_3$  is decreased, the frequency increases and the amplitude decreases.

The modified SP subsystem is shown in Figure 4-2B. To induce the model into *sustained* oscillation, the gain, P1, must be raised above its original value of 1.1. (This parameter is *separate* from the *steady-state* SP gain, set to 0.95.) As this value is increased, the magnitude of the velocity of the oscillation increases accordingly, taking longer and longer to reach steady state. Above 1.3, the oscillation becomes sustained, and its peak velocity increases with P1. As the gain surpasses 3.9 the oscillation becomes exponentially increasing. Initially, as a tradeoff between amplitude of the velocity oscillation and time to reach steady state, we chose a value 3.025 for the model. This value is no longer so restricted because we can decrease the required time to steady state with an initiating impulse as described below.

Because even an unstable system requires an inducement to begin oscillating, we initially added a low-energy velocity noise source to the junction where the input and

feedback sum. This small disturbance insured continuous oscillation of the system even in the absence of a pursuit signal. However, the model required more than two seconds before the oscillation achieved its steady-state amplitude. When we substituted a very short duration, biphasic pulse for the noise source, the output reached full amplitude in under a second; this latter stimulus simulates the abrupt onset of *fixation attempt*, which has been shown to be necessary for the CN oscillation to become manifest (Dell'Osso, 1973a).

To use this SP subsystem in our OMS model, we changed the plant dynamics from a single pole (time constant 15 ms) to a double pole (time constants 7 ms and 180 ms). This was necessary to achieve more realistic eye trajectories when combined with the saccadic portion of the model. While a two-pole, one-zero plant would be more physiologically correct, this extra degree of complexity (including the concomitant change of the motor signal to the ocular motor neurons (see below) to a pulse-slide-step mechanism—see below) would provide no additional insight into the overall system behavior beyond saccadic trajectories (Jacobs et al., 2001).

It was also necessary to convert the SP subsystem from one that operated in a velocity-in, velocity-out model to one that could operate in a position-in, position-out model to facilitate interaction with the saccadic subsystem. There is evidence that both position and velocity are afferent signals to the brain, encoded by signals present in the optic nerve, with the velocity created by calculations between retinal ganglion cells (Korth, Rix, & Sembritzki, 2000), although most motion processing may take place cortically (Bach & Hoffmann, 2000). This was accomplished in our model by adding a

differentiator following the retinal summing junction at the input, converting the position error signal into velocity error signal (retinal “slip” velocity). The common neural integrator converts the pursuit subsystem’s velocity output signals back into position signals. Because the eye must be driven by a *step-ramp* signal if it is to pursue constant-velocity targets (ramps), we then added the pursuit subsystem’s output to the direct pathway that sums with the integrated one at the ocular motor neurons.

These last two modifications required further changes to the SP portion of the IM, to its “virtual” plant that acts upon the efference signal that is fed back to the input summing junction of the model. First we added a second pole to match the one added to the actual plant. Second, we added a zero to account for the integrator/direct path added before the final motor pathway.

**SACCADIC SUBSYSTEM:** We built a saccadic subsystem composed of a pulse generator, saccadic internal monitor and ocular motor neuron and connected it to the two-pole plant used in the SP subsystem. The pulse generator was based on a resettable neural integrator (Abel, Dell’Osso, & Daroff, 1978; Abel, Dell’Osso, Schmidt, & Daroff, 1980; Kustov & Robinson, 1995), (RNI), distinct from the common neural integrator that appears in the final motor pathway. The RNI is part of the circuit that determines saccade duration: the output of the RNI is compared to a piece-wise linear function. When the output surpasses the function-value, the RNI resets, ending the saccade. The saccadic durations are based on a combination of published physiological data (Zuber & Stark, 1965; Yarbus, 1967) and data analyses performed in this lab over three decades. Once the saccade duration was set, pulse amplitude was determined by an adaptive algorithm that

varied the magnitude of the pulse applied to the two-pole plant until the steady-state amplitude of the eye matched the intended target position. An exponential function was then fit to these magnitudes and used in the pulse generator.

**THE COMMON NEURAL INTEGRATOR:** Because a pulse-step is required to drive the eye in a saccade, it is necessary to take the signal from the pulse generator and integrate it (analogous to the above discussion regarding step-ramp signals and smooth pursuit) in preparation for combination with the original pulse with the step. The integration is performed by the common neural integrator shown in Figures 4-1 and 4-2, which consists of a leaky integrator (time constant equal to the normal dark-drift time constant of 25 sec) around which is a positive feedback gain to offset that leak and produce a non-leaky integrator. Provision was also made to include two such elements to simulate gaze-evoked nystagmus caused by a leak in a sub-population of the neural integrator cells (Abel et al., 1978).

**THE OCULAR MOTOR NEURONS:** The combination of the pulse and the step is done by the ocular motor neurons (OMN). This combination of signals is *not* a simple addition of the pulse and the step, for that would not yield a true pulse-step, as the integrated signal is ramping up during the pulse and does not attain its final height until the pulse has concluded. Instead, the signal from the pulse generator is passed to the output at the moment when the pulse starts (summed with any constant offset present at the output of the common NI). Upon termination of the pulse, the integrated step from the common NI is then passed to the output, yielding a pulse-step motor command.

INTERNAL MONITOR: The Internal Monitor (IM) is the “brains” of this model, performing all the computation necessary to insure proper smooth pursuit velocities, saccades and neural integrator control, among other functions. The IM has a long pre-history in models of ocular motor function in the presence of dysfunction (Dell'Osso, 1968; Weber & Daroff, 1972; Dell'Osso, Troost, & Daroff, 1975; Abel et al., 1978; Doslak, Dell'Osso, & Daroff, 1979; Dell'Osso & Daroff, 1981; Doslak, Dell'Osso, & Daroff, 1982). What emerges with this model is the realization that the IM is also necessary for the *normal* operation of the OM system. The IM makes use of visual signals from the *moving oculocentric coordinate system* (i.e., the retina), as well as position and velocity efference signals recorded in the *moving or stationary craniocentric space* (i.e., the brainstem). Using this information, delayed appropriately, it is possible to reconstruct target position and velocity in *stationary, earth-centric space* independent of any confounding “noise,” e.g. CN or latent/manifest latent nystagmus oscillations. The model can then respond appropriately to target changes, providing proper commands to the SP and saccadic subsystems.

Due to the complexity of tasks that the IM is required to perform, it was designed in a modular fashion, facilitating testing of each function before adding it to the IM, and allowing for simpler debugging of the module after incorporating it into the IM. Each functional block makes use of a combination of afferent and efferent signals to achieve its goal of providing needed signals to either other internal monitor blocks or to external functional subsystems. Working together, these logic and signal-reconstruction blocks allow the ocular motor system to properly differentiate target position/velocity from eye

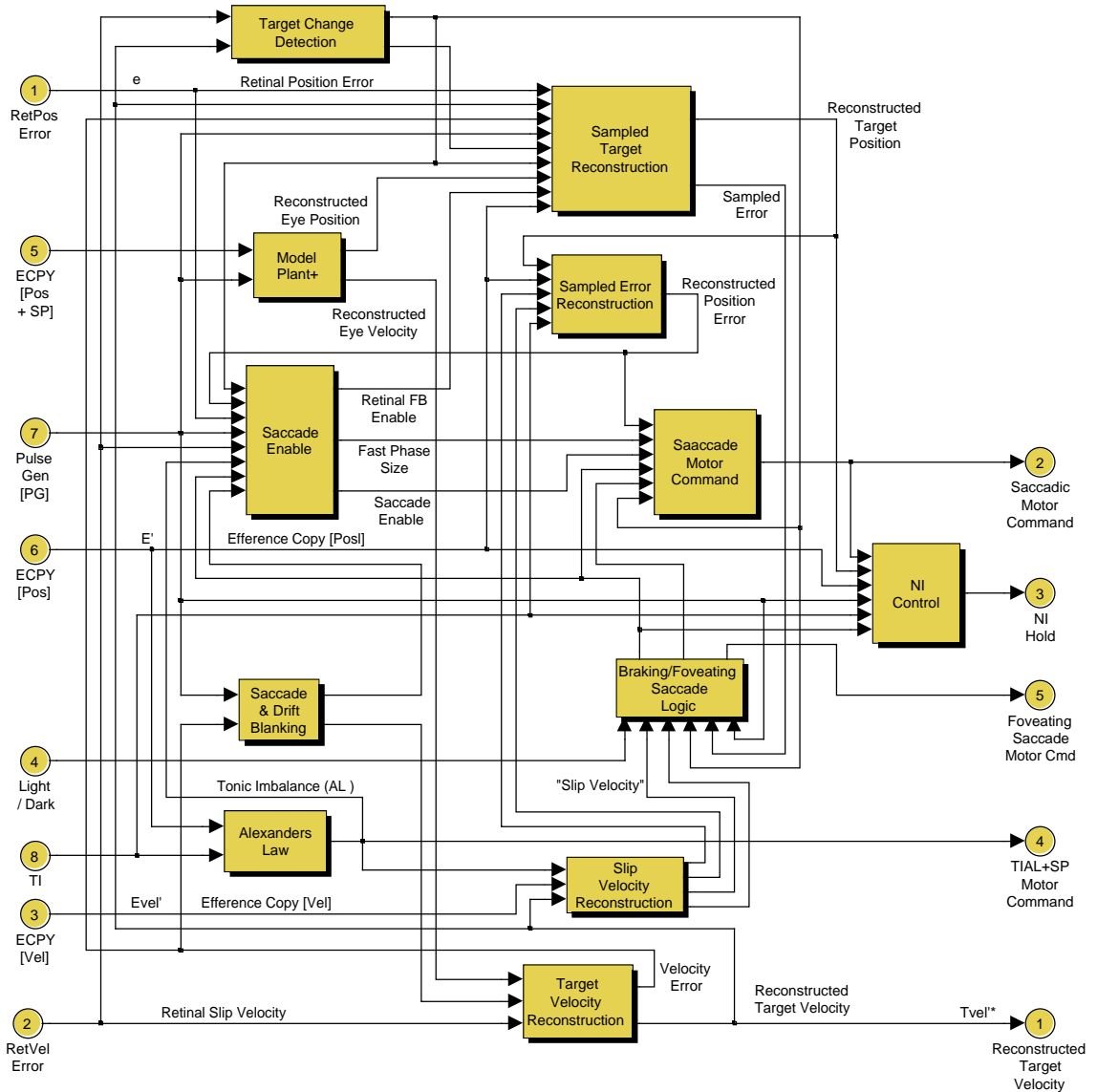
position/velocity and make appropriate decisions to generate accurate, responsive eye movements.

As the number of behaviors the IM was required to simulate increased, there was an associated increase in the number of *interconnections* between its internal blocks. Compare Figure 4-3A with Figure A-3 of the LMLN model (Dell'Osso & Jacobs, 2001), that appears in Appendix A. This is intuitively pleasing, for by analogy, a biological brain's interconnectedness greatly increases with its degree of sophistication.

Examination of the structure of the IM in Figure 4-3A only hints at its complexity. The drop shadows on functional blocks indicate that they, too, contain functional blocks. For example, the block labeled "Saccade Enable," in Figure 4-3B determines whether a corrective saccade is to be made based on visual feedback or efference copy information. This block is further composed of sub-blocks. It is beyond the scope of this chapter to provide a detailed description of each block in the model; see Appendix B for a summary of the major and supporting blocks. Here it is sufficient to state that at the model's most basic level, all the building blocks are composed of elemental operations that simulate functions (e.g., timing or summation) that could be reproduced easily by analog methods (e.g., RC simulation of membrane time constants) or by neural networks. As a result, any departures from known neuroanatomical structures or their presumed functions do not detract from the model's functional accuracy.

A

### INTERNAL MONITOR [Sacc,FS/BS,SP,AL,NI Control]



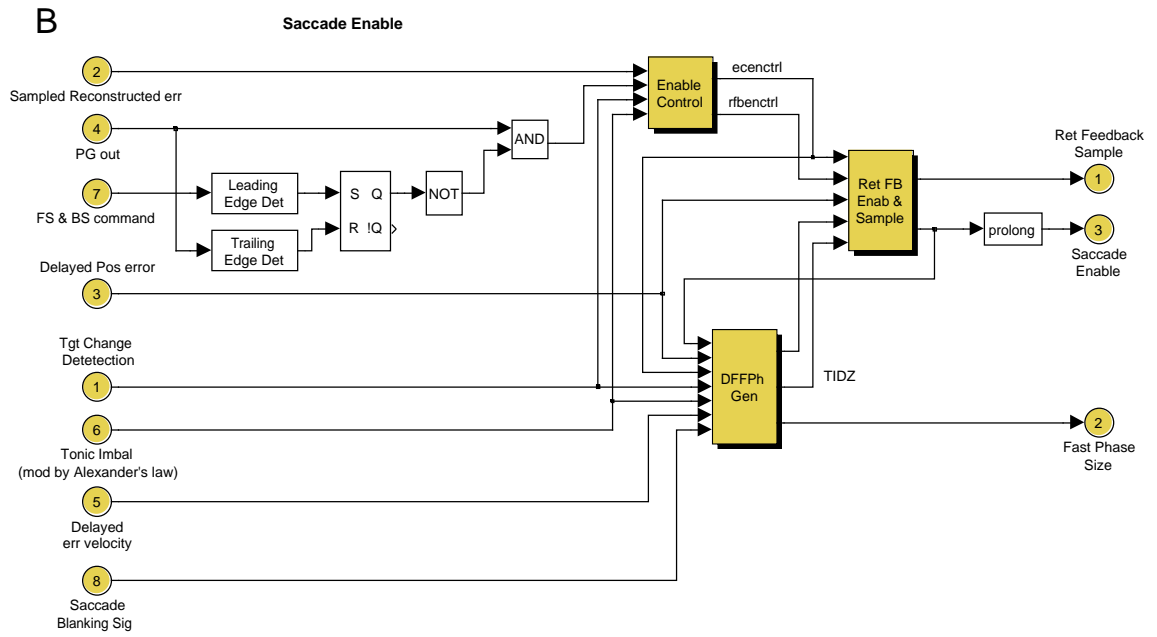


Figure 4-3

A.) The arrangement and interconnections of the functional blocks contained within the internal monitor. The major functions of the internal monitor are: detecting target changes; reconstructing target position and velocity; controlling the neural integrator; and determining the timing and amplitudes of saccades and fast phases of nystagmus. The input, output and other signal labels are consistent with those shown in Figures 4-1, 4-2, and 4-4. B.) The arrangement and interconnections within one of the major functional blocks within the internal monitor, the Saccade Enable and Timing block. As the drop shadows indicate, each of these functional blocks contain additional functional blocks within.

One of the IM's most important functions is to ensure a level of separation between the SP and saccadic subsystems so that they respond only to their appropriate input signals. For example, it is crucial that when saccades are made, the SP subsystem does not act upon them and attempt to pursue, but instead ignores perceived movement until the saccade has ended. To accomplish this, the IM "blanks" out saccades so that SP doesn't see and try to react to their large velocity changes. The complexity of this task is greatly increased by the presence of internal oscillations.

**BRAKING/FOVEATING SACCADE LOGIC:** Braking saccades are automatically generated to brake runaway eye velocities. Simple inspection of the  $PP_{fs}$  waveform reveals the basic logic necessary to decide whether a saccade will be braking or foveating. If the eye is *running away from* the target at the time of saccade programming (which precedes the actual time the saccade is generated), the velocity exceeds a user-settable threshold (default =  $4^\circ/\text{sec}$ ), and has passed its point of maximum velocity (i.e., is not still accelerating), a braking saccade will be generated. If, however, the eye is *approaching* the target at that time, and the velocity exceeds the threshold, and falls below the acceleration threshold, then the saccade will be foveating, with the magnitude calculated by the predicting where the eye will be 60 ms (default value) later, a time corresponding to the actual commission of saccade. This reinforces our initial definition of a braking saccade (Dell'Osso & Daroff, 1976; Jacobs et al., 1999): it should *oppose* the slow phase. (Note that although it is a special case, the foveating saccade is

also a braking saccade since it too acts to brake the slow phase at the time of its execution).

**FIXATION SUBSYSTEM:** The fixation subsystem is a velocity-limiting system aimed at reducing retinal slip velocity (Luebke & Robinson, 1988; Epelboim & Kowler, 1993). Fixation is most effective when the target image falls within the fovea, and the slip velocity is relatively low. These, therefore, are the activation conditions for the model's fixation subsystem. A further condition is that fixation only follows foveating (including volitional) saccades. This is based on observation of data from CN subjects that never show extended foveation in the absence of saccades or after simple braking saccades. We initially created position- and velocity-sensitivity functions that approximated the general sensitivity of the visual system: highly sensitive (scale factor = 1) for the central portion of the fovea and for lower velocities, with approximately exponentially decreasing sensitivity at increasing distance from the center of the fovea or higher velocities. This function is plotted in Appendix Figure B-7C. Position and velocity error are passed through these functions and then multiplied by a gating signal that is "on" only in the presence of a foveating saccade, to create a "quality of foveation" signal that ranges from 0 to 1. We found that the position component was, at best, redundant and therefore could be eliminated. This is supported by observations of actual CN data that show the presence of apparent "extended foveation" even following improperly programmed foveating saccades that did not achieve target foveation.

We modeled fixation using two distinct approaches: first (Figure 4-4, and Figure B-7A), to provide a “counter-signal” equal and opposite to the nystagmus velocity (the difference between the reconstructed target and eye velocities) to cancel out a portion of that oscillation; and second, to use a variable gain to modulate the velocity signal that is fed to the input of the NI and its associated linear gain pathway. The counter-signal approach is derived from the method employed to cancel the nystagmus motor signal from the retinal error signal in the first model of a normal ocular motor system capable of simulating CN (Dell'Osso, 1968). In this case, however, the subtraction is a velocity signal and is limited to periods following a foveating saccade. It is the product of the aforementioned quality signal, the nystagmus velocity, and an additional constant factor of 4 (to compensate for the 0.25 gain of the velocity signal that is passed to the ocular motor neurons). The resulting product is subtracted from the velocity signal just before the input to the NI.

In the second method, variable-gain (Figure B-7B), the quality signal is subtracted from 1 to create an overall gain. When foveation is poor, this gain is 1, allowing the full velocity signal to pass unimpeded. When foveation criteria are met, the total gain drops towards zero and permits less of the velocity signal to pass, slowing the eye. The present OMS model utilizes the first approach in its simulation of the fixation subsystem.

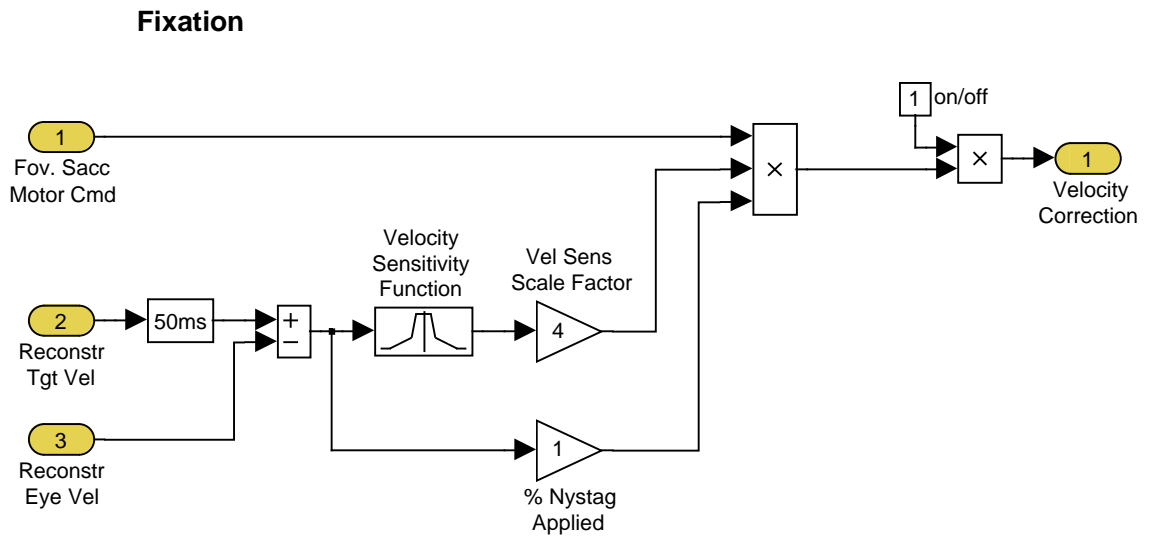


Figure 4-4

Fixation subsystem using the counter-signal approach. The velocity sensitivity function is a piecewise approximation of a Gaussian function.

#### *4.2.6 Generation of CN*

After interconnecting the SP and saccadic subsystems, it is possible to generate the underlying oscillation for pendular CN—the velocity instability of pursuit-system nystagmus. As before, we first induced the SP subsystem into spontaneous, sustained oscillation by increasing the gain in the PMC+ block. Classic CN waveforms would then result from the appropriate interjection of braking and foveating saccades during fixation and in conjunction with target-induced voluntary saccades and pursuit.

### **4.3 RESULTS**

Because we propose that the ocular motor system in subjects with CN is essentially normal, it is necessary to demonstrate that the model can perform all the behaviors seen in normals, including some commonly seen basic pathologies, such as saccadic dysmetrias, NI dysfunction, and muscle paresis. Furthermore, the presence of the internal nystagmus oscillations should not interfere with the goal-directed operation of the system, for it does not in individuals with CN.

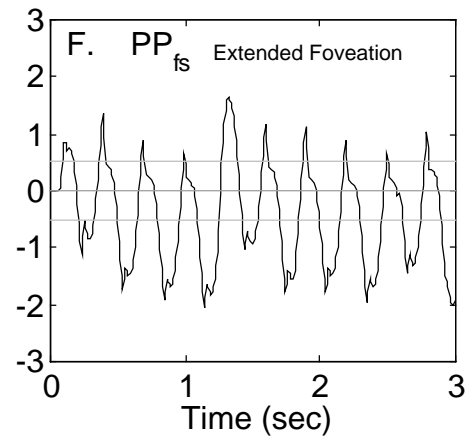
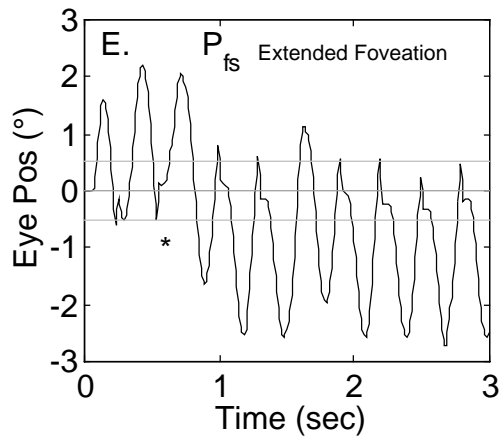
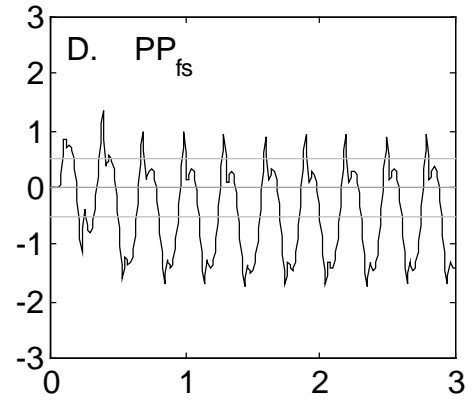
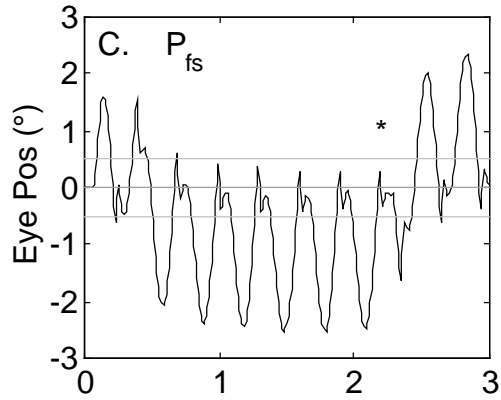
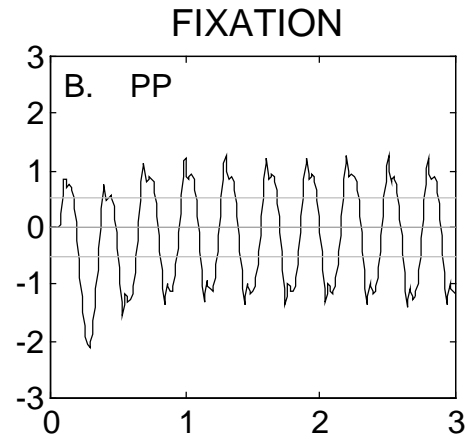
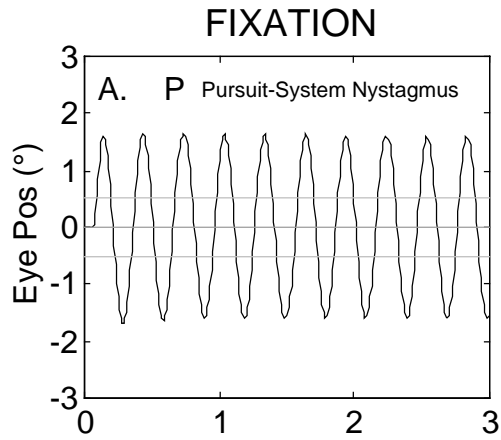
#### *4.3.1 Normal Behavior*

This model shares a common development path with our LMLN model (Dell'Osso & Jacobs, 2001). Therefore it is capable of reproducing the same range of normal behaviors as the LMLN model, such as the ability to make orthometric saccades over a wide range ( $<\pm 1^\circ$  to  $\pm 50^\circ$ ) (Dell'Osso and Jacobs, Figure A-5) and it can also

reproduce several common ocular motor dysfunctions, such as saccadic dysmetria and macrosaccadic oscillation (Dell'Osso and Jacobs, Figure A-6), gaze-evoked nystagmus, and the muscle paresis of myasthenia gravis (Dell'Osso and Jacobs, Figure A-7). In addition, as will be shown below, the current model reproduces proper responses to more complex stimuli. Comparison of the Internal Monitor of the present model with that of its predecessor, demonstrates how it is the *interconnections* of functional blocks that allows this new behavior, not the addition of new functional blocks.

#### 4.3.2 'Evolution' of CN Waveforms

The panels in Figure 4-5 show the progression of CN from the simple, initial underlying pendular velocity oscillation (panel A) that straddles the intended fixation point at  $0^\circ$ . In panel B, only braking saccades have been enabled (using the criteria described in Section 4.2.5—BRAKING/FOVEATING SACCADE LOGIC), resulting in the pseudopendular (PP) waveform. Because they all have the same fixed amplitude and do not attempt to achieve foveation, the oscillation remains symmetric around the fixation point at  $0^\circ$ . Note that in both of these waveforms, the fovea spends a bare minimum of time on the target, therefore neither is conducive to good acuity and both are seen only transiently in individuals with CN as they shift between more visually-useful waveforms.



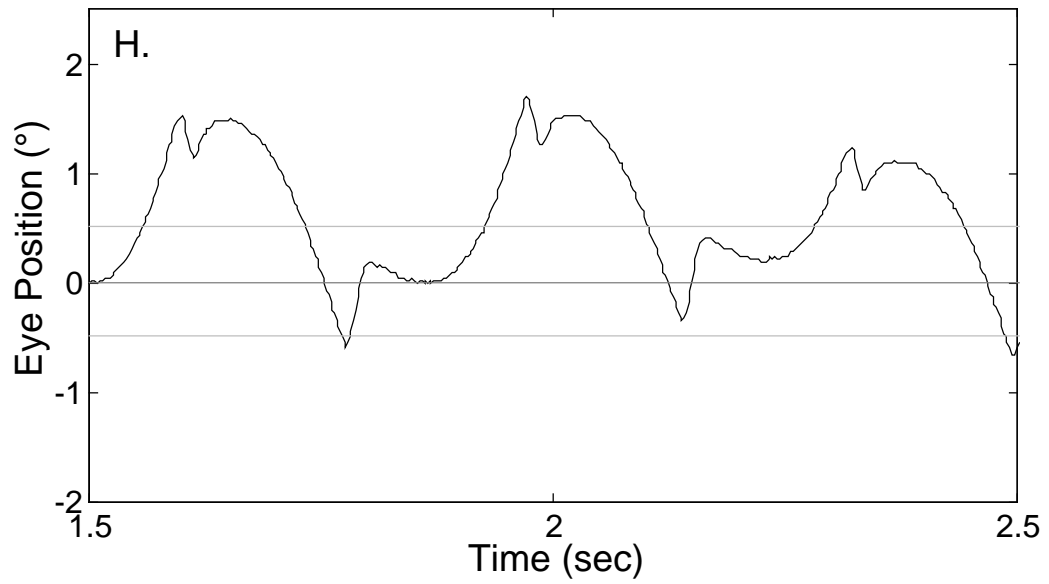
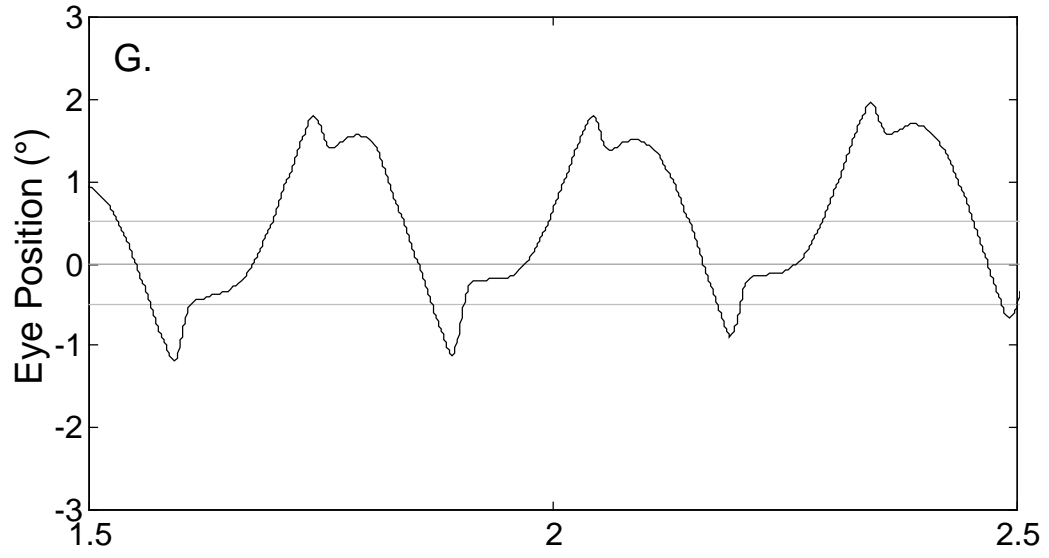


Figure 4-5

Evolution of pendular waveform of *pursuit-system* nystagmus. A.) Pendular (P) oscillation about the fixation point caused by the underlying velocity instability. B.) Braking saccades of the pseudopendular (PP) waveform damp the oscillation but do not alter its position. Foveating saccades alone in the pendular with foveating saccade ( $P_{fs}$ ) waveform [C.) and E.)] or with braking saccades in the pseudopendular with foveating saccade ( $PP_{fs}$ ) waveform [D.) and F.)] shift the eye position to allow target foveation at one peak or the other. E.) and F.) the fixation subsystem extends foveation, allowing increased visual acuity. G.) Portion of model output of  $PP_{fs}$  waveform for comparison to H.) data from a CN subject. Note the similar frequency and amplitude of the two, and compare the extended foveation periods following the foveating saccades; the model allows less eye movement during these intervals.

In panel C, the model has been directed to make foveating saccades (also as described in Section 4.2.5). Braking saccades have been disabled. This resulting waveform is  $P_{fs}$ , which no longer straddles the fixation point. The foveating saccades make use of reconstructed eye position error to foveate the target, effectively *shifting* the waveform (“bias shift”) so it is no longer symmetric about the target (Dell’Osso, 1973a). Now the periods following the foveating saccades can make a useful contribution to visual acuity, as they are both within the fovea and of low enough retinal slip velocity. In panel D, braking and foveating saccades are both active, and the result is the complex-appearing  $PP_{fs}$  waveform. (For comparison, see panels G and H, which compare the model’s  $PP_{fs}$  output with data recorded from a human subject.) An important feature in panels C and E are the spontaneous reversals of foveating saccade direction. This is known as *bias reversal*; it is commonly seen in CN and was not specifically designed into the model—it is an emergent property. The origin of bias reversals had been hypothesized to be due to a mildly unstable null making small shifts. However, the model’s behavior is due to small variations in the timing of braking/foveating saccade generation. Look at the  $P_{fs}$  case in panel C: following the foveating saccade marked with a “\*,” a second foveating saccade occurs shortly thereafter, rather than waiting for the cycle to complete. This is most probably due to conditions at the time of the second saccade’s programming (60 ms prior to its appearance) still favor a foveating saccade, for the effect of the first foveating saccade may not have been predicted to be sufficient. In panel E, the bias reversal occurs for a different reason: here the foveating saccade

expected to follow the starred saccade is skipped entirely, and the oscillation completes a turn-around before conditions again favor the programming of a foveating saccade. The saccade was skipped because the times when both the velocity and acceleration criteria, mentioned earlier, were satisfied did not overlap long enough for a saccade to be programmed. Thus, the model's emergent property has suggested new hypotheses for bias reversals.

Note the size of the braking saccades in panels B and D: they appear to be less than  $1^\circ$ , despite the fact that  $1^\circ$  was their programmed magnitude, reflected in the size of the motor command sent to the plant. This effect has been discussed in detail in previous work (Jacobs & Dell'Osso, 1997; Jacobs et al., 2001), and can be explained by the mechanical interaction between the fast and slow phases, as the saccades must overcome the opposing velocity of the slow phase, although it does not rule out any neural interaction between the SP and saccadic subsystems.

Panel E also demonstrates the effects of failure to make a foveating saccade (for reasons described above). The resulting oscillation is larger and straddles the fixation point until the next foveating saccade re-establishes target foveation and waveform bias. Compare this to Figure 2-5, from the second chapter, that shows a CN subject who, when not making braking saccades (waveform  $P_{fs}$ ), has a larger-magnitude oscillation than when braking saccades are made (waveform  $PP_{fs}$ ).

Finally, in panels E and F, the effect of the fixation subsystem upon the oscillation is shown, decreasing the effect of the oscillation when the conditions specified earlier in this chapter (Section 4.2.5—FIXATION SUBSYSTEM) are met. Note the distinct

flattening of the waveform immediately following the foveating saccades—this is *extended foveation*, a prolonging of the low-velocity, on-target period when visual acuity can achieve its highest value. Compare this to panels C and D, where the position continues sinusoidally after the saccade, reflecting the ongoing drive of the nystagmus signal. Even though the target falls on the fovea, its velocity relative to the fovea is higher than the case when foveation has been extended; therefore visual acuity will be reduced.

#### 4.3.3 Responses to Step, Pulse-Step, Ramp, and Step-Ramp Stimuli: Normal and with CN

In the first recordings of the responses of an individual with CN to step, pulse-step, ramp, and step-ramp changes in target position, it was found that, despite the ongoing oscillation, the responses to each of these stimuli were normal in both accuracy during foveation periods and timing (Dell'Osso, 1968). All of the LMLN model's previously demonstrated responses (Dell'Osso & Jacobs, 2001), are properly executed by the present evolution of the model—even when CN oscillations, and their attendant foveating and braking saccades are present. Figures 4-6 through 4-10 show the model's responses to various target stimuli in the presence of both  $P_{fs}$  and  $PP_{fs}$  waveforms analogous to the responses from our LMLN model.

Figure 4-6 shows normal saccades made over the range of  $1^\circ$  to  $30^\circ$ . Note that saccades up to  $17^\circ$  are accurate, while larger ones require an additional, corrective saccade, after a 130 msec latency, to reach the target, as is commonly seen in normal subjects. Especially noteworthy, in this and subsequent Figures, is that the presence of

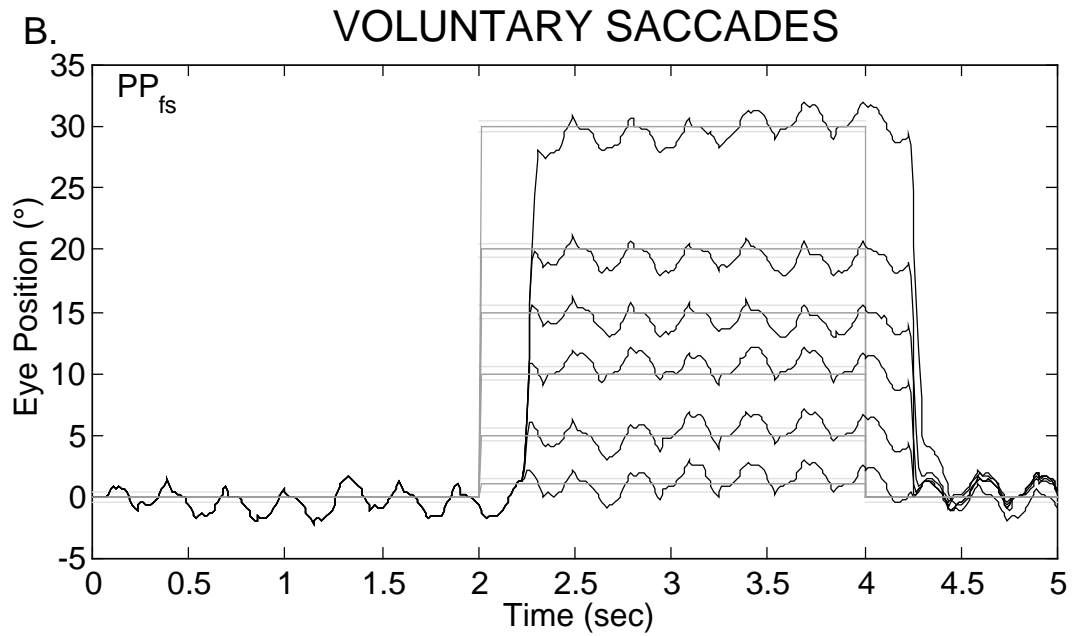
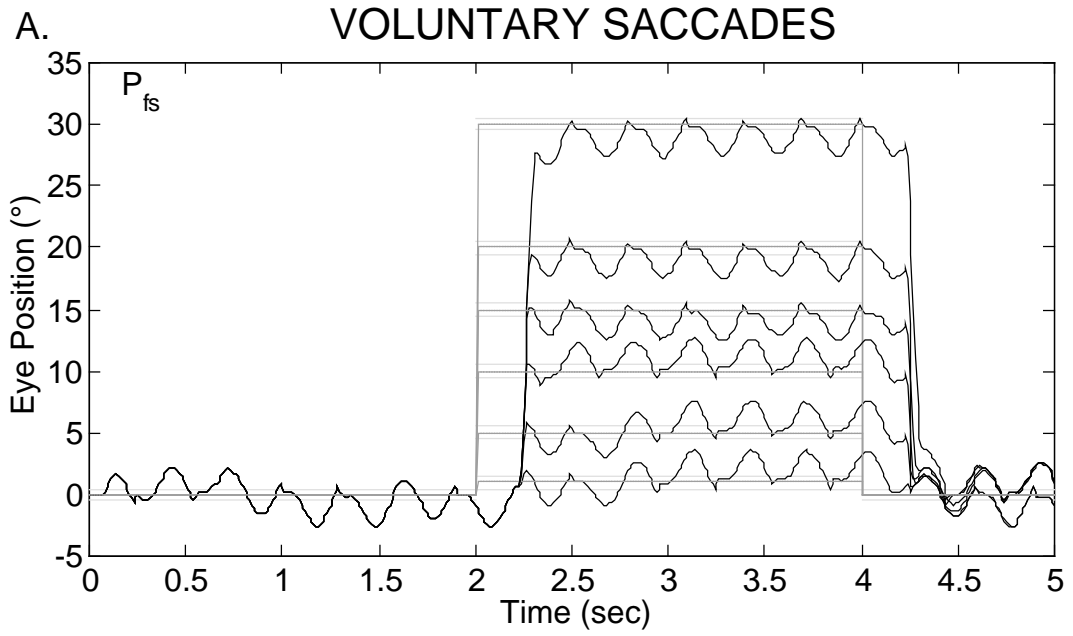


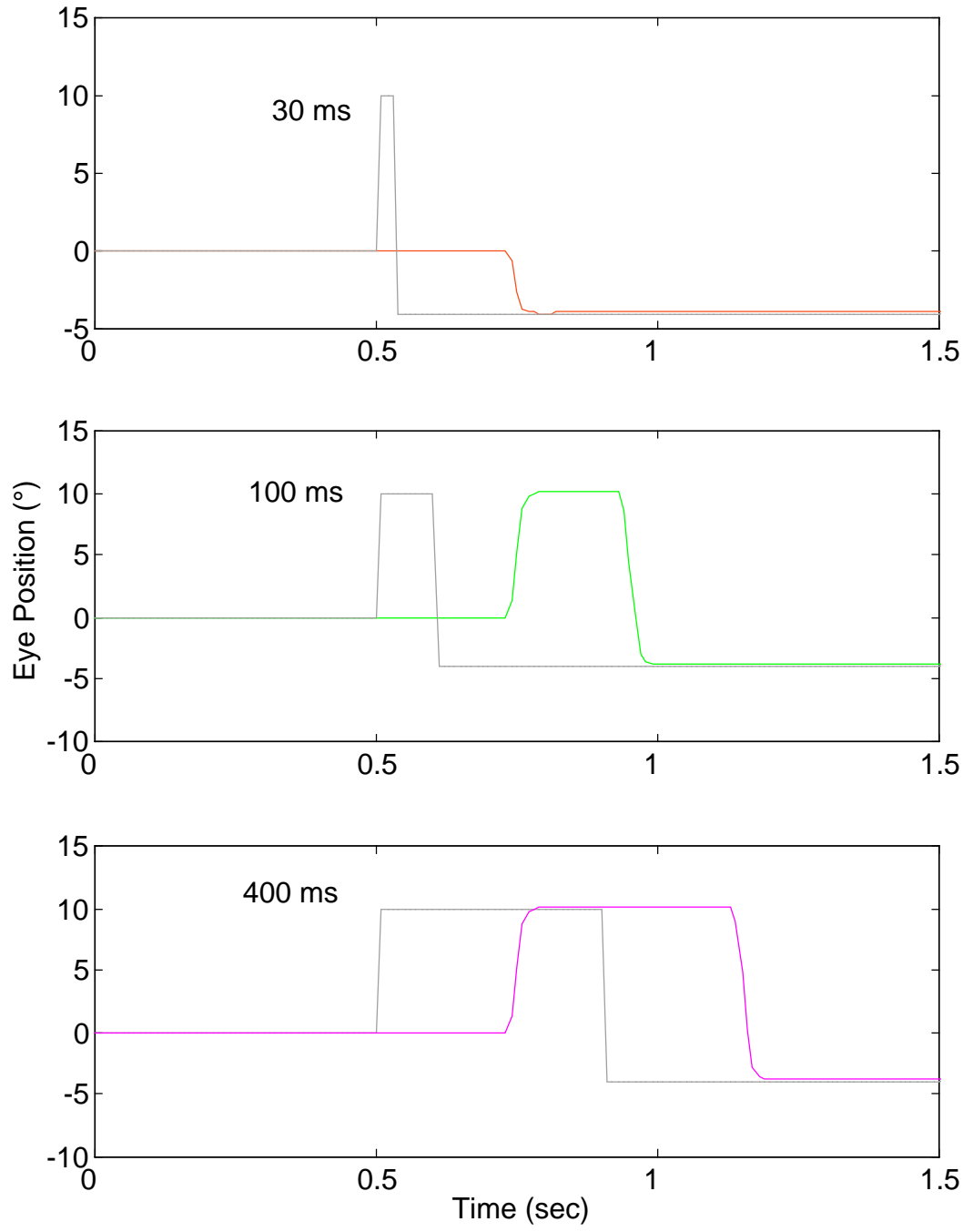
Figure 4-6

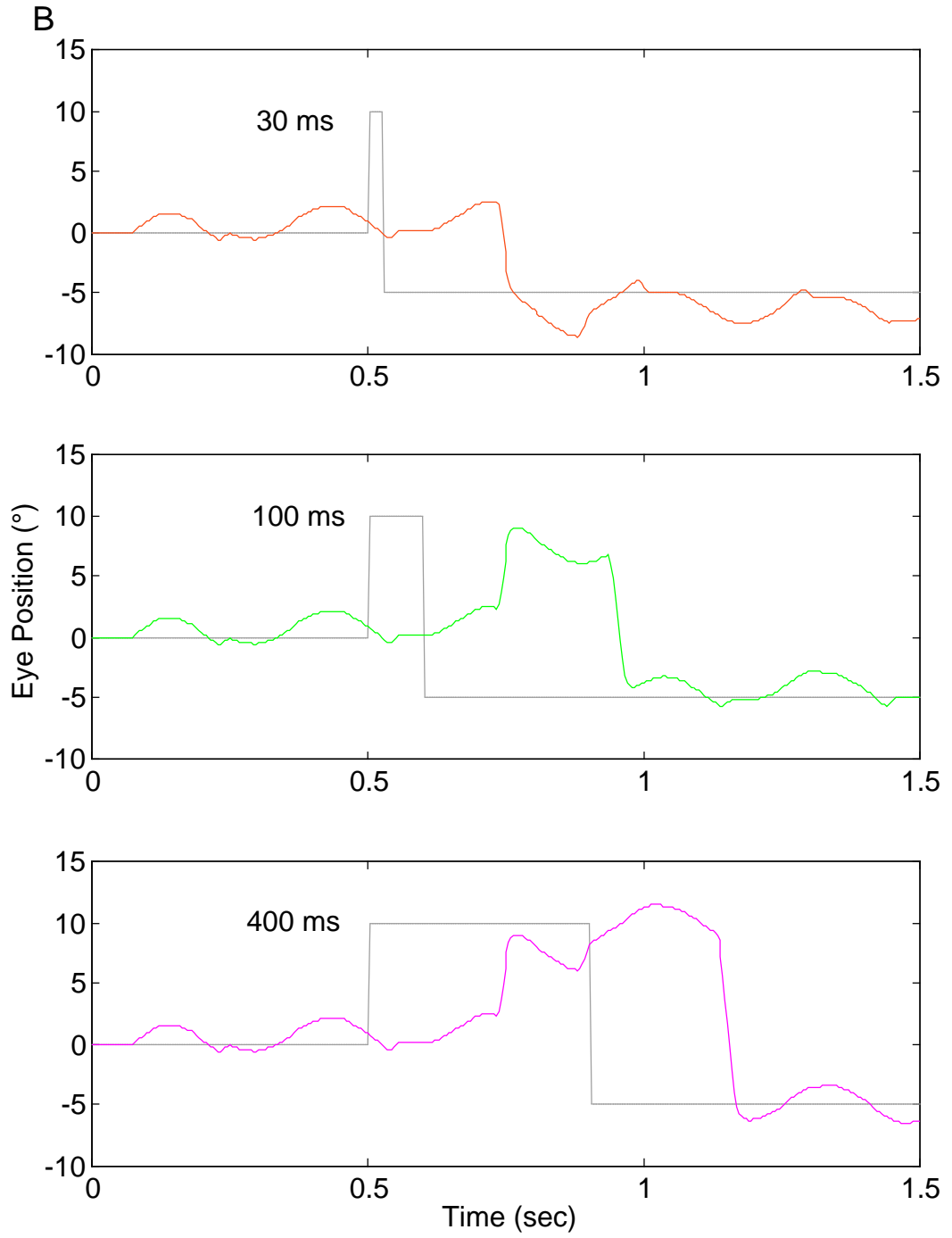
Accurate voluntary saccades made to target step changes in position ( $1-30^\circ$ ) made despite the presence of either A.)  $P_{fs}$  or B.)  $PP_{fs}$  nystagmus waveforms. Note the periods of extended foveation and spontaneous *bias shifts* about the fixation point.

nystagmus quick phases does *not* interfere with voluntary refixations. In the event that two saccadic commands compete for control of the saccadic pulse generator, the first one to arrive will be programmed, and the other one must wait for the saccadic refractory period to conclude before it is executed. This behavior duplicates that exhibited by individuals with CN. The responses made during both the  $P_{fs}$  and  $PP_{fs}$  waveforms are accurate and foveation may occur at either peak of the oscillation. Occasional bias reversals occur when a foveating or braking saccade is not made. The amplitudes of the foveating saccades vary but foveation is maintained. The responses to a  $30^\circ$ -step change in target position during  $P_{fs}$  and  $PP_{fs}$  contain short-latency corrective saccades followed by foveating saccades that quickly establish target foveation at the rightmost peaks of the oscillation. The return saccades from  $30^\circ$  do not contain corrective saccades; instead, the slow phase of the nystagmus is used to reach the target. After return to primary position, foveation may occur at either peak of the oscillation. These emergent behaviors of the model duplicate recorded responses from individuals with CN.

In Figure 4-7A, the model has been set to “normal” mode, i.e. the CN oscillation has been turned off by resetting the gain of the SP subsystem’s internal parameters (in the PMC+ block) back to their default values. Operating in this mode, responses to pulse-step stimuli are demonstrated. The model properly ignores pulses shorter than 50 msec, responding only to the second step (Becker & Jürgens, 1979). A pulse longer than 50 msec will trigger a saccade to that location, followed, 200 msec later by a second saccade in response to the step. These responses duplicate those of normal individuals. In Figures 4-7 B and C, the responses in the presence of  $P_{fs}$  and  $PP_{fs}$  CN are shown, respectively.

A





C

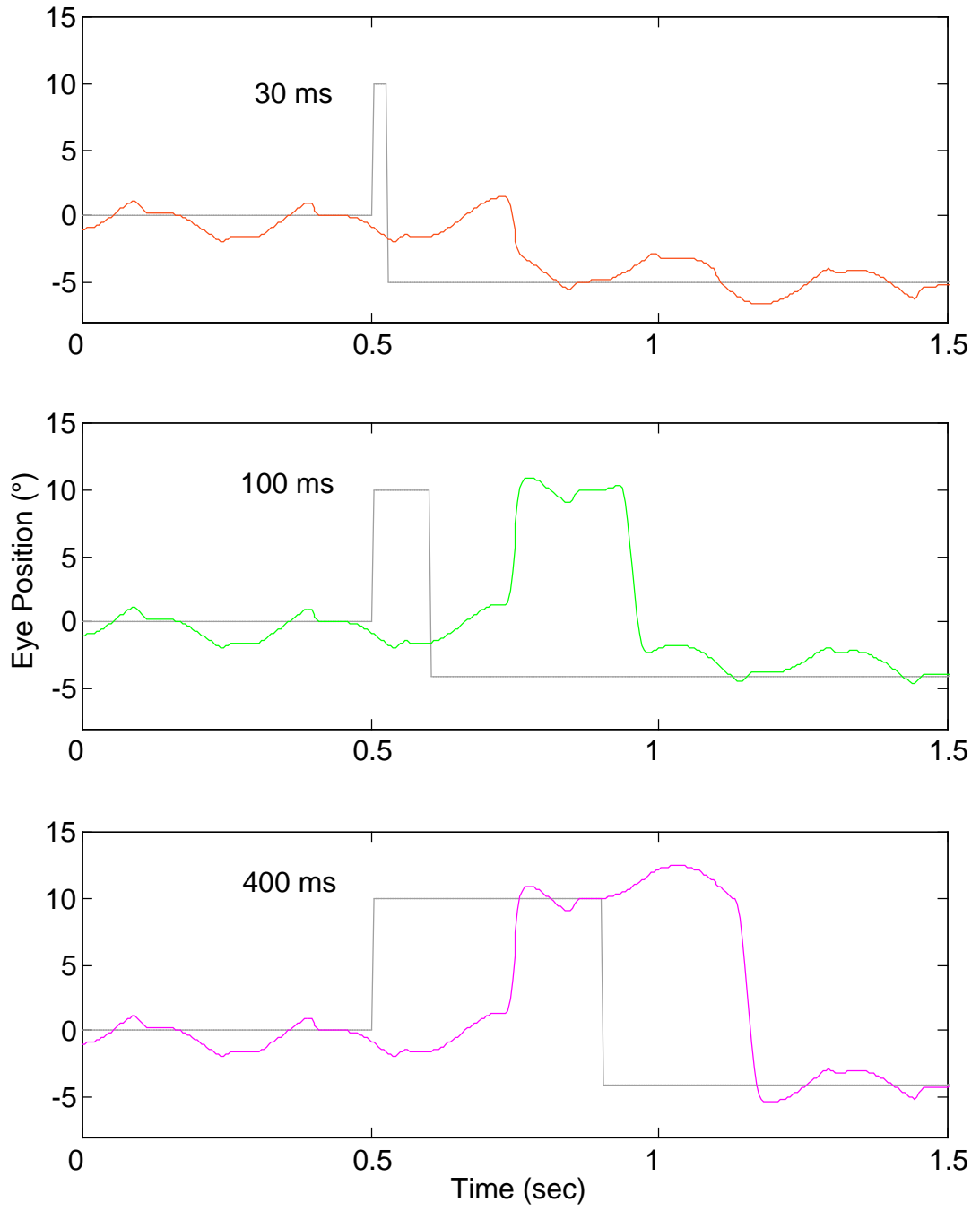


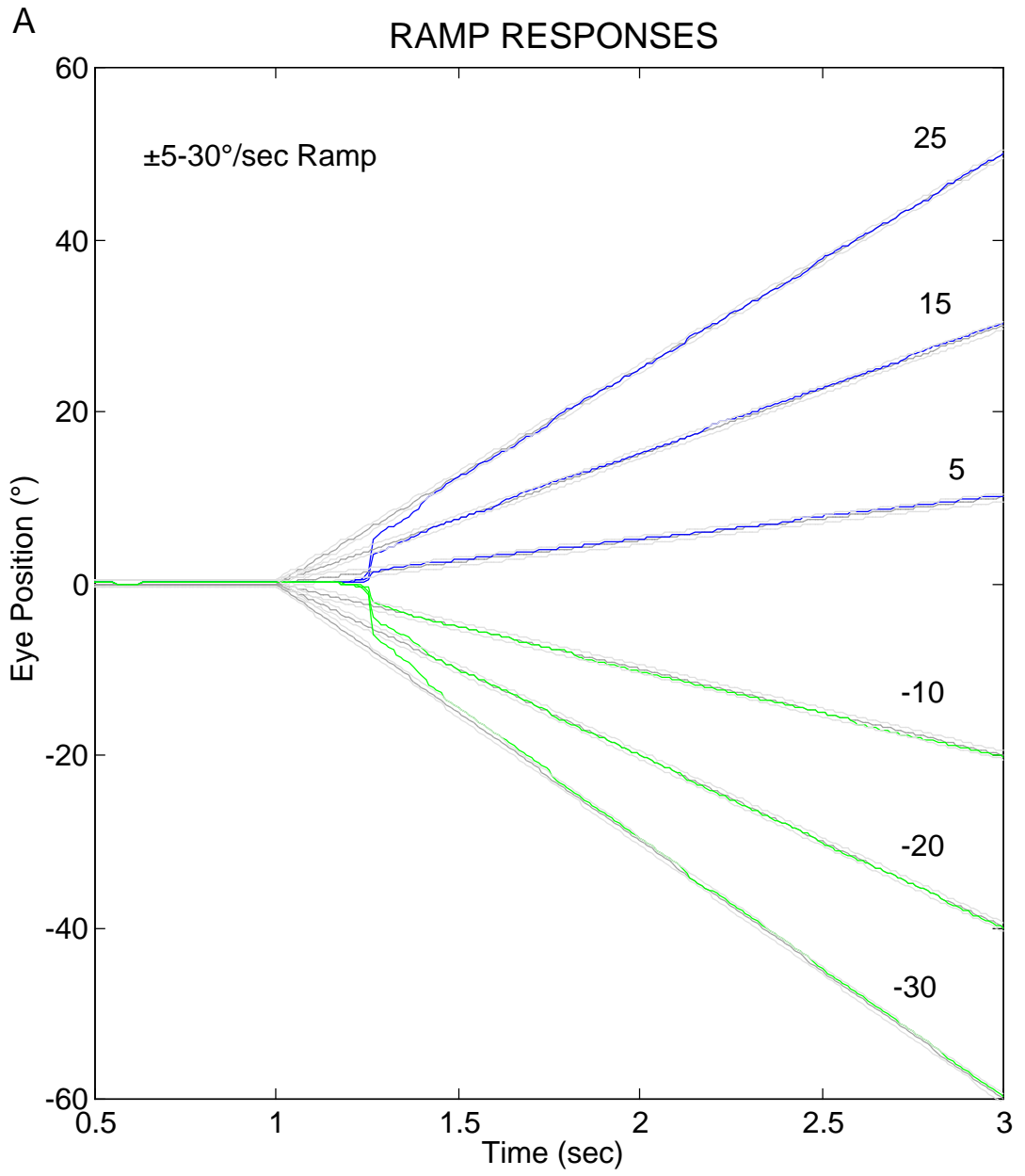
Figure 4-7

Accurate responses to pulse-step changes in target position made under A.) normal conditions and B.) either  $P_{fs}$  or C.)  $PP_{fs}$  nystagmus waveforms. In all cases, short pulse widths ( $<50$  ms) are ignored and a response is made to the second step after the appropriate saccadic latency. Longer pulse widths ( $>50$  and  $<200$  ms) result in a two-saccade response with an intersaccadic interval of 200 ms. Pulse widths  $>200$  ms are responded to as individual step responses, each after the normal saccadic latency.

Again, the responses are normal with the addition of the CN waveforms and they duplicate those of individuals with CN (Dell'Osso & Daroff, 1975).

Figure 4-8A shows that the model is capable of accurately pursuing ramps ranging from very low to moderately high velocities ( $30^\circ/\text{sec}$ ); the ramps can be to either the right or the left. The initial latency before pursuit begins is 130 ms. The eye, although off-target, almost immediately matched the target's velocity, and 100 ms later (at 230 ms) the model generated a catch-up saccade that put the eye onto the target. At high stimulus speeds, the initial catch-up saccade may be followed by a 130 ms-latency corrective saccade. Also, since the overall SP gain is 0.95, there are several more catch-up saccades made over the duration of the stimulus; catch-up saccades increase in amplitude and frequency as target velocity increases. In Figure 4-8B, the responses to step-ramp (or Rashbass) changes in target position are shown. The initial steps can be to either the right or the left and are followed by a ramp that either continues in the same direction, or goes against the initial step. The same behavior of initial and catch-up saccades described for ramp responses is exhibited in step-ramp responses.

In addition to the above normal behaviors that demonstrate separate and synergistic functioning of the SP and saccadic subsystems, the model is also capable of accurate responses to ramp and step-ramp stimuli, despite the presence of nystagmus. Figure 4-9 shows the model's responses in the presence of  $P_{fs}$  to both ramp and step-ramp changes in target position. The initial catch-up saccades for ramp stimuli are diminished by the ongoing nystagmus slow phases, an emergent behavior. Similarly, for step-ramp



### B STEP-RAMP RESPONSES

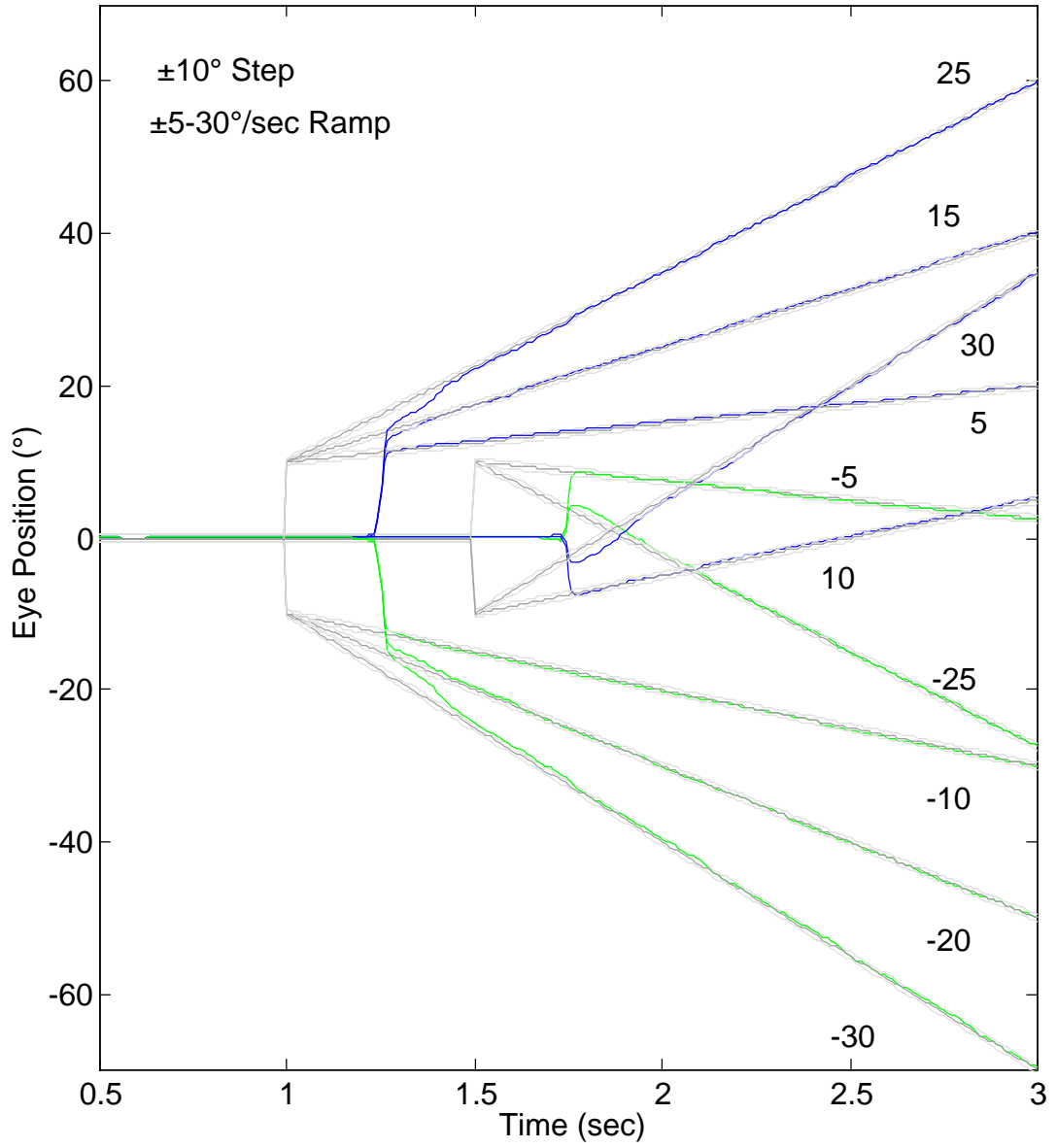
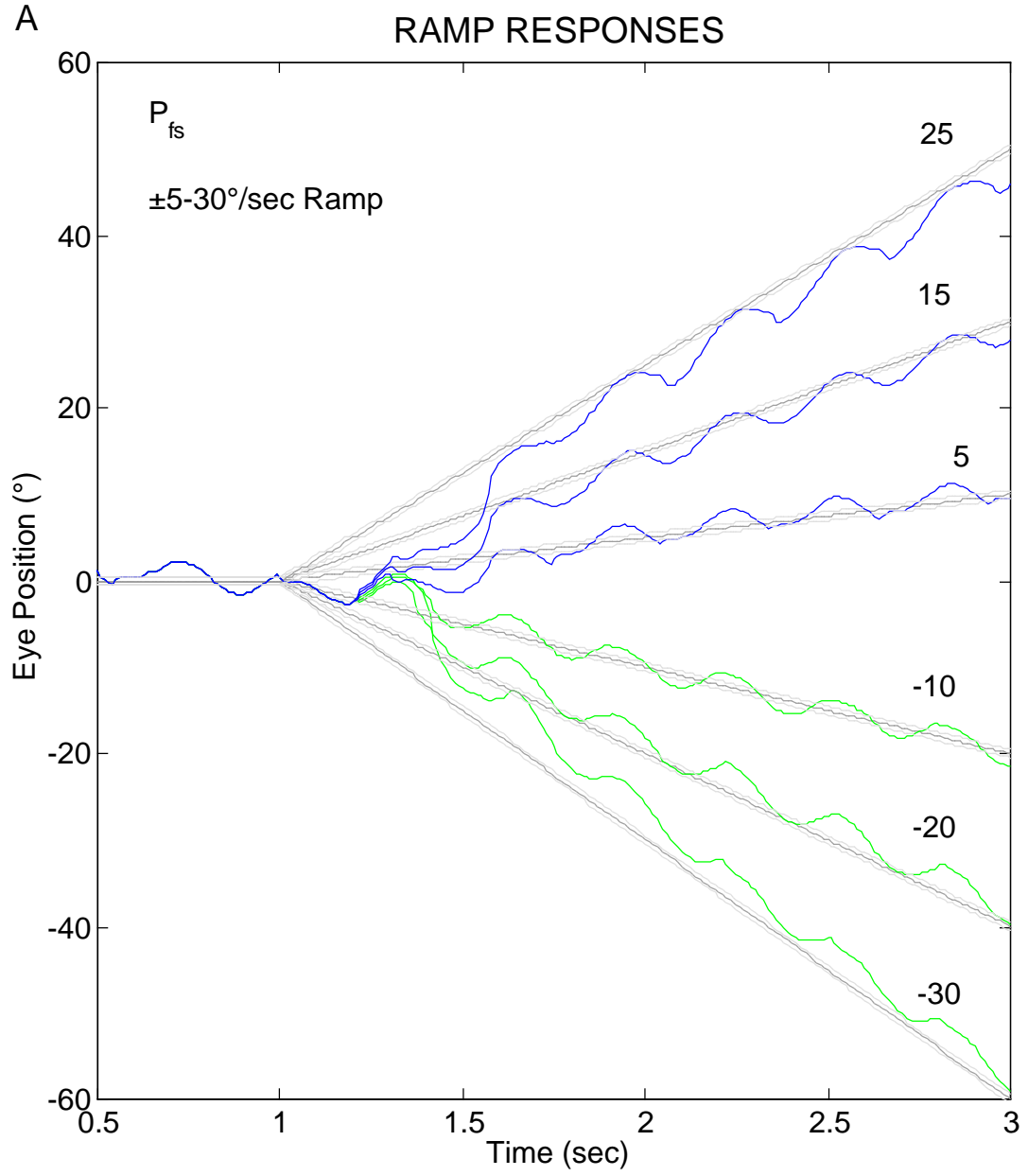


Figure 4-8

Accurate responses to A.) ramp and B.) step-ramp changes in target position made by the normal model. In both types of response, the pursuit subsystem responds first and is followed by either a catch-up saccade (ramps) or a modified refixation saccade (step-ramps). Note the corrective saccade following large initial saccades and the increased occurrence of catch-up saccades at the higher ramp velocities. In this and the following Figures, dotted lines around the target stimuli indicate the foveal extent and, ramp velocities are indicated.



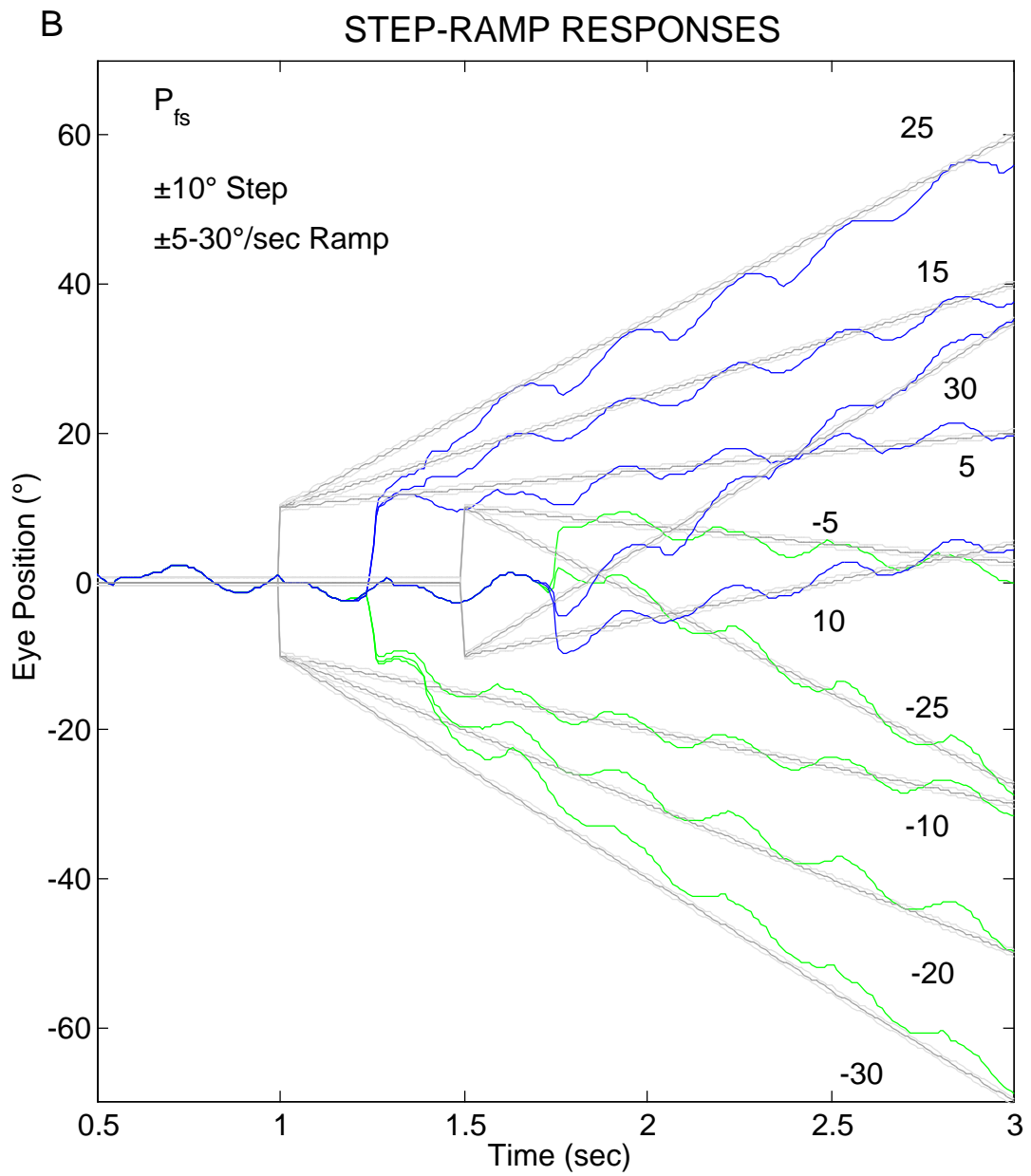
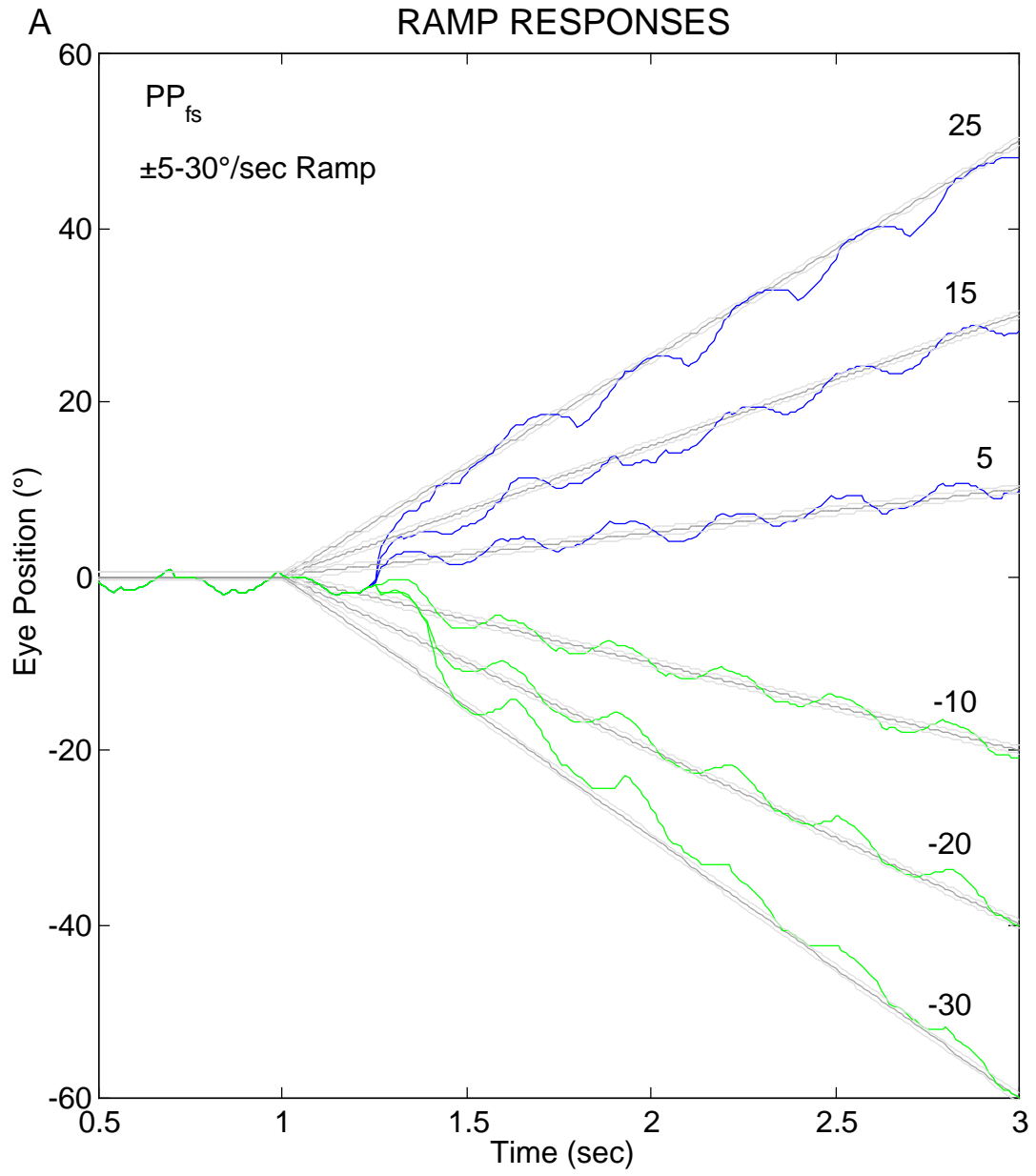


Figure 4-9

Accurate responses to A.) ramp and B.) step-ramp changes in target position made despite the presence of the  $P_{fs}$  nystagmus waveform. In this and the following Figure, note the presence of corrective saccades after larger initial saccades and the distortion of the underlying waveforms during pursuit at higher velocities, due to the required catch-up saccades. Pursuit during the periods of extended foveation is accurate.



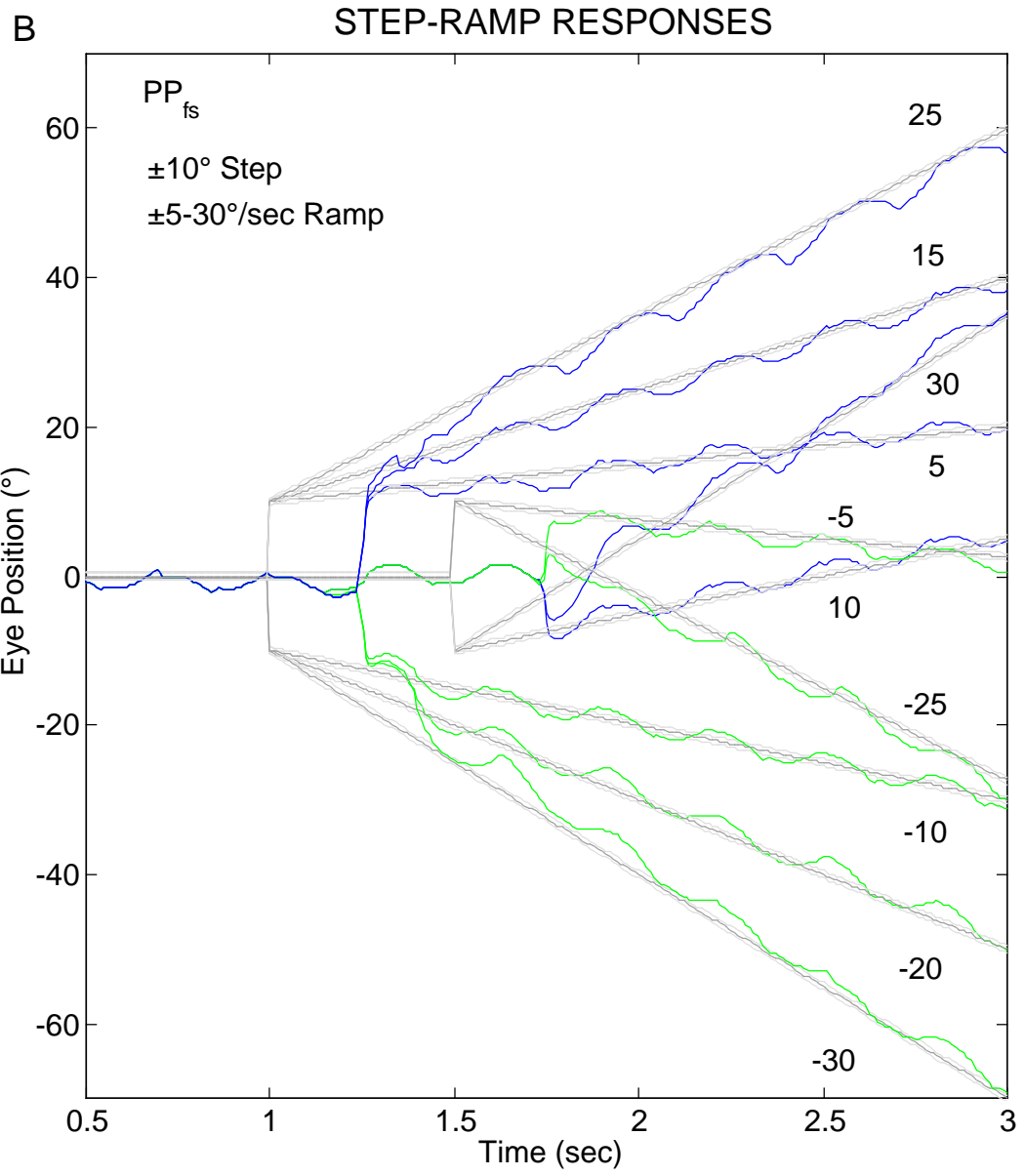


Figure 10

Accurate responses to A.) ramp and B.) step-ramp changes in target position made despite the presence of the  $PP_{fs}$  nystagmus waveform.

stimuli, the initial saccade is diminished by the nystagmus slow phase and corrective saccades may be replaced by the slow phase. As pursuit is attempted for high-velocity target motion, the eye falls behind more quickly and more, larger catch-up saccades are needed. This distorts the waveform from that exhibited during fixation of a static target. Each of the above emergent behaviors duplicates responses of individuals with CN.

In Figure 4-10, the model's responses to both ramp and step-ramp changes in target position in the presence of  $PP_{fs}$  nystagmus are shown. The observations and emergent behaviors discussed above for  $P_{fs}$  also apply to the responses made during  $PP_{fs}$  nystagmus.

## **4.4 DISCUSSION**

We constructed a computer model of the normal ocular motor system that simulates normal saccadic, pursuit, and saccade-pursuit combination responses. It also simulates saccadic dysfunctions, gaze-evoked nystagmus, myasthenia gravis, and the dual-mode waveforms of LMLN (Dell'Osso & Jacobs, 2001). To it, we have added the ability to simulate the pendular-CN responses during fixation, saccades, pursuit, and combinations of the latter two, based on the following hypotheses and foundations.

### *4.4.1 Conceptual Basis for the Model*

We hypothesized that within the OMS, an internal monitor makes use of afferent retinal and efferent motor information to detect changes in target position and to

accurately reconstruct target position and velocity from internally generated eye position and velocity, such as those resulting from CN oscillations. We further hypothesized that these oscillations are merely an extension of the ringing observed in the normal SP subsystem at the onset of pursuit. By a small gain-change, we forced the ringing to continue, rather than let it decay exponentially. Thus, our hypothetical source for pendular CN is an otherwise normal SP subsystem acting within a normal ocular motor system. This OMS model uses the abilities necessary for *normal* operation to react to the pendular velocity oscillation, inserting foveating and braking saccades, and most importantly, using efference copy to properly reconstruct a stable percept of the outside world (i.e., one without oscillopsia). Furthermore, this reconstruction effort does not diminish the model's ability to respond to complex stimuli with the appropriate accuracy and latency. The underlying pendular nystagmus is, therefore, a *pursuit-system* nystagmus—PSN, and the resulting waveforms (some pathognomonic for CN) and eye repositioning are generated by normal saccadic responses.

It should be made clear that we are *in no way* proposing a discrete anatomical structure that we purport to be “The Internal Monitor,” but rather have adopted a top-down, engineering-based approach by gathering all the disparate signals and functions proposed for the IM, and grouping them in one block for the purpose of clarity. Interestingly enough, however, recent work has uncovered the presence of many of these signals in the paramedian tract (PMT) (Buttner-Ennever, Horn, & Schmidtke, 1989; Nakamagoe, Iwamoto, & Yoshida, 2000).

#### *4.4.2 Fixation Subsystem Method*

We elected to use the counter-signal method over the variable gain method in the final model because we felt that the variable gain method could lead to problems with SP performance, perhaps even removing the model's ability to pursue moving targets. It is possible that this method can be improved by incorporating a non-linearity, driven by reconstructed target velocity that only reduces gain for velocities above a selected threshold value. This threshold value would have to be selected with great care to separate oscillations from true pursuit. The counter-signal method, while perhaps seeming to be the less obvious approach, is just as easy to implement, and offers good results with no obvious drawbacks that need be worked around.

#### *4.4.3 Foundations of the Model*

The quality of this model's performance owes to its lineage. It is the latest in a series of models of ocular motor function (and dysfunction) that have been built on some very basic foundations that have come from years of observation and analysis of normal and abnormal eye movement data, and wherever applicable, adherence to demonstrated neurophysiological structure. By taking this approach, we could ensure that the model be "robust" in its behavior, meaning that: 1) it could respond realistically to a broad range of inputs, simulating a broad range of behaviors; and 2) in the more classical control-systems definition of the term, it could recover from internal errors in a realistic manner, rather than simply failing or yielding wildly uncontrolled outputs. Drawing on these previous models, we expanded them, adding new features. Among these were a

redesigned saccadic pulse generator, still based on the resettable neural integrator (separate from the NI present in the final common motor pathway); a modified SP subsystem to generate sustained pendular oscillation; and a vastly improved, albeit complex, internal monitor that could separate eye movement from target movement and generate braking and foveating saccades.

#### *4.4.4 Development of the Model*

It is possible to learn much from simple, limited models; however, such models tend to be incapable of performing beyond their limitations. Models designed to simulate normal ocular motor control may succeed when tested against a limited repertoire of behaviors, but almost inevitably they will fail rapidly when challenged by injury to their structure, or inputs beyond their intended range. This is often due to gross oversimplifications in their design (the parsimonious false economy of ‘engineering elegance’) as well as unjustifiable assumptions about the operation of the ocular motor system. Only a model that can adequately reproduce normal functions is likely to be able, eventually, to also simulate dysfunctions, as each new insult to the system suggests a possible set of remedies that might be used both in nature and in the model. It was because of this approach that our simulation makes extensive use of efference copy of motor output signals (the *internal monitor*), as first required in a model of CN (Dell’Osso, 1968), later in a study of normal corrective saccades (Weber & Daroff, 1972), and in models of square-wave pulses (originally designated “macro square-wave jerks”) (Dell’Osso et al., 1975), gaze-evoked nystagmus, and myasthenia gravis. It also contains

a resettable neural integrator in the pulse generator (Abel et al., 1978; Abel et al., 1980) that is distinct from the common neural integrator responsible for maintaining eye position, and it utilizes feedback control of the saccadic pulse input to the common neural integrator, as required by the gaze-evoked nystagmus model (Abel et al., 1978).

As we added individual features to the model to broaden its range of simulations, each was followed by an extensive retesting of all previous simulations to ensure that no loss of function occurred. Specific attempts that failed to accomplish their goal or interfered with existing functions were discarded and those that worked, retained and refined. In this manner we interactively *evolved* the model over a period of several years. Finally, the CN model contains internal-monitor features required by our recent model of LMLN (Jacobs & Dell'Osso, 1999) that, although not necessary for CN simulations, were retained and did not interfere with them. In particular, we have not yet applied the Alexander's Law functionality towards changing the CN waveform at different gaze angles. Other features will be implemented in future work, and will be discussed in the next chapter.

Thus, in addition to expanding the range of normal responses and adding those with pendular CN, this model retains the capability of simulating normal eye movements and, with proper settings (i.e., "lesions"), other neurological conditions of its predecessors (e.g., gaze-evoked nystagmus, myasthenia gravis, and latent/manifest latent nystagmus). It represents a major step in our goal to marry previous models of ocular motor dysfunction into a unitary ocular motor control system model that can be used to

study and simulate many, if not all, of the behaviors exhibited by both normal individuals and those with specific ocular motor dysfunction.

The most important achievement of this model springs from the fact that complex-appearing behavior arises from the interaction of many simpler interconnected subsystems, as is seen in nature. We started with a SP subsystem capable of being induced into instability, and by connecting it with a saccadic subsystem and reconstructing and keeping track of commands issued by each subsystem, and monitoring the resulting eye movements to provide commands to the SP and saccadic subsystems, we were able to reproduce the most difficult pendular CN waveforms.

#### 4.5 WORKS CITED

Abadi, R. V., & Dickinson, C. M. (1985). The influence of preexisting oscillations on the binocular optokinetic response. *Ann Neurol*, **17**, 578-586.

Abadi, R. V., & Worfolk, R. (1989). Retinal slip velocities in congenital nystagmus. *Vision Research*, **29**(2), 195-205.

Abadi, R. V., Dickinson, C. M., & Lomas, M. S. (1982) Inverted and asymmetrical optokinetic nystagmus. In: G. Lennerstrand, D. S. Zee, & E. L. Keller, *Functional Basis of Ocular Motility Disorders* (pp. 143-146). Oxford, Pergamon Press.

Abel, L. A., Dell'Osso, L. F., & Daroff, R. B. (1978). Analog model for gaze-evoked nystagmus. *IEEE Trans Biomed Engng*, **BME**(25), 71-75.

Abel, L. A., Dell'Osso, L. F., Schmidt, D., & Daroff, R. B. (1980). Myasthenia gravis: Analogue computer model. *Exp Neurol*, **68**, 378-389.

Bach, M., & Hoffmann, M. B. (2000). Visual motion detection in man is governed by non-retinal mechanisms. *Vision Research*, **40**(18), 2379-2785.

- Becker, W., & Jürgens, R. (1979). An analysis of the saccadic system by means of double step stimuli. *Vision Research*, **19**, 967-983.
- Broomhead, D. S., Clement, R. A., Muldoon, M. R., Whittle, J. P., Scallan, C., & Abadi, R. V. (2000). Modelling of congenital nystagmus waveforms produced by saccadic system abnormalities. *Biological Cybernetics*, **82**(5), 391-399.
- Buttner-Ennever, J. A., Horn, A. K., & Schmidtke, K. (1989). Cell groups of the medial longitudinal fasciculus and paramedian tracts. *Revue Neurologique*, **145**(8-9), 533-539.
- Dell'Osso, L. F. (1968) *A Dual-Mode Model for the Normal Eye Tracking System and the System with Nystagmus. (Ph.D. Dissertation)*, University of Wyoming.
- Dell'Osso, L. F. (1973a). Fixation characteristics in hereditary congenital nystagmus. *Am J Optom Arch Am Acad Optom*, **50**, 85-90.
- Dell'Osso, L. F. (1973b) Improving Visual Acuity in Congenital Nystagmus. In: J. L. Smith, & J. S. Glaser, *Neuro-Ophthalmology Symposium of the University of Miami and the Bascom Palmer Eye Institute, Vol. VII* (pp. 98-106). St. Louis: CV Mosby Company.

- Dell'Osso, L. F. (1986). Evaluation of smooth pursuit in the presence of congenital nystagmus. *Neuro ophthalmol*, **6**, 383-406.
- Dell'Osso, L. F. (1994). Evidence suggesting individual ocular motor control of each eye (muscle). *J Vestib Res*, **4**, 335-345.
- Dell'Osso, L. F., & Daroff, R. B. (1975). Congenital nystagmus waveforms and foveation strategy. *Doc Ophthalmol*, **39**, 155-182.
- Dell'Osso, L. F., & Daroff, R. B. (1976). Braking saccade—A new fast eye movement. *Aviat Space Environ Med*, **47**, 435-437.
- Dell'Osso, L. F., & Daroff, R. B. (1981) Clinical disorders of ocular movement. In: B. L. Zuber, *Models of Oculomotor Behavior and Control* (pp. 233-256). West Palm Beach, CRC Press Inc.
- Dell'Osso, L. F., & Daroff, R. B. (1997) Nystagmus and saccadic intrusions and oscillations. In: W. Tasman, & E. A. Jaeger, *Duane's Clinical Ophthalmology*, Vol. II, Chap. 11 (pp. 1-33). Philadelphia: Lippincott-Raven.

Dell'Osso, L. F., & Jacobs, J. B. (2001). A normal ocular motor system model that simulates the dual-mode fast phases of latent/manifest latent nystagmus(submitted). *Biological Cybernetics*, 000-000.

Dell'Osso, L. F., Troost, B. T., & Daroff, R. B. (1975). Macro square wave jerks. *Neurology*, **25**, 975-979.

Dell'Osso, L. F., Gauthier, G., Liberman, G., & Stark, L. (1972). Eye movement recordings as a diagnostic tool in a case of congenital nystagmus. *Am J Optom Arch Am Acad Optom*, **49**, 3-13.

Dell'Osso, L. F., Van der Steen, J., Steinman, R. M., & Collewijn, H. (1992a). Foveation dynamics in congenital nystagmus III: Vestibulo-ocular reflex. *Doc Ophthalmol*, **79**, 51-70.

Dell'Osso, L. F., Van der Steen, J., Steinman, R. M., & Collewijn, H. (1992b). Foveation dynamics in congenital nystagmus II: Smooth pursuit. *Doc Ophthalmol*, **79**, 25-49.

Dell'Osso, L. F., Van der Steen, J., Steinman, R. M., & Collewijn, H. (1992c). Foveation dynamics in congenital nystagmus I: Fixation. *Doc Ophthalmol*, **79**, 1-23.

- Dell'Osso, L. F., Weissman, B. M., Leigh, R. J., Abel, L. A., & Sheth, N. V. (1993). Hereditary congenital nystagmus and gaze-holding failure: The role of the neural integrator. *Neurology*, **43**, 1741-1749.
- Doslak, M. J., Dell'Osso, L. F., & Daroff, R. B. (1979). A model of Alexander's law of vestibular nystagmus. *Biol Cyber*, **34**, 181-186.
- Doslak, M. J., Dell'Osso, L. F., & Daroff, R. B. (1982). Alexander's law: A model and resulting study. *Ann Otol Rhinol Laryngol*, **91**, 316-322.
- Epelboim, J., & Kowler, E. (1993). Slow control with eccentric targets: evidence against a position-corrective model. *Vision Res*, **33**, 361-380.
- Harris, C. M. (1995) Problems in modeling congenital nystagmus: Towards a new model. In: J. M. Findlay, R. Walker, & R. W. Kentridge, *Eye Movement Research: Mechanisms, Processes and Applications* (pp. 239-253). Amsterdam, Elsevier.
- Hertle, R. W., & Dell'Osso, L. F. (1999). Clinical and ocular motor analysis of congenital nystagmus in infancy. *J Am Assoc Pediatr Ophthalmol Strab*, **3**, 70-79.
- Jacobs, J. B., & Dell'Osso, L. F. (1997). Congenital nystagmus braking saccade characteristics. ARVO abstracts. *Invest Ophthalmol Vis Sci*, **38**, S650.

- Jacobs, J. B., & Dell'Osso, L. F. (1999). A Dual-Mode Model of Latent Nystagmus. ARVO abstracts. *Invest Ophthalmol Vis Sci*, **40**, S962.
- Jacobs, J. B., Dell'Osso, L. F., & Erchul, D. M. (1999). Generation of braking saccades in congenital nystagmus. *Neuro-Ophthalmol*, **21**, 83-95.
- Jacobs, J. B., Dell'Osso, L. F., & Leigh, R. J. (2001). Characteristics of braking saccades in congenital nystagmus (submitted). *Vision Research*, **40**, 000-000.
- Kommerell, G., & Mehdorn, E. (1982) Is an optokinetic defect the cause of congenital and latent nystagmus? In: G. Lennerstrand, D. S. Zee, & E. L. Keller, *Functional Basis of Ocular Motility Disorders* (pp. 159-167). Oxford: Pergamon Press.
- Korth, M., Rix, R., & Sembritzki, O. (2000). The sequential processing of visual motion in the human electroretinogram and visually evoked potential. *Vis. Neurosci.*, **17**(4), 631-646.
- Krauzlis, R. J., & Lisberger, S. G. (1989). A control systems model of smooth pursuit eye movements with realistic emergent properties. *Neural Computation*, **1**, 116-122.

- Krauzlis, R. J., & Miles, F. A. (1996). Transitions between pursuit eye movements and fixation in the monkey: Dependence on context. *J Neurophysiol*, **76**, 1622-1638.
- Kurzan, R., & Büttner, U. (1989). Smooth pursuit mechanisms in congenital nystagmus. *Neuro ophthalmol*, **9**, 313-325.
- Kustov, A. A., & Robinson, D. L. (1995). Modified saccades evoked by stimulation of the Macaque superior colliculus account for properties of the resettable integrator. *J Neurophysiol*, **00**, 000-000.
- Luebke, A. E., & Robinson, D. A. (1988). Transition dynamics between pursuit and fixation suggest different systems. *Vision Res*, **28**, 941-946.
- Lueck, C. J., Tanyeri, S., Mossman, S., Crawford, T. J., & Kennard, C. (1989). Unilateral reversal of smooth pursuit and optokinetic nystagmus. *Rev Neurol (Paris)*, **145**, 656-660.
- Nakamagoe, K., Iwamoto, Y., & Yoshida, K. (2000). Evidence for brainstem structures participating in oculomotor integration. *Science*, **288**, 857-859.
- Optican, L. M., & Zee, D. S. (1984). A hypothetical explanation of congenital nystagmus. *Biol Cyber*, **50**, 119-134.

- Reinecke, R. D., Suqin, G., & Goldstein, H. P. (1988). Waveform evolution in infantile nystagmus: An electro-oculo-graphic study of 35 cases. *Binoc Vision*, **3**, 191-202.
- Robinson, D. A., Gordon, J. L., & Gordon, S. E. (1986). A model of smooth pursuit eye movements. *Biol Cyber*, **55**, 43-57.
- Shallo-Hoffmann, J., Wolsley, C. J., Acheson, J. F., & Bronstein, A. M. (1998). Reduced duration of a visual motion aftereffect in congenital nystagmus. *Documenta Ophthalmologica*, **95**(3-4), 301-314.
- St. John, R., Fisk, J. D., Timney, B., & Goodale, M. A. (1984). Eye movements of human albinos. *Am J Optom Physiol Optics*, **61**, 377-385.
- Tusa, R. J., Zee, D. S., Hain, T. C., & Simonsz, H. J. (1992). Voluntary control of congenital nystagmus. *Clin Vis Sci*, **7**, 195-210.
- Weber, R. B., & Daroff, R. B. (1972). Corrective movements following refixation saccades: Type and control system analysis. *Vision Res*, **12**, 467-475.

Yamazaki, A. (1979) Abnormalities of smooth pursuit and vestibular eye movements in congenital jerk nystagmus. In: K. Shimaya, *Ophthalmology* (pp. 1162-1165). Amsterdam: Excerpta Medica.

Yarbus, A. L. (1967) *Eye movements and vision.*, Plenum Press: New York.

Yee, R. D., Baloh, R. W., & Honrubia, V. (1980). Study of congenital nystagmus: optokinetic nystagmus. *British Journal of Ophthalmology*, **64**(12), 926-932.

Zuber, B. L., & Stark, L. (1965). Microsaccades and the velocity-amplitude relationship for saccadic eye movements. *Science*, **150**, 1459-1460.

## Chapter 5

# CONCLUSIONS

### 5.1 SUMMARY

The goals of this dissertation were to examine the role and characteristics of braking (and foveating) saccades in congenital nystagmus, and to incorporate this knowledge into the development, testing and presentation of a model of the ocular motor system capable of simulating a family of CN waveforms that contain these saccades.

#### *5.1.1 Generation of Braking Saccades*

In Chapter 2, the conditions responsible for the generation of braking saccades were presented, based on the study of subjects who each displayed two of the most common waveforms ( $PP_{fs}$  and PC) containing braking saccades. It was shown that braking saccades (which, as a class, include foveating saccades) act to oppose the runaway slow-phase velocity that characterizes CN. However, there are also differences between braking and foveating saccades, for foveating saccades are goal-directed, serving to move the eye to the target, whereas braking saccades do not, contributing to visual acuity only indirectly. As a consequence, braking saccades tend to be small, usually only around  $1^\circ$  or so for  $PP_{fs}$ , and more regular in magnitude from cycle to cycle than foveating saccades, which tend to be larger and more variable in magnitude, but exceedingly regular in their end position.

It was shown that the crucial factor for triggering a braking saccade was the eye's velocity relative to the target. When this error, known as "slip velocity" exceeded a particular threshold, the resulting decrease in visual acuity was the necessary impetus to attempt slowing of the eye by the execution of that saccade. By examination of phase planes (plots of eye position vs velocity) it was determined that the most probable time for saccade programming was between 40 and 70 msec prior to its appearance, most probably closer to 40 msec. These data were crucial for designing the model presented in Chapter 4, guiding the development of the logic that incorporated these saccades into the CN waveform.

### *5.1.2 Characteristics of Braking Saccades*

Just as important as learning how and why braking saccades are generated, is understanding the effects on them (and on foveating saccades) due to the high-velocity, slow-phase oscillation. This was answered by the study presented in Chapter 3, that examined how well they conformed to several standard relationships governing their most basic characteristics and also noting how they differed. These results turned out to have implications beyond nystagmus; by the use of stimuli that could invoke analogous responses in normal subjects, a basic model demonstrated that the simple mechanical interaction between slow and fast eye movement subsystems was sufficient to explain the occasional "failure" of braking saccades to match the relationships. In such cases it was possible to regain a sense of normalcy by reexamining the methods used to measure the saccades, and devise minor corrections based on the findings. The failure to understand

this phenomenon can lead to the finding of pathological behavior where none truly exists, and lead to the positing of special or damaged structures in the brain of nystagmus subjects that do not exist in normals, such as reversed pathways (Optican & Zee, 1984; Tusa, Zee, Hain, & Simonsz, 1992; Harris, 1995), or a deficient saccadic system (Broomhead, Clement, Muldoon, Whittle, Scallan, & Abadi, 2000). In these examples, the resulting models could produce outputs that resembled particular waveforms of CN, but they also produced unrealistic outputs when trying to reproduce others. Furthermore, their repertoire of behaviors was quite limited, incapable of simulating anything they were not specifically designed to do, most especially normal behavior.

### *5.1.3 Model*

The model at the center of this dissertation attempts to avoid these potential pitfalls by taking a different approach to the problem of modeling CN. A key hypothesis driving this approach is that the ocular motor system in a subject with CN (and no other visual system or neurological problems) is not structurally different than that of a normal subject, and that any differences that may exist are due to the adaptations that must be made to function effectively despite the confounding stimuli produced by the oscillation. By this reasoning, the waveforms produced in CN are *not* the result of an abnormal or damaged brain, but rather the response of an otherwise unremarkable ocular motor system making use of its inherent abilities to reconstruct eye and target positions and velocities, even under adverse conditions. From a control-systems-engineering point of view, this makes perfect sense, for it is only by stressing a system do we really begin to

understand its most basic properties and discover what otherwise-hidden capabilities it has.

The model was designed following a traditional engineering approach, favoring the use of discrete components, connected together to make functional subsystems. These subsystems are in turn connected to other subsystems by lines that carry distinct, traceable signals representing information about the state of each subsystem of the model and its inputs and outputs. It is then possible to implement behaviors by acting upon these signals with deliberately specified linear and nonlinear arithmetic functions, filters, delays and combinatorial and sequential logic functions and using the resulting information to control each subsystem.

Following this engineering approach does not mean, however, that less attention is paid to biology. Whenever practical, known anatomical structures were implemented as blocks in the model, based on their known characteristics. For example, the saccadic subsystem is built around a resettable neural integrator, separate from the neural integrator that is part of the final common motor pathway. The necessity for this resettable NI was first demonstrated theoretically in a model by Abel et al. (1978).

Sometimes there is not enough evidence to favor one anatomical explanation over another; the true benefit of a modular approach becomes most apparent in these cases, for it gives the freedom to create a (hopefully temporary) “place-holding” block that simply must be capable of transforming known or hypothesized inputs from the subsystems that feed into it, and create outputs that can be used to drive its dependent subsystems. This practice is called sometimes referred to as “black-boxing,” based on a term from

engineering jargon, but which has become part of common language meaning, somewhat disparagingly (and most unfairly), a thing that is mysterious, especially as to function. An example occurs in the internal monitor. To calculate reconstructed target position, the eye's position must be known. Whether this information were to come from proprioception or from efference copy is unimportant; simply having it is sufficient for the purpose at hand.

In contrast, the use of neural networks for modeling, while quite powerful at solving difficult problems, does not offer the same access to internal details. Their greatest strength lies in their approximation of the actual neural structure of the systems they simulate, by the complete interconnection of many identical nodes. A neural network achieves its proper functionality not through its design, but rather by the training it receives. To reach the desired outputs for a given set of inputs, the connection weights between nodes are modified systematically by the error in the current outputs. If sufficiently trained, the network can also respond appropriately to inputs that did not fall within its original training set. However, examination of the network's final state offers no clues to the "reasoning" by which these results are actually achieved. This can be viewed as the ultimate black-box approach, and there is no reason that a large complex model such as the one presented in this dissertation could not contain subsystems developed in this manner.

Regardless of the methods used to implement the whole model, or parts of it, in order to be considered as a starting point for modeling CN, the model first needs to be able to reproduce the behavior of a normal ocular motor system, and to do so with

stability and robustness; unusual or ill-conditioned inputs should not cause unstable outputs. As stated previously, a chief hypothesis of this dissertation is that the factors that shape CN waveforms are the built-in capabilities of the OMS brought to light by having to provide the best possible visual acuity despite the presence of an internally-generated velocity noise. Therefore the greatest concentration of modeling effort was initially applied towards these normal (and non-CN-related pathological) behaviors, since they remain recognizably present in people with CN. Only after such normal behavior can be replicated is it then “safe” to start expanding the model to produce the waveforms of CN.

If this goal is met, the model might be able to fill the same role as a “digital animal” model of CN, since at present there are vanishingly few animal models of CN, though several have been proposed, but invariably these animals turned out *not* to have CN, but either LMLN or an acquired nystagmus. At present, there is only one verified animal model, a family of Belgian Sheepdogs with a mutation that affects the optic chiasm (Williams, Garraghty, & Goldowitz, 1991; Williams & Dell'Osso, 1993; Dell'Osso, 1994; Dell'Osso & Williams, 1995; Dell'Osso, Hertle, Williams, & Jacobs, 1999). In the most extreme case, *achiasma*, the chiasm is totally eliminated and visual input remains ipsilateral from retina to visual cortex, although there is a lesser form, *hemichiasma*, that causes partial, unequal decussation so that a much smaller fraction of the axons cross over from each eye to the contralateral lateral geniculate nucleus (Hogan & Williams, 1995). Dogs with either of these conditions display pendular and jerk horizontal CN and vertical *see-saw nystagmus*, where when one eye moves up and intorts, the other moves down and extorts. These dogs have been extensively studied, and

have been used to test a new surgical treatment for several forms of nystagmus.

Unfortunately, the mutation has been found only in this one pedigree, and severe fertility problems, and limited understanding of the genetics of the defect have endangered the line's survival. In this light, a robust, reliable, easily accessible computer model of CN may prove invaluable.

## **5.2 FUTURE WORK**

Although the model presented here is quite powerful and informative, it is not complete; many features still need to be added. Perhaps the biggest omission is that at this time it only simulates pendular CN waveforms. Jerk and pseudocycloid waveforms are just as important, and may have a different genesis. Alexander's law will be used to cause changes in the CN waveform as it varies around the null point. Similarly, the null will shift in the direction opposite of pursuit. Further integration of the currently separate LMLN and CN functionality will allow both to exist simultaneously (some individuals have both types of nystagmus), and the CN can also have a latent component (i.e. produce CN waveforms that change as a function of which eye is fixating).

The next major change will deal with the model's uniocular nature, i.e. currently it controls only one eye. (It is possible to drive a second eye, as shown by the myasthenia gravis simulations made with the LMLN version of the model, but in this case it is the same control signal driving two plants with different characteristics, demonstrating the paresis and the normal eye for comparison.) The real ocular motor system is binocular,

making decisions for two eyes, with a variable degree of yoking between them (Dell'Osso, 1994). Also, the two halves of the system are connected in push-pull, so each half actually provides only a unidirectional drive signal; movement in the other direction is provided by the complementary half. Binocularity will allow the simulation of convergence effects on nystagmus, such as the damping of CN.

Another future goal is extending the functionality of the fixation subsystem so that the duration of foveation extension periods can exceed 100 msec, as is commonly seen in CN subjects with the best visual acuity. Currently the fixation system can only “flatten” the slow phase when it meets the criteria for foveation, slowing the eye so that portion of the waveform spent in foveation has a minimal velocity. To achieve this extension, it might be necessary to allow the fixation subsystem to directly influence the nystagmus oscillation at its source, resetting the phase so that after the end of a foveating saccade the oscillation has to build up from zero again, rather than simply continuing onward from where it was interrupted, as it currently does. This modification may also be necessary for the generation of the pseudocycloid waveform, which looks like half of a pendular waveform with large braking saccades to bring the fovea towards (but not onto) the target.

Eventually the model will be further enhanced by the addition of VOR and optokinetic subsystems to study the effects of movement on nystagmus, for both normal and abnormal function. This is of particular importance, because phylogenetically, VOR is one of the oldest components of the OMS, and therefore has greatly affected the evolution of the subsystems that developed later. The addition of optokinetic function

will enable the simulation of the effect of extra-foveal stimuli, such as full-field patterned movement on nystagmus. This will parallel future studies with CN (and LMLN) subjects who will be exposed to such stimuli to learn how they react when presented with such stimuli.

### **5.3 CONCLUSIONS**

Recall the first two quotes that appeared at the very beginning of this dissertation: “Do not write about nystagmus; it will lead you nowhere,” and “There are only two things we do not know about nystagmus—the origin of the fast phase, and the origin of the slow phase.” With any luck, after reading this dissertation these quotes can be seen in the humorous vein intended. During Wilbrand’s life, nystagmus was more or less a mystery, not particularly amenable to study or understanding, for the tools available to investigators at the beginning of the century were quite limited. As discussed in the first chapter of this dissertation, the past fifty years have been a sort of renaissance for eye movement research, as sensors, electronics, computers and engineering methods have become increasingly affordable, powerful and refined, allowing for ever-increasing quantitative studies. This happy confluence has allowed us to greatly increase our understanding, and over the past decades the body of knowledge in the field has grown explosively. This model is submitted with the hope that it, too, will become part of the ocular motor system researcher’s toolbox, for it provides a remarkably robust insight into the presumed workings of the OMS. It will be made freely available to all who wish to

examine, evaluate and experiment with it, adding to, refining and, if need be, fixing the many subsystems presented here. (By no stretch of the imagination should it be inferred that this model is being presented as flawless, the Platonic ideal of the ocular motor system. That would be a disastrously ridiculous claim to make, given a tenet in computer science that says, in effect: the more complex a system is, the harder to prove it is “correct,” and this is actually pretty difficult for all but the most trivial systems (Dijkstra, 1976; Gries, 1981; Holzmann, 1991), not to mention how much there is left to learn about the workings of the OMS.) As this model matures, it will be possible to use it as a cornerstone for investigating nystagmus, since major hypotheses can be tested by the construction and implementation of new subsystems. Indeed, as has been the case with the development to date, design choices can be seen as hypotheses, although some will remain untestable for some time to come, while anatomical study of the OMS progresses.

A potential consequence of any non-trivially complex model is the possibility that it may produce behaviors for which it was not specifically designed. If these unexpected behaviors reproduce features seen in real-world data, and if the model design has mirrored the organization of the system being studied, they are *emergent properties*, and understanding how and why they occur may shed some light on how the real system works.

Careful observation of this model’s outputs, as it was presented with a variety of inputs, has turned up several emergent properties, involving interactions between the fast- and slow eye-movement subsystems. Perhaps the most important result is that the magnitude of goal-directed saccades are calculated after accounting for the slow-phase

oscillation, rather than simply calculating the difference between where the target is, and where the eye is “supposed” to be; the resulting hypometric saccade plus the CN slow phase foveates the target.

Another striking result is that the addition of foveating saccades is enough to convert the underlying pendular velocity oscillation that caused the eye to straddle the intended point of regard, into nystagmus that is ‘biased’ to one side or the other of that point. In fact, calling this a “bias” exposes a bias in the thought process during the early analysis of CN data (Dell'Osso, 1973), namely that in addition to these foveating saccades, it would be necessary to add a constant position offset to the output of the model to achieve this aim. As shown in Chapter 4, Figures 4-5A and 4-5C, this was not necessary.

Figure 4-5B also demonstrates that the addition of braking saccades will change the peak-to-peak amplitude of the oscillation, obviating the need to modify it at its source, as was originally thought necessary.

Another emergent property can be seen in later panels in that figure. In Figures 4-5C, D and F, the waveform switches between left- and right-beating, without changing the point of fixation, i.e., remaining centered around 0°. This is bias reversal, and this model is the first to simulate this commonly observed behavior and propose hypotheses for the cause.

Figure 4-9B illustrates another common observation that the model was not specifically programmed to emulate. When the target moves, the eye can catch up with it either by making a saccade, or, if conditions allow (the slow phase is already accelerating

in the direction of the new target position), it can simply “ride” the slow phase to the desired position.

Finally, it should be noted that the CN outputs of this model display *variability* in waveform from cycle to cycle instead of machine-like regularity. This gives the results a very lifelike appearance that had not been anticipated during the design of the model. The differences in saccade timing and magnitude, and their interactions with smooth pursuit are due to noise, in the form of small errors in the velocity signals (biologically, an intrinsically noisy signal) that can affect the dependent subsystems that use this information to make decisions about the programming of upcoming eye movements.

Shortly after the end of the second World War the Scottish ophthalmologist Sir Stewart Duke-Elder (GCVO, MA, LL.D., PhD, DSc, BSc, MB, ChB, MD, FRCS, FRCS(Edin), FACS, FRACS, FRCP, FRS), arguably one of the most influential and respected visual scientists of his time, published volume 4—Ocular Motility and Strabismus—of what would be his *magnum opus* “System of Ophthalmology,” a 15-volume set (completed shortly before his death in 1978) that covered just about every conceivable topic in the field. In the brief section on congenital nystagmus Duke-Elder included a short clinical description, with little or no speculation as to the cause or origin of the oscillation, and then summarized: “[O]n the whole it is a permanent and untreatable anomaly which should be eliminated by eugenic prophylaxis.” (Duke-Elder & Wybar, 1949).

Even if this statement is to be interpreted most generously, considering the term “eugenic prophylaxis” from a pre-war point of view, and assuming that his phrasing

“should be eliminated” was not a *directive* to prevent people with CN from reproducing, but a statement of cause and effect that such an approach *would* be effective, as no other options existed at the time, it is still a horrifying statement. At best, it is in effect a white flag, surrendering all hope of understanding a puzzling, and often benign, condition for no justifiable reason other than to be rid of it. It is quite difficult to reconcile this attitude with the many scientific achievements of his distinguished life’s work.

Fortunately, at the time of this writing, we have much greater reason for optimism. In the half century since Duke-Elder penned those words, the many advances in tools and techniques—including observation, recording and analysis, animal studies and, of course, modeling—have yielded an improved understanding of CN. It is no longer mysterious and unassailable; there are now many therapies that can greatly lessen the impact that it has on the day-to-day existence of those who live with it. Some of these treatments appeared at the end of Duke-Elder’s career, and some are being developed today. Perhaps it is possible that even more effective treatments, maybe even a cure, might be found in the not-too-distant future.

## 5.4 WORKS CITED

- Abel, L. A., Dell'Osso, L. F., & Daroff, R. B. (1978). Analog model for gaze-evoked nystagmus. *IEEE Trans Biomed Engng*, **BME(25)**, 71-75.
- Broomhead, D. S., Clement, R. A., Muldoon, M. R., Whittle, J. P., Scallan, C., & Abadi, R. V. (2000). Modelling of congenital nystagmus waveforms produced by saccadic system abnormalities. *Biological Cybernetics*, **82**, 391-399.
- Dell'Osso, L. F., Hertle, R. W., Williams, R. W., & Jacobs, J. B. (1999). A new surgery for congenital nystagmus: effects of tenotomy on an achiasmatic canine and the role of extraocular proprioception. *J Am Assoc Pediatr Ophthalmol Strab*, **3**, 166-182.
- Dell'Osso, L. F. (1994). Evidence suggesting individual ocular motor control of each eye (muscle). *J Vestib Res*, **4**, 335-345.
- Dell'Osso, L. F., & Williams, R. W. (1995). Ocular motor abnormalities in achiasmatic mutant Belgian sheepdogs: Unyoked eye movements in a mammal. *Vision Res*, **35**, 109-116.
- Dell'Osso, L. F. (1973). Fixation characteristics in hereditary congenital nystagmus. *Am J Optom Arch Am Acad Optom*, **50**, 85-90.
- Dijkstra, E. W. (1976) *A discipline of programming.*, Prentice Hall: Englewood Cliffs, NJ.
- Duke-Elder, S., & Wybar, K. (1949) *Ocular motility and strabismus (Vol IV)*. System of Ophthalmology., Mosby: St. Louis.

- Gries, D. (1981) *The science of programming.*, Springer-Verlag: New York.
- Harris, C. M. (1995) Problems in modeling congenital nystagmus: Towards a new model.  
In: J. M. Findlay, R. Walker, & R. W. Kentridge, *Eye Movement Research: Mechanisms, Processes and Applications* (pp. 239-253). Amsterdam: Elsevier.
- Hogan, D., & Williams, R. W. (1995). Analysis of the retinas and optic nerves of achiasmatic Belgian sheepdogs. *J Comp Neurol*, **352**, 367-380.
- Holzmann, G. J. (1991) *Design and validation of computer protocols.*, Prentice Hall: Englewood Cliffs, NJ.
- Optican, L. M., & Zee, D. S. (1984). A hypothetical explanation of congenital nystagmus. *Biol Cyber*, **50**, 119-134.
- Tusa, R. J., Zee, D. S., Hain, T. C., & Simonsz, H. J. (1992). Voluntary control of congenital nystagmus. *Clin Vis Sci*, **7**, 195-210.
- Williams, R. W., Garraghty, P. E., & Goldowitz, D. (1991). A new visual system mutation: Achiasmatic dogs with congenital nystagmus. *Soc Neurosci Abstr*, **17**, 187.
- Williams, R. W., & Dell'Osso, L. F. (1993). Ocular motor abnormalities in achiasmatic mutant Belgian sheepdogs. *Invest Ophthalmol Vis Sci*, **34**, 1125.

## Appendix A

# A NORMAL OCULAR MOTOR SYSTEM MODEL THAT SIMULATES THE DUAL-MODE FAST PHASES OF LATENT/MANIFEST LATENT NYSTAGMUS

### **A.0 ABSTRACT**

The fast phases of latent/manifest latent nystagmus (LMLN) may either cause the target image to fall within (foveating) or outside (defoveating) the foveal area. We previously verified that both types are generated by the same mechanism as voluntary saccades and propose a hypothetical, dual-mode mechanism (computer model) for LMLN that utilizes normal ocular-motor control functions. Fixation data recorded during the past 30 years from 97 subjects with LMLN using both infrared and magnetic search coil oculography were used as a basis for our simulations. The MATLAB/Simulink software was used to construct a robust, modular, ocular motor system model, capable of simulating LMLN. Fast-phase amplitude vs. both peak velocity and duration of simulated saccades were equivalent to those of saccades in normal subjects. Based on our LMLN studies, we constructed a hypothetical model in which the slow-phase velocity acted to

trigger the change between foveating and defoveating LMLN fast phases. Foveating fast phases were generated during lower slow-phase velocities whereas, defoveating fast phases occurred during higher slow-phase velocities. The bidirectional model simulated Alexander's law behavior under all viewing and fixation conditions. Our ocular-motor model accurately simulates LMLN patient ocular motility data and provides a hypothetical explanation for the conditions that result in both foveating and defoveating fast phases. As is the case for normal physiological saccades, position error determined saccadic amplitudes for foveating fast phases. However, final slow-phase velocity determined amplitudes of defoveating fast phases. In addition, we suggest that individuals with LMLN use their fixation subsystem to further decrease the slow-phase velocity as the target image approaches the foveal center.

## **A.1 INTRODUCTION**

Latent/manifest latent nystagmus (LMLN) is a specific type of infantile nystagmus that occurs subsequent to strabismus in some patients (Dell'Osso, Schmidt, & Daroff, 1979; Dell'Osso, Traccis, & Abel, 1983). It may be confused with another type of infantile nystagmus, congenital nystagmus (CN) in patients with strabismus and a latent component to their CN (Dell'Osso, 1985; Dell'Osso, 1994), or the nystagmus blockage syndrome (Dell'Osso, Ellenberger, Abel, & Flynn, 1983); the presence of a head turn further confounds the identification. Accurate eye-movement recordings can reliably differentiate LMLN from CN by identifying the respective waveforms and their variation

with gaze and convergence angle. Unlike CN, whose amplitude grows as gaze is directed to either side of the null position, the amplitude of LMLN usually follows Alexander's law (i.e., it increases as the fixating eye moves into abduction and decreases in adduction (see Figures A-9 and A-10 (Dell'Osso et al., 1979))). The slow phases of LMLN may be either linear or of decreasing velocity in the same patient (Dell'Osso, Leigh, Sheth, & Daroff, 1995). Studies of the fast phases confirmed that they satisfied saccadic velocity- and duration-amplitude relationships (Erchul, Jacobs, & Dell'Osso, 1996; Erchul & Dell'Osso, 1997). However, depending on the slow-phase velocity, LMLN fast phases could be programmed to cause the target image to fall either within (foveating) or outside (defoveating) the foveal area (Dell'Osso et al., 1995). Higher slow-phase velocities were found to precipitate defoveating fast phases (Erchul, Dell'Osso, & Jacobs, 1998). Also, as presaccadic slow-phase velocities grew, fast-phase amplitude followed.

Several mechanisms have been proposed as the cause of LMLN. Confusion of egocentric direction secondary to strabismus may result in a constant-velocity drift of the eyes in the direction opposite to the fixating eye (Dell'Osso et al., 1979; Dell'Osso & Daroff, 1981). Alternatively, it has been suggested that a naso-temporal asymmetry in the optokinetic system may cause the tonic drift of the eyes (Kommerell & Mehdorn, 1982). Finally, a proprioceptive imbalance has also been suggested as being responsible for the slow-phase genesis of LMLN (Ishikawa, 1979). Each of these putative mechanisms results in a linear slow phase in the direction opposite to the fixating eye although, the proprioception hypothesis is limited to esotropia.

Our approach to modeling the ocular motor system is primarily based on function, dysfunction, and system-level responses. Although specific neuroanatomy and neurophysiology are incorporated into the model as much as possible (e.g., the retina, the extraocular muscle and globe plant, the ocular motor neurons, the common neural integrator in the vestibular and prepositus hypoglossi nuclei, and the pulse-generator burst cells of the pons), the absence of functional correlation for more centrally located sites does not preclude the incorporation of necessary hypothetical function into the model. Indeed, it is not clear that neurophysiological signals exist that parallel the functional signals of their models (Robinson, 1994). Many neurological signals appear to be composites of several functional signals that cannot be decomposed into recognizable parts. With that caveat, It is interesting to note, however, that recent work suggests that structures in the paramedian tract may contain many of the signals required by the functional block we describe as the Internal Monitor (Nakamagoe, Iwamoto, & Yoshida, 2000). Models at *both* the neuronal and systems levels are useful; the former to elucidate specific behavior of neural populations and the latter, to predict system behavior. It is doubtful that system behavior can ever be predicted by studying small neural populations; the activity of hidden layers in neural networks tells us nothing about how signals are processed. The essence of feedback control system behavior lies *not* in the individual building blocks but in their *interconnections*; from such models, we cannot learn about specific neuronal behavior but we can use them to study and predict system behavior and to test specific hypothetical mechanisms for dysfunction.

In order for a model to simulate ocular motor dysfunction (e.g., nystagmus or saccadic intrusions and oscillations) in a truly robust and meaningful manner, it must do more than generate the particular waveform(s) characteristic of that dysfunction. There are an infinite number of ways one can simulate any specific waveform and merely demonstrating that one model, using one method, can do so is insufficient evidence that the model is biologically relevant. What is needed to support a hypothetical model for a specific dysfunction is its demonstrated function within a robust large-scale model of the ocular motor system that contains many, if not all, of the subsystems that are normally present and that might be adversely affected by the dysfunction introduced. Small, limited-scope models of equally small portions of the ocular motor system fail to meet this critical requirement. Although such “bottom-up” models are instructive and may suggest possible mechanisms or anatomical locations, they must be tested within a working model of the whole system before they can rise to the level of realistic, working hypotheses.

A large-scale “top-down” control system model is needed to demonstrate: a broad range of normal responses when the dysfunction is not present; responses equivalent to those of human patients with the dysfunction; no secondary activation of subsystems that might respond erroneously to the oscillation produced by the dysfunction; and no unexpected neurophysiological interaction with other subsystems. Because of these last points, one cannot eliminate known subsystems to “simplify” the model nor limit it to those subsystems responsible for the desired responses (e.g., one needs to have an intact, *active* pursuit system when testing the saccadic responses of an ocular motor system with

an ongoing oscillation to prove that the slow phases do not erroneously activate smooth pursuit). The assumptions commonly made in normal models simply do not apply in the presence of abnormal, internally generated eye movement (e.g., motion on the retina causing retinal slip does *not* imply target motion and must *not* initiate a response). Thus, a robust model, capable of simulating dysfunction, must be more sophisticated than those limited to duplicating stereotypical responses of normals to a limited range of stimuli, or “waveform generators” that are presented as putative hypothetical mechanisms for complex ocular motor dysfunction.

The benefits of such an ocular motor model capable of duplicating both normal and abnormal ocular motor responses are many. First, such a model serves to codify and quantify one’s thinking about the mechanisms responsible for the complex responses of the ocular motor system to various known stimuli. Second, if a particular hypothetical subsystem malfunction can be tested in the context of the whole ocular motor system and it performs as expected from recordings of humans with that dysfunction without either introducing new, uncharacteristic behavior or loss of previously demonstrated behavior, that hypothesis is more strongly supported. Third, such a complex model will, by its nature, contain many hypothetical mechanisms and interactions between subsystems, which may lend themselves to further testing. Finally, if constructed in a modular, subsystem manner, the model can be easily modified by changing specific subsystems as new neurophysiological information about their mechanisms is uncovered. To ensure that the overall model remains robust, each new change or addition must undergo a thorough

“backwards-compatibility” testing to verify the retention of all previously demonstrated behavior and the absence of new, non-physiological behavior.

In this paper we present the beginnings of such a robust ocular motor system model. Specifically, it is a dual-mode, control-system model that is capable of producing normal saccades and both foveating and defoveating fast phases in LMLN. Additionally, the model contains a mechanism by which linear slow phases undergo the transition to decreasing velocity slow phases. We made no attempt to differentiate between the hypothetical causes of LMLN but constructed a model that is consistent with each of them; the model’s constant-velocity input to the neural integrator (equivalent to an imbalance in the bilateral, push-pull integrators) may stem from any of the putative causes. A preliminary attempt to model LMLN was presented elsewhere (Erchul & Dell’Osso, 1997). The current model includes programmable Alexander’s law behavior (zero to maximal) and fixation conditions (e.g., either eye fixating under either monocular (LN) or binocular (MLN) viewing conditions and is, therefore, capable of simulating the idiosyncratic characteristics of a broad spectrum of individuals with LMLN (Jacobs & Dell’Osso, 1999).

Using a robust ocular motor system model with demonstrated capabilities in the simulation of both normal saccadic behavior and that of patients with several saccadic, central, and peripheral dysfunction, we will test the above hypothetical mechanism for LMLN. The ongoing LN or MLN oscillation should not interfere with the normal saccadic system’s ability to make accurate and timely saccadic responses to target steps despite (these will include short-latency corrective saccades where required). The

changes in slow-phase velocity induced by the Alexander's Law variation with gaze angle should not interfere with the saccadic responses. Waveform transitions resulting from the above slow-phase velocity changes should not interfere with saccadic responses. Direction reversals in LN induced by alternate cover or spontaneous reversals in MLN should not interfere with accurate fixation of a stationary target. Finally, simultaneous Alexander's Law variation with gaze angle, waveform transitions, and direction reversals with gaze angle ("adducting-eye fixation") should not interfere with normal saccadic responses.

## **A.2 METHODS**

### *A.2.1 Recording and Protocol*

The data from 97 LMLN patients of both sexes, ranging in age from infants to the elderly, and including 6 with Down syndrome (Averbuch-Heller, Dell'Osso, Jacobs, & Remler, 1999) were used as foundations for our model. The data were recorded in our laboratory over a period of 30 years by either of two methods. Some horizontal eye movement recordings were made using infrared reflection and the remaining data were recorded by means of a phase-detecting revolving magnetic field. Details of the respective equipment, methods, and protocols used may be found in the referenced papers. Written consent was obtained from subjects before the testing.

### *A.2.2 Analysis*

Data analysis (and filtering, if required), statistical computation of means and standard deviations, and graphical presentation were performed using custom software written in MATLAB (The MathWorks, Natick MA), a development environment for scientific computing.

### *A.2.3 Computer Simulation*

The computer simulation of the control-system model was accomplished using the Simulink component of MATLAB. As the block diagram of Figure A-1 shows, the model is of modular design, consisting of functional building blocks thought to be required for accurate ocular motor control. This allows for easy substitution of any block by an equivalent block, based on new data or personal preference. The modular design facilitates expansion of the model to include additional subsystems and preserves the separation of functions required to produce the wide variety of ocular motor responses exhibited by humans, both normals and those with specific dysfunction. In addition to modularity, the model contains distributed delays (see Figure A-2) that duplicate those known to exist from neurophysiological studies. Figure A-2 also shows details of both the smooth pursuit subsystem we used and the pulse generator to neural integrator connections. The model output is that of the fixating eye (either right or left) or of both eyes if conjugacy is assumed.

### LMLN Block Diagram

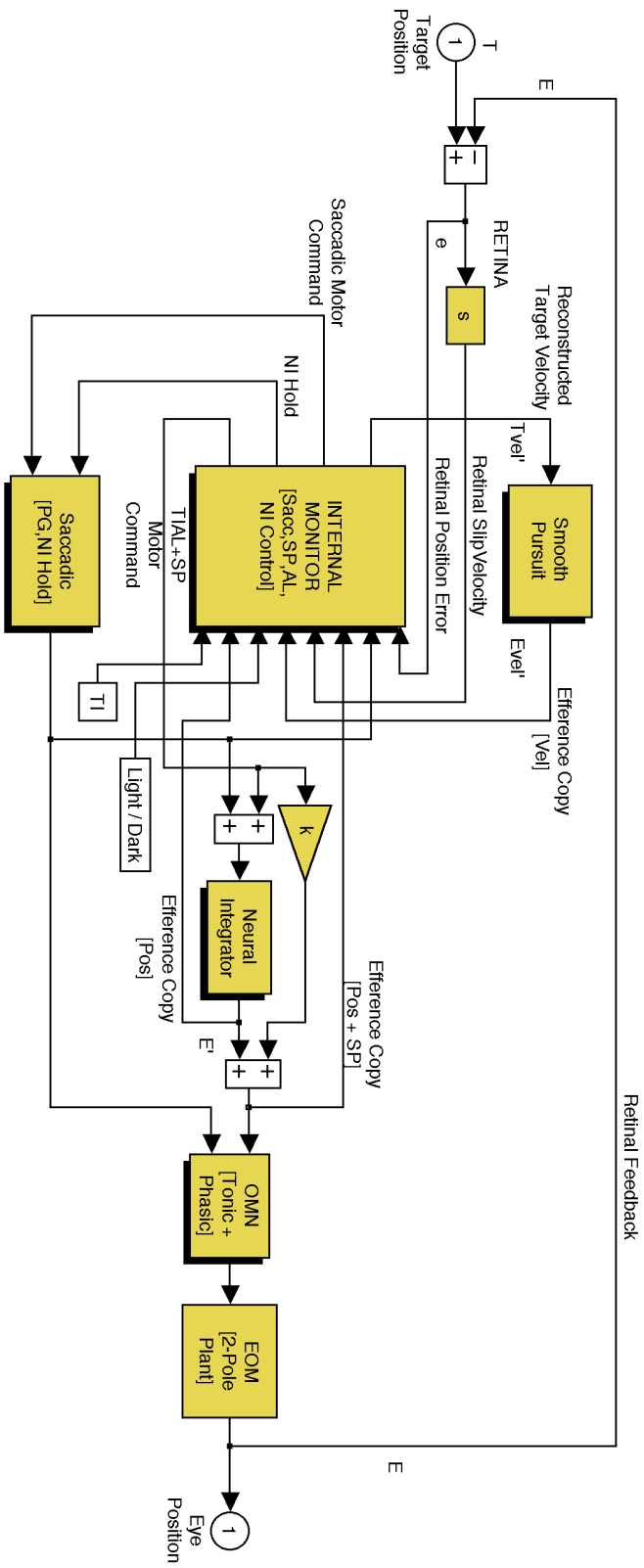


Figure A-1

A functional block diagram of the latent/manifest latent nystagmus model showing the basic organization of subsystems and major components. In this and the following Figures, T—target, E—eye, e—retinal error, Tvel'—reconstructed (perceived) target velocity, Evel'—eye-velocity motor command, E'—eye-position motor command, OMN—ocular motor neuron, EOM—extraocular muscle (plant), TI—tonic imbalance, TIAL+SP—tonic imbalance adjusted by Alexander's law plus smooth pursuit motor command, NI Hold—neural integrator hold signal, PG—pulse generator, [Sacc,SP,AL,NI Control]—saccadic, smooth pursuit, Alexander's law, and neural integrator control functional blocks (respectively) in the internal monitor, and other symbols within square brackets are signals used by other blocks. Transfer functions of various blocks are shown in their Laplace notation within the block. Drop shadows on a functional block indicate that other functional blocks are contained within.

### LMLN Model

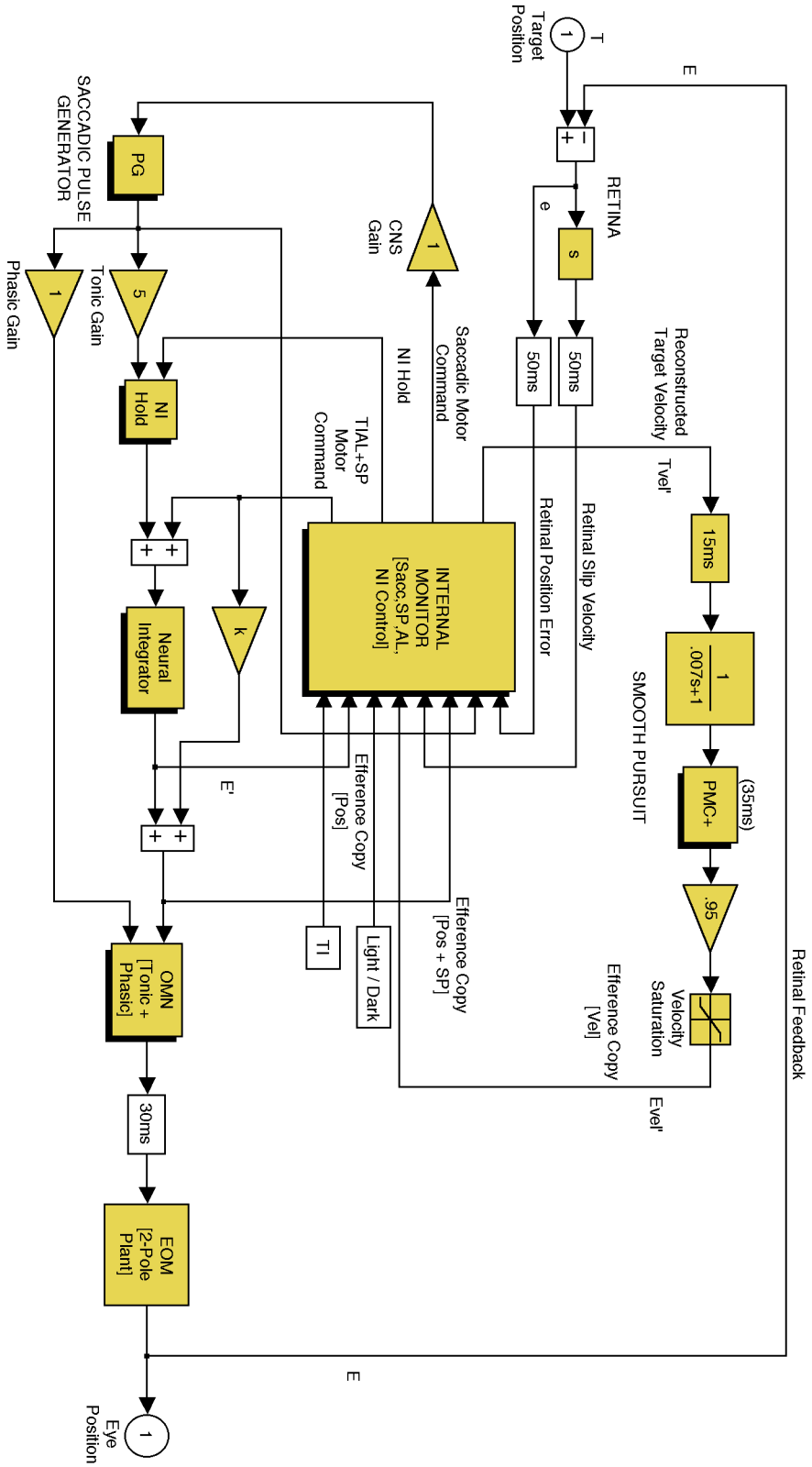


Figure A-2

An expansion of Figure A-1 showing the specific components of both the smooth pursuit and saccadic subsystems and also the distributed delays throughout the model. The smooth pursuit system contains distributed delays and gains, a velocity saturation, and a pre-motor command feedback circuit ('PMC+') that is responsible for the oscillatory nature of smooth pursuit. The saccadic pulse generator circuitry feeds to the neural integrator through a hold circuit ('NI Hold') that limits the portion of the pulse that is integrated.

#### *A.2.4 Model Subsystems*

THE PLANT—Because this is a model of the complex control of several subsystems (see Figures A-1 and A-2), a two-pole transfer function was used for the eye plant. It provides an adequate saccadic trajectory, being far better than a single-pole plant and almost as accurate as a one-zero, two-pole plant. It has become apparent that a truly realistic simulation of the plant should contain a proprioceptive feedback loop and some form of gain control. Until such a model is derived, the two-pole plant is adequate for our purposes. For simulations requiring the outputs of an additional eye, such as the covered, normal eye in myasthenia gravis, a second plant, driven by the ocular motor neurons, was added.

THE OCULAR MOTOR NEURONS—The summation of tonic and phasic signals at the ocular motor neurons (see Figures A-1 and A-2) was simulated by a summation with logic to ensure that the output was that of the pulse when a pulse was present. This was done because the very high frequencies exhibited by the burst cells probably serve as an upper limit on the frequency of the motor neurons.

THE COMMON NEURAL INTEGRATOR—The common neural integrator (see Figures A-1 and A-2) consists of a leaky integrator (time constant equal to the normal dark drift time constant of 25 sec) around which is a positive feedback gain to offset that leak and produce a non-leaky integrator. Provision was also made to include two such elements to simulate gaze-evoked nystagmus caused by a leak in a sub-population of the neural integrator cells (Abel, Dell'Osso, & Daroff, 1978).

**THE PULSE GENERATOR**—The pulse generator (see Figures A-1 and A-2) produces a pulse whose height is determined by a saturation non-linearity and whose duration is determined by a resettable neural integrator and another non-linearity (Abel et al., 1978). A saccadic motor command is passed by a sample-and-hold to both nonlinearities. The pulse-height signal is maintained until the pulse-width signal terminates it. The trailing edge of the pulse generator signal is used to initiate a user-definable refractory period after which another saccade can be generated. The non-linear functions were tuned to yield acceptable saccadic trajectories from the two-pole plant and to make hypometric saccades for target steps greater than  $17^\circ$ .

**THE SACCADIC SUBSYSTEM**—The saccadic system, which includes the pulse generator, (see Figures A-1 and A-2) responds to abrupt changes in target position and is capable of making short-latency (130 msec) corrective saccades, based on efference copy of eye position motor commands. Such corrective saccades are part of the normal responses to large target changes and to abnormal hypometria or hypermetria. The saccadic system must respond properly to step changes in target position despite the presence of LMLN, ignoring eye position changes due to either the slow or fast phases.

**THE SMOOTH PURSUIT SUBSYSTEM**—The smooth pursuit system (see Figures A-1 and A-2) is a modified version of that proposed by Robinson, Gordon, & Gordon (1986). It was chosen for its transient oscillatory characteristics that we required for our modeling of CN (Dell'Osso & Jacobs, 1998). The open-loop gain was set to 0.95 to simulate normal smooth pursuit. It responds to the perceived motion of the target, generating an equivalent velocity signal. The forward path contains a low-pass filter,

gain, velocity saturation, and a premotor circuit (PMC+ in Figure A-2). The PMC+ circuit contains an acceleration saturation and an integrator in a negative feedback loop; it controls the oscillatory behavior of the pursuit subsystem. During the saccadic simulations of both normals and those with abnormalities, such as LMLN, it must *not* respond inappropriately to internally generated slow phases during either fixation or in response to target steps.

THE INTERNAL MONITOR—The internal monitor is a block that subsumes all the computation required for the reconstruction of eye and target position and velocity, and for the programming of saccades and pursuit. Such a grouping is not made on an anatomical basis, but purely on a functional basis; it is *essential* for this model (see Figures A-1 and A-2), as the functions it performs have been required by *all* of our past models of ocular motor dysfunction (Dell'Osso, 1968; Weber & Daroff, 1972; Dell'Osso, Troost, & Daroff, 1975; Abel et al., 1978; Doslak, Dell'Osso, & Daroff, 1979; Abel, Dell'Osso, Schmidt, & Daroff, 1980; Dell'Osso & Daroff, 1981; Doslak, Dell'Osso, & Daroff, 1982). Because a moving *oculocentric* coordinate system (the retina) that must be used to infer the position and velocity of objects in a head-fixed, real-world coordinate system (*craniocentric*), the internal monitor of afferent and efferent information (or its equivalent) is necessary for all robust models of ocular motor control, normal and abnormal. It makes use of afferent signals from the retina and efferent signals from the brainstem (each with its own distributed delay) to enable the model to detect target changes, to accurately reconstruct target position and velocity, and to differentiate them from eye position and velocity in the presence of motor instabilities. It calculates saccadic

motor commands for voluntary and corrective saccades and for fast phases, perceived target position and velocity, and a signal to control the percentage of every saccadic pulse that should be integrated. Provision is also made for Alexander's law variation of nystagmus slow phases (Doslak et al., 1979; Doslak et al., 1982). Without such abilities, we contend that the human ocular motor system could not function (as we know it does function) in the presence of either nystagmus or saccadic instabilities. Additional inputs to the internal monitor are: a light/dark signal (L/D), for future simulations of eye movements in the dark; and tonic imbalance (TI) that may be a result of any of a number of mechanisms hypothesized to cause LMLN. As shown in Figure A-3, the Internal Monitor consists of the following individual functional blocks: Target Change Detection, Target Position Reconstruction (consisting of model OMN and plant plus Saccade Logic), Target Velocity Reconstruction (consisting of model velocity circuitry and Plant+), Saccade Enable & Timing, Saccade & Drift Blanking, Neural Integrator Control, Alexander's Law, and Braking Saccade Logic. Figure A-4 shows the functional blocks within the Saccade Enable & Timing block. Each functional block makes use of a combination of afferent and efferent signals to achieve its goal of providing needed signals to either other internal monitor blocks or to external functional blocks. Working together, these logic and signal-reconstruction blocks allow the ocular motor system to properly differentiate target position/velocity from eye position/velocity and make appropriate decisions to generate responsive eye movements. Further details about the operation of the functional blocks that make up the internal monitor may be found in Section A.7.

### INTERNAL MONITOR [Sacc,SP,AL,NI Control]

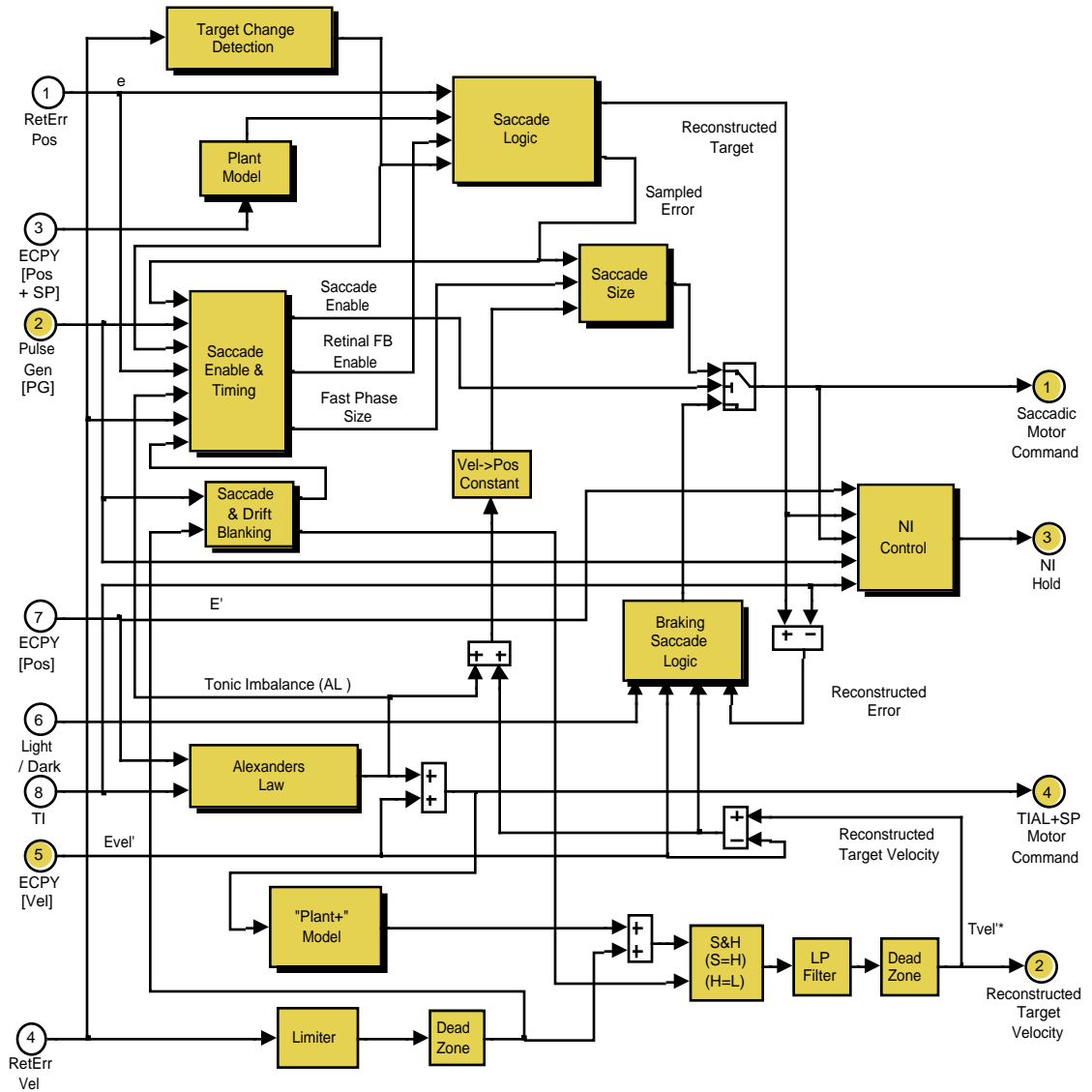


Figure A-3

The arrangement and interconnections of the functional blocks contained within the internal monitor. The major functions of the internal monitor are: detecting target changes; reconstructing target position and velocity; controlling the neural integrator; modifying tonic imbalances (Alexander's law); and determining the timing and amplitudes of saccades and fast phases of nystagmus. The input, output and other signal labels are consistent with those shown in Figures A-1, A-2, and A-4.

### Saccade Enable & Timing

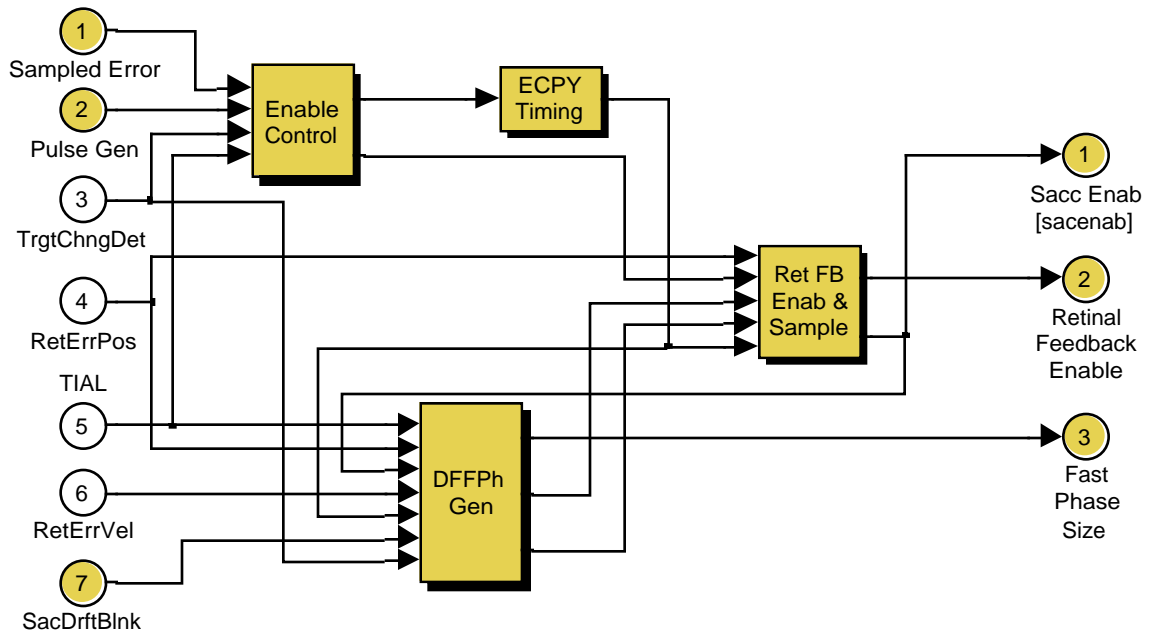


Figure A-4

The arrangement and interconnections of one of the major functional blocks within the internal monitor, the saccade enable and timing block. As the drop shadows indicate, each of these functional blocks contains additional functional blocks within.

FAST-PHASE GENERATION—For generation of a *foveating* fast phase, the output of the neural integrator is compared with a desired eye-position signal and the difference between them is subjected to a position-signal error threshold. If this error exceeds the threshold, a saccade proportional to the error is generated. When the slow-phase velocity exceeds the velocity threshold ( $4^\circ/\text{sec}$ ), a *defoveating* fast phase is generated instead. The transition from foveating to defoveating saccades in the model is based on phase-plane data from LMLN subjects (Dell'Osso et al., 1995). The phase planes showed a significant difference in the pre-saccadic velocities for the foveating and defoveating cases. However, some showed a region of overlapping slow-phase velocities where either foveating or defoveating fast phases can occur. This could be simulated in the model by a change in the position-error threshold.

DECREASING VELOCITY SLOW PHASES—Previous studies also showed correlation of fast-phase size with pre- and post-saccadic velocity (Erchul et al., 1996; Erchul & Dell'Osso, 1997; Erchul et al., 1998). The linear relationship of the size and post-saccadic velocity suggested that an unintegrated pulse (i.e., a saccadic pulse or “stepless” saccade) was being used by the system. The post-saccadic velocities indicated that the pulse was not totally unintegrated and the data suggested that the fast-phase generator produces a pulse width and height for a saccade of a relatively small size. Larger saccades are a result of this pulse and a *higher, velocity-driven* pulse gain. In order to generate the decreasing velocity profiles of LMLN slow phases, additional mechanisms were required in the model. Increasing the pulse to values that produce

saccades greater than that required to foveate the target leads to a larger unintegrated pulse, which is summed with the output from the neural integrator and produces a decreasing velocity slow phase.

### **A.3 RESULTS**

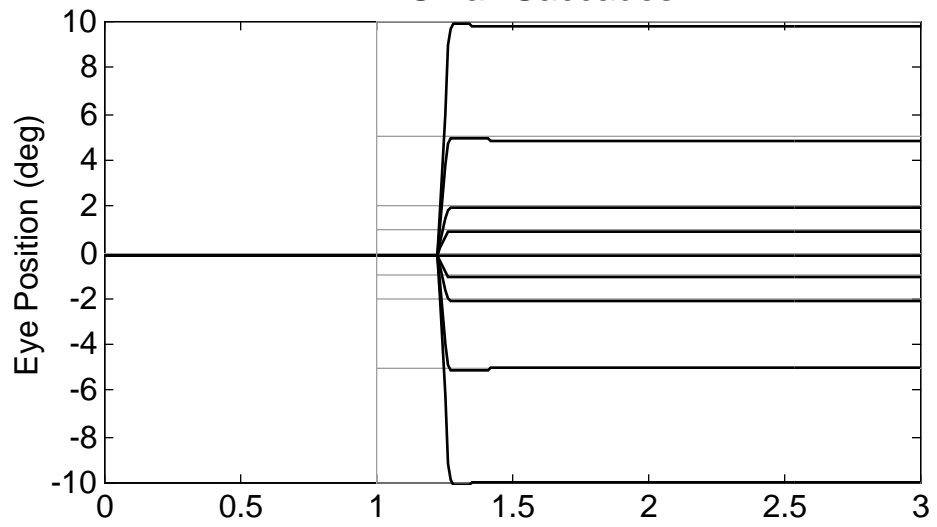
#### *A.3.1 Normal Saccades*

Figure A-5 illustrates the range over which the model simulates normal saccades. Saccades from 1° to approximately 17° are accurately executed in one movement. Larger saccades show characteristic hypometria followed by a short-interval, non-visually driven (130 msec) corrective saccade. The model correctly responds to target-position changes occurring at any time.

#### *A.3.2 Abnormal Saccades*

DYSMETRIA AND OSCILLATIONS – Simulations of various types of saccadic dysfunction are illustrated in Figure A-6. Hypometria and hypermetria are signs of cerebellar dysfunction and result when the saccadic gain is either too low or high and macro saccadic oscillations occur when the saccadic gain is  $\geq 2.0$ .

A. Small Saccades



B. Large Saccades

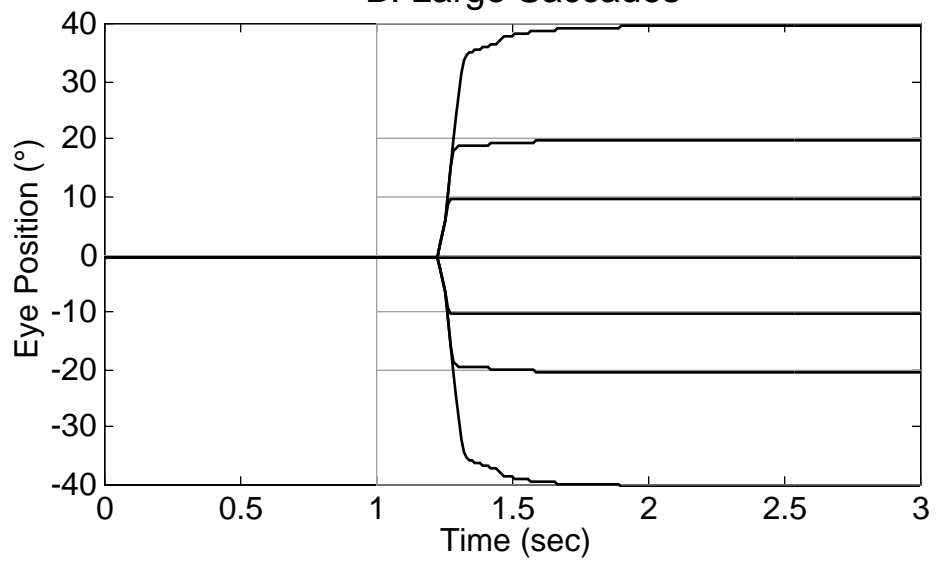


Figure A-5

Model simulations of normal saccadic refixations made by the model from  $\pm 1-40^\circ$  in amplitude. Note that larger refixations are accomplished by primary saccades followed by short-latency corrective saccades, mimicking normal humans. In this and the following Figures, target changes and positions are shown dashed and in this and Figures A-7A, A-8, A-9, and A-11, individual model responses to target steps of differing amplitudes (including  $0^\circ$ ) were superimposed.

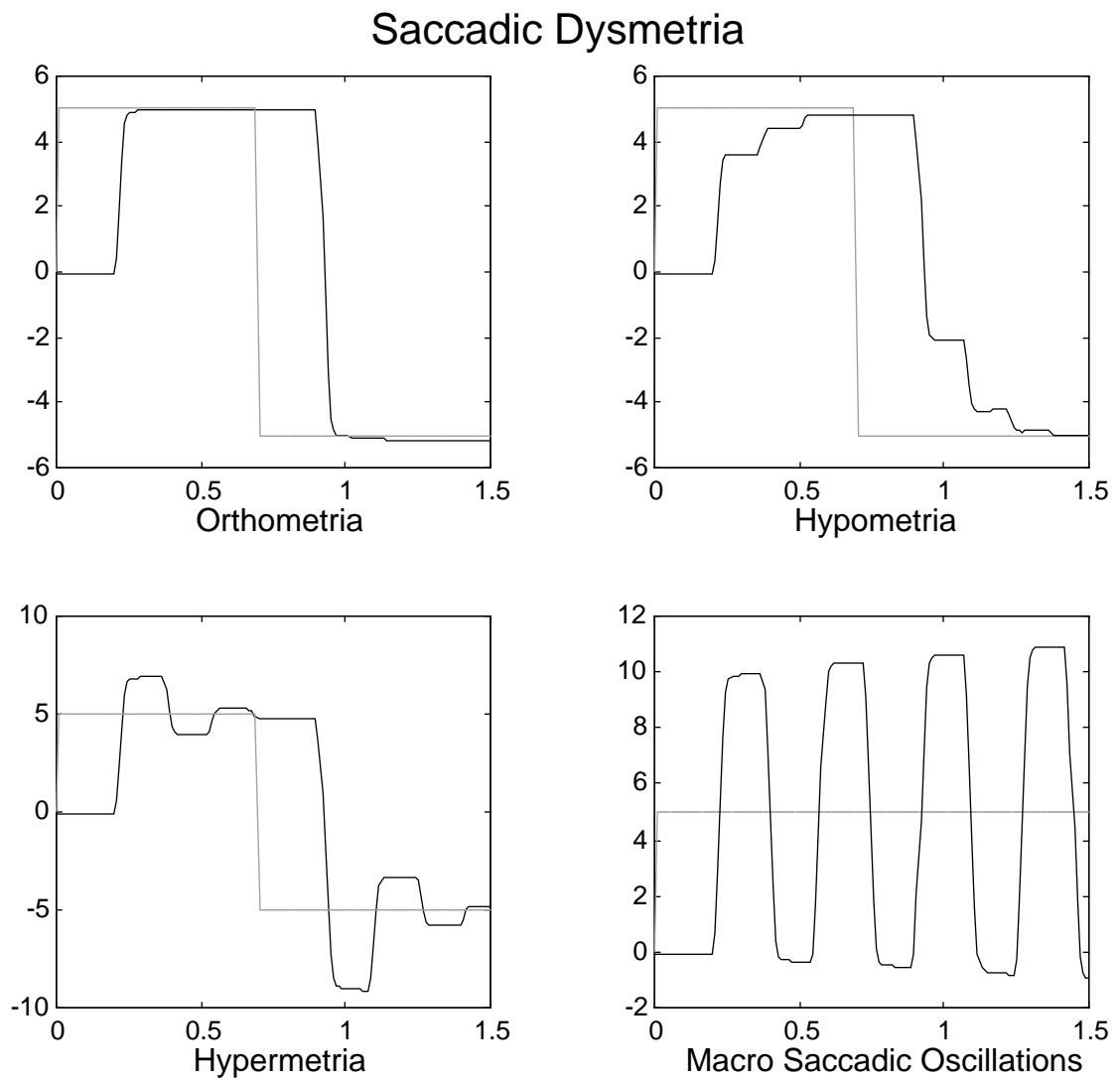


Figure A-6

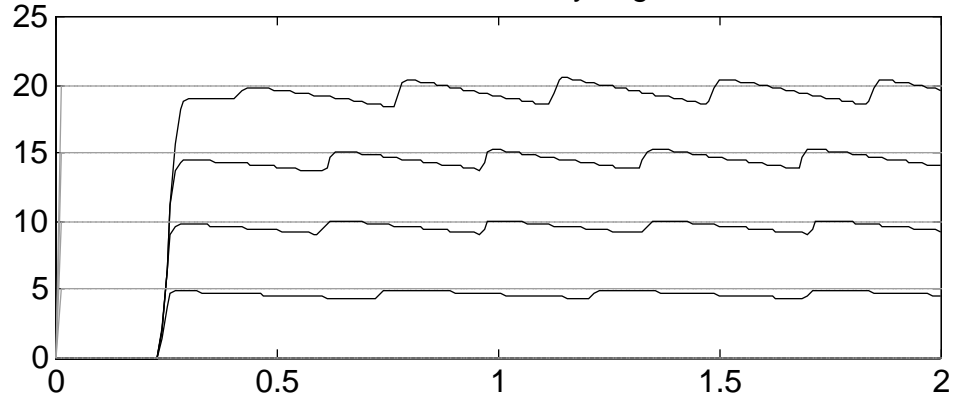
Model simulations of various types of saccadic dysmetria, including macro saccadic oscillations, mimicking those recorded in human patients.

GAZE-EVOKED NYSTAGMUS AND MYASTHENIA GRAVIS – The panels in Figure A-7 illustrate the model's simulation of gaze-evoked nystagmus and myasthenia gravis. Gaze-evoked nystagmus (A) was simulated by making the common neural integrator leaky. The two myasthenia gravis examples were simulated by lesioning the plant slightly (B) and with a paresis (C). The movements of the unaffected eye (under cover) were simulated by adding a normal plant to the output of the ocular motor neuron (see Figures A-1 and A-2). For a more complete demonstration of the simulated variations in gaze-evoked nystagmus, see Abel et al. (1978) and for myasthenia gravis, see Abel et al. (1980).

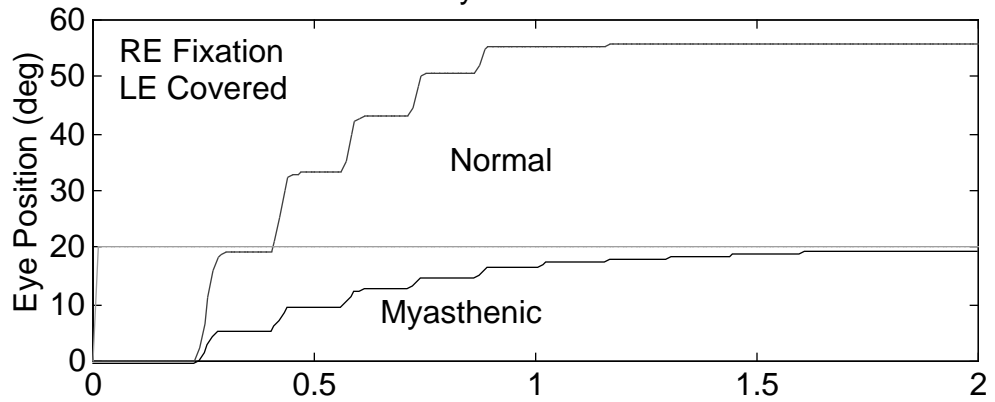
### *A.3.3 Manifest Latent Nystagmus (MLN)*

The nystagmus of individuals with MLN (both eyes open) contains linear slow phases and foveating fast phases throughout most gaze angles. Figure A-8 shows the movements of the fixating eye during periods of both MLN and LN, the latter being caused by the alternate cover test. This subject preferred to fixate with the left eye while the right eye was in an esotropic position; the resulting MLN was jerk left. When the left eye was covered, the right eye moved from its esotropic position to take up fixation while the left eye moved to an esophoric position; the resulting LN was jerk-right. When the right eye was covered, the left eye moved from its esophoric position to take up fixation while the right eye moved to an esophoric position; the resulting LN was jerk-left.

A. Gaze-Evoked Nystagmus



B. Myasthenia Gravis



C. Myasthenia Gravis

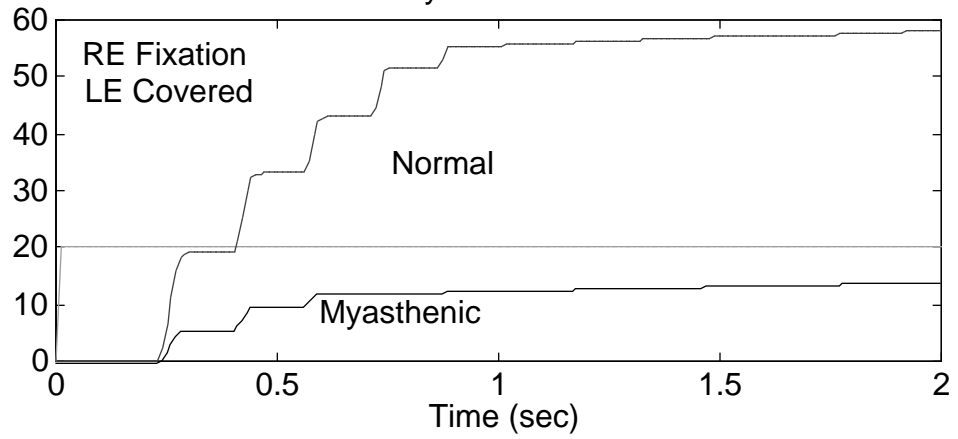


Figure A-7

Demonstration of additional types of ocular motor dysfunction that the model is capable of simulating. A.) Simulated gaze-evoked nystagmus produced by lesioning (making leaky) the model's common neural integrator. The nystagmus amplitude increases as gaze is directed from primary position in either direction; there is no nystagmus in primary position. B.) Simulated saccades of myasthenia gravis, showing both the hypometric saccadic trajectories of the fixating myasthenic eye and the saccades of the normal, covered eye (shown dashed). The ocular plant was lesioned to produce this simulation. C.) Simulated saccades in myasthenia gravis where the myasthenic eye is paretic (i.e., the plant was made to saturate). In B.) and C.), an additional normal ocular plant was added in parallel to the fixating myasthenic eye to obtain the responses of the normal, covered eye. In this and the following Figures, RE—right eye, LE—left eye.

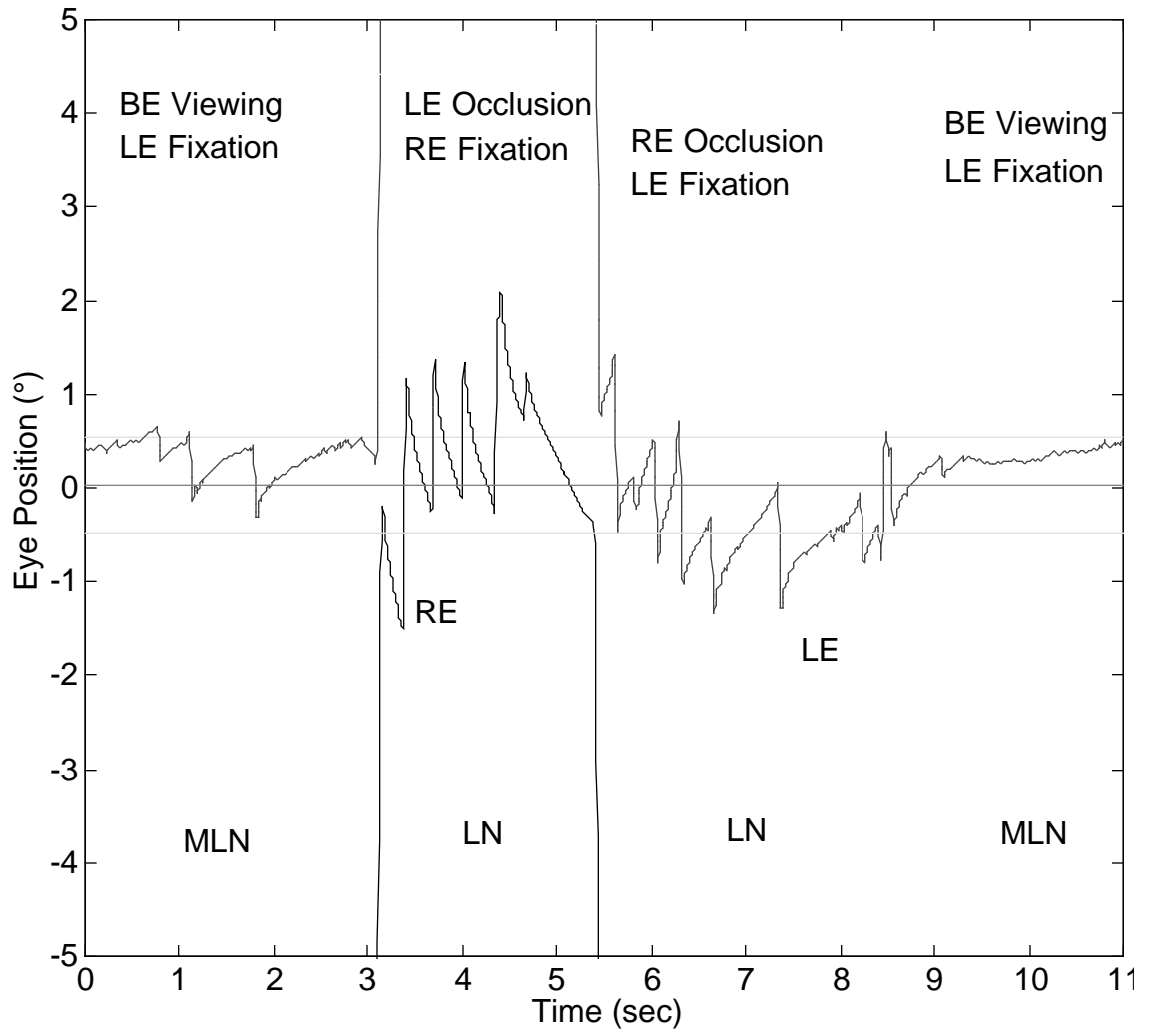


Figure A-8

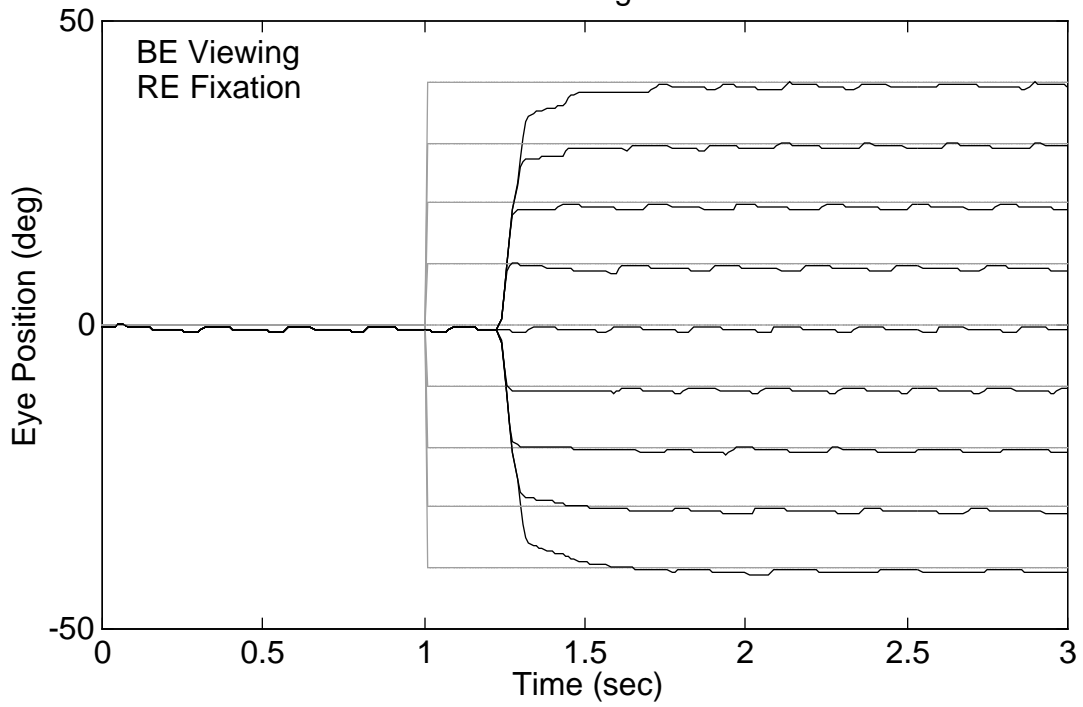
Ocular motor recordings of the fixating eye from a typical subject with esotropia and LMLN during binocular viewing and the alternate cover test. Shown are the transitions from binocular viewing (MLN with left-eye fixation in this case), left eye occluded (LN with right-eye fixation), right eye occluded (LN with left-eye fixation), and a return to binocular viewing (MLN with left-eye fixation). During MLN the slow phases were linear with foveating fast phases and during LN the slow phases were decelerating with defoveating fast phases. Some of the fast phases have dynamic overshoots. In this and Figure A-11, RE is solid, LE is dashed, and dashed lines at  $\pm 0.5^\circ$  indicate the extent of the fovea.

Finally, when the left eye was uncovered, the LN waveform transitioned to an MLN waveform. The Figure demonstrates both the linear slow phases with foveating fast phases of MLN and the decelerating slow phases with defoveating fast phases of LN. Figure A-9 shows the model simulation of MLN during saccades and fixation. In Figure A-9A, a small gaze-angle (Alexander's law) effect is simulated and, although slow-phase velocity increases as the fixating right eye abducts, the fast phases remain foveating. In Figure A-9B, a larger gaze-angle effect increases slow-phase velocity faster as fixation moves in the fixating right eye's abducting direction and when it exceeds  $4^\circ/\text{sec}$ , the fast phases become larger and defoveating and the slow phases exhibit a decreasing velocity. Note that neither type of MLN interferes with the ability of the saccadic subsystem to accurately foveate the target, including making corrective saccades when necessary. The amount of Alexander's Law effect in a particular simulation is governed by a settable slope parameter.

#### *A.3.4 Latent Nystagmus (LN)*

The nystagmus of individuals with LN (one eye occluded) contains decelerating slow phases and defoveating fast phases throughout most gaze angles (refer to Figure A-8). Figure A-10 shows the model simulation of LN during saccades and fixation. In Figure A-10A, a small gaze-angle Alexander's law effect is simulated and, although slow-phase velocity decreases as the fixating right eye adducts, the fast phases remain defoveating except in far adduction. In Figure A-10B, a larger gaze-angle effect decreases slow-phase

A. Small Gaze-Angle Effect - MLN



B. Large Gaze-Angle Effect - MLN

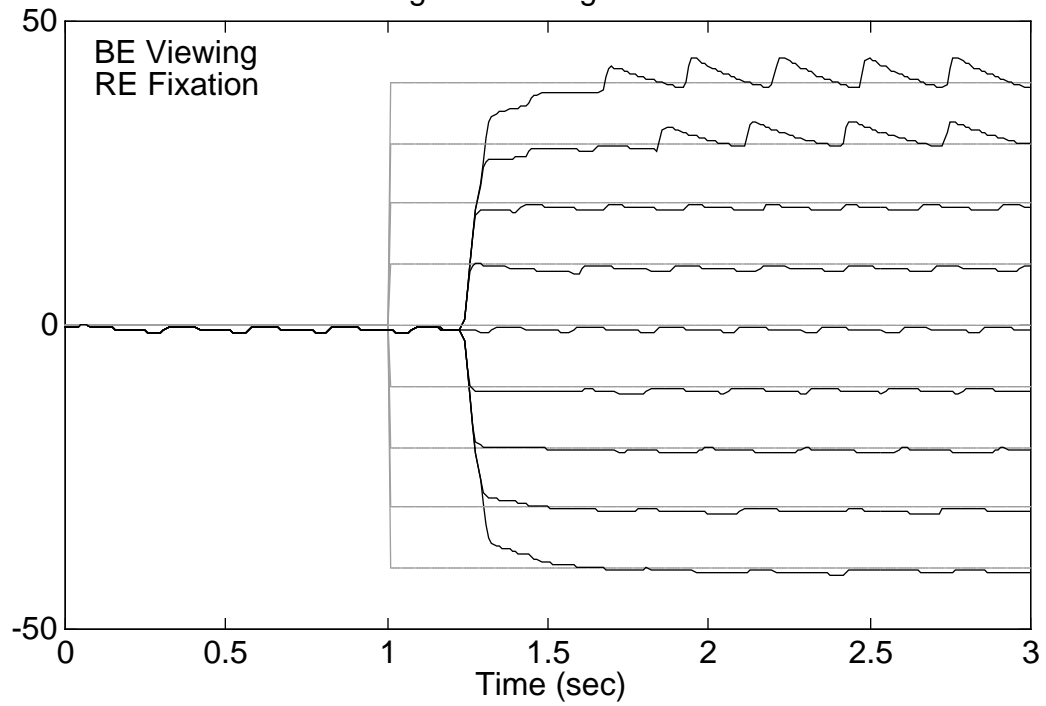
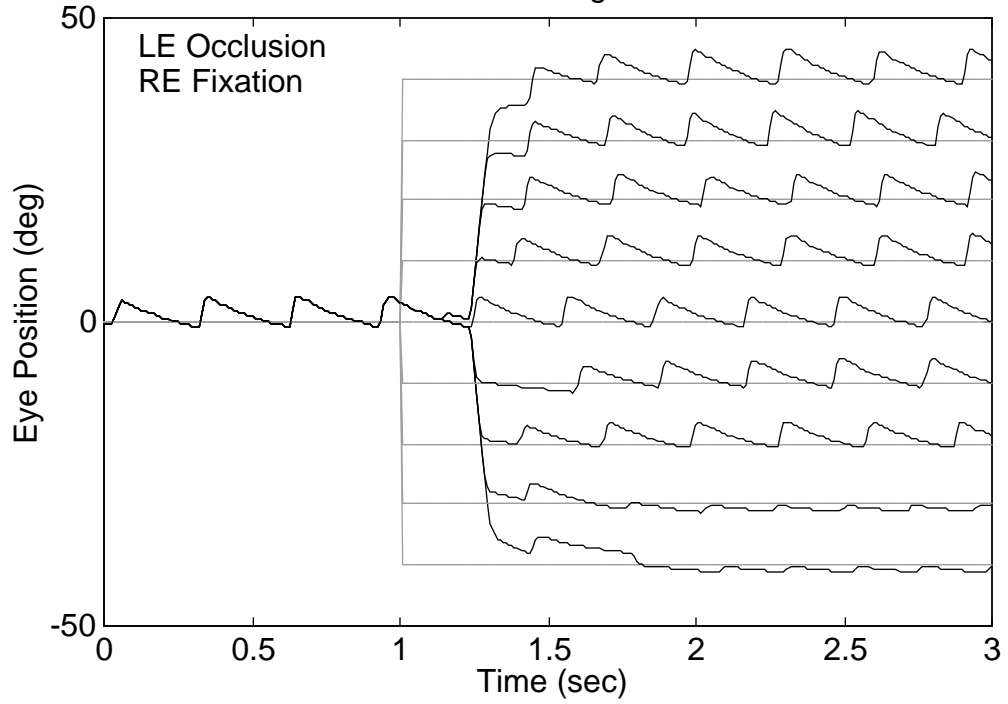


Figure A-9

Simulations of the refixations and fixation at various gaze angles of an individual with manifest latent nystagmus and A.) Small Alexander's law effect or B.) Large effect. In A.) the slow phases remained linear with foveating fast phases, whereas in B.) there was a transition to larger, decelerating slow phases and to defoveating fast phases in far abduction of the right, fixating eye. In this and the following Figures, BE – both eyes.

A. Small Gaze-Angle Effect - LN



B. Large Gaze-Angle Effect - LN

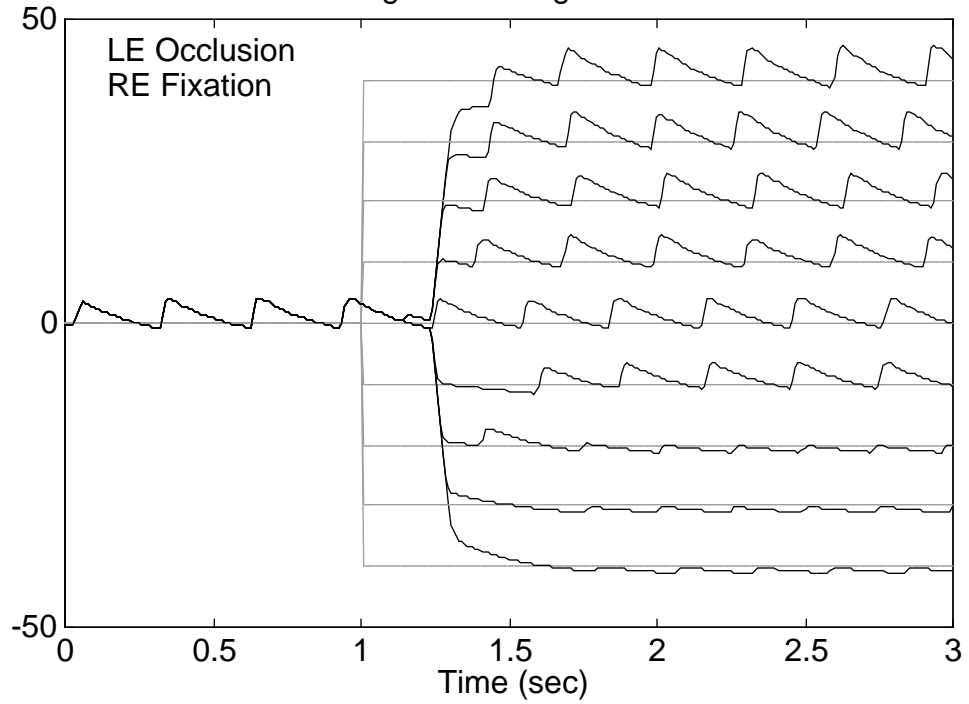


Figure A-10

Simulations of the refixations and fixation at various gaze angles of an individual with latent nystagmus and A.) Small Alexander's Law effect or B.) Large effect. In A.) the large, decelerating slow phases and defoveating fast phases did not transition to smaller, linear slow phases and foveating fast phases until far adduction of the fixating right eye whereas in B.) the transition occurred closer to primary position.

velocity faster as fixation moves in the fixating right eye's adducting direction and the slow phases become  $<4^\circ/\text{sec}$  at a more central gaze angle, causing smaller, foveating fast phases and linear slow phases. Note again that neither type of LN interferes with the ability of the saccadic subsystem to accurately foveate the target, including making corrective saccades when necessary.

#### *A.3.5 Alternating Fixation*

The effects of spontaneous alternating fixation on MLN (Figure A-11A) and forced alternating fixation (e.g., as a result of the alternate cover test) on LN (Figure A-11B) is realistically simulated by the model. This was done by simply reversing the sign of the tonic imbalance such that the resulting slow phases were directed toward the non-fixing eye, as would occur in the individual with LMLN under the above two conditions. In Figure 11A, the MLN slow phases remain linear and the small fast phases remain foveating; in Figure A-11B, larger LN slow phases remain decelerating and fast phases, defoveating.

#### *A.3.6 Abducting-Eye Fixation*

As a final demonstration of the model's flexibility and ability to simulate common characteristics of LMLN while simultaneously responding correctly to step changes in target position, the phenomenon of fixation with the adducting eye (i.e., looking over the nose) is demonstrated in Figure A-12. This usually results in a head turn to the opposite direction and often produces confusion with CN and the mistaken impression that CN can

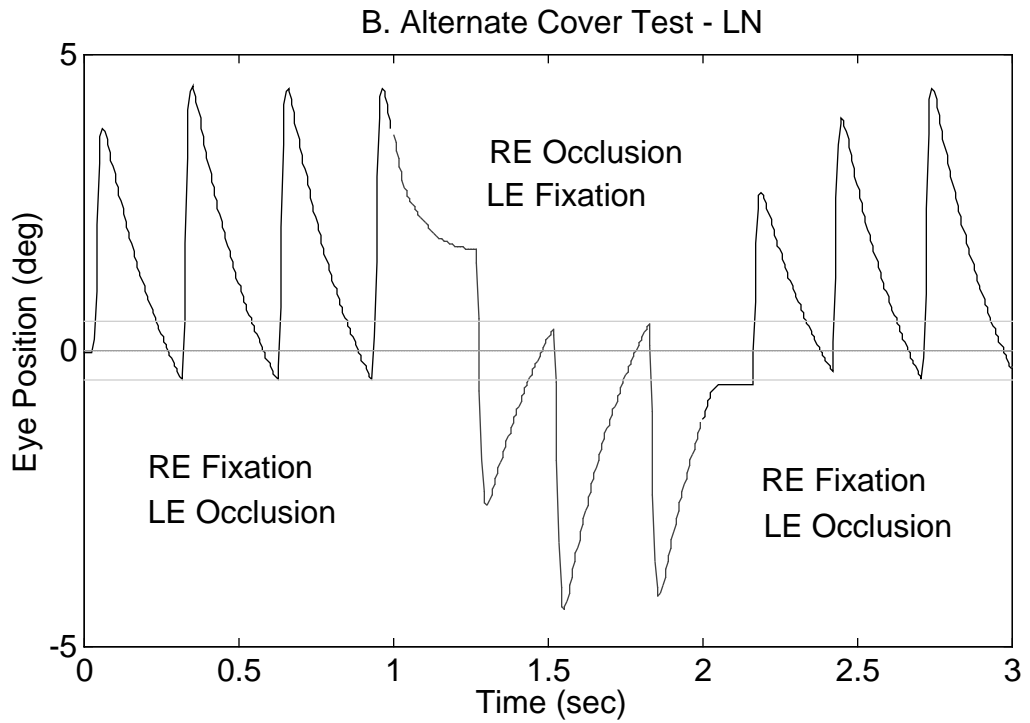
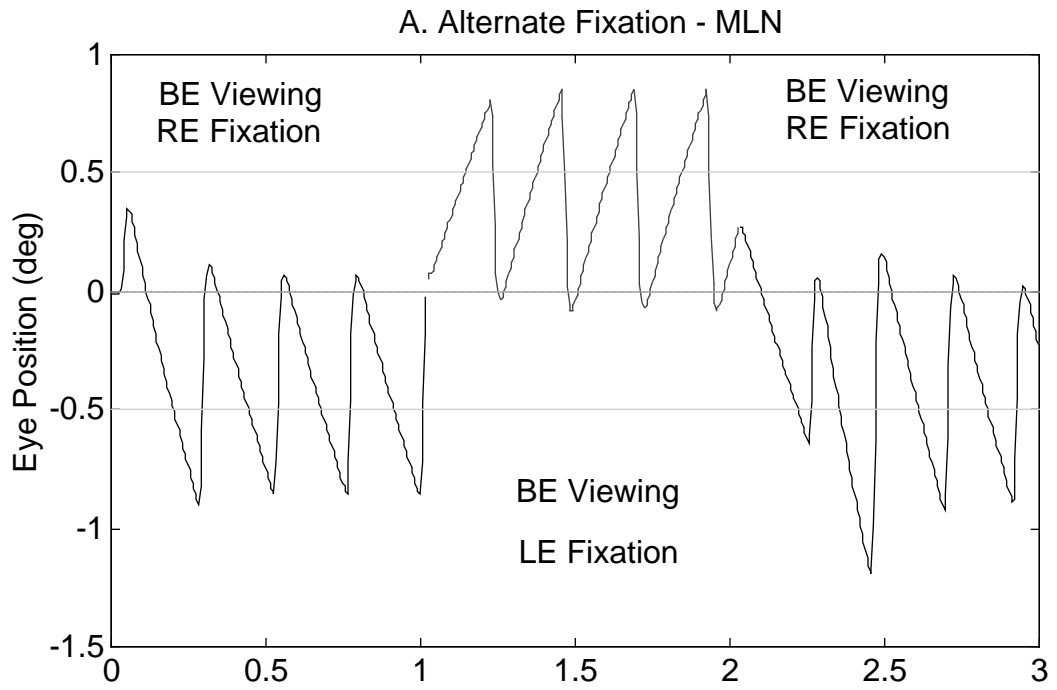
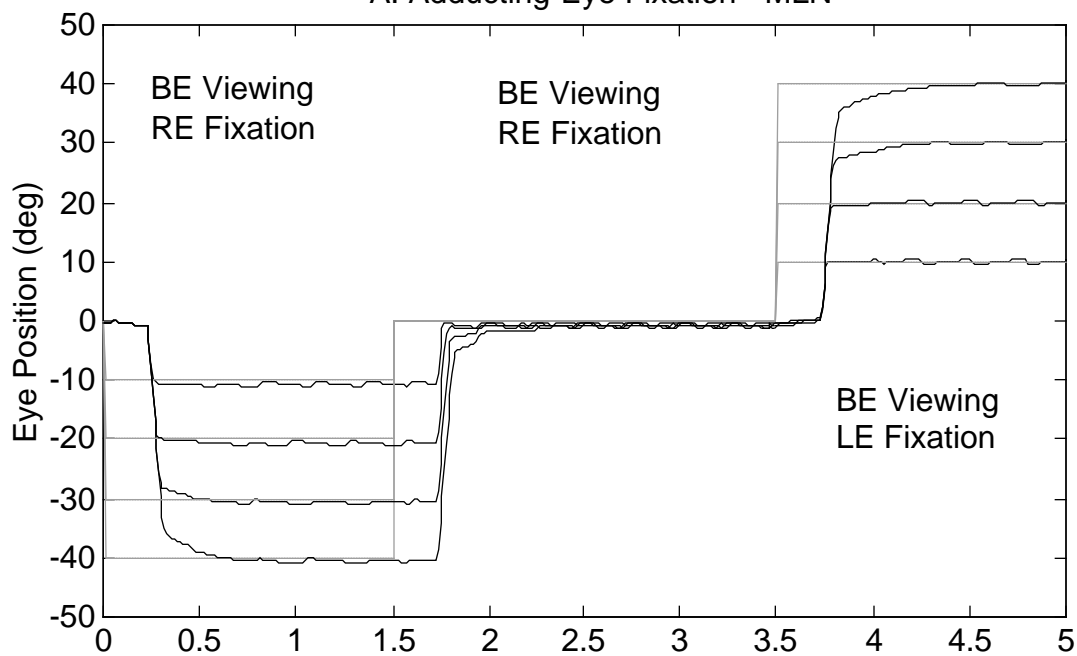


Figure A-11

A.) Simulation of the spontaneous alternation in the fixating eye, and the accompanying reversal in nystagmus direction, during fixation seen in individuals with manifest latent nystagmus. In this simulation, the slow phases of the fixating eye (right—left—right) were linear and the fast phases, foveating. B.) Simulation of the responses seen in an individual with latent nystagmus when given the alternate cover test; the nystagmus direction is always that of the fixating eye (right—left—right). In this simulation, the larger slow phases were decelerating and the fast phases, defoveating.

A. Adducting-Eye Fixation - MLN



B. Adducting-Eye Fixation - MLN

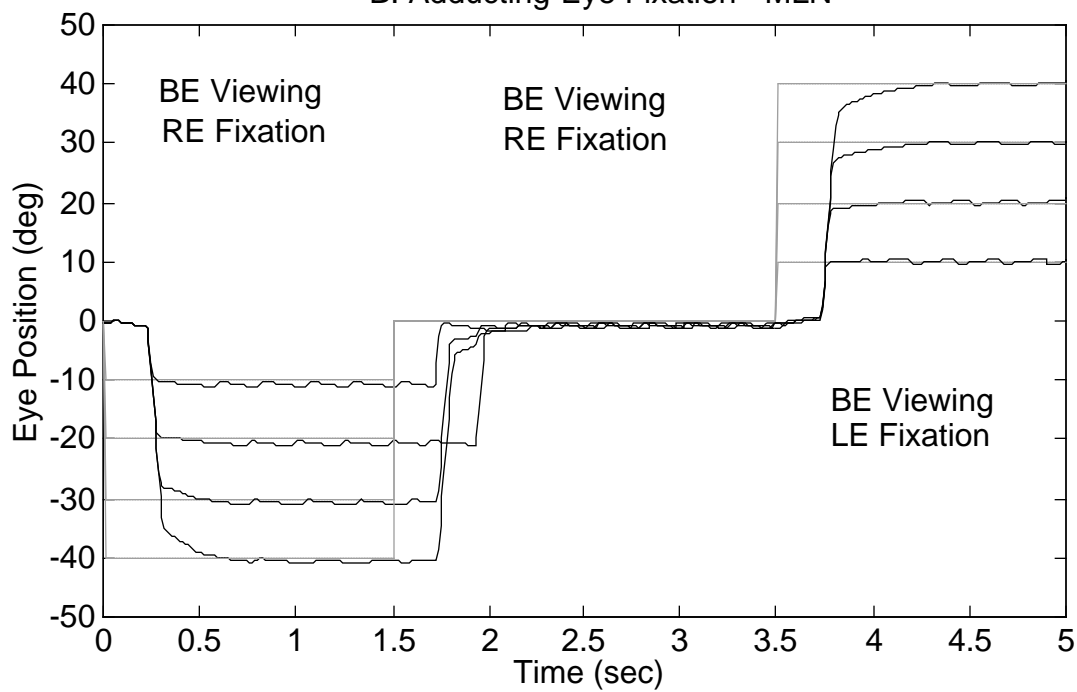


Figure A-12

Simulations of the condition of fixation with the adducting eye, commonly seen in individuals with manifest latent nystagmus. In both A.) and B.) the jerk right nystagmus seen during fixation with the right eye in left gaze, diminishes as gaze is directed farther to the left and the jerk left nystagmus seen during fixation with the left eye in right gaze, diminishes as gaze is directed farther to the right. In B.) the target change from  $-20^\circ$  to  $0^\circ$  occurred too late to cancel the next rightward fast phase and the model made the saccade to primary position after a suitable refractory period.

have two nulls. In both Figure A-12A and A-12B, the fixating eye has minimal MLN in far adduction (due to Alexander's law) and the direction spontaneously reverses from jerk right in left gaze to jerk left in right gaze with the accompanying change in the fixating eye. Again, the MLN does not prevent the saccadic subsystem from foveating the target and, as is illustrated in B, when the target change occurs too late to suppress the next fast phase, the voluntary saccade is correctly made following an intersaccadic refractory interval (saccade from  $-20^\circ$  to  $0^\circ$ ).

#### **A.4 DISCUSSION**

We constructed a model of the normal ocular motor control system that includes a hypothetical mechanism for generating LMLN and the transition between foveating and defoveating fast phases. This transition is based on the following observations and assumptions: the stimulus for the oscillation is a tonic imbalance signal that produces a linear slow eye movement directed opposite to the fixating eye; normally foveating fast phases become defoveating when the speed of the linear slow phases exceed an idiosyncratic threshold value (due to cover of one eye or Alexander's law variation (Doslak et al., 1979; Doslak et al., 1982)); and the transition from linear to decelerating slow phases is a consequence of common neural integrator control, allowing integration of only that portion of saccadic pulses that make the integrator output signal equivalent to that of the desired eye position (Abel et al., 1978). This is consistent with the observed shape of the slow phases responsible for the generation of LMLN in human subjects. The

model also simulates saccadic dysfunctions, gaze-evoked nystagmus, and myasthenia gravis. Although the model contains a smooth pursuit system, we present only the saccadic and fixation responses in this study; *neither the smooth pursuit system nor the braking saccade logic (needed for CN simulations) was improperly activated during any of the simulations.*

#### *A.4.1 Hypotheses of the Model*

We hypothesized that an internal monitor could make use of afferent retinal and efferent motor information to detect changes in target position and to accurately differentiate target position and velocity from internally generated eye position and velocity (e.g., resulting from LMLN). We also hypothesized that LMLN is ultimately caused by a tonic imbalance (i.e., constant-velocity signal) to the common neural integrator that causes both eyes to move in a direction opposite to the fixating eye and with greater velocity when one eye was occluded. In addition, we hypothesized that when slow-phase velocity exceeded  $4^\circ/\text{sec}$ , the foveating fast phases of the LMLN would undergo a transition to defoveating fast phases and the resulting slow phases become decreasing velocity due to unintegrated portions of the fast-phase pulses. Finally, we hypothesized that, due to Alexander's law, slow-phase velocity increased as gaze was directed in the abducting direction of the fixating eye and that would ultimately cause the transition from foveating to defoveating fast phases.

#### *A.4.2 Foundations of the Model*

This model was built on the foundations laid in previous models of ocular motor dysfunction with the aim that the model be *robust* in its range of simulations and its insensitivity to internal errors (i.e., the model produces a wide variety of realistic, goal-directed outputs and recovers from “mistakes”). From those models, we incorporated a pulse generator with a resettable neural integrator, an internal monitor to reconstruct target position and velocity, and a common neural integrator under feedback control to determine what percentage of each pulse requires integration. In addition, we incorporated a tonic imbalance signal whose primary-position amplitude depended on whether both eyes were open or one was occluded and whose final amplitude varied with gaze angle to a settable degree. We demonstrated the ability of this model to simulate both normal and abnormal saccadic responses, several types of ocular motor dysfunction, and saccadic and fixation responses of subjects with LMLN under different viewing conditions.

#### *A.4.3 ‘Evolving’ the Model*

Although these previous models were limited in the scope of their simulations, all were designed to simulate both normal and abnormal responses and, thereby, yielded insights into normal ocular motor control. In contrast, models that were restricted to normal responses did not reveal the complexities inherent in accurate control of eye movement. As a result, such models tended to be simplistic (e.g., the final common neural integrator was used for both eye position and to control the pulse width of the

saccadic burst neurons), usually contained unjustifiable assumptions (e.g., retinal image motion equals target motion), and were inadequate representations of the wide range of human ocular motor control. It was only attempts to simulate dysfunction that were responsible for recognizing: the necessity of employing efference copy of motor commands; the existence of a separate *resettable* neural integrator for pulse generation; and that the common neural integrator does not, and *should not*, integrate all pulses it receives but only those (or part of those) required to match the eye-position motor command to perceived target position. Thus, our simulation makes extensive use of efference copy of motor output signals (the *internal monitor*), as first required in a model of CN (Dell'Osso, 1968), later in a study of normal corrective saccades (Weber & Daroff, 1972), and in models of square-wave pulses (previously designated, macro square-wave jerks) (Dell'Osso et al., 1975), gaze-evoked nystagmus, (Abel et al., 1978) and myasthenia gravis (Abel et al., 1980). It also contains a resettable neural integrator in the pulse generator (Abel et al., 1978; Abel et al., 1980) that is distinct from the common neural integrator responsible for maintaining eye position, and it utilizes feedback control of the saccadic pulse input to the common neural integrator, as required by the gaze-evoked nystagmus model (Abel et al., 1978).

As we added individual features to the model to broaden its range of simulations, each was followed by an extensive retesting of all previous simulations to ensure that no loss of function occurred. Specific attempts that failed to accomplish their goal or interfered with existing functions were discarded and those that worked, retained and refined. In this manner, we interactively *evolved* the model over a period of several years.

Finally, the LMLN model contains internal-monitor features required by our preliminary model of CN (Dell'Osso & Jacobs, 1998) that, although not necessary for LMLN simulations, were retained and did not interfere with them. Specifically, the determination of perceived target velocity (used to drive the smooth pursuit subsystem) was not confounded by the slow phases (linear or decelerating) of LMLN and neither braking nor foveating saccades were mistakenly generated by the functional block responsible for their insertion into CN waveforms. Thus, in addition to LMLN, this model retains the capability of simulating normal eye movements and, with proper settings (i.e., “lesions”), the other neurological conditions of its predecessors (e.g., gaze-evoked nystagmus and myasthenia gravis). It is our goal to marry the LMLN and CN models into a unitary ocular motor control system model that can be used to simulate many, if not all, of the behaviors exhibited by both normal individuals and those with specific ocular motor dysfunction.

#### *A.4.4 The Dual-Mode Nature of the Model*

The automatic transition between foveating and defoveating fast phases in this simulation is affected by the interaction of the dynamics of the eye plant with pre-saccadic slow-phase velocity and position-error threshold. Although the decelerating slow phases could have significant implications for visual acuity, the method for their generation is not critical for the basic mechanism proposed here as an explanation for foveating and defoveating fast phases in LMLN. The model demonstrates how visual acuity could be improved by the defoveating fast-phase strategy if the final slowing of

decelerating LMLN slow phases could be accomplished by a fixation subsystem. A more sophisticated model of LMLN should include a fixation mechanism that uses position- and velocity-signal feedback to further decrease the slow-phase velocity. In addition, the model could include a mechanism for the generation of dynamic overshoots. However, this is not critical for the simulation presented here concerning the transition between foveating and defoveating fast phases.

#### *A.4.5 Emergent Behavior of the Model*

One of the marks of the biological relevance of a model is its ability to exhibit behavior not designed into it. Examination of some of the responses shown in Figures A-9, A-10, and A-12 reveal such behavior. In Figure A-9A the corrective saccades needed to acquire the targets at 20 and 30° were altered by the fast phases of the MLN; the post-saccadic drift after the corrective saccade to 40° was diminished by the oppositely directed slow phase of the MLN; extended slow phases after the initial saccades to -10 and -20° acquired the target and suppressed the corrective saccade that would have occurred for -20°; and the corrective saccades to -30 and -40° were diminished by the MLN slow phases. In Figure A-9B, in addition to similar interactions, the transitions from foveating to defoveating fast phases at 30 and 40° were delayed by the interaction between post-saccadic drift and oppositely directed MLN slow phases. In Figure A-10A post-saccadic drift delayed the transition to foveating fast phases at -30 and -40° (the same thing occurred at -20° in the plots shown in part B). Also, the defoveating fast phase occurring just after the initial saccade to -40° delayed but did not prevent the

needed corrective saccade (i.e., the model acted to correct itself). Figure A-10B also demonstrates how post-saccadic drift and slow phases combined to supplant the otherwise required corrective saccades needed to acquire the  $-30$  and  $-40^\circ$  targets. Figure A-12 exhibited similar emergent behavior and in part B), the initial saccade to  $-20^\circ$  was delayed by the timing of a fast phase that occurred before the normal saccadic latency (again, the model corrected itself). All of these responses, predicted by the model, were due to interactions of different hypothetical mechanisms for both normal and abnormal behavior and, significantly, these behaviors have all been documented in ocular motility recordings of subjects with LMLN.

#### *A.4.6 A Robust Ocular Motor System Model as a Research Tool*

Because MATLAB/Simulink is widely used and this model is of modular construction, it can serve as a *test bed* for other investigators to test hypothetical mechanisms. The existing simulations of specific subsystems can be replaced by newer ones as they are developed, models of other subsystems can be added as needed (e.g., vestibular or optokinetic), models of other dysfunctions can be tested (e.g., saccadic intrusions and oscillations), and both students and researchers can use it to study the ocular motor system under both normal and abnormal conditions. Toward that end, we plan to make all of the constituent subsystems available as MATLAB files to investigators who request them and, eventually place them on a web site for easy downloading.

## **A.5 ACKNOWLEDGEMENTS**

The authors wish to acknowledge the contributions of D. M. Erchul to preliminary simulations that helped lead to the present model.

## **A.6 LITERATURE CITED**

Abel, L. A., Dell'Osso, L. F., & Daroff, R. B. (1978). Analog model for gaze-evoked nystagmus. *IEEE Trans Biomed Engng*, BME(25), 71-75.

Abel, L. A., Dell'Osso, L. F., Schmidt, D., & Daroff, R. B. (1980). Myasthenia gravis: Analogue computer model. *Exp Neurol*, 68, 378-389.

Averbuch-Heller, L., Dell'Osso, L. F., Jacobs, J. B., & Remler, B. F. (1999). Latent and congenital nystagmus in Down syndrome. *J Neuro-Ophthalmol*, 19, 166-172.

Dell'Osso, L. F. (1968) A Dual-Mode Model for the Normal Eye Tracking System and the System with Nystagmus. (Ph.D. Dissertation)., University of Wyoming.

Dell'Osso, L. F. (1985). Congenital, latent and manifest latent nystagmus - similarities, differences and relation to strabismus. *Jpn J Ophthalmol*, 29, 351-368.

Dell'Osso, L. F. (1994). Congenital and latent/manifest latent nystagmus: Diagnosis, treatment, foveation, oscillopsia, and acuity. *Jpn J Ophthalmol*, 38, 329-336.

Dell'Osso, L. F., & Daroff, R. B. (1981) Clinical disorders of ocular movement. In: B. L. Zuber, *Models of Oculomotor Behavior and Control* (pp. 233-256). West Palm Beach, CRC Press Inc.

Dell'Osso, L. F., & Jacobs, J. B. (1998). An preliminary model of congenital nystagmus (CN) incorporating braking saccades. *Invest Ophthalmol Vis Sci*, 39, S149.

Dell'Osso, L. F., Troost, B. T., & Daroff, R. B. (1975). Macro square wave jerks. *Neurology*, 25, 975-979.

Dell'Osso, L. F., Schmidt, D., & Daroff, R. B. (1979). Latent, manifest latent and congenital nystagmus. *Arch Ophthalmol*, 97, 1877-1885.

Dell'Osso, L. F., Traccis, S., & Abel, L. A. (1983). Strabismus - A necessary condition for latent and manifest latent nystagmus. *Neuro ophthalmol*, 3, 247-257.

Dell'Osso, L. F., Ellenberger, J. C., Abel, L. A., & Flynn, J. T. (1983). The nystagmus blockage syndrome: Congenital nystagmus, manifest latent nystagmus or both? *Invest Ophthalmol Vis Sci*, 24, 1580-1587.

- Dell'Osso, L. F., Leigh, R. J., Sheth, N. V., & Daroff, R. B. (1995). Two types of foveation strategy in 'latent' nystagmus. Fixation, visual acuity and stability. *Neuro Ophthalmol*, 15, 167-186.
- Doslak, M. J., Dell'Osso, L. F., & Daroff, R. B. (1979). A model of Alexander's law of vestibular nystagmus. *Biol Cyber*, 34, 181-186.
- Doslak, M. J., Dell'Osso, L. F., & Daroff, R. B. (1982). Alexander's law: A model and resulting study. *Ann Otol Rhinol Laryngol*, 91, 316-322.
- Erchul, D. M., & Dell'Osso, L. F. (1997). Latent nystagmus fast-phase generation. ARVO abstracts. *Invest Ophthalmol Vis Sci*, 38, S650.
- Erchul, D. M., Jacobs, J. B., & Dell'Osso, L. F. (1996). Latent nystagmus fast-phase generation. ARVO abstracts. *Invest Ophthalmol Vis Sci*, 37, S277.
- Erchul, D. M., Dell'Osso, L. F., & Jacobs, J. B. (1998). Characteristics of foveating and defoveating fast phases in latent nystagmus. *Invest Ophthalmol Vis Sci*, 39, 1751-1759.

Ishikawa, S. (1979) Latent nystagmus and its etiology. In: R. D. Reinecke, Strabismus, Proceedings of the Third Meeting of the International Strabismological Association (pp. 203-214). New York, Grune and Stratton.

Jacobs, J. B., & Dell'Osso, L. F. (1999). A Dual-Mode Model of Latent Nystagmus. ARVO abstracts. Invest Ophthalmol Vis Sci, 40, S962.

Kommerell, G., & Mehdorn, E. (1982) Is an optokinetic defect the cause of congenital and latent nystagmus? In: G. Lennerstrand, D. S. Zee, & E. L. Keller, Functional Basis of Ocular Motility Disorders (pp. 159-167). Oxford, Pergamon Press.

Nakamagoe, K., Iwamoto, Y., & Yoshida, K. (2000). Evidence for brainstem structures participating in oculomotor integration. Science, 288, 857-859.

Robinson, D. A. (1994) Implications of neural networks for how we think about brain function. In: P. Cordo, & S. Harnad, Movement Control (pp. 42-53). Cambridge: Cambridge University Press.

Robinson, D. A., Gordon, J. L., & Gordon, S. E. (1986). A model of smooth pursuit eye movements. Biol Cyber, 55, 43-57.

Weber, R. B., & Daroff, R. B. (1972). Corrective movements following refixation saccades: Type and control system analysis. *Vision Res*, 12, 467-475.

## **A.7 APPENDIX—MODEL DETAILS**

The major functions of the internal monitor are described in the Methods. Below are descriptions of the operating principles of each functional sub-block whose interconnections (shown in Figures A-3 and A-4) form the internal monitor.

### *A.7.1 Target Change Detection*

There are four implementations of this circuitry. The first uses retinal error velocity to detect all target changes of  $\geq 1^\circ$  at all times. The second also uses the pulse generator (Pulse Gen) signal to detect all target changes of  $>0.1^\circ$  except during a saccade. The third uses the same two signals and sampled, reconstructed retinal error to detect all target changes  $>0.1^\circ$  except during a saccade, when it detects all target changes  $>0.2^\circ$ . The fourth uses the initial two signals and sampled, reconstructed retinal slip velocity to detect all target changes  $>0.1^\circ$  except during a saccade, when it detects all target changes  $>1^\circ$ . At present, we are using the first implementation.

### *A.7.2 Plant Model and Saccadic Logic*

Retinal error position is summed with the efference copy of eye position after the latter is passed through a model of the OMN and 2-pole plant; appropriate delays are in place. The resulting signal is reconstructed target position which is sampled when either a target change is detected or a retinal feedback sample is called for by the Saccade Enable and Timing circuitry.

### *A.7.3 Target Velocity Reconstruction*

Retinal error velocity is limited and passed through a dead zone (0.1°/sec) and then summed with the efference copy of eye velocity after the latter is summed with tonic imbalance and passed through a model of the 1-zero, 2-pole (Plant+); appropriate delays are in place. The resulting signal is sampled or held, based on the signal from the Saccade and Drift Blanking circuit. This signal is low-pass filtered and passed through a dead zone (0.2°/sec) to yield reconstructed target velocity, which is the input motor command signal to the Smooth Pursuit circuitry.

### *A.7.4 Saccade Enable and Timing*

Using the inputs shown in Figure A-4, these blocks determine when to output commands that enable saccades to be generated, to sample the retina, and to produce a defoveating fast phase of a particular size. The sub-blocks are: Enable Control, Efference Copy (ECPY) Timing, Retinal Feedback (Ret FB) Enable & Sample, and Defoveating Fast-Phase Generation (DFFPh Gen). The Enable Control circuitry sends output signals to both the ECPY Timing and Ret FB Enable & Sample circuits. The output from the latter directly enables a saccade to be initiated. Its second output is Retinal FB Enable, that allows sampling of a new reconstructed target signal; Target Change Detection also allows such sampling. The third output (from Defoveating Fast-Phase Generation) is Fast-Phase Size, that is added to a sampled, reconstructed retinal error signal to determine saccade size via the Saccadic Motor Command, which is sent to the Pulse Generator.

*Enable Control* - uses sampled, reconstructed retinal error (after a  $0.3^\circ$  dead zone), Pulse Gen, Target Change Detection, and tonic imbalance acted on by Alexander's law (TIAL) to determine if an ECPY (i.e., "corrective") saccade or a Ret FB (i.e., "fixation") saccade should be enabled. If the Sampled Error is non-zero and it has been less than 150 ms since the last detected change in target position, Pulse Gen is passed to the output, "ECPY Timing". If, on the other hand, 150 ms elapsed since the last detected target change, the "Ret FB Enab" output will be high; that output passes to the Ret FB Enab & Sample circuitry.

*ECPY Timing* - acts on the input signal from Enable Control. It outputs a signal to the Ret FB Enable & Sample circuitry that is 10 ms long and starts 130 ms after Pulse Gen concludes.

*Ret FB Enable & Sample* - uses five inputs: retinal error position, a signal from the Enable Control circuitry, two signals from the DFFPh Gen circuitry (see below), and one from the ECPY Timing circuitry. Its outputs are signals that enable either retinal feedback or saccades. The first signal allows sampling of reconstructed target position. Each input from ECPY Timing resets the circuitry until a latency of 330 ms expires and sets the output high. The "Ret FB Enable" signal produces "Sacc Enab" (see above). Before a "Ret FB Enab" signal is created, one of five criteria must be satisfied, several of which depend on specific combinations of the five inputs to the Ret FB Enable & Sample circuitry. Two criteria that directly trigger a "Ret FB Enable" output are a "Ret FB Enab & Spl" signal from the Enable Control circuitry and a signal from within this block. Each of two other criteria results from the outputs of multi-input AND gates. The first AND

gate requires that four conditions be met: 200 ms has elapsed since the last saccade enabling signal, the tonic imbalance signal must be zero, the retinal error signal must have a magnitude  $>0.5^\circ$ , and the retinal error velocity signal must be high. The second AND gate also requires that four conditions be met: 200 ms have elapsed since the last saccade enabling signal, retinal error has to be non-zero, retinal error velocity must be high, and tonic imbalance must be non-zero. The final criterion that triggers “Ret FB Enab” is the output of an AND gate when the magnitude of the retinal error is higher than a  $0.5^\circ$  threshold. This triggers a “corrective” saccade.

*Defoveating Fast-Phase Generation* - uses seven inputs “TIAL,” “Ret Err Pos,” “Ret FB Enable” from the Ret FB Enable & Sample circuitry, “Ret Err Vel,” “ECPY Enable” from the ECPY Enable circuitry, “Sac Drft Blnk,” and “Trgt Chng Det.” Its major output is “Fast Phase Size,” which is “TIAL” multiplied by -0.8 after passing through a dead zone of  $4^\circ/\text{sec}$ . It is an output if either “Ret FB Enable” or “ECPY Timing” signals are high and at least 200 ms has elapsed since the last “Trgt Chng Det” signal; if both are low, “Fast Phase Size” is zero. Two other outputs are signals related to “Ret Err Vel” and “TIAL” that are used by Ret FB Enab & Sample.

#### *A.7.5 Saccade Size*

This uses “Fast Phase Size,” “Sampled Error” (retinal), and a modified velocity signal to calculate the magnitude of the saccade to be generated by the Pulse Generator.

#### *A.7.6 Saccade and Drift Blanking*

The Saccade and Drift Blanking circuitry prevents other logic from evaluating steady-state target, eye, or retinal variables during, or immediately after saccades. It creates a blanking signal that lasts for 70 ms beyond the length of the saccadic pulse, using a delayed “Pulse Gen” signal. The output signal is also used to prevent the effects of post-saccadic drift from adversely affecting calculation of reconstructed target velocity.

#### *A.7.7 Neural Integrator Control*

When a TI is present, the NI Control circuitry allows the NI to integrate the output of the Pulse Generator until its output (desired eye position) is equal to the reconstructed target position. When NI Control is active, the “Pulse Gen” signal is not integrated by the NI. “NI Hold” is set to zero when both “Pulse Gen” and the reconstructed error signal are non-zero. During “Pulse Gen,” “NI Hold” remains low until a reconstructed retinal error signal crosses zero, whereupon “NI Hold” is set high. It is also set high if “Pulse Gen” terminates. In the absence of a tonic imbalance (TI=0), the NI integrates all “Pulse Gen” signals. Other conditions (e.g., for gaze-evoked nystagmus, smooth pursuit, etc.) need to be added to activate this circuitry that allows the NI to hold its value when it has arrived at the correct eye position.

#### *A.7.8 Alexander's Law*

This mechanism uses efference copy of eye position to modulate the TI input and produce "TIAL." The eye-position signal is multiplied by the Alexander's law slope and filtered before summing with TI. Depending on the sign of TI, this sum is kept greater than or less than 0, and is passed on to a final switch that only produces an output if TI is present. Differing amounts of Alexander's Law effect are simulated by the value of the Alexander's Law slope.

#### *A.7.9 Braking Saccade Logic*

This circuitry uses sampled, "Reconstructed Error"(retinal position), sampled, reconstructed retinal slip velocity, and desired eye velocity to determine if the conditions for generating a braking saccade are met. Braking saccades occur in many CN waveforms and always occur in the direction opposite to eye motion if the eye is moving away from the target. First, "Reconstructed Error" is used by the Braking Saccade Logic circuit to determine if retinal error is increasing (calling for a braking saccade) or decreasing (no braking saccade). If this criterion for a braking saccade is met, its magnitude is determined within limits. Second, an estimate of retinal slip velocity is compared to a threshold; if it exceeds it, the second criterion for a braking saccade is met. Third, the direction of desired eye velocity is determined and used to assign the direction of the braking saccade. If desired eye acceleration falls below threshold, a braking saccade is enabled for a period of time determined by a timing circuit.

## APPENDIX B

### OPERATIONAL DESCRIPTION OF THE MAJOR BLOCKS IN THE OMS MODEL

It would be impractical to fully reproduce all the blocks of the OMS model presented in Chapter 4, and quite difficult for the reader to reproduce the model from such a paper description. The goal of the diagrams in this appendix is to give a greater feel for the complexity and structure of the model, and the design decisions that were made at each level.

The model will be made available on the Ocular Motor Neurophysiology Laboratory's World Wide Web home page. In addition, it is possible to contact the author at [Jonathan.Bruce.Jacobs@cornell.edu](mailto:Jonathan.Bruce.Jacobs@cornell.edu) for updated information.

Figure B-1. Overview of OMS model and internal monitor.

Figure B-2. Saccadic enable subsystem and sub-blocks.

Figure B-3. Target change detect, model plant, saccadic motor command,  
and associated sub-blocks.

Figure B-4. Reconstruction of position and velocity of eye and target.

Figure B-5. Saccadic and post-drift blanking.

Figure B-6. Braking/Foveating saccade logic and sub-blocks.

Figure B-7. Fixation subsystem and sub-blocks.

Figure B-8. Neural integrator hold controller.

Figure B-9. Saccadic pulse generator and sub-blocks.

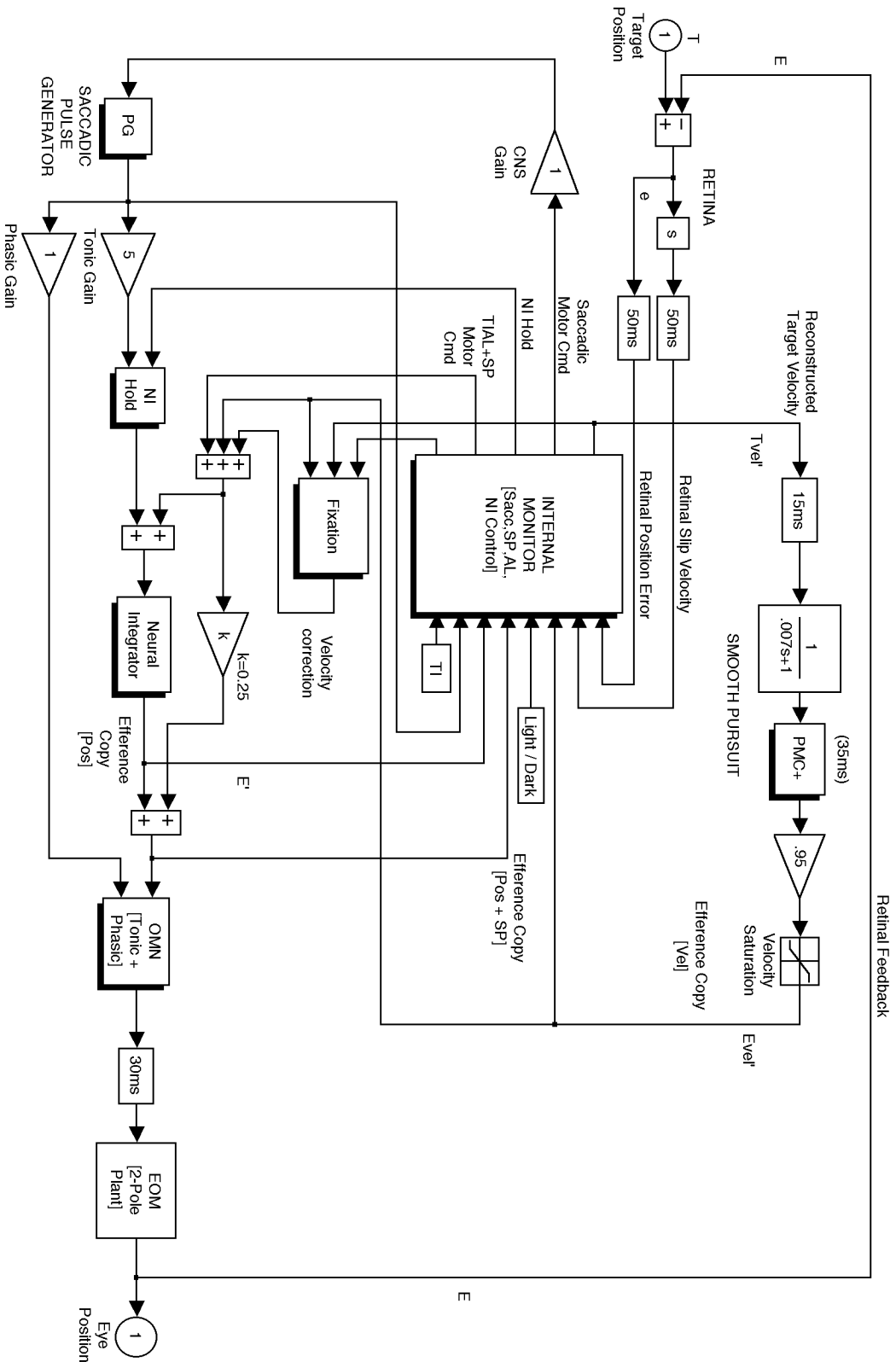
Figure B-10. Neural integrator and ocular motor neurons.

Figure B-11. Resettable event timer.

Program Listing: Pulse Height Function (phfn\_ss.m).

A

### OMS Model



B

**INTERNAL MONITOR [Sacc,FS/BS,SP,AL,NI Control]**

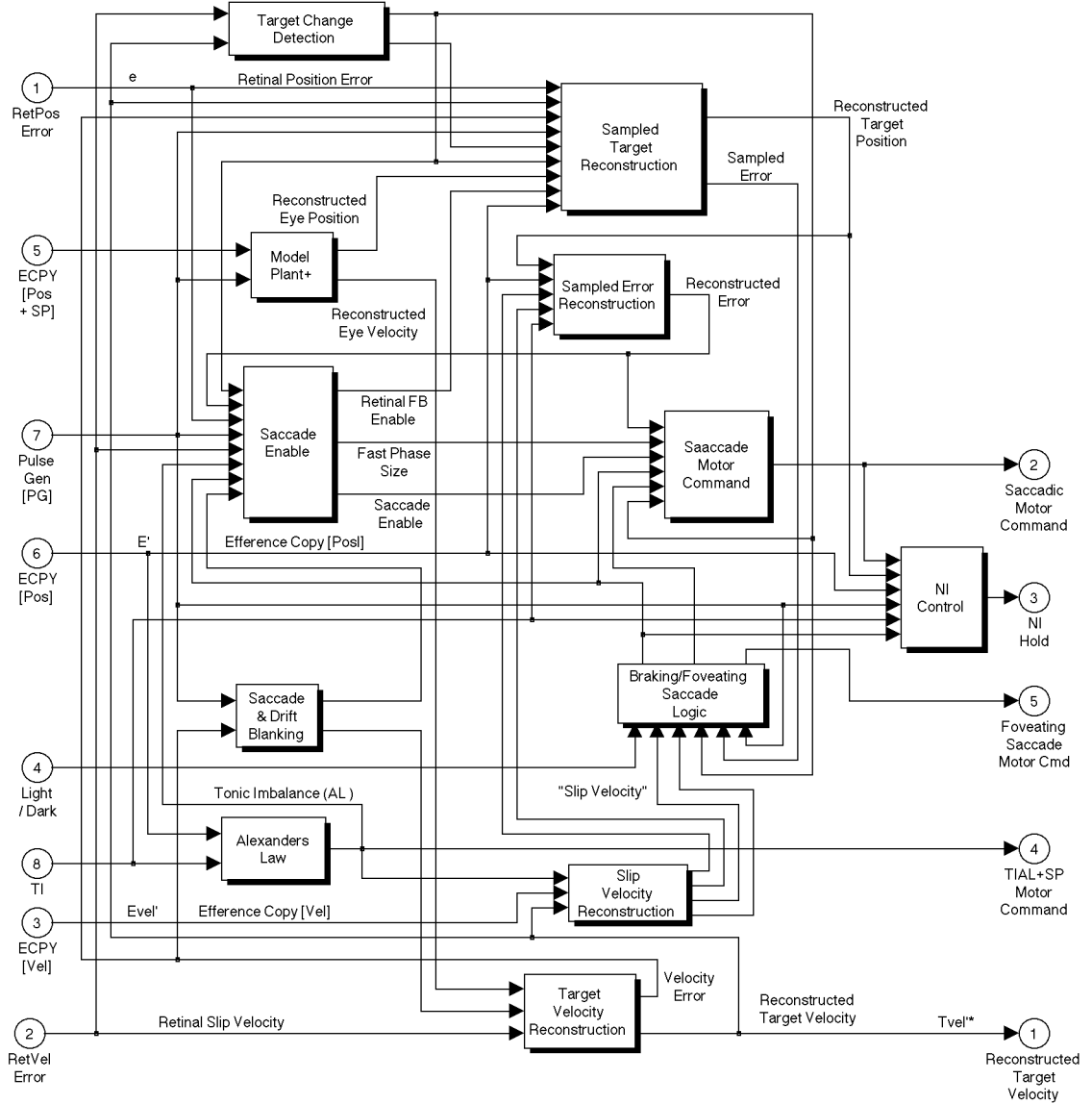
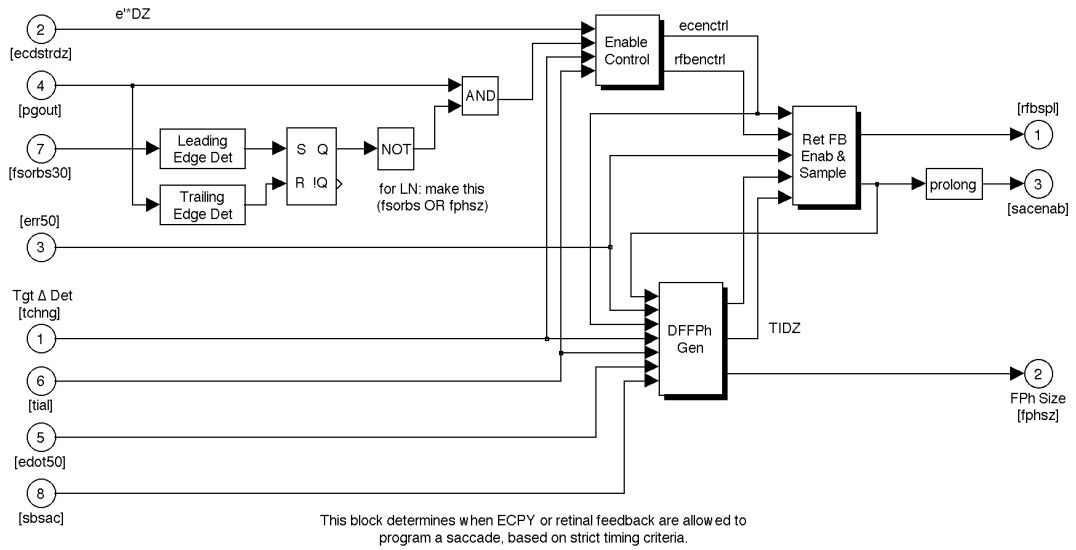


Figure B-1

A.) Ocular motor system (OMS) model showing distributed delays, pursuit subsystem components, pulse generator and neural integrator hold. (This Figure also appears as Figure 4-2A.) B.) The arrangement and interconnections of the functional blocks contained within the internal monitor. The major functions of the internal monitor are: detecting target changes; reconstructing target position and velocity; controlling the neural integrator; and determining the timing and amplitudes of saccades and fast phases of nystagmus. The input, output and other signal labels are consistent with those shown in Figures 4-1, 4-2, and 4-4. (This Figure also appears as Figure 4-3A.)

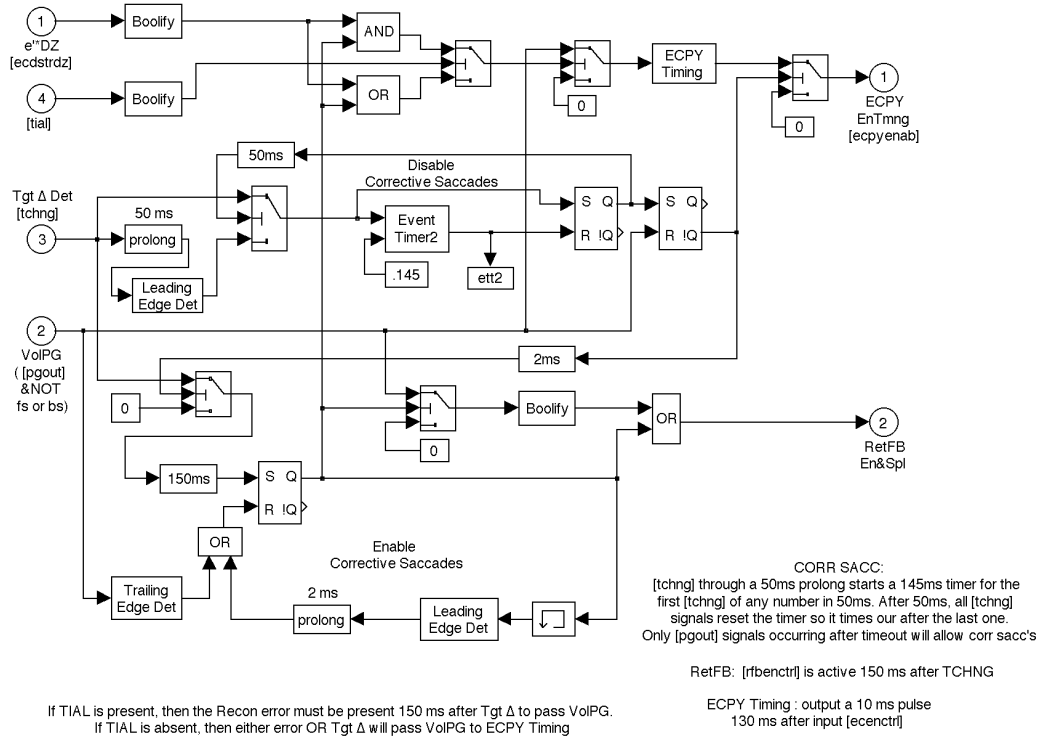
A

**Saccade Enable**



B

**Enable Control**



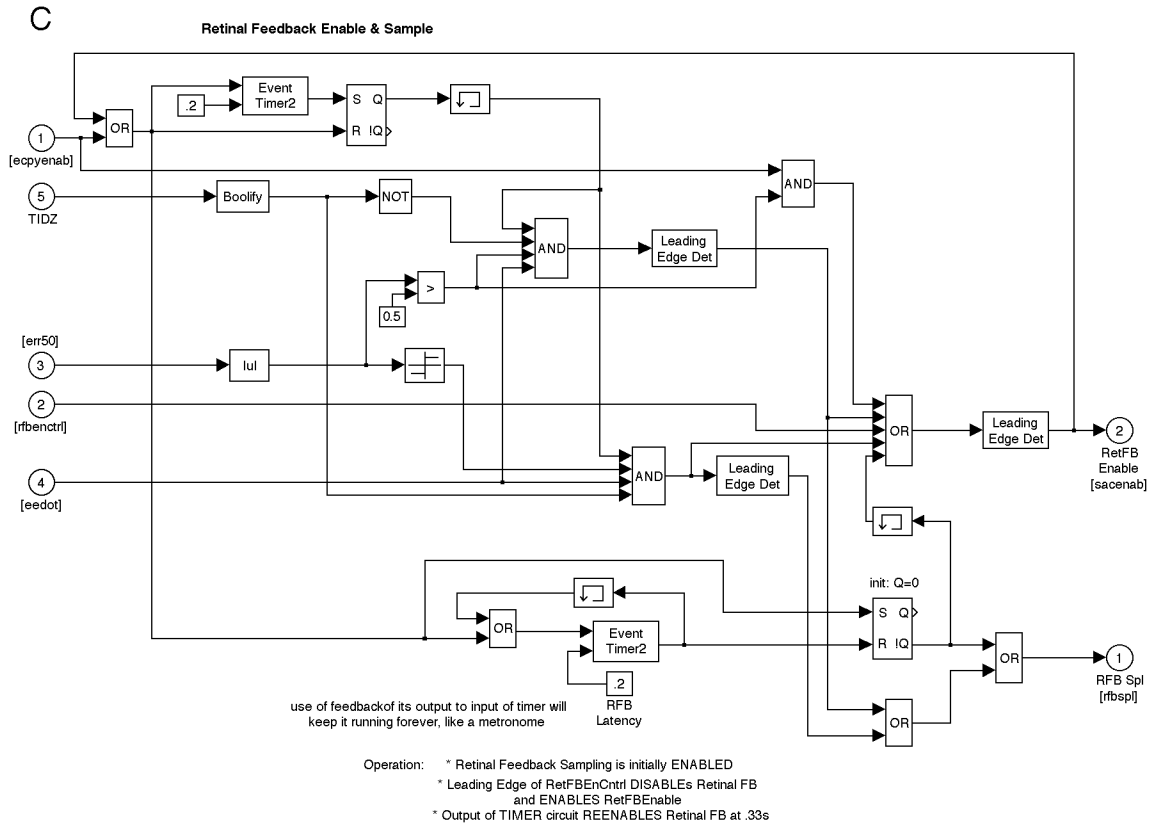


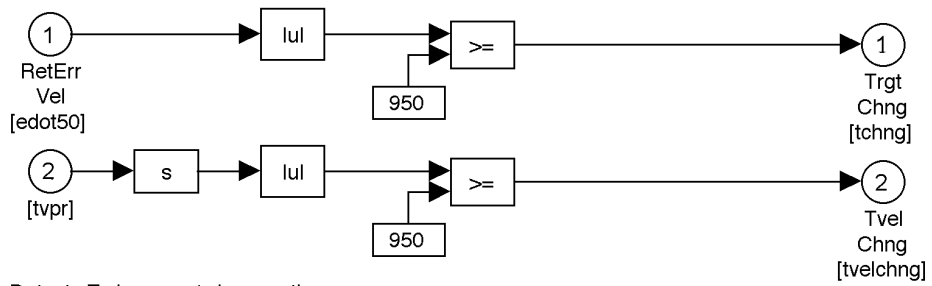
Figure B-2

A.) The arrangement and interconnections within one of the major functional blocks of the internal monitor, the Saccade Enable and Timing block, that determines when to output commands that enable saccades to be generated and when to sample the retina. As the drop shadows indicate, each of these functional blocks contain additional functional blocks within. The sub-blocks relevant to the CN function of this model are: Enable Control (which contains Efference Copy (ECPY) Timing) and Retinal Feedback (Ret FB) Enable & Sample. B.) The Enable Control sub-block determines if and when saccades due to retinal feedback or ECPY can be made, and enforces their priority of execution by sending control signals to the ECPY Timing and Ret FB Enable & Sample circuits. Enable Control uses sampled, reconstructed retinal error (after a  $0.3^\circ$  dead zone), Pulse Gen, and Target Change Detection to determine if an ECPY (i.e., “corrective”) saccade or a Ret FB (i.e., “fixation”) saccade should be enabled. If the Sampled Error is non-zero and it has been less than 150 ms since the last detected change in target position, Pulse Gen is passed to the output, “ECPY Timing,” which outputs a signal to the Ret FB Enable & Sample circuitry that is 10 ms long and starts 130 ms after Pulse Gen concludes. If, on the other hand, 150 ms elapsed since the last detected target change, the “Ret FB Enab” output will be high; that output passes to the Ret FB Enab & Sample circuitry.

Figure B-2 (cont.)

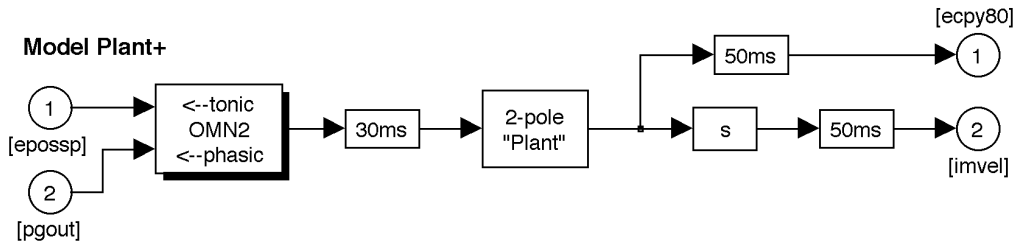
C.) The Retinal Feedback Enable & Sample sub-block provides the timing signal to Sampled Target Reconstruction, telling it when to sample position and velocity errors to calculate saccadic magnitudes. It takes as inputs: retinal error position; a signal from the Enable Control circuitry; and one from the ECPY Timing circuitry. Its output signals enable either retinal feedback or saccades. The first, “RFB spl,” allows sampling of reconstructed target position. Each input from ECPY Timing resets the circuitry until a latency of 330 ms expires and sets the output high. The second, “Ret FB Enable,” produces “Sacc Enab” (see above). Before a “Ret FB Enable” signal is created, one of five criteria must be satisfied, several of which depend on specific combinations of the inputs to the Ret FB Enable & Sample circuitry. Two criteria that directly trigger a “Ret FB Enable” output are a “Ret FB Enab & Spl” signal from the Enable Control circuitry and a signal from within this block. Each of two other criteria results from the outputs of multi-input AND gates. The first AND gate requires that four conditions be met: 200 ms have elapsed since the last saccade enabling signal; the tonic imbalance signal must be zero; the retinal error signal must have a magnitude  $>0.5^\circ$ ; and the retinal error velocity signal must be high. The second AND gate also requires that four conditions be met: 200 ms have elapsed since the last saccade enabling signal; non-zero retinal error; retinal error velocity must be high; and non-zero tonic imbalance (seen in LMLN). The final criterion that triggers “Ret FB Enable” is the output of an AND gate when the magnitude of the retinal error is higher than a  $0.5^\circ$  threshold. This triggers a “corrective” saccade.

### A Target Change Detection

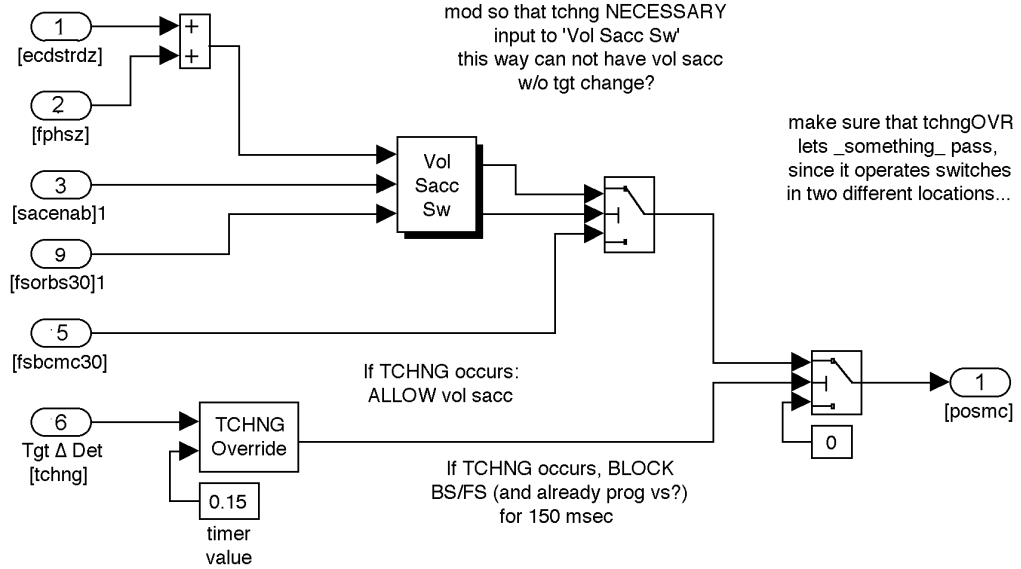


Detects T change >1 deg any time

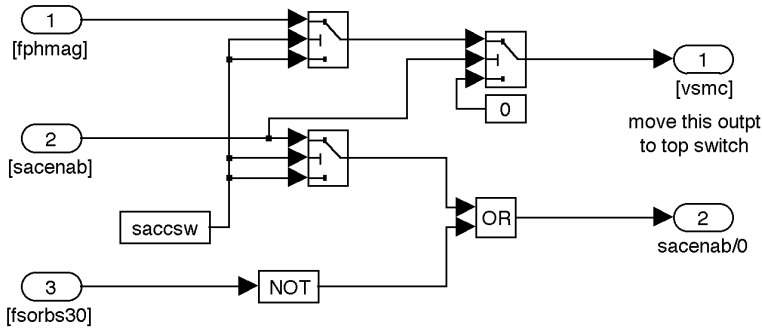
### B Model Plant+



### C Saccadic Motor Command



### Voluntary Saccade Switch



### TCHNG Override

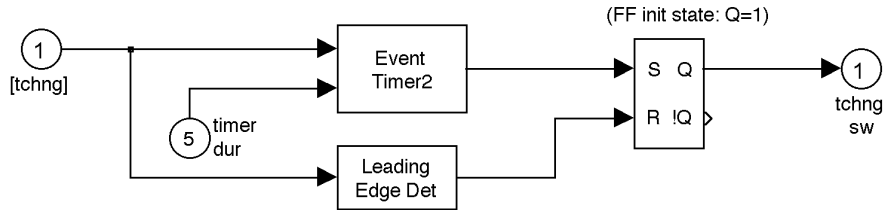
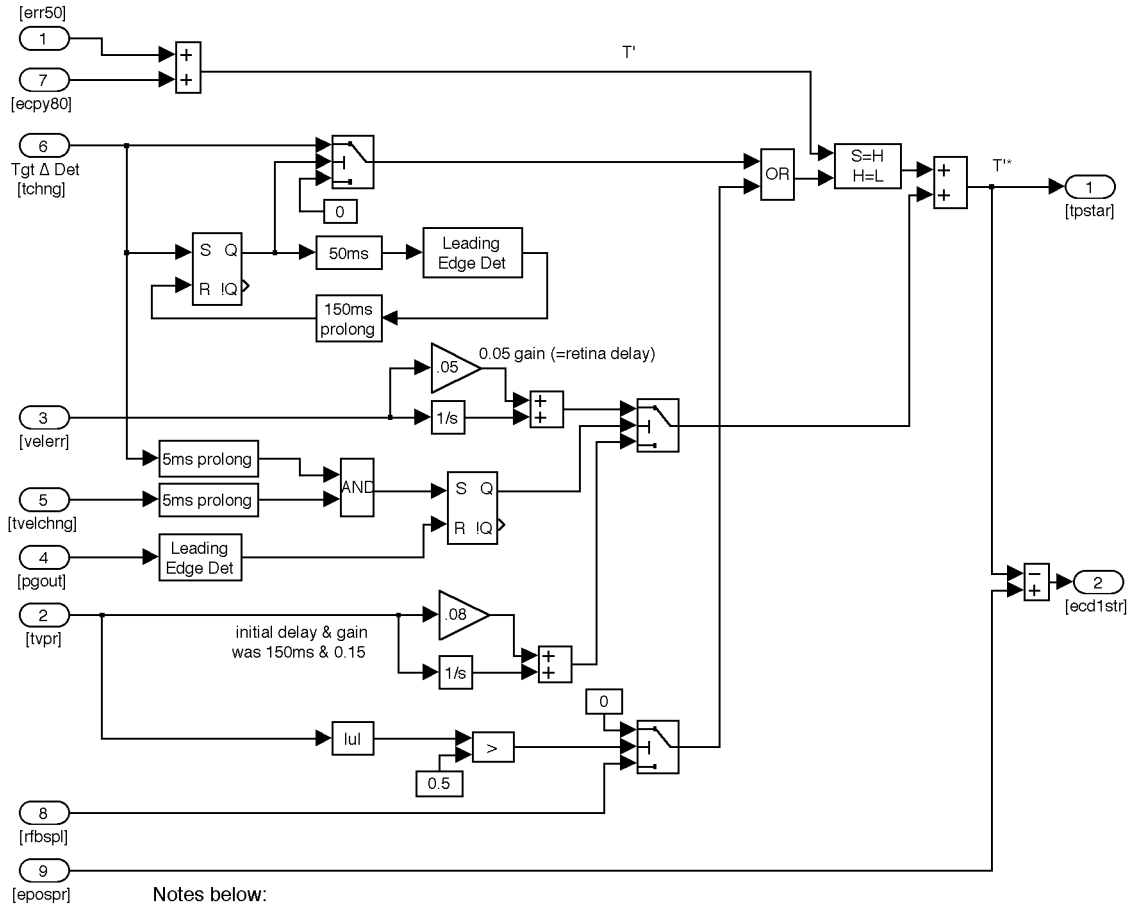


Figure B-3

A.) The Target Change Detection function compares the retinal error velocity to an empirically set threshold to determine if the target position has changed. Likewise, it looks at the acceleration of the reconstructed target velocity to determine if the target has changed velocity. B.) The Model Plant+ simulates the effect of motor commands on the plant, providing the IM with information about the consequences of its motor commands earlier than would be possible if it had to wait for the information to come back from the moving eye. This is the source of ECPY for the IM. C.) The Saccadic Motor Command and internal blocks determine the final magnitude and timing of the saccade to be executed, and whether a voluntary saccade or braking/foveating saccade will be allowed. (The “Event Timer” is shown in Figure B-10.)

### A Sampled Target Position Reconstruction

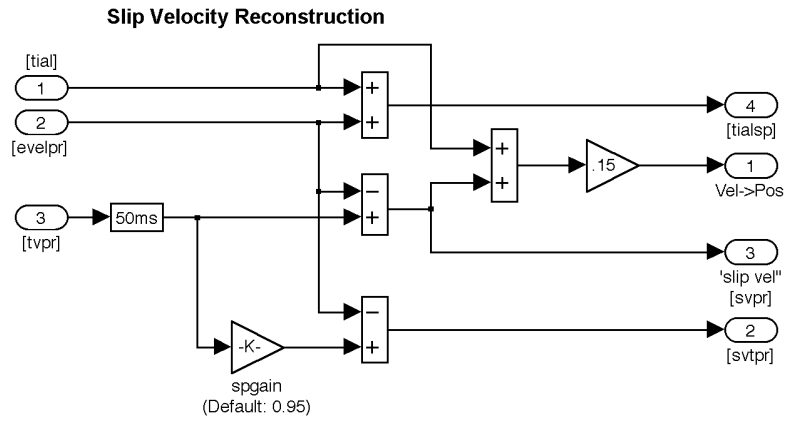


For a step-ramp stim, [velerr] is integrated to mimic target position change before the SP system starts to pursue. It is then shut off at 200ms by [pgout] after 150ms of integration. The .05 gain is for the initial lost 50ms.

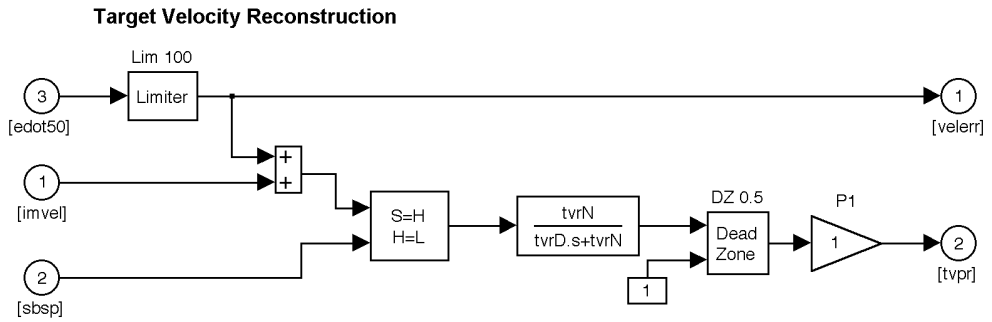
The integral of [tvpr] is used to move [tpstar] to mimic the target motion based on reconstructed target velocity. The .08 gain exceeds the value of integrating [velerr] for 50ms (retinal delay) due to slow buildup of tvpr so values match when switching between velerr and tvposd)

If pursuit is active (tvpr > .5), rbspl does not sample [tprime] because the target is moving and the change from its initial position would result in an inappropriate saccade

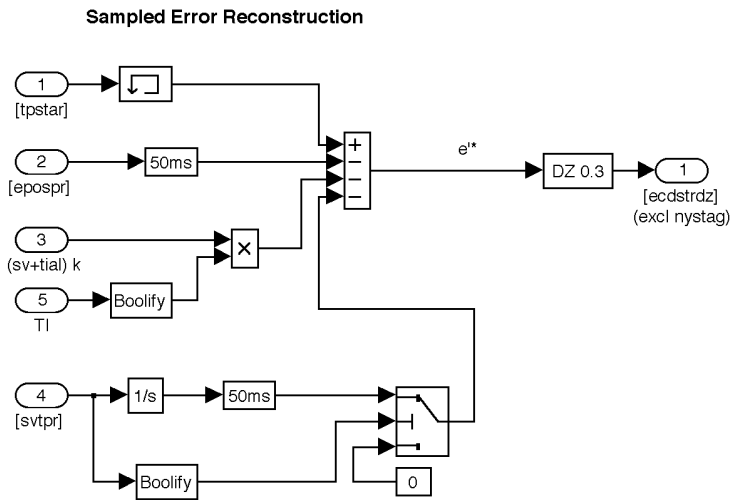
B



C



D



[svtpr] is approx = to the CNvel signal and is used for CN simulations; for normals, [svtpr] should be = 0 and sptpr50 would not be switched into the summer

[sv+tial]\*k is used for the LMLN model and needs to be automatically switched off for normals or CN simulations

Figure B-4

These sub blocks work together to reconstruct the position and velocity information the IM needs to control the saccadic and smooth pursuit subsystems. A.) Sampled Target Position Reconstruction: Retinal error position (epos50), is summed with ecpy80 (the efference copy of eye position (epospr) after being passed through a model of the OMN and 2-pole plant in the “Plant+” block). Appropriate delays are in place. The resulting signal is reconstructed target position,  $T'$ , which is sampled to yield  $T'^*$  (tpstar) when either a target change (tchnng) is detected or a sample of retinal feedback information (rfspl) is called for by the Saccade Enable circuitry. B.) Reconstructed slip velocity (svpr) is the difference between the reconstructed target velocity (tvpr) and velocity efference copy (evelpr). (Evelpr differs from the retinal velocity error at the input to the IM, as the latter also contains the effects of saccadic movement.) The “svtpr” output calculates slip velocity accounting for the actual gain of the SP system, 0.95.

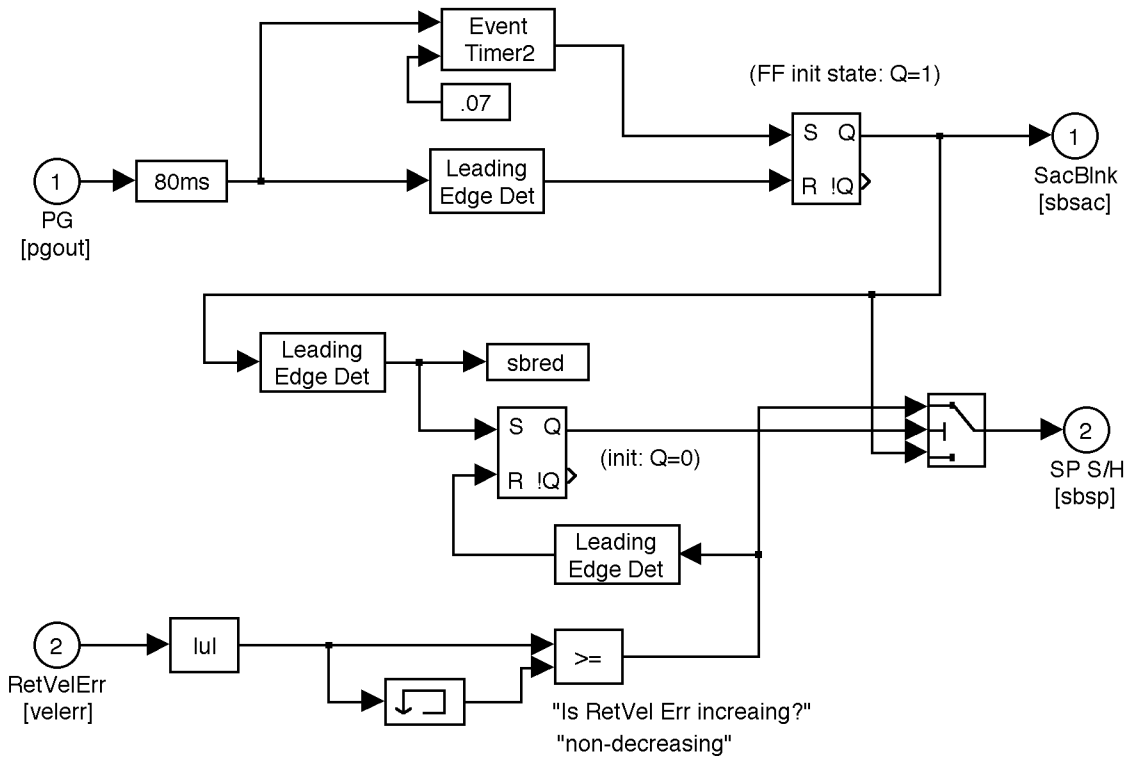
Figure B-4 (cont.)

C.) Target Velocity Reconstruction: Retinal error velocity ( $\dot{e}_{50}$ ) is hard-limited to  $100^\circ/\text{sec}$  (to prevent attempted pursuit of stimuli that are beyond human ability to pursue) and passed through a dead zone ( $0.1^\circ/\text{sec}$ ) and then summed with the reconstructed eye velocity “imvel” (created by summing the efference copy of eye velocity ( $e_{velpr}$ ) with tonic imbalance (TI) and passed through a model of the 1-zero, 2-pole “Plant+”).

Appropriate delays are in place. The resulting signal is sampled or held, based on the “sbsp” signal from the Saccade and Drift Blanking (SP) circuit. This signal is low-pass filtered ( $5/[s+5]$ ) and passed through a dead zone ( $0.2^\circ/\text{sec}$ ) to yield reconstructed target velocity ( $T_{vel}^*$ ), which is the motor command signal to the SP system.

D.) The reconstructed, sampled error is calculated from: the reconstructed, sampled target position ( $tpstar$ ); position efference copy ( $e_{pospr}$ ); any tonic imbalances that are present (see LMLN model); and reconstructed slip velocity ( $svtpr$ ) that has been integrated into a position signal. This sum is passed through a  $0.3^\circ$  dead zone to provide a driving signal to the saccadic subsystem that is free of the nystagmus oscillation.

### Saccade and Post-Saccadic Drift Blanking



Rationale: We do not want the model to look at the slow phase information that immediately follows a saccade. We want to disable both the saccadic and SP systems appropriately.

Saccadic: [sbsac] is initially ENABLED, and is DISABLED by the leading edge of a saccade (after an 80ms delay). 70 ms later the timer REENABLES [sbsac] (Because of the 80ms delay, actual time of reenables is 150 ms after end of PG)

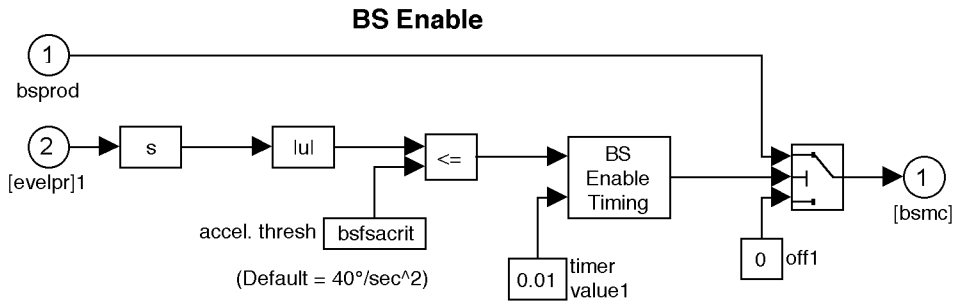
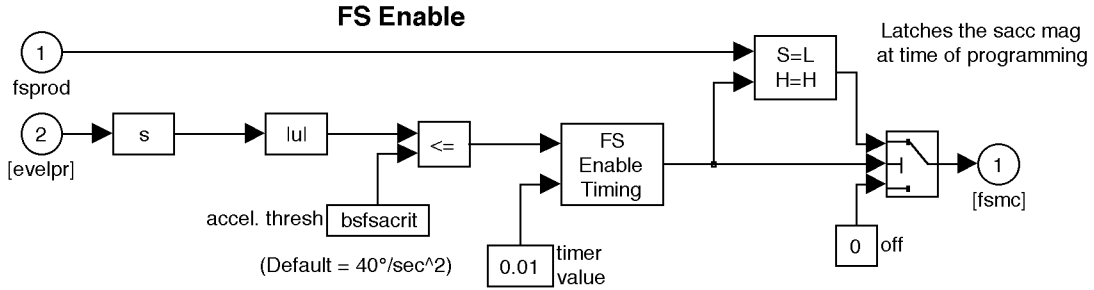
SP: Lower SR latch is SET by [sbsac] going high. The switch will now pass information about the change in velocity error (whether it is decreasing or increasing). If it is increasing, [sbsp] is 1, and the beginning of this increase sets the switch so that [sbsp] = [sbsac]. If the error is decreasing, then [sbsp] = 0, and should stay 0 for as long as [velerr] is decreasing \*\*\*and hasn't crossed zero\*\*\*

Figure B-5

Saccade and Drift Blanking: The Saccade and Drift Blanking circuitry prevents other functions from evaluating steady-state target, eye, or retinal variables during, or for up to 70 ms after saccades. This allows the eye to reach its final position before the reconstruction functions are allowed to sample it, so that they are reacting to the true eye position, not an intermediate value. It creates a blanking signal (sbsac) that lasts for  $PW + 70$  ms, using a delayed PG signal (pg80). The “sbsac” signal is also used to prevent the effects of post-saccadic drift from adversely affecting calculation of reconstructed target velocity. The “sbsac” signal causes the “SP S/H” (sbsp) signal to go low (after “sbsac” goes high at  $80+PW+70$  ms) until the velocity error signal (velerr) begins to increase, at which time “sbsp” goes high.

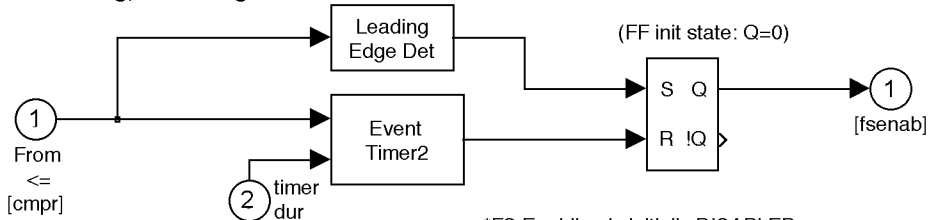


**B**



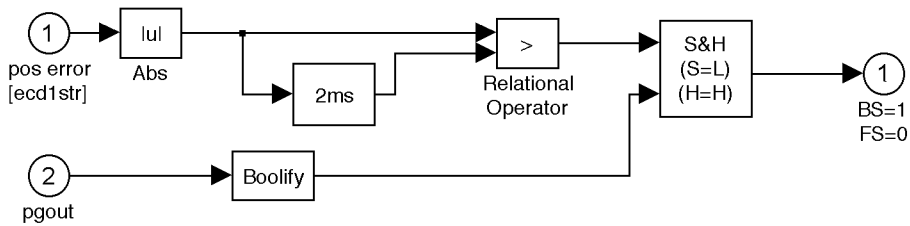
These blocks allow a BS or FS for up to xx ms (set by "timer value") after the acceleration criterion is met (i.e., drops below threshold)

**BS Timing, FS Timing**



Operation: \*FS Enabling is initially DISABLED  
 \* Leading Edge of input ENABLEs output  
 \* Output of TIMER circuit DISABLES output

**FS or BS?**



The position error is compared to its value 3 ms earlier. If the error is increasing, we want to make a braking saccade to oppose the runaway.

If the position error is decreasing, then the eye is approaching the target, and we would like to generate a foveating saccade, since this is our best time to consider capturing the target.

Figure B-6

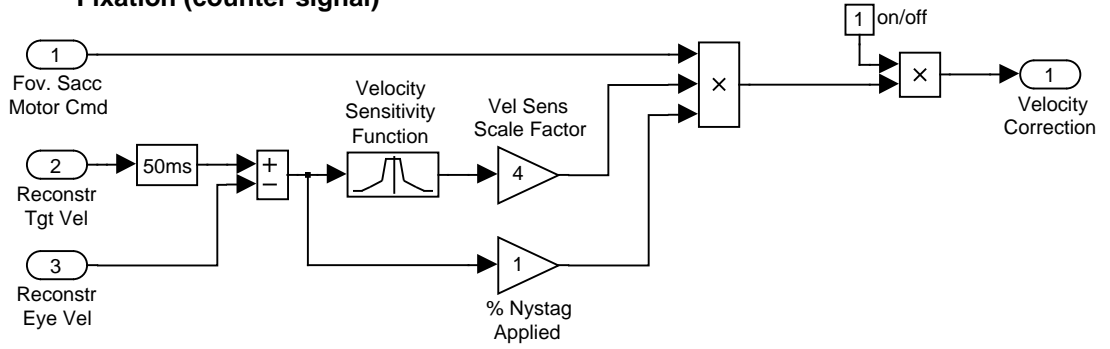
A.) The Braking & Foveating Saccade Logic function determines whether to make a braking saccade or a foveating saccade based on the eye's position, velocity and direction. If the eye is running away from the target, and exceeds the position and velocity criteria, and has stopped accelerating, a fixed-magnitude braking saccade (default =  $1^\circ$ ) is programmed. If the eye is heading towards the target, then a foveating saccade is calculated using the eye's velocity to predict how much larger the saccade will have to be to counteract the effect of the opposing runaway oscillation to be accurate. It makes this prediction by extrapolating eye position 60 ms (default value) into the future assuming a constant velocity. The saccade is also scaled by a factor "fs\_scale," that depends on velocity. "BS Enable" and "FS Enable" determine the times when braking and foveating saccades are allowed to execute. Operation and design notes appear in the figure.

Figure B-6 (cont.)

B.) The subsystems in the BS/FS Logic subsystem that determine braking and foveating saccade timing and eligibility. FS and BS Enable are based on timer circuits to specifically enable the execution of braking and foveating saccades for up to 10 ms (default) after the eye's position, velocity and/or acceleration meet the specified criteria. For foveating saccades, the magnitude of the saccade to be made is latched at the time of initial eligibility. "FS or BS?" determines whether the eye is moving towards or away from the target by comparing the position error signal to its value 2 ms earlier. If the error is increasing, a braking saccade is indicated, and the output will be high. If the error is decreasing, a foveating saccade is indicated, and the output will be low. The output is latched during the execution of the saccade so it can not change.

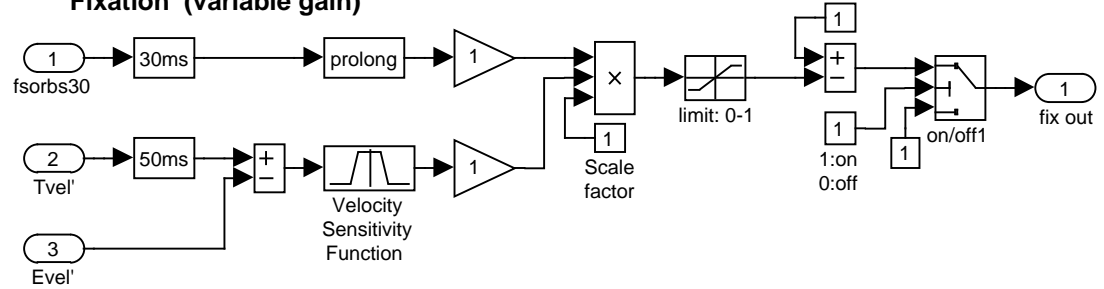
A

**Fixation (counter signal)**



B

**Fixation (variable gain)**



C

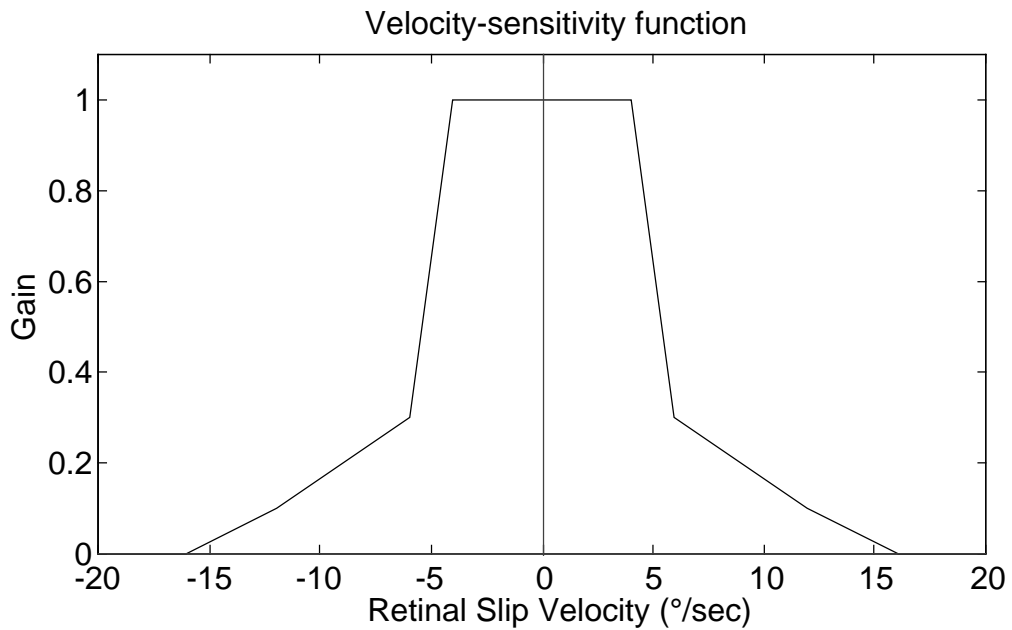
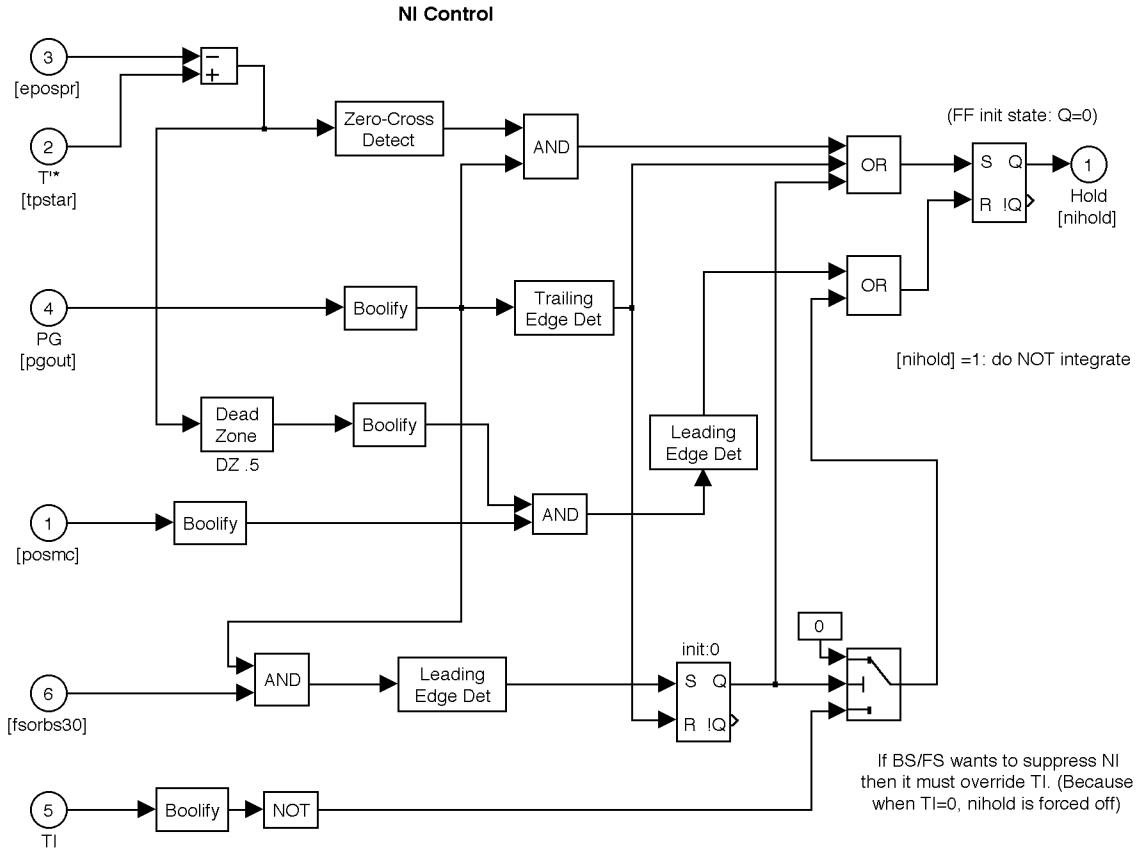


Figure B-7

Two approaches to modeling the fixation subsystem discussed in Chapter 4, section 4.2.5.

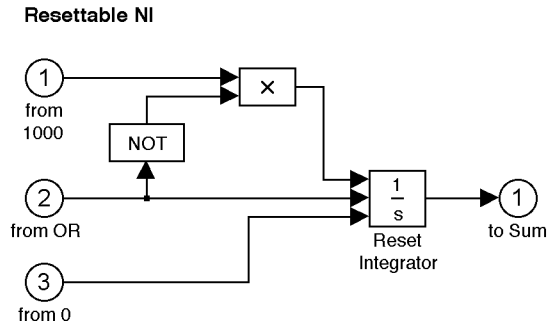
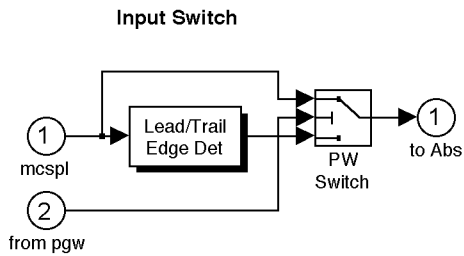
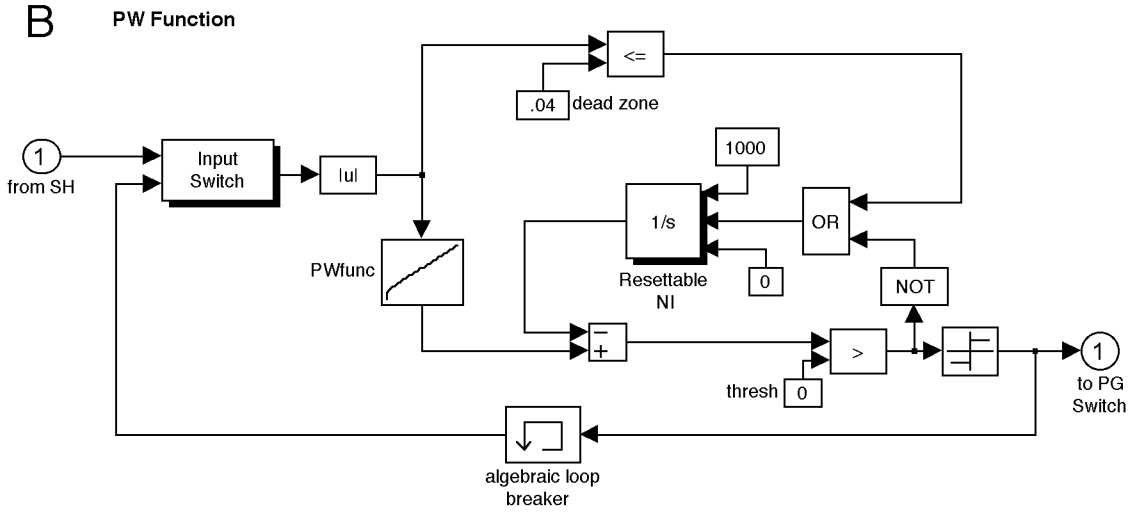
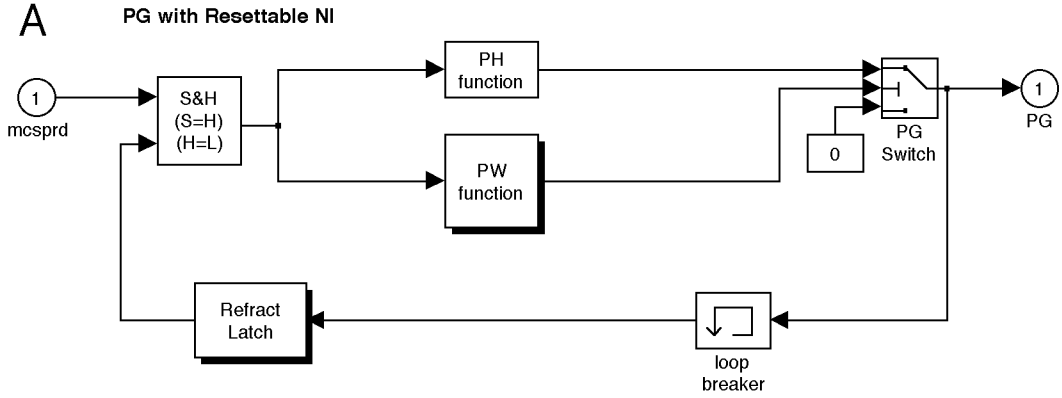
A) The “counter-signal” approach calculates the nystagmus oscillation as the difference between reconstructed target velocity and reconstructed eye velocity. This reconstructed oscillation is passed through a velocity sensitivity function that approximates the relationship between slip velocity and visual acuity. The result is multiplied by four to compensate for the 0.25 gain in the velocity branch around the neural integrator (see Figure B-1A) and combined with other pursuit commands at the input to the NI, and is applied only after the execution of a foveating saccade. B.) The “variable gain” approach also passes the reconstructed nystagmus signal through a velocity sensitivity function, but subtracts the result from 1 to provide a gain signal (ranging from 0-1) that directly affects overall SP gain. C.) The velocity sensitivity function is piecewise-linear, with breakpoints set at  $\pm 4$ , 8, 12 and  $16^\circ/\text{sec}$  in a rough approximation of a Gaussian function.

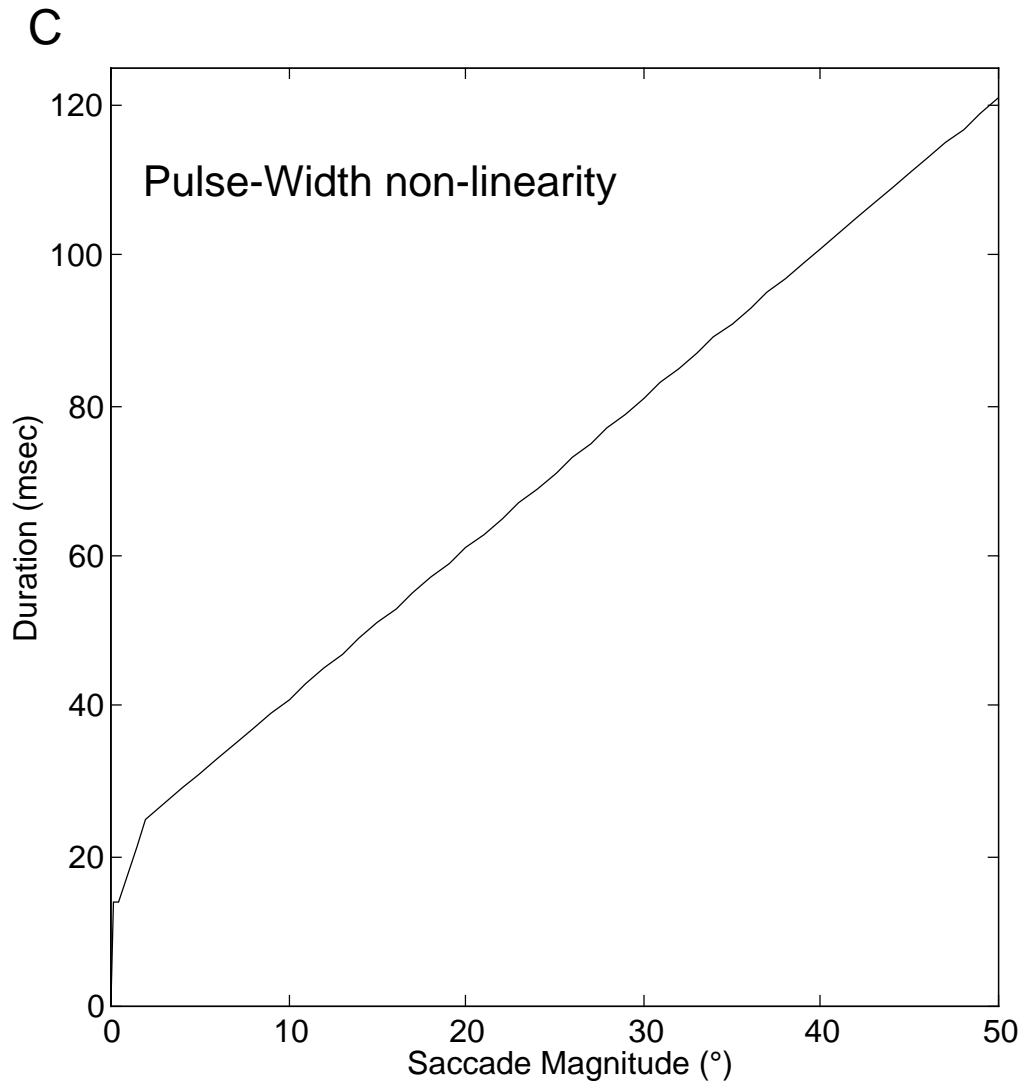


Rationale: We do not always want the NI to integrate every step. E.g. defoveating saccades in LN  
 Don't integrate for any of these conditions: 1) BS/FS pulse, 2) error crosses zero during PG, 3) before end of PG?  
 Resume integration when: 1) as soon as posmc is present while error>0.5°, or 2) NO TI is present

Figure B-8

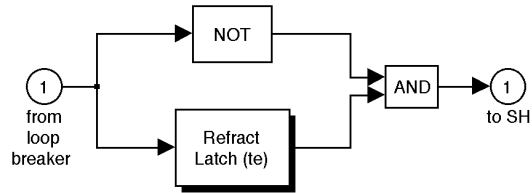
The Neural Integrator Control detects when the eye has reached the target during the execution of a saccade and prevents the neural integrator from continuing to integrate the rest of the pulse. This condition occurs during braking and foveating saccades during CN, and defoveating saccades during LMLN. The Neural Integrator Control circuitry allows the NI to integrate the output of PG until its output (desired eye position) is equal to the reconstructed target position. The output signal (H) is used to remove the PG input from the NI via a control switch. H is set low when both PG and the reconstructed error signal (epr) are non-zero. During PG, H remains low until “epr” crosses zero, whereupon H is set high. H is also set high if PG terminates. In the absence of a tonic imbalance (TI=0), the NI integrates all PG signals. Other conditions (e.g., for GEN, SP, etc.) need to be added to activate this circuitry that allows the NI to hold its value when it has arrived at the correct eye position.



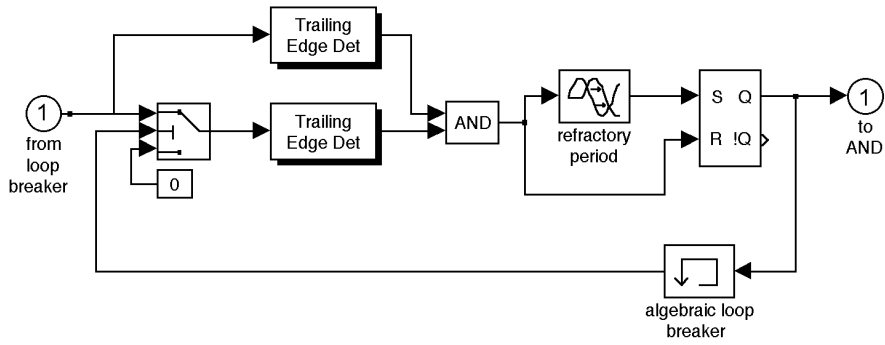


D

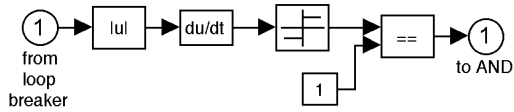
Refractory Latch



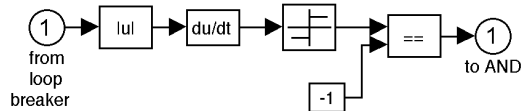
Refractory Latch (te)



Leading Edge Detector



Trailing Edge Detector



Lead/Trail Edge Detector

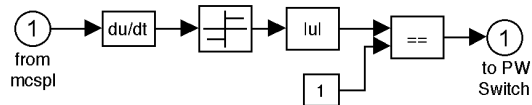
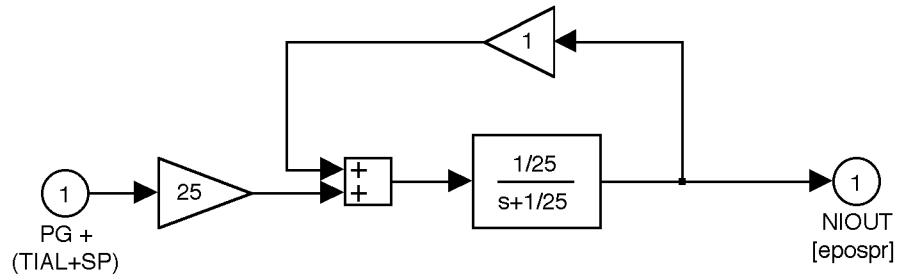


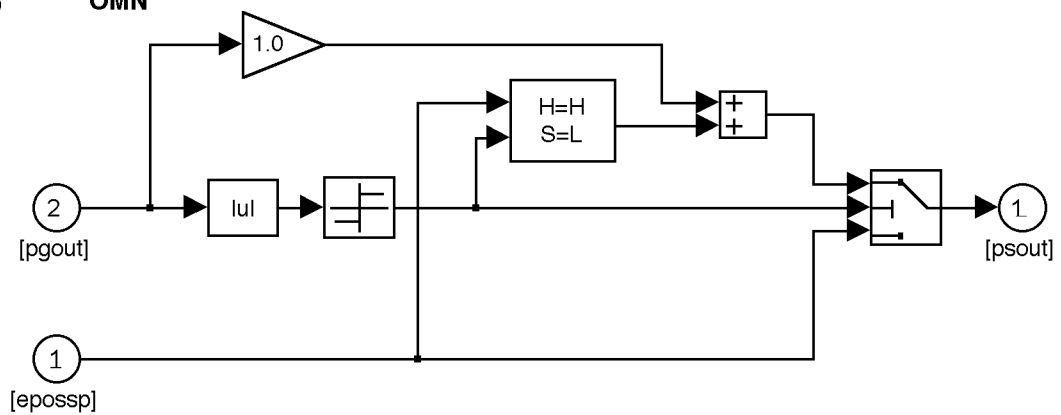
Figure B-9

A.) The Saccadic Pulse Generator uses discrete pulse height (PH) and pulse width (PW) functions to create an appropriately-sized pulse. The pulse width function and its components are shown in this figure. The pulse height function, a MATLAB m-file, appears at the end of this appendix. The saccadic motor command is passed by the Sample/Hold (S/H) circuit to both the PH and PW functions. B.) The pulse width function operates by rapidly integrating the input signal until it matches the value in the nonlinear function “PWfunc,” shown in panel C. The integrator is reset when they match, or when the saccadic command falls below the “dead zone” threshold of  $0.4^\circ$ . C.) The nonlinear function used by the resettable neural integrator to calculate duration. This function is based on observations and published data for saccadic duration vs. magnitude. D.) The Refractory Latch sets the refractory period between saccades, preventing the execution of another saccade until the designated refractory time (default = 50 ms) beyond the end of the PG signal has elapsed. During this refractory period, the S/H circuit is set to “hold,” so no saccades commands can be accepted.

**A NI Real**



**B OMN**



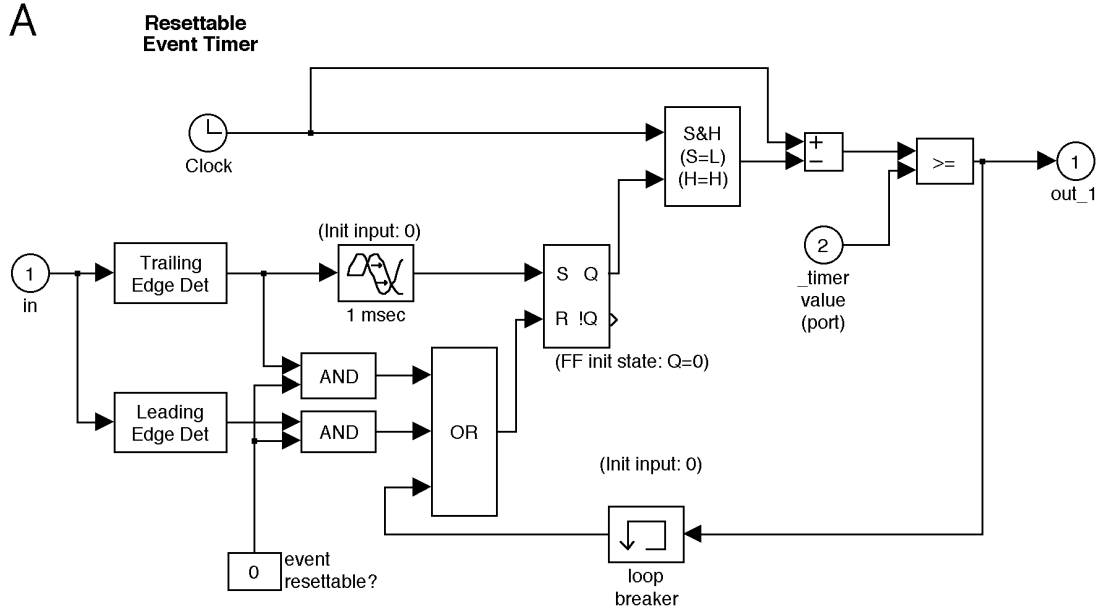
This block behaves like the ocular motor neurons, combining a phasic pulse (from PG) with the tonic step produced by integration of the step, yielding a Pulse-Step to drive the plant.

Operation: when the pulse is active ("from PG") it activates the switch, passing the upper input through to the output. When the pulse is over, the switch changes, allowing the lower input (from the NI) to pass.

Note that the OMN properly combines the pulse with the output of the NI, by latching that output to its value at the moment the pulse appears.

Figure B-10

A.) The Neural Integrator has slight leak, with a time constant of 25 seconds, so that in the absence of a visual target, the eye will slowly drift back to zero. B.) The Ocular Motor Neurons combine the pulse from the saccadic pulse generator with a step that is an integrated version of that pulse. This is not a simple summation of the two signals; rather the pulse is latched at its initial value until it has terminated, and the step has integrated to its final value. See the figure for operational details.



This block is an RESETTABLE EVENT TIMER. It outputs a spike of unit height xx milliseconds (set by "timer value") after it detects an event ( i.e a TRAILING edge which represents the end of a saccadic pulse)

It has TWO modes: 1) Event resettable and 2) Event Non-resettable

In 1), Any event (leading or trailing edge) will reset the counter so that it counts down from the end trailing edge) of that event.

In 2) Subsequent events DO NOT reset the counter; it only resets when it reaches zero

The real trick here is understanding how to reload the countdown.

It resets if either of two conditions is met:

- 1) The count reaches its limit (set in "timer value") -- Both case 1) and 2)
- 2) A new event (leading or trailing edge) is detected. -- Only case 1)

The "OR" gate allows either of these conditions to reset the circuit. The delay before the "S" input of the flip-flop prevents both "S" and "R" from being set simultaneously, because this would put the flip-flop in an undefined state.

Therefore, an event first RESETS and then SETS the flip-flop.

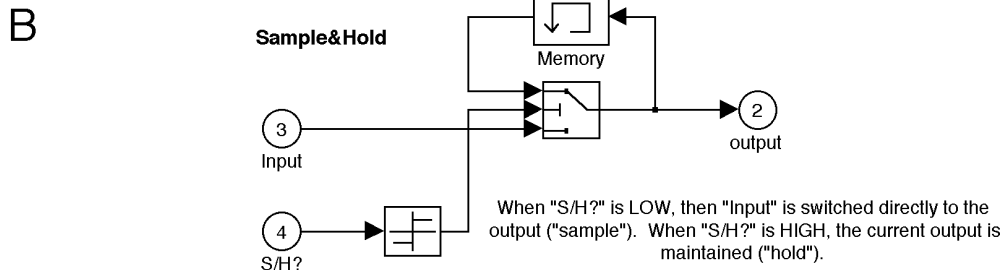


Figure B-11

A.) The Resettable Event Timer is non-physiological in implementation, but simply substitutes for an analog function such as integration until a set threshold is achieved. It is the basis of almost all the timing functions in the model. When the trailing edge of an input is detected, the time is latched, and at each subsequent time step compared to the current time. When the difference reaches the value set on the “Timer Value” port, the timer resets. B.) The Sample & Hold passes its input to the output while the control signal (S/H) is low. When this control goes high, it continues to pass the last sampled value until the control returns to zero. There is also a variant where the control signal is inverted so that sample is high and hold is low. The required control signal is marked on the block, e.g. “S=H” or “S=L” for “sample when high” or “sample when low,” respectively.

```
% PHfn_ss.m: Function to produce pulse height to complement the pulse width
% produced by the pulse width function used in the PGrNI (2P)
% Eye position was measured at its steady state (400ms after end of pulse),
% and a constant tonic gain of 5.25.
%
% Written by: Jonathan Jacobs
%      October 1998 - February 1999 (last mod: 02/18/99)

function out = PHfn_ss(in);

sgn = sign(in);
in = abs(in);

if in > 50
    in = 50;
end

% teeny tiny saccades -- 0.05 to 0.09 degrees
smallmag = [0.6366 0.7635 0.8903 1.0170 1.1438];
if in < 0.05, out = 0; return; end
if (in >= 0.05) & (in < 0.1)
    ind = fix((in-0.04)*100);
    if ind==0; ind=1;end
    out = smallmag(ind)*sgn;
    return
end

% we go by 2.5 degree increments so that we only have to load
% small (25 element) matrices. If we had to load in values for
% all fifty degrees at once, it would make the model unbearably slow.
%% this seems to be the best tradeoff between speed and partitioning effort
if (in >= 0.1) & (in < 2.55)
    mag = [...
        1.2732 2.5449 3.8155 5.0852 6.3542 ... %% 0.1 - 0.5
        7.6228 8.8910 10.1590 11.4269 12.6946 ... %% 0.6 - 1
        13.9623 15.2300 16.4977 17.7654 19.0331 ... %% 1.1 - 1.5
        20.3009 21.5688 22.8366 24.1046 25.3725 ... %% 1.6 - 2
        26.6406 27.9086 29.1767 30.4449 31.7131 ... %% 2.1 - 2.5
    ];
    ind = round(in*10);
    out = mag(ind)*sgn;
    return
end

if (in > 2.5) & (in < 5.05)
    mag = [...
        32.9813 34.2495 35.5177 36.7860 38.0543 ... %% 2.6 - 3
        39.3226 40.5910 41.8593 43.1277 44.3961 ... %% 3.1 - 3.5
        45.6644 46.9328 48.2012 49.4696 50.7380 ... %% 3.6 - 4
        52.0064 53.2749 54.5433 55.8117 57.0801 ... %% 4.1 - 4.5
        58.3486 59.6170 60.8854 62.1538 63.4223 ... %% 4.6 - 5
    ];
    ind = round((in-2.5)*10);
    if ind==0; ind=1;end
    out = mag(ind)*sgn;
    return
end
end
```

```
if (in > 5) & (in < 7.55)
    mag = [...
        64.6907 65.9592 67.2276 68.4960 69.7645 ... %% 5.1 - 5.5
        71.0329 72.3014 69.2340 70.3865 71.5447 ... %% 5.6 - 6
        72.7076 73.8747 75.0451 76.2185 77.3944 ... %% 6.1 - 6.5
        78.5724 79.7522 76.4592 77.5283 78.6059 ... %% 6.6 - 7
        79.6905 80.7809 81.8763 82.9757 84.0786 ... %% 7.1 - 7.5
    ];
    ind = round((in-5)*10);
    if ind==0; ind=1;end
    out = mag(ind)*sgn;
    return
end

if (in > 7.5) & (in <= 10.05)
    mag = [...
        85.1843 86.2924 82.8469 83.8477 84.8586 ... %% 7.6 - 8
        85.8779 86.9042 87.9361 88.9727 90.0131 ... %% 8.1 - 8.5
        91.0566 92.1028 88.5749 89.5126 90.4626 ... %% 8.6 - 9
        91.4226 92.3907 93.3654 94.3455 95.3298 ... %% 9.1 - 9.5
        96.3176 97.3083 93.6681 94.5619 95.4677 ... %% 9.6 - 10
    ];
    ind = round((in-7.5)*10);
    if ind==0; ind=1;end
    out = mag(ind)*sgn;
    return
end

if (in > 10) & (in <= 12.55)
    mag = [...
        96.3829 97.3057 98.2346 94.7130 95.5548 ... %% 10.1 - 10.5
        96.4106 97.2775 98.1530 94.8065 95.5987 ... %% 10.6 - 11
        96.4076 97.2295 98.0613 94.8181 95.5822 ... %% 11.1 - 11.5
        96.3616 97.1527 97.9528 94.8341 95.5726 ... %% 11.6 - 12
        96.3249 97.0877 97.8583 94.9234 95.6205 ... %% 12.1 - 12.5
    ];
    ind = round((in-10)*10);
    if ind==0; ind=1;end
    out = mag(ind)*sgn;
    return
end

if (in > 12.5) & (in <= 15.0)
    mag = [...
        96.3345 97.0612 97.7973 94.9418 95.6175 ... %% 12.6 - 13
        96.3089 97.0117 97.7229 94.9630 95.6190 ... %% 13.1 - 13.5
        96.2892 96.9698 97.6577 95.0522 95.6710 ... %% 13.6 - 14
        96.3081 96.9581 97.6175 95.0731 95.6755 ... %% 14.1 - 14.5
        96.2948 96.9259 97.5654 95.0959 95.6831 ... %% 14.6 - 15
    ];
    ind = round((in-12.5)*10);
    if ind==0; ind=1;end
    out = mag(ind)*sgn;
    return
end
```

```
if (in > 15) & (in < 17.75)
    mag = [...
        96.2857  96.8990  97.5197  95.1874  95.7388 ... %% 15.1 - 15.5
        96.3112  96.8978  97.4940  95.2086  95.7475 ... %% 15.6 - 16
        96.3058  96.8771  97.4572  95.2310  95.7583 ... %% 16.1 - 16.5
        96.3034  96.8603  97.4250  95.2555  95.7715 ... %% 16.6 - 17
        96.3039  96.8470  97.3971  95.2816  95.7868 ... %% 17.1 - 17.5
    ];
    ind = round((in-15.0)*10);
    if ind==0; ind=1;end
    out = mag(ind)*sgn;
    return
end
```

```
if (in > 17.5) & (in < 20.05)
    mag = [...
        96.3070  96.8370  97.3730  95.3693  95.8416 ... %% 17.6 - 18
        96.3361  96.8445  97.3617  95.3926  95.8562 ... %% 18.1 - 18.5
        96.3406  96.8377  97.3426  95.4167  95.8722 ... %% 18.6 - 19
        96.3468  96.8331  97.3264  95.4421  95.8896 ... %% 19.1 - 19.5
        96.3549  96.8307  97.3128  95.4685  95.9083 ... %% 19.6 - 20
    ];
    ind = round((in-17.5)*10);
    if ind==0; ind=1;end
    out = mag(ind)*sgn;
    return
end
```

```
if (in > 20) & (in < 22.55)
    mag = [...
        96.3645  96.8302  97.3016  95.4958  95.9282 ... %% 20.1 - 20.5
        96.3755  96.8315  97.2925  95.5239  95.9489 ... %% 20.6 - 21
        96.3877  96.8343  97.2853  95.6043  95.9992 ... %% 21.1 - 21.5
        96.4169  96.8473  97.2848  95.6291  96.0185 ... %% 21.6 - 22
        96.4292  96.8516  97.2802  95.6544  96.0386 ... %% 22.1 - 22.5
    ];
    ind = round((in-20.0)*10);
    if ind==0; ind=1;end
    out = mag(ind)*sgn;
    return
end
```

```
if (in > 22.5) & (in < 25.05)
    mag = [...
        96.4425  96.8571  97.2772  95.6805  96.0594 ... %% 22.6 - 23
        96.4568  96.8637  97.2757  95.7071  96.0810 ... %% 23.1 - 23.5
        96.4718  96.8714  97.2754  95.7343  96.1031 ... %% 23.6 - 24
        96.4877  96.8800  97.2763  95.7619  96.1258 ... %% 24.1 - 24.5
        96.5041  96.8895  97.2784  95.7899  96.1489 ... %% 24.6 - 25
    ];
    ind = round((in-22.5)*10);
    if ind==0; ind=1;end
```

```
out = mag(ind)*sgn;  
return  
end
```

```
if (in > 25) & (in < 27.55)  
mag = [...  
96.5212 96.8998 97.2814 95.8182 96.1724 ... %% 25.1 - 25.5  
96.5388 96.9108 97.2854 95.8914 96.2169 ... %% 25.6 - 26  
96.5663 96.9267 97.2923 95.9165 96.2388 ... %% 26.1 - 26.5  
96.5836 96.9383 97.2976 95.9418 96.2612 ... %% 26.6 - 27  
96.6013 96.9505 97.3038 95.9676 96.2840 ... %% 27.1 - 27.5  
];  
ind = round((in-25.0)*10);  
if ind==0; ind=1;end  
out = mag(ind)*sgn;  
return  
end
```

```
if (in > 27.5) & (in < 30.05)  
mag = [...  
96.6195 96.9633 97.3106 95.9937 96.3071 ... %% 27.6 - 28  
96.6381 96.9766 97.3182 96.0202 96.3304 ... %% 28.1 - 28.5  
96.6570 96.9903 97.3264 96.0469 96.3541 ... %% 28.6 - 29  
96.6763 97.0045 97.3351 96.0738 96.3780 ... %% 29.1 - 29.5  
96.6959 97.0191 97.3445 96.1010 96.4021 ... %% 29.6 - 30  
];  
ind = round((in-27.5)*10);  
if ind==0; ind=1;end  
out = mag(ind)*sgn;  
return  
end
```

```
if (in > 30) & (in < 32.55)  
mag = [...  
96.7157 97.0341 97.3543 96.1283 96.4263 ... %% 30.1 - 30.5  
96.7358 97.0494 97.3646 96.1558 96.4507 ... %% 30.6 - 31  
96.7560 97.0650 97.3754 96.1834 96.4752 ... %% 31.1 - 31.5  
96.7764 97.0809 97.3866 96.2110 96.4998 ... %% 31.6 - 32  
96.7970 97.0971 97.3982 96.2388 96.5245 ... %% 32.1 - 32.5  
];  
ind = round((in-30.0)*10);  
if ind==0; ind=1;end  
out = mag(ind)*sgn;  
return  
end
```

```
if (in > 32.5) & (in < 35.05)  
mag = [...  
96.8178 97.1135 97.4101 96.2981 96.5592 ... %% 32.6 - 33  
96.8418 97.1312 97.4227 96.3230 96.5827 ... %% 33.1 - 33.5  
96.8623 97.1478 97.4353 96.3481 96.6064 ... %% 33.6 - 34  
96.8829 97.1647 97.4482 96.3734 96.6303 ... %% 34.1 - 34.5  
96.9037 97.1818 97.4613 96.3988 96.6542 ... %% 34.6 - 35  
];
```

```
ind = round((in-32.5)*10);  
if ind==0; ind=1;end  
out = mag(ind)*sgn;  
return  
end
```

```
if (in > 35) & (in < 37.55)  
mag = [...  
96.9246 97.1991 97.4748 96.4245 96.6782 ... %% 35.1 - 35.5  
96.9456 97.2166 97.4885 96.4502 96.7023 ... %% 35.6 - 36  
96.9667 97.2342 97.5025 96.4761 96.7264 ... %% 36.1 - 36.5  
96.9878 97.2519 97.5167 96.5020 96.7506 ... %% 36.6 - 37  
97.0091 97.2698 97.5311 96.5281 96.7749 ... %% 37.1 - 37.5  
];  
ind = round((in-35.0)*10);  
if ind==0; ind=1;end  
out = mag(ind)*sgn;  
return  
end
```

```
if (in > 37.5) & (in < 40.05)  
mag = [...  
97.0304 97.2879 97.5458 96.5542 96.7991 ... %% 37.6 - 38  
97.0517 97.3060 97.5606 96.5804 96.8234 ... %% 38.1 - 38.5  
97.0731 97.3242 97.5756 96.6066 96.8476 ... %% 38.6 - 39  
97.0945 97.3426 97.5908 96.6328 96.8719 ... %% 39.1 - 39.5  
97.1160 97.3610 97.6062 96.6591 96.8961 ... %% 39.6 - 40  
];  
ind = round((in-37.5)*10);  
if ind==0; ind=1;end  
out = mag(ind)*sgn;  
return  
end
```

```
if (in > 40) & (in < 42.55)  
mag = [...  
97.1374 97.3795 97.6217 96.6854 96.9203 ... %% 40.1 - 40.5  
97.1589 97.3981 97.6374 96.7117 96.9445 ... %% 40.6 - 41  
97.1804 97.4168 97.6532 96.7380 96.9687 ... %% 41.1 - 41.5  
97.2019 97.4355 97.6691 96.7642 96.9928 ... %% 41.6 - 42  
97.2234 97.4543 97.6852 96.7904 97.0168 ... %% 42.1 - 42.5  
];  
ind = round((in-40.0)*10);  
if ind==0; ind=1;end  
out = mag(ind)*sgn;  
return  
end
```

```
if (in > 42.5) & (in < 45.05)  
mag = [...  
97.2449 97.4731 97.7014 96.8166 97.0408 ... %% 42.6 - 43  
97.2664 97.4920 97.7177 96.8428 97.0648 ... %% 43.1 - 43.5  
97.2878 97.5109 97.7341 96.8775 97.0895 ... %% 43.6 - 44  
97.3094 97.5299 97.7506 96.9018 97.1131 ... %% 44.1 - 44.5  
];
```

```
    97.3308  97.5490  97.7672  96.9262  97.1367 ... %% 44.6 - 45
];
ind = round((in-42.5)*10);
out = mag(ind)*sgn;
return
end

if (in > 45) & (in <= 47.55)
mag = [...
    97.3522  97.5680  97.7839  96.9507  97.1603 ... %% 45.1 - 45.5
    97.3736  97.5871  97.8006  96.9754  97.1838 ... %% 45.6 - 46
    97.3949  97.6062  97.8175  97.0001  97.2073 ... %% 46.1 - 46.5
    97.4163  97.6253  97.8344  97.0250  97.2308 ... %% 46.6 - 47
    97.4376  97.6445  97.8514  97.0500  97.2542 ... %% 47.1 - 47.5
];
ind = round((in-45.0)*10);
if ind==0; ind=1;end
out = mag(ind)*sgn;
return
end

if (in > 47.5) & (in < 50.05)
mag = [...
    97.4589  97.6637  97.8684  97.0751  97.2776 ... %% 47.6 - 48
    97.4802  97.6829  97.8855  97.1002  97.3008 ... %% 48.1 - 48.5
    97.5015  97.7021  97.9027  97.1255  97.3241 ... %% 48.6 - 49
    97.5227  97.7213  97.9199  97.1508  97.3472 ... %% 49.1 - 49.5
    97.5439  97.7405  97.9372  97.1763  97.3703 ... %% 49.6 - 50
];
ind = round((in-47.5)*10);
if ind==0; ind=1;end
out = mag(ind)*sgn;
return
end
```

## BIBLIOGRAHY

- Abadi, R. V., & Dickinson, C. M. (1985). The influence of preexisting oscillations on the binocular optokinetic response. *Ann Neurol*, **17**, 578-586.
- Abadi, R. V., & Dickinson, C. M. (1986). Waveform characteristics in congenital nystagmus. *Doc Ophthalmol*, **64**, 153-167.
- Abadi, R. V., & Worfolk, R. (1989). Retinal slip velocities in congenital nystagmus. *Vision Research*, **29**, 195-205.
- Abadi, R. V., Dickinson, C. M., & Lomas, M. S. (1982) Inverted and asymmetrical optokinetic nystagmus. In: G. Lennerstrand, D. S. Zee, & E. L. Keller, *Functional Basis of Ocular Motility Disorders* (pp. 143-146). Oxford, Pergamon Press.
- Abadi, R. V., Scallan, C. J., & Clement, R. A. (2000). The characteristics of dynamic overshoots in square-wave jerks, and in congenital and manifest latent nystagmus. *Vision Research*, **40**, 2813-2829.
- Abel, L. A., & Hertle, R. W. (1988) Effects of psychoactive drugs on ocular motor behavior. In: C. W. Johnston, & F. J. Pirozzolo, *Neuropsychology of Eye Movements* (pp. 83-114). Hillsdale, Lawrence Erlbaum Associates.
- Abel, L. A., & Dell'Osso, L. F. (1988). Correlations between saccadic latency and velocity in neurologic patients and elderly, but not young, normal subjects. *Investigative Ophthalmology and Visual Science*, **29**, 347.
- Abel, L. A., Dell'Osso, L. F., & Daroff, R. B. (1978). Analog model for gaze-evoked nystagmus. *IEEE Trans Biomed Engng*, **BME(25)**, 71-75.
- Abel, L. A., Dell'Osso, L. F., Schmidt, D., & Daroff, R. B. (1980). Myasthenia gravis: Analogue computer model. *Exp Neurol*, **68**, 378-389.
- Averbuch-Heller, L., Dell'Osso, L. F., Jacobs, J. B., & Remler, B. F. (1999). Latent and congenital nystagmus in Down syndrome. *J Neuro-Ophthalmol*, **19**, 166-172.
- Bach, M., & Hoffmann, M. B. (2000). Visual motion detection in man is governed by non-retinal mechanisms. *Vision Research*, **40**(18), 2379-2785.
- Bahill, A. T., Clark, M. R., & Stark, L. (1975). The main sequence: A tool for studying human eye movements. *Mathematical Bioscience*, **24**, 191-204.

- Bahill, A. T., Brockenbrough, A., & Troost, B. T. (1981). Variability and development of a normative database for saccadic eye movements. *Investigative Ophthalmology and Visual Science*, **21**, 116-125.
- Becker, W. (1989) Metrics. In: R. M. Wurtz, & M. E. Goldberg, *The neurobiology of saccadic eye movements* (pp. 13-67). Amsterdam: Elsevier Science Publishers BV.
- Becker, W., & Jürgens, R. (1979). An analysis of the saccadic system by means of double step stimuli. *Vision Research*, **19**, 967-983.
- Bedell, H. E., & Currie, D. C. (1993). Extraretinal signals for congenital nystagmus. *Invest Ophthalmol Vis Sci*, **34**, 2325-2332.
- Blumer, R., Lukas, J.-R., Aigner, M., Bittner, R., Baumgartner, I., & Mayr, R. (1999). Fine structural analysis of extraocular muscle spindles of a two-year-old human infant. *Invest Ophthalmol Vis Sci*, **40**, 55-64.
- Boghen, D., Troost, B. T., Daroff, R. B., Dell'Osso, L. F., & Birkett, J. E. (1974). Velocity characteristics of normal human saccades. *Invest Ophthalmol*, **13**, 619-623.
- Brindley, G. S., & Merton, P. A. (1960). The absence of position sense in the human eye. *J. Physiol.*, **153**, 127-130.
- Broomhead, D. S., Clement, R. A., Muldoon, M. R., Whittle, J. P., Scallan, C., & Abadi, R. V. (2000). Modelling of congenital nystagmus waveforms produced by saccadic system abnormalities. *Biological Cybernetics*, **82**, 391-399.
- Broomhead, D. S., Clement, R. A., Muldoon, M. R., Whittle, J. P., Scallan, C., & Abadi, R. V. (2000). Modelling of congenital nystagmus waveforms produced by saccadic system abnormalities. *Biological Cybernetics*, **82**(5), 391-399.
- Bruce, C. J., & Goldberg, M. E. (1985). Primate frontal eye fields. I. Single neurons discharging before saccades. *J Neurophysiol*, **53**, 603-635.
- Burr, D. C., & Ross, J. (1982). Contrast sensitivity at high velocities. *Vision Res*, **22**, 479-484.
- Buttner-Ennever, J. A., Horn, A. K., & Schmidtke, K. (1989). Cell groups of the medial longitudinal fasciculus and paramedian tracts. *Revue Neurologique*, **145**(8-9), 533-539.
- Carl, J. R., & Gellman, R. S. (1987). Human smooth pursuit: stimulus-dependent responses. *Journal of Neurophysiology*, **57**(5), 1446-1463.

- Carpenter, R. H. S. (1988) *Movements of the Eyes, 2nd Edition.*, Pion: London.
- Chung, S. T. L., & Bedell, H. E. (1995). Effect of retinal image motion on visual acuity and contour interaction in congenital nystagmus. *Vision Res*, **35**, 3071-3082.
- Collewijn, H., & Tamminga, E. P. (1984). Human smooth and saccadic eye movements during voluntary pursuit of different target motions on different backgrounds. *J Physiol*, **351**, 217-250.
- de la Barre, E. B. (1898). A method of recording eye-movements. *American Journal of Psychology*, **9**, 572-574.
- Dell'Osso, L. F. (1968) *A Dual-Mode Model for the Normal Eye Tracking System and the System with Nystagmus. (Ph.D. Dissertation)*. In: Electrical Engineering (Biomedical), University of Wyoming: Laramie. p. 1-131
- Dell'Osso, L. F. (1968) *A Dual-Mode Model for the Normal Eye Tracking System and the System with Nystagmus. (Ph.D. Dissertation)*, University of Wyoming.
- Dell'Osso, L. F. (1973). Fixation characteristics in hereditary congenital nystagmus. *Am J Optom Arch Am Acad Optom*, **50**, 85-90.
- Dell'Osso, L. F. (1973) Improving Visual Acuity in Congenital Nystagmus. In: J. L. Smith, & J. S. Glaser, *Neuro-Ophthalmology Symposium of the University of Miami and the Bascom Palmer Eye Institute, Vol. VII* (pp. 98-106). St. Louis: CV Mosby Company.
- Dell'Osso, L. F. (1976) Prism exploitation of gaze and fusional null angles in congenital nystagmus. In: S. Moore, *Orthoptics : Past, Present, Future* (pp. 135-142). New York: Symposia Specialists.
- Dell'Osso, L. F. (1985). Congenital, latent and manifest latent nystagmus - similarities, differences and relation to strabismus. *Jpn J Ophthalmol*, **29**, 351-368.
- Dell'Osso, L. F. (1986). Evaluation of smooth pursuit in the presence of congenital nystagmus. *Neuro ophthalmol*, **6**, 383-406.
- Dell'Osso, L. F. (1994). Congenital and latent/manifest latent nystagmus: Diagnosis, treatment, foveation, oscillopsia, and acuity. *Jpn J Ophthalmol*, **38**, 329-336.
- Dell'Osso, L. F. (1994). Evidence suggesting individual ocular motor control of each eye (muscle). *J Vestib Res*, **4**, 335-345.

- Dell'Osso, L. F. (1997). Extraocular muscle tenotomy, dissection, and suture: A hypothetical therapy for congenital nystagmus. *J Pediatr Ophthalmol Strab*, **35**, 232-233.
- Dell'Osso, L. F., & Daroff, R. B. (1975). Congenital nystagmus waveforms and foveation strategy. *Doc Ophthalmol*, **39**, 155-182.
- Dell'Osso, L. F., & Daroff, R. B. (1976). Braking saccade—A new fast eye movement. *Aviat Space Environ Med*, **47**, 435-437.
- Dell'Osso, L. F., & Flynn, J. T. (1979). Congenital nystagmus surgery: a quantitative evaluation of the effects. *Arch Ophthalmol*, **97**, 462-469.
- Dell'Osso, L. F., & Daroff, R. B. (1981) Clinical disorders of ocular movement. In: B. L. Zuber, *Models of Oculomotor Behavior and Control* (pp. 233-256). West Palm Beach, CRC Press Inc.
- Dell'Osso, L. F., & Daroff, R. B. (1986) Abnormal head position and head motion associated with nystagmus. In: E. L. Keller, & D. S. Zee, *Adaptive Processes In Visual and Oculomotor Systems* (pp. 473-478). Oxford: Pergamon Press.
- Dell'Osso, L. F., & Leigh, R. J. (1995). Oscillopsia suppression: Efference copy or foveation periods? *Invest Ophthalmol Vis Sci*, **36**, S174.
- Dell'Osso, L. F., & Williams, R. W. (1995). Ocular motor abnormalities in achiasmatic mutant Belgian sheepdogs: Unyoked eye movements in a mammal. *Vision Res*, **35**, 109-116.
- Dell'Osso, L. F., & Daroff, R. B. (1997) Nystagmus and saccadic intrusions and oscillations. In: W. Tasman, & E. A. Jaeger, *Duane's Clinical Ophthalmology, Vol. II, Chap. 11* (pp. 1-33). Philadelphia: Lippincott-Raven.
- Dell'Osso, L. F., & Jacobs, J. B. (1998). An preliminary model of congenital nystagmus (CN) incorporating braking saccades. *Invest Ophthalmol Vis Sci*, **39**, S149.
- Dell'Osso, L. F., & Daroff, R. B. (1999) Eye movement characteristics and recording techniques. In: J. S. Glaser, *Neuro-Ophthalmology, 3rd Edition* (pp. 327-343). Baltimore: Lippincott Williams & Wilkins.
- Dell'Osso, L. F., & Daroff, R. B. (1999) Nystagmus and saccadic intrusions and oscillations. In: J. S. Glaser, *Neuro-Ophthalmology* (pp. 369-401). Baltimore: Lippincott Williams & Wilkins.

Dell'Osso, L. F., & Jacobs, J. B. (2000) A robust, normal ocular motor system model with latent/manifest latent nystagmus (LMLN) and dual-mode fast phases. In: J. A. Sharpe, *Neuro-ophthalmology at the Beginning of the New Millennium* (pp. 113-118). Englewood: Medimond Medical Publications.

Dell'Osso, L. F., & Jacobs, J. B. (2001). A normal ocular motor system model that simulates the dual-mode fast phases of latent/manifest latent nystagmus (submitted). *Biological Cybernetics*, 000-000.

Dell'Osso, L. F., Flynn, J. T., & Daroff, R. B. (1974). Hereditary congenital nystagmus: An intrafamilial study. *Arch Ophthalmol*, **92**, 366-374.

Dell'Osso, L. F., Troost, B. T., & Daroff, R. B. (1975). Macro square wave jerks. *Neurology*, **25**, 975-979.

Dell'Osso, L. F., Schmidt, D., & Daroff, R. B. (1979). Latent, manifest latent and congenital nystagmus. *Arch Ophthalmol*, **97**, 1877-1885.

Dell'Osso, L. F., Traccis, S., & Abel, L. A. (1983). Strabismus - A necessary condition for latent and manifest latent nystagmus. *Neuro ophthalmol*, **3**, 247-257.

Dell'Osso, L. F., Averbuch-Heller, L., & Leigh, R. J. (1997). Oscillopsia suppression and foveation-period variation in congenital, latent, and acquired nystagmus. *Neuro ophthalmol*, **18**, 163-183.

Dell'Osso, L. F., Gauthier, G., Liberman, G., & Stark, L. (1972). Eye movement recordings as a diagnostic tool in a case of congenital nystagmus. *Am J Optom Arch Am Acad Optom*, **49**, 3-13.

Dell'Osso, L. F., Ellenberger, J. C., Abel, L. A., & Flynn, J. T. (1983). The nystagmus blockage syndrome: Congenital nystagmus, manifest latent nystagmus or both? *Invest Ophthalmol Vis Sci*, **24**, 1580-1587.

Dell'Osso, L. F., Van der Steen, J., Steinman, R. M., & Collewijn, H. (1992). Foveation dynamics in congenital nystagmus I: Fixation. *Doc Ophthalmol*, **79**, 1-23.

Dell'Osso, L. F., Van der Steen, J., Steinman, R. M., & Collewijn, H. (1992). Foveation dynamics in congenital nystagmus II: Smooth pursuit. *Doc Ophthalmol*, **79**, 25-49.

Dell'Osso, L. F., Van der Steen, J., Steinman, R. M., & Collewijn, H. (1992). Foveation dynamics in congenital nystagmus III: Vestibulo-ocular reflex. *Doc Ophthalmol*, **79**, 51-70.

Dell'Osso, L. F., Leigh, R. J., Sheth, N. V., & Daroff, R. B. (1995). Two types of foveation strategy in 'latent' nystagmus. Fixation, visual acuity and stability. *Neuro ophthalmol*, **15**, 167-186.

Dell'Osso, L. F., Hertle, R. W., Williams, R. W., & Jacobs, J. B. (1999). A new surgery for congenital nystagmus: effects of tenotomy on an achiasmatic canine and the role of extraocular proprioception. *J Am Assoc Pediatr Ophthalmol Strab*, **3**, 166-182.

Dell'Osso, L. F., Hogan, D., Jacobs, J. B., & Williams, R. W. (1999). Eye movements in canine hemichiasma: does human hemichiasma exist? *Neuro-ophthalmol*, **22**, 47-58.

Dell'Osso, L. F., Weissman, B. M., Leigh, R. J., Abel, L. A., & Sheth, N. V. (1993). Hereditary congenital nystagmus and gaze-holding failure: The role of the neural integrator. *Neurology*, **43**, 1741-1749.

Dickinson, C. M., & Abadi, R. V. (1985). The influence of nystagmoid oscillation on contrast sensitivity in normal observers. *Vision Res*, **25**, 1089-1096.

Dijkstra, E. W. (1976) *A discipline of programming.*, Prentice Hall: Englewood Cliffs, NJ.

Doslak, M. J., Dell'Osso, L. F., & Daroff, R. B. (1979). A model of Alexander's law of vestibular nystagmus. *Biol Cyber*, **34**, 181-186.

Doslak, M. J., Dell'Osso, L. F., & Daroff, R. B. (1982). Alexander's law: A model and resulting study. *Ann Otol Rhinol Laryngol*, **91**, 316-322.

Doslak, M. J., Dell'Osso, L. F., & Daroff, R. B. (1983). Multiple double saccadic pulses occurring with other saccadic intrusions and oscillations. *Neuro ophthalmol*, **3**, 109-116.

Duke-Elder, S., & Wybar, K. (1949) *Ocular motility and strabismus (Vol IV)*. System of Ophthalmology., Mosby: St. Louis.

Epelboim, J., & Kowler, E. (1993). Slow control with eccentric targets: evidence against a position-corrective model. *Vision Res*, **33**, 361-380.

Erchul, D. M., & Dell'Osso, L. F. (1997). Latent nystagmus fast-phase generation. ARVO abstracts. *Invest Ophthalmol Vis Sci*, **38**, S650.

Erchul, D. M., Jacobs, J. B., & Dell'Osso, L. F. (1996). Latent nystagmus fast-phase generation. ARVO abstracts. *Invest Ophthalmol Vis Sci*, **37**, S277.

- Erchul, D. M., Dell'Osso, L. F., & Jacobs, J. B. (1998). Characteristics of foveating and defoveating fast phases in latent nystagmus. *Invest Ophthalmol Vis Sci*, **39**, 1751-1759.
- Evarts, E. V. (1971) Feedback and corollary discharge: a merging of the concepts. In: E. V. Evarts, E. Bizzi, R. E. Burke, M. DeLong, & W. T. Thach Jr., *Central Control of Movement, Chap. V* (pp. 86-112). Cambridge: Neurosci Res Prog Bull.
- Flynn, J. T., & Dell'Osso, L. F. (1979). The effects of congenital nystagmus surgery. *Ophthalmol AAO*, **86**, 1414-1425.
- Forssman, B. (1971). Hereditary studies of congenital nystagmus in a Swedish population. *Ann Hum Genet (London)*, **35**, 119-138.
- Glaser, J. S. (1999) *Neuro-ophthalmology*. 3 ed., Lippincott Williams & Wilkins: Philadelphia.
- Goldreich, D., Krauzlis, R. J., & Lisberger, S. G. (1992). Effect of changing feedback delay on spontaneous oscillations in smooth pursuit eye movements of monkeys. *J Neurophysiol*, **67**, 625-638.
- Goldstein, H. P. (1995). Extended slow phase analysis of foveation, waveform and null zone in infantile nystagmus. *Invest Ophthalmol Vis Sci*, **36**, S174.
- Gresty, M. A., Halmagyi, G. M., & Leech, J. (1978). The relationship between head and eye movement in congenital nystagmus with head shaking: objective recordings of a single case. *Br J Ophthalmol*, **62**, 533-535.
- Gresty, M. A., Leech, J., Sanders, M. D., & Eggars, H. (1976). A study of head and eye movement in spasmus nutans. *Br J Ophthalmol*, **160**, 652-654.
- Gresty, M. A., Bronstein, A. M., Page, N. G., & Rudge, P. (1991). Congenital-type nystagmus emerging in later life. *Neurology*, **41**, 653-656.
- Gries, D. (1981) *The science of programming.*, Springer-Verlag: New York.
- Guthrie, B. L., Porter, J. D., & Sparks, D. L. (1983). Corollary discharge provides accurate eye position information to the oculomotor system. *Science*, **221**, 1193-1195.
- Hainline, L. (1988) Normal lifespan developmental changes in saccadic and pursuit eye movements. In: C. W. Johnston, & F. J. Pirozzolo, *Neuropsychology of Eye Movements* (pp. 31-64). Hillsdale: Lawrence Erlbaum Associates.

Halmagyi, G. M., Gresty, M. A., & Leech, J. (1980). Reversed optokinetic nystagmus (OKN): mechanism and clinical significance. *Ann Neurol*, **7**, 429-435.

Harris, C. M. (1995) Problems in modeling congenital nystagmus: Towards a new model. In: J. M. Findlay, R. Walker, & R. W. Kentridge, *Eye Movement Research: Mechanisms, Processes and Applications* (pp. 239-253). Amsterdam: Elsevier.

Hayasaka, S. (1986). Hereditary congenital nystagmus. A Japanese pedigree. *Ophthalmic Pediatr Genet*, **7**, 73-76.

Helmholtz, H. v. (1866) *Handbuch der Physiologen Optik.*, Voss: Leipzig.

Hering, E. (1879). Über Muskelgeräusche des Auges. *Sitzungsberichte der Akademie der Wissenschaften un Wien: Mathematisch-Naturwissenschaftliche Klasse, Abteilung 3*, **79**, 137-159.

Hertle, R. W., & Dell'Osso, L. F. (1999). Clinical and ocular motor analysis of congenital nystagmus in infancy. *J Am Assoc Pediatr Ophthalmol Strab*, **3**, 70-79.

Hertle, R. W., Dell'Osso, L. F., & Movaghar, M. (1995). Clinical and oculographic analysis of congenital nystagmus (CN) in infancy. *Invest Ophthalmol Vis Sci*, **36**, S174.

Hertle, R. W., Dell'Osso, L. F., Williams, R. W., & Jacobs, J. B. (1998). Extraocular muscle tenotomy (the Dell'Osso procedure): Damping of congenital (CN) and see-saw (SSN) nystagmus in the achiasmatic Belgian sheepdog (ABS). [ARVO Abstract]. *Invest Ophthalmol Vis Sci*, **39**, S149.

Hertle, R. W., Tabuchi, A., Dell'Osso, L. F., Abel, L. A., & Weissman, B. M. (1988). Saccadic oscillations and intrusions preceding the postnatal appearance of congenital nystagmus. *Neuro ophthalmol*, **8**, 37-42.

Hogan, D., & Williams, R. W. (1995). Analysis of the retinas and optic nerves of achiasmatic Belgian sheepdogs. *J Comp Neurol*, **352**, 367-380.

Holzmann, G. J. (1991) *Design and validation of computer protocols.*, Prentice Hall: Englewood Cliffs, NJ.

Ishikawa, S. (1979) Latent nystagmus and its etiology. In: R. D. Reinecke, *Strabismus, Proceedings of the Third Meeting of the International Strabismological Association* (pp. 203-214). New York, Grune and Stratton.

- Jacobs, J. B., & Dell'Osso, L. F. (1997). Congenital nystagmus braking saccade characteristics. ARVO abstracts. *Investigative Ophthalmology and Visual Science*, **38**, S650.
- Jacobs, J. B., & Dell'Osso, L. F. (1999). A dual-mode model of latent nystagmus [ARVO Abstract]. *Invest Ophthalmol Vis Sci*, **40**, S962.
- Jacobs, J. B., & Dell'Osso, L. F. (1999). A dual-mode model of latent nystagmus. ARVO abstracts. *Investigative Ophthalmology and Visual Science*, **40**, S962.
- Jacobs, J. B., & Dell'Osso, L. F. (2000). A model of congenital nystagmus (CN) incorporating braking and foveating saccades. ARVO abstracts. *Investigative Ophthalmology and Visual Science*, **41**, S701.
- Jacobs, J. B., Erchul, D. M., & Dell'Osso, L. F. (1996). Braking saccade generation in congenital nystagmus. ARVO abstracts. *Investigative Ophthalmology and Visual Science*, **37**, S277.
- Jacobs, J. B., Dell'Osso, L. F., & Erchul, D. M. (1999). Generation of braking saccades in congenital nystagmus. *Neuro-Ophthalmology*, **21**, 83-95.
- Jacobs, J. B., Dell'Osso, L. F., & Leigh, R. J. (2001). Characteristics of braking saccades in congenital nystagmus (submitted). *Vision Research*, **40**, 000-000.
- Juhola, M., & Pyykkö, I. (1987). Effects of sampling frequencies on the velocity of slow and fast phases of nystagmus. *Int J Bio Med Comp*, **20**, 253-263.
- Jürgens, R., Becker, W., Reiger, P., & Widderich, A. (1981) Interaction between goal-directed saccades and the vestibulo-ocular reflex (VOR) is different from interaction between quick phases and VOR. In: A. F. Fuchs, & W. Becker, *Progress in Oculomotor Research* (pp. 11-18). Amsterdam: Elsevier.
- Kapoula, Z. A., Robinson, D. A., & Hain, T. C. (1986). Motion of the eye immediately after a saccade. *Experimental Brain Research*, **61**, 386-394.
- Keller, E. L., & Edelman, J. A. (1994). Use of interrupted saccade paradigm to study spatial and temporal dynamics of saccadic burst cells in superior colliculus in monkey. *Journal of Neurophysiology*, **72**(6), 2754-2770.
- Kelly, B. J., Rosenberg, M. L., Zee, D. S., & Optican, L. M. (1989). Unilateral pursuit-induced congenital nystagmus. *Neurology*, **39**, 414-416.

Kerrison, J. B., Koenekoop, R. K., Arnould, V. J., D., Z., & Maumenee, I. H. (1998). Clinical features of autosomal dominant congenital nystagmus linked to chromosome 6p12. *Am J Ophthalmol*, **125**, 64-70.

Komatsu, H., & Wurtz, R. H. (1989). Modulation of pursuit eye movements by stimulation of cortical areas MT and MST. *J Neurophysiol*, **62**, 31-47.

Kommerell, G., & Mehdorn, E. (1982) Is an optokinetic defect the cause of congenital and latent nystagmus? In: G. Lennerstrand, D. S. Zee, & E. L. Keller, *Functional Basis of Ocular Motility Disorders* (pp. 159-167). Oxford: Pergamon Press.

Korth, M., Rix, R., & Sembritzki, O. (2000). The sequential processing of visual motion in the human electroretinogram and visually evoked potential. *Vis. Neurosci.*, **17**(4), 631-646.

Krauzlis, R. J., & Lisberger, S. G. (1989). A control systems model of smooth pursuit eye movements with realistic emergent properties. *Neural Computation*, **1**, 116-122.

Krauzlis, R. J., & Miles, F. A. (1996). Transitions between pursuit eye movements and fixation in the monkey: Dependence on context. *J Neurophysiol*, **76**, 1622-1638.

Kurzan, R., & Büttner, U. (1989). Smooth pursuit mechanisms in congenital nystagmus. *Neuro ophthalmol*, **9**, 313-325.

Kustov, A. A., & Robinson, D. L. (1995). Modified saccades evoked by stimulation of the Macaque superior colliculus account for properties of the resettable integrator. *J Neurophysiol*, **00**, 000-000.

Leigh, R. J., & Zee, D. S. (1980). Eye movements of the blind. *Invest Ophthalmol Vis Sci*, **19**, 328-330.

Leigh, R. J., & Zee, D. S. (1999) *The Neurology of Eye Movements, Edition 3 (Contemporary Neurology Series)*., Oxford University Press: New York.

Ludveigh, E. (1952). Possible role of proprioception in the extraocular muscles. *A. M. A. Arch. Opth.*, **48**(436-441).

Ludveigh, E. (1952). Control of ocular movements and visual interpretation of environment. *A. M. A. Arch. Opth.*, **48**(442-448).

Luebke, A. E., & Robinson, D. A. (1988). Transition dynamics between pursuit and fixation suggest different systems. *Vision Res*, **28**, 941-946.

- Lueck, C. J., Tanyeri, S., Mossman, S., Crawford, T. J., & Kennard, C. (1989). Unilateral reversal of smooth pursuit and optokinetic nystagmus. *Revue Neurologique*, **145**, 656-660.
- Lynch, J. C., Mountcastle, V. B., Talbot, W. H., & Yin, T. C. T. (1977). Parietal lobe mechanisms for directed visual attention. *J Neurophysiol*, **40**, 362-389.
- May, J. G., Keller, E. L., & Crandall, J. (1988). Changes in eye velocity during smooth pursuit tracking induced by microstimulation in the dorsolateral pontine nucleus of the macaque. *Soc Neurosci Abstr*, **11**, 79.
- Melzack, R. (1992). Phantom limbs. *Scientific American*, (April), 120-126.
- Merton, P. A. (1964) Absence of conscious position sense in the human eyes. In: M. B. Bender, *The Oculomotor System* (pp. 314-320). New York: Harper and Row.
- Nakamagoe, K., Iwamoto, Y., & Yoshida, K. (2000). Evidence for brainstem structures participating in oculomotor integration. *Science*, **288**, 857-859.
- Nakamagoe, K., Iwamoto, Y., & Yoshida, K. (2000). Evidence for brainstem structures participating in oculomotor integration. *Science*, **288**, 857-859.
- Oetting, W. S., Armstrong, C. M., Holleschau, A. M., DeWan, A. T., & Summers, G. C. (2000). Evidence for genetic heterogeneity in families with congenital motor nystagmus (CN). *Ophthalmic Genetics*, **21**(4), 227-233.
- Ohm, J. (1928). Die Hebelnystagmographie. *Albrecht von Graefes Archiv für Ophthalmologie*, **120**, 235-252.
- Optican, L. M., & Zee, D. S. (1984). A hypothetical explanation of congenital nystagmus. *Biol Cyber*, **50**, 119-134.
- Optican, L. M., Zee, D. S., Chu, F. C., & Cogan, D. G. (1983). Open loop pursuit in congenital nystagmus. [ARVO Abstract]. *Invest Ophthalmol Vis Sci*, **24**(Suppl), 271.
- Orschansky, J. (1898). Eine Methode die Augenbewegungen direkt zu untersuchen (Ophthalmographie). *Zentralblatt für Physiologie*, **12**, 785-790.
- Porter, J. D. (1986). Brainstem terminations of extraocular muscle primary afferent neurons in the monkey. *J Comp Neurol*, **247**, 133-143.

- Reinecke, R. D. (1995) Development of congenital and infantile nystagmus. In: R. J. Tusa, & S. A. Newman, *Neuro-Ophthalmological Disorders - Diagnostic Workup and Management* (pp. 175-186). New York, Basel, Hong Kong: Marcel Dekker, Inc.
- Reinecke, R. D., Suqin, G., & Goldstein, H. P. (1988). Waveform evolution in infantile nystagmus: An electro-oculo-graphic study of 35 cases. *Binoc Vision*, **3**, 191-202.
- Robinson, D. A. (1963). A method of measuring eye movement using a scleral search coil in a magnetic field. *IEEE Trans Bio Med Electron*, **BME(10)**, 137-145.
- Robinson, D. A. (1994) Implications of neural networks for how we think about brain function. In: P. Cordo, & S. Harnad, *Movement Control* (pp. 42-53). Cambridge: Cambridge University Press.
- Robinson, D. A., Gordon, J. L., & Gordon, S. E. (1986). A model of smooth pursuit eye movements. *Biol Cyber*, **55**, 43-57.
- Rottach, K. G., Zivotofsky, A. Z., Das, V. E., Averbuch-Heller, L., DiScenna, A. O., Poonyathalang, A., & Leigh, R. J. (1996). Comparison of horizontal, vertical and diagonal smooth pursuit eye movements in normal human subjects. *Vision Res*, **36**, 2189-2195.
- Russell, S. J., & Norvig, P. (1995) Learning in Neural and Belief Networks. In: *Artificial Intelligence, A Modern Approach* (pp. 563-598). Englewood Cliffs, NJ: Prentice Hall.
- Sacks, O. W. (1987) The disembodied lady. In: *The man who mistook his wife for a hat and other clinical tales* (pp. 43-54). New York: Harper and Row—Perennial Library.
- Schmidt, D., Dell'Osso, L. F., Abel, L. A., & Daroff, R. B. (1980). Myasthenia gravis: Saccadic eye movement waveforms. *Experimental Neurology*, **68**, 346-364.
- Schmidt, D., Dell'Osso, L. F., Abel, L. A., & Daroff, R. B. (1980). Myasthenia gravis: Dynamic changes in saccadic waveform, gain and velocity. *Experimental Neurology*, **68**, 365-377.
- Sekuler, R., & Blake, R. (1994) *Perception.*, McGraw-Hill, Inc.: New York.
- Shallo-Hoffmann, J., Wolsley, C. J., Acheson, J. F., & Bronstein, A. M. (1998). Reduced duration of a visual motion aftereffect in congenital nystagmus. *Documenta Ophthalmologica*, **95**(3-4), 301-314.
- Sharpe, J. A., & Zackon, D. H. (1987). Senescent saccades. *Acta Oto-Laryngologica (Stockholm)*, **104**, 422-428.

Sharpe, J. A., Troost, B. T., Dell'Osso, L. F., & Daroff, R. B. (1975). Comparative velocities of different types of fast eye movements in man. *Investigative Ophthalmology*, **14**, 689-692.

Sherrington, C. S. (1918). Observation on the sensual role of the proprioceptive nerve supply of the extrinsic ocular muscles. *Brain*, **41**, 332-343.

Sheth, N. V., Dell'Osso, L. F., Leigh, R. J., Van Doren, C. L., & Peckham, H. P. (1995). The effects of afferent stimulation on congenital nystagmus foveation periods. *Vision Res*, **35**, 2371-2382.

Shu, F. H. (1982) Evolution of the Stars. In: *The Physical Universe. An Introduction to Astronomy* (pp. 144-158). Mill Valley, California: University Science Books.

Skavenski, A. A. (1972). Inflow as a source of extraretinal eye position information. *Vision Res*, **12**, 221-229.

Smit, A. C., Van Gisbergen, J. A. M., & Cools, A. R. (1987) Dynamics of saccadic tracking responses: Effects of task complexity. In: J. K. O'Reagan, & A. Levy-Schoen, *Eye movements: from physiology to cognition* (pp. 7-16). North Holland: Elsevier Science Publishers BV.

Smit, A. C., Van Gisbergen, J. A. M., & Cools, A. R. (1987). A parametric analysis of human saccades in different experimental paradigms. *Vision Research*, **27**, 1745-1762.

Sperry, R. W. (1950). Neural basis of the spontaneous optokinetic response produced by visual inversion. *J Comp Physiol Psychol*, **43**, 482-489.

St. John, R., Fisk, J. D., Timney, B., & Goodale, M. A. (1984). Eye movements of human albinos. *Am J Optom Physiol Optics*, **61**, 377-385.

Steinman, R. M., & Collewijn, H. (1980). Binocular retinal image motion during active head rotation. *Vision Res*, **20**, 415-429.

Steinman, R. M., Haddad, G. M., Skavenski, A. A., & Wyman, D. (1973). Miniature eye movement. *Science*, **181**, 810-819.

Tusa, R. J., Zee, D. S., Hain, T. C., & Simonsz, H. J. (1992). Voluntary control of congenital nystagmus. *Clin Vis Sci*, **7**, 195-210.

- Van Opstal, A. J., & Van Gisbergen, J. A. M. (1987). Skewness of saccadic velocity profiles: A unifying parameter for normal and slow saccades. *Vision Research*, **27**, 731-745.
- Van Opstal, A. J., & Van Gisbergen, J. A. M. (1989). Scatter in the metrics of saccades and properties of the collicular motor map. *Vision Research*, **29**, 1183-1196.
- Von Holst, E., & Mittelstaedt, H. (1950). Das Reafferenzprinzip (Wechselwirkungen zwischen Zentralnervensystem und Peripherie). *Naturwiss*, **37**, 464-476.
- Weber, R. B., & Daroff, R. B. (1972). Corrective movements following refixation saccades: Type and control system analysis. *Vision Res*, **12**, 467-475.
- Weissman, B. M., Dell'Osso, L. F., Abel, L. A., & Leigh, R. J. (1987). Spasmus nutans: A quantitative prospective study. *Arch Ophthalmol*, **105**, 525-528.
- Whittaker, S. G., & Cummings, R. W. (1990). Foveating saccades. *Vision Research*, **30**, 1363-1366.
- Williams, R. W., & Dell'Osso, L. F. (1993). Ocular motor abnormalities in achiasmatic mutant Belgian sheepdogs. *Invest Ophthalmol Vis Sci*, **34**, 1125.
- Williams, R. W., Garraghty, P. E., & Goldowitz, D. (1991). A new visual system mutation: Achiasmatic dogs with congenital nystagmus. *Soc Neurosci Abstr*, **17**, 187.
- Winson, J. (1990). The meaning of dreams. *Scientific American*, (Nov 1990), 86-96.
- Winters, J. M., Nam, M. H., & Stark, L. W. (1984). Modeling dynamical interactions between fast and slow movements: Fast saccadic eye movement behavior in the presence of the slower VOR. *Math Biosci*, **68**, 159-185.
- Wirtschafter, J. D., & Weingarden, A. S. (1988) Neurophysiology and central pathways in oculomotor control: Physiology and anatomy of saccadic and pursuit movements. In: C. W. Johnston, & F. J. Pirozzolo, *Neuropsychology of Eye Movements* (pp. 5-30). Hillsdale: Lawrence Erlbaum Associates.
- Yamazaki, A. (1979) Abnormalities of smooth pursuit and vestibular eye movements in congenital jerk nystagmus. In: K. Shimaya, *Ophthalmology* (pp. 1162-1165). Amsterdam: Excerpta Medica.
- Yarbus, A. L. (1967) *Eye movements and vision.*, Plenum Press: New York.

- Yee, R. D., Baloh, R. W., & Honrubia, V. (1980). Study of congenital nystagmus: optokinetic nystagmus. *British Journal of Ophthalmology*, **64**(12), 926-932.
- Yee, R. D., Baloh, R. W., & Honrubia, V. (1981). Eye movement abnormalities in rod monochromacy. *Ophthalmology*, **88**, 1010-1018.
- Young, L. R., & Stark, L. (1963). Variable feedback experiments testing a sampled data model for eye tracking movements. *IEEE Trans Prof Tech Group Human Factors Electron*, **HFE**(4), 38-51.
- Zee, D. S., & Robinson, D. A. (1979). A hypothetical explanation of saccadic oscillations. *Annals of Neurology*, **5**(5), 405-414.
- Zee, D. S., Fitzgibbon, E. J., & Optican, L. M. (1992). Saccade-vergence interactions in humans. *Journal of Neurophysiology*, **68**, 1624-1641.
- Zee, D. S., Optican, L. M., Cook, J. D., Robinson, D. A., & Engel, W. K. (1976). Slow saccades in spinocerebellar degeneration. *Archives of Neurology*, **33**, 243-251.
- Zuber, B. L., & Stark, L. (1965). Microsaccades and the velocity-amplitude relationship for saccadic eye movements. *Science*, **150**, 1459-1460.